

Hieronim Jakubowski

Homocysteine in Protein Structure/ Function and Human Disease

Chemical Biology of Homocysteine-
containing Proteins

 Springer

Homocysteine in Protein Structure/Function and Human Disease

Hieronim Jakubowski

Homocysteine in Protein Structure/Function and Human Disease

Chemical Biology of
Homocysteine-containing
Proteins



Springer

Hieronim Jakubowski
Department of Microbiology and Molecular Genetics
UMDNJ-New Jersey Medical School
International Center for Public Health
Newark, NJ, USA

ISBN 978-3-7091-1409-4 ISBN 978-3-7091-1410-0 (eBook)
DOI 10.1007/978-3-7091-1410-0
Springer Wien Heidelberg New York Dordrecht London

Library of Congress Control Number: 2013939562

© Springer-Verlag Wien 2013

This work is subject to copyright. All rights are reserved by the Publisher, whether the whole or part of the material is concerned, specifically the rights of translation, reprinting, reuse of illustrations, recitation, broadcasting, reproduction on microfilms or in any other physical way, and transmission or information storage and retrieval, electronic adaptation, computer software, or by similar or dissimilar methodology now known or hereafter developed. Exempted from this legal reservation are brief excerpts in connection with reviews or scholarly analysis or material supplied specifically for the purpose of being entered and executed on a computer system, for exclusive use by the purchaser of the work. Duplication of this publication or parts thereof is permitted only under the provisions of the Copyright Law of the Publisher's location, in its current version, and permission for use must always be obtained from Springer. Permissions for use may be obtained through RightsLink at the Copyright Clearance Center. Violations are liable to prosecution under the respective Copyright Law.

The use of general descriptive names, registered names, trademarks, service marks, etc. in this publication does not imply, even in the absence of a specific statement, that such names are exempt from the relevant protective laws and regulations and therefore free for general use.

While the advice and information in this book are believed to be true and accurate at the date of publication, neither the authors nor the editors nor the publisher can accept any legal responsibility for any errors or omissions that may be made. The publisher makes no warranty, express or implied, with respect to the material contained herein.

Printed on acid-free paper

Springer is part of Springer Science+Business Media (www.springer.com)

To my wife, Alina Barbara

Preface

Proteins, the major functional macromolecules of life, are composed of long chains of L- α -amino acids linked by amide bonds between the α -carboxyl group of one residue and the α -amino group of the next. Although proteins contain several dozens to thousands of amino acid residues, only the 20 canonical coded amino acids, including two that contain sulfur—cysteine and methionine—are involved. Many diseases originate from mutations or modifications in proteins that affect their structure and cause a loss of function.

Recent studies provide evidence that in humans and animals, the noncoded sulfur-containing amino acid homocysteine (Hcy) becomes a constituent of proteins via two mechanisms: (a) protein *N*-homocysteinylation by Hcy-thiolactone and (b) protein *S*-thiolation in thiol–disulfide exchange reactions. Protein *N*-homocysteinylation is absolutely specific for Hcy because Hcy-thiolactone, the actual agent creating the modification, can only arise from Hcy in any cell type. In contrast, protein *S*-thiolation is not limited to Hcy but occurs with other thiols as well, generating a variety of *S*-thiolated proteins such as *S*-glutathionyl-protein, *S*-cysteinyl-protein, and *S*-cysteinyl-glycyl-protein, in addition to *S*-Hcy-protein. Thus, while *N*-Hcy-protein is unique, *S*-Hcy-protein is a quantitatively minor component of the total *S*-thiolated-protein species. Furthermore, as described in this book, physiological responses to *N*-Hcy-protein are also unique and distinct from the responses to *S*-Hcy-protein.

In the first sections of this book, I have described fundamental aspects of protein-related chemical biology of Hcy and emphasized the importance of Hcy-thiolactone-mediated protein *N*-homocysteinylation in Hcy pathobiology. Of many known naturally occurring Hcy species, only the thioester Hcy-thiolactone, a product of an error-correcting reaction in protein biosynthesis, can mediate the incorporation of Hcy into proteins via stable isopeptide bonds. Protein *N*-homocysteinylation creates altered proteins with newly acquired interactions. With the development of novel analytical methods within the last few years, studies of the role of Hcy-thiolactone and protein *N*-linked Hcy in humans and experimental animals became possible. So far, these studies have identified about three dozens of individual *N*-Hcy-proteins and specific sites of *N*-homocysteinylation in some of them. These studies also show

that the genetic or dietary hyperhomocysteinemia greatly elevates levels of Hcy-thiolactone and protein *N*-linked Hcy in humans and mice. Other studies provide evidence that *N*-Hcy-proteins are immunogenic in humans and experimental animals. In humans, *N*-homocysteinylation causes the formation of neo-self *N*ε-Hcy-Lys epitopes in proteins, which induce an adaptive immune response, manifested by the generation of anti-*N*-Hcy-protein IgG autoantibodies. Levels of these autoantibodies are elevated in stroke and coronary artery disease (CAD) patients and thus may play an important role in atherosclerosis. Other data show that *N*-homocysteinylation of fibrinogen by Hcy-thiolactone contributes to thrombogenic effects of elevated plasma tHcy levels in humans. Furthermore, these studies also show that primary Hcy lowering by B-vitamin therapy is beneficial in that it improves fibrin clot properties and lowers the levels of anti-*N*-Hcy-protein autoantibodies in healthy individuals. In contrast, secondary B-vitamin intervention appears to be ineffective: although it lowers plasma tHcy, *it does not affect anti-N-Hcy-protein autoantibody titers in CAD patients*. Finally, roles of Hcy-thiolactone-detoxifying enzymes, paraoxonase 1 and bleomycin hydrolase, as well as urinary Hcy-thiolactone elimination are discussed.

The final sections of this book are devoted to protein *S*-homocysteinylation. About a dozen of individual proteins are described that have been shown to be susceptible to *S*-homocysteinylation in vitro, and some of them are also found to be *S*-homocysteinylation in vivo. *S*-homocysteinylation, or more generally *S*-thiolation, causes profound changes in protein structure and function, but the physiological significance of these changes is not fully understood. The function of several proteins has been shown to be affected by Hcy and other thiols in vitro, and some of them are also affected in cultured cells and in vivo.

Newark, NJ
January 2013

Hieronim Jakubowski

List of Abbreviations

AARS	Aminoacyl-tRNA synthetase
A β	Amyloid β -peptide
ADMA	Asymmetric dimethylarginine
AdoHcy	S-adenosylhomocysteine
ApoA1	Apolipoprotein A1
ApoB	Apolipoprotein B
AuNPs	Gold nanoparticles
BHMT	Betaine-homocysteine methyltransferase
Blmh	Bleomycin hydrolase
CAD	Coronary artery disease
cbEGF	Calcium-binding epidermal growth factor
CBS	Cystathionine β -synthase
CD	Circular dichroism
CKD	Chronic kidney disease
CMQT	2-Chloro-1-methylquinolinium tetrafluoroborate
CRP	C-reactive protein
Cse	Cystathionine γ -lyase
DDAH	Dimethylarginine dimethylaminohydrolase
DHFR	Dihydrofolate reductase
DLS	Dynamic light scattering
ER	Endoplasmic reticulum
ESI-MS	Electrospray ionization-mass spectrometry
FSN	Fluorosurfactant
GC-MS	Gas chromatography-mass spectrometry
GSH	Glutathione
HCA	Homocysteic acid
Hcy	Homocysteine
HDL	High-density lipoprotein
hnRNP-E1	Heterogenous nuclear ribonucleoprotein E1

HPLC	High-performance liquid chromatography
HSA	Homocysteine sulfinic acid
HPV	Human papilloma virus
HTL	Hcy-thiolactone
HUVECs	Human umbilical vein endothelial cells
ICAM	Intercellular adhesion molecule
IgG	Immunoglobulin G
KLH	Keyhole limpet hemocyanin
LC-MS	Liquid chromatography-mass spectroscopy
LDL	Low-density lipoprotein
MCP	Monocyte chemotactic protein
MetRS	Methionyl-tRNA synthetase
MS	Methionine synthase
MTHFR	Methylenetetrahydrofolate reductase
MTP	Microtubule proteins
NF	Nuclear factor
<i>N</i> -Hcy-protein	<i>N</i> -homocysteinylated protein or Hcy bound to protein by an isopeptide linkage
NMDA	<i>N</i> -methyl-D-aspartate
NMR	Nuclear magnetic resonance
OPA	<i>o</i> -Phthalaldehyde
TCEP	Tris(2-carboxyethyl)phosphine
tHcy	total Hcy, i.e., Hcy present after reductive cleavage of all disulfide bonds in a sample
tRNA	transfer RNA
Pcft	Proton-coupled folate transporter
Pon 1	Paraoxonase 1
PSEA	Polysulfoethylaspartamide
PTH	Phenylthiohydantoin
SDS-PAGE	Sodium dodecyl sulfate-polyacrylamide gel electrophoresis
<i>S</i> -Hcy-protein	<i>S</i> -homocysteinylated protein or Hcy bound to protein by a disulfide linkage
TLC	Thin-layer chromatography
TNF	Tissue necrosis factor
TTR	Transthyretin
VCAM	Vascular cell adhesion molecule
UPR	Unfolded protein response
UV	Ultraviolet

Contents

1	Introduction	1
2	An Overview of Homocysteine Metabolism	7
2.1	Homocysteine Metabolite Levels	8
2.1.1	“Total Homocysteine”	9
2.1.2	<i>S</i> -Homocysteinyl-Protein	9
2.1.3	Homocysteine-Thiolactone	10
2.1.4	<i>N</i> -Homocysteinyl-Protein	10
2.1.5	<i>Nε</i> -Homocysteinyl-Lysine	11
2.1.6	<i>S</i> -Adenosylhomocysteine	11
2.1.7	Cystathionine	11
2.1.8	Homocysteic Acid and Homocysteine Sulfinic Acid	11
2.2	Toxicity of Homocysteine Metabolites	12
2.2.1	Free Reduced Homocysteine	13
2.2.2	<i>S</i> -Homocysteinyl-Protein	13
2.2.3	Homocysteine-Thiolactone	14
2.2.4	<i>N</i> -Homocysteinyl-Protein	16
2.2.5	<i>Nε</i> -Homocysteinyl-Lysine	17
2.2.6	<i>S</i> -Adenosylhomocysteine	17
2.2.7	Cystathionine	18
2.2.8	Homocysteic Acid	18
3	Homocysteine-Thiolactone	19
3.1	Chemical Synthesis	19
3.1.1	Demethylation of Methionine	19
3.1.2	Acid-Dependent Cyclization of Homocysteine	20
3.2	Physicochemical Properties	20
3.2.1	UV Spectrum	20
3.2.2	pK_a value	23
3.2.3	Stability	23
3.2.4	Reactivity Toward Amino Groups	25
3.2.5	Reactivity Toward Carbonyl Compounds	27

3.3	Quantification Methods	29
3.3.1	Assays Based on Radiolabeling	29
3.3.2	Assays Based on Direct UV Monitoring	29
3.3.3	High-Performance Liquid Chromatography-Based Assays	29
3.3.4	Gas Chromatography/Mass Spectrometry Assay	32
3.3.5	Gold Nanoparticle Homocysteine-Thiolactone Sensor	32
3.4	Biosynthesis	33
3.4.1	The Involvement of Methionyl-tRNA Synthetase	33
3.4.2	Molecular Mechanism	37
3.5	Turnover	45
3.5.1	Enzymatic Turnover	45
3.5.2	Urinary Excretion	50
3.6	Clinical Significance	51
4	Discoveries of Protein S- and N-Homocysteinylation	55
5	N-Homocysteinyl-Proteins	59
5.1	Synthesis In Vitro	59
5.2	Biological Formation	62
5.2.1	N-Hcy-Protein Levels In Vivo	62
5.2.2	Site-Specific N-Homocysteinylation In Vivo	69
5.3	Turnover	71
5.3.1	N ϵ -Homocysteinyl-Lysine	71
5.4	Structural and Functional Consequences	76
5.4.1	N-Homocysteinylation and Redox Function	78
5.4.2	N-Hcy-Fibrinogen and Fibrin Clot Properties	83
5.4.3	N-Homocysteinylation and LDL Function	84
5.4.4	N-Homocysteinylation and HDL Function	85
5.4.5	N-Homocysteinylation Induces Protein Aggregation and Amyloid Conversion	86
5.5	Quantification of N-Hcy-Protein	94
5.5.1	High-Performance Liquid Chromatography Assay with UV Detection	95
5.5.2	High-Performance Liquid Chromatography Assays with Fluorescence Detection	96
5.5.3	Immunoassays with Rabbit Polyclonal Anti-N-Hcy-Protein Antibodies	99
5.5.4	Western Blot Immunoassay for N-Hcy-ApoAI	99
5.5.5	Detection of Protein N-Homocysteinylation by Selective Reactions with Aldehydes	100
5.5.6	Liquid Chromatography/Mass Spectrometry Analysis of the Site-Specific Protein N-Homocysteinylation In Vivo	102
6	Pathophysiological Consequences of Protein N-Homocysteinylation	107
6.1	The Hcy-Thiolactone Hypothesis	108
6.1.1	Hcy-Thiolactone Levels in Hyperhomocysteinemia	109
6.1.2	Protein N-Linked Hcy in Hyperhomocysteinemia	110

6.2	<i>N</i> -Hcy-Protein and Adaptive Autoimmune Responses	111
6.2.1	Atherosclerosis Is an Inflammatory Disease	111
6.2.2	<i>N</i> -Hcy-Protein Is Immunogenic in Rabbits	112
6.2.3	<i>N</i> -Hcy-Protein Is Autoimmunogenic in Humans	112
6.2.4	Anti- <i>N</i> -Hcy-Protein Autoantibodies in Atherosclerosis	114
6.3	<i>N</i> -Hcy-Protein and Innate Immune Responses	115
6.4	<i>N</i> -Hcy-Fibrinogen and Thrombosis	117
6.5	<i>N</i> -Hcy-Collagen and Connective Tissue Abnormalities	119
7	S-Homocysteinylated Proteins	121
7.1	Plasma <i>S</i> -Homocysteinyl-Proteins	123
7.1.1	<i>S</i> -Hcy-Albumin	123
7.1.2	<i>S</i> -Hcy-Transferrin	124
7.1.3	Apolipoprotein B and Lipoprotein[a]	126
7.2	Extracellular Matrix Proteins	127
7.2.1	Fibrillins	127
7.2.2	Fibronectin	129
7.2.3	Tropoelastin	129
7.3	Blood Homeostasis Proteins	130
7.3.1	Factor Va	130
7.3.2	Annexin A2	131
7.4	Intracellular Proteins	132
7.4.1	Heterogenous Nuclear Ribonucleoprotein E1 (hnRNP-E1)	132
7.4.2	Metallothionein	134
7.4.3	Dimethylarginine Dimethylaminohydrolase	134
	References	137
	Index	161

Chapter 1

Introduction

That homocystine itself might be present in proteins is a possibility that should be borne in mind and will be worth investigating
—Vincent Du Vigneaud, 1955 Nobel Prize in Chemistry laureate

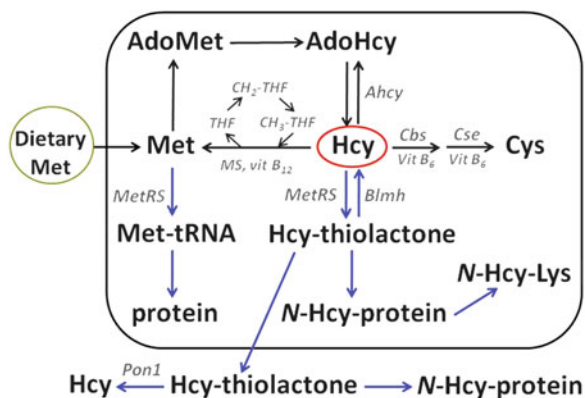
In living organisms, homocysteine (Hcy) is a universal intermediate in the metabolic pathways of two other sulfur-containing amino acids: cysteine and methionine. Relative to cysteine, Hcy has in its side chain an extra methylene ($-\text{CH}_2-$) group that makes it a higher homolog of cysteine. Compared with methionine, Hcy is missing a methyl (CH_3-) group and thus is a lower homolog of methionine. Methionine and cysteine are two canonical coded amino acids that are incorporated by the ribosomal biosynthetic apparatus into polypeptide chains of protein at positions specified by AUG and UGU/UGC codons, respectively. In contrast, Hcy does not normally participate in protein biosynthesis (there is no codon triplet for Hcy) and is considered to be a nonprotein amino acid.

The disulfide cystine, the first sulfur-containing amino acid to be discovered, was originally isolated from a urinary calculus by Wallstone in 1810 and, by the end of nineteenth century, established to be a major component of proteins [1]. Since the mid-1800s accumulating experimental evidence from the Liebig's laboratory and from other investigators indicated that cysteine does not account for all the sulfur present in proteins [1]. The nature of this non-cystine protein sulfur has been clarified in the 1923 studies of Mueller which led to the isolation of a new sulfur-containing amino acid, methionine, from protein hydrolysates [2].

Hcy, the last of the three major sulfur-containing amino acids, was first obtained in 1932 in the oxidized disulfide form—homocystine—by the demethylation of methionine with sulfuric acid [3]. Three years later, in 1935, Hcy was prepared by reduction of homocystine with metallic sodium in liquid ammonia [4]. Subsequent studies clarified the physiological role of Hcy as an intermediate in the metabolism of methionine and cysteine via the classical remethylation and transsulfuration pathways, respectively [5].

Elucidation of the genetic code and of the ribosomal protein biosynthesis mechanism established that Hcy is not a coded amino acid. However, because of

Fig. 1.1 Schematic representation of human homocysteine metabolism



its close structural similarity to the coded amino acid methionine, Hcy does enter the first step of protein biosynthesis. In fact, the active site of methionyl-tRNA synthetase (MetRS), in addition to activating the cognate substrate methionine and forming Met-AMP, also activates Hcy and forms homocysteinyl adenylate (Hcy-AMP). Met-AMP proceeds to form Met-tRNA, which then donates Met to growing peptide chains in the ribosomal protein biosynthetic apparatus. In contrast, the Hcy-AMP intermediate is converted to Hcy-thiolactone by an editing mechanism of MetRS, which prevents the attachment of Hcy to tRNA^{Met} and thus precludes Hcy from entering the genetic code [6, 7]. The editing mechanism of MetRS is universal and is responsible for the biosynthesis of the thioester Hcy-thiolactone in all organisms, from bacteria to human. The conversion to Hcy-thiolactone, catalyzed by MetRS, initiates a novel pathway of Hcy metabolism in humans and animals (Fig. 1.1).

Methionine, one of the eight essential amino acids that must be provided in the form of dietary protein, is the only source of Hcy in the human body (Fig. 1.1). Under normal circumstances, Hcy does not accumulate because it is metabolized to methionine and cysteine. However, the inability to metabolize Hcy via the classical remethylation and transsulfuration pathways, caused by certain genetic or nutritional deficiencies, leads to Hcy accumulation, which is associated with numerous pathological conditions in humans. Over the past two decades, studies of Hcy have experienced unprecedented growth fueled primarily by the desire to understand its role in cardiovascular and neurological diseases in humans [8–10].

Early studies have shown that high-protein diets can be harmful to experimental animals. Subsequent studies of individual dietary amino acids have led to the conclusion that methionine, the ultimate metabolic precursor of Hcy (Fig. 1.1), ingested in excess, is the most toxic amino acid [11–13]. Excessive consumption of methionine leads to elevation of Hcy levels (hyperhomocysteinemia). In fact, animals fed with high-methionine diets are often used as models of experimental hyperhomocysteinemia [14]. For instance, female rats fed with a diet containing 5 % methionine have no successful pregnancies [15], while animals fed with high-protein or high-methionine diets for 2 years develop hyperhomocysteinemia and vascular disease [16, 17]. Apolipoprotein E-deficient mice fed with a high-methionine diet (2.2 % or

4.4 % methionine) experience accelerated atherosclerosis (at 3 months), start to lose weight, and die prematurely (48 % animals die at 8 months) [18]. Chicks fed with a high-methionine (2 %) diet develop hyperhomocysteinemia, neurological seizures, and severe aortic pathology resulting from aberrant assembly of elastic fibers [19]. Elevation of Hcy in body tissues, further exacerbated when intake of B vitamins and folate (cofactors of Hcy-metabolizing enzymes; Fig. 1.1) is inadequate, contributes to the toxicity of methionine excess [20]. Conversely, methionine restriction increases life span in rats [21] and inhibits age-related disease processes [22], including cancer [23]. The administration of Hcy itself is often used to study mechanisms underlying the pathology of hyperhomocysteinemia in experimental animals [18, 24, 25].

In humans, the administration of methionine at a dose of 0.1 g/kg body weight is used to test for deficiencies in Hcy metabolism and to study relationships between elevation of plasma Hcy and cardiovascular and neurodegenerative diseases. The oral methionine loading test is generally very safe [26, 27]. However, a larger dose of methionine may cause severe, potentially lethal cerebral effects: one case of death of a control subject participating in a study of relationships between Hcy and Alzheimer's disease has been reported to result from a substantial overdose of methionine (80 g instead of the usual 8 g) [28].

Inborn errors in human Hcy metabolism due to mutations in the cystathionine β -synthase (CBS), 5,10-methylenetetrahydrofolate reductase (MTHFR), or methionine synthase (MS) genes (Fig. 1.1) cause severe hyperhomocysteinemia and homocystinuria as well as pathologies in multiple organs, including the cardiovascular system and the brain, and lead to premature death due to vascular complications, usually thromboembolism in affected arteries and veins [20, 29–32]. Observations of advanced arterial lesions in children with inborn errors in Hcy metabolism have led to a proposal that Hcy causes vascular disease [33]. Severe hyperhomocysteinemia is rare. For example, CBS deficiency occurs at an estimated worldwide frequency of 1 in 300,000, with higher frequency in Ireland (1 in 65,000) and Qatar (1 in 1,800). In contrast, mild hyperhomocysteinemia is quite prevalent in the general population (some estimates indicate a frequency as high as 1 in 10) and is also associated with an increased risk [34] of cardiovascular disease and mortality [35–37], neurological complications [38], pregnancy complications and birth defects [39], and osteoporosis [40]. Although associations alone do not prove causality, preponderance of experimental evidence indicates that it is biologically plausible that excess Hcy can damage and impair normal cellular and physiological function and cause disease [9, 41].

Atherosclerosis is a disease of the vascular wall and is initiated by endothelial damage [42, 43]. Endothelial dysfunction, immune activation, and thrombosis, characteristic features of vascular disease [42, 43], are all observed in hyperhomocysteinemic individuals [20] and experimental hyperhomocysteinemia in animals [14, 44, 45]. The degree of endothelial function impairment in hyperhomocysteinemic organisms is similar to that observed in subjects with hypercholesterolemia or hypertension [44].

The strongest evidence that elevated Hcy plays a causal role in atherothrombotic disease comes from studies of severe genetic hyperhomocysteinemia in humans and

the finding that Hcy lowering by B-vitamin supplementation significantly improves vascular outcomes in CBS-deficient patients [20, 29, 30]. For instance, while untreated CBS-deficient patients suffer one vascular event per 25 patient-years [46], B-vitamin-treated CBS-deficient patients suffer only one vascular event per 263 patient-years (relative risk 0.091, $p < 0.001$) [30]. Hcy-lowering therapy initiated early in life also prevents brain disease from severe MTHFR deficiency [31, 47]. Furthermore, studies of genetic or nutritional hyperhomocysteinemia in animal models also provide a strong support for a causative role of Hcy [14, 44, 48].

In humans, lowering plasma Hcy by B-vitamin supplementation improves cognitive function in the general population [49] and leads to a 21–24 % reduction of vascular outcomes in high-risk stroke patients [50, 51], but not in myocardial infarction patients [51, 52]. Meta-analysis of Hcy-lowering trials provides evidence that folic acid supplementation can significantly reduce the risk of stroke in primary prevention, provided that the intervention lasts >3 years and results in tHcy lowering >20 % [53]. Among possible reasons cited for the failure of B-vitamin intervention trials to prevent adverse vascular outcomes is that the beneficial effect of B-vitamin therapy in lowering plasma Hcy is counteracted by adverse effects of high B-vitamin levels on the cardiovascular system [10].

As demonstrated by a post hoc subanalysis of the VITATOPS trial [54], benefits of B-vitamin therapy to lower Hcy are offset by concomitant use of antiplatelet therapy. Combined analyses of two randomized Hcy-lowering B-vitamin trials, the Norwegian Vitamin Trial (NORVIT) and the Western Norway B Vitamin Intervention Trial (WENBIT), suggest that cardiovascular risk prediction is confined to the fraction of Hcy that does not respond to B vitamins [55]. Hcy lowering by B-vitamin treatment slows the rate of accelerated brain atrophy [56] and cognitive decline [57] in mild cognitive impairment patients, which may slow or prevent the conversion to dementia and Alzheimer's disease.

Although it is a common metabolite in all living organisms, Hcy in excess of basal levels can be extremely toxic to human [58–61], animal [62], yeast [63–65], and bacterial cells [66, 67]. Why Hcy is toxic is not entirely clear and is a subject of intense investigations, particularly in the context of human pathophysiology [41, 44, 68–71].

Hcy is one of the most reactive amino acids and participates in at least seven reactions in biological systems [68]. In addition to its elimination by remethylation to methionine, transsulfuration to cysteine (via cystathionine), and oxidation to disulfides, Hcy is also metabolically converted to other, potentially toxic, metabolites (Fig. 1.1), such as Hcy-thiolactone, *N*-Hcy-protein, *Ne*-Hcy-Lys [72], AdoHcy, homocysteic acid, or *S*-nitroso-Hcy; these conversions can be greatly enhanced in genetic or nutritional deficiencies in Hcy metabolism. Possible mechanisms accounting for the toxicity of specific Hcy metabolites have been proposed. However, because of parallel changes in the concentrations of Hcy metabolites under most clinical and experimental circumstances, it is often difficult to unequivocally assign the observed toxicity to a specific Hcy metabolite.

As discovered at the end of 1990s, two of these metabolites, Hcy-thiolactone [73, 74] and *S*-nitroso-Hcy [75, 76], mediate Hcy incorporation into protein [77].

Hcy-thiolactone-mediated Hcy incorporation affects the protein's structure/function and leads to protein damage [7, 68]. Accumulating evidence, discussed in the following chapters in this book, strongly suggests that Hcy-thiolactone and *N*-Hcy-protein contribute to the pathophysiology of hyperhomocysteinemia.

It is interesting to note that in his 1932 article describing the discovery of homocystine [3], the 1955 Nobel Prize in Chemistry laureate Vincent Du Vigneaud stated "*That homocystine itself might be present in proteins is a possibility that should be borne in mind and will be worth investigating.*" This possibility has turned into reality in a more recent times [73, 78], and Hcy is now known to be a component of proteins [79]. Mechanisms of Hcy incorporation into protein and chemical biology of Hcy-containing proteins, with emphasis on mechanisms by which such Hcy-proteins could contribute to human cardiovascular and neurological diseases, are the subjects of this book.

Chapter 2

An Overview of Homocysteine Metabolism

Mammals, in contrast to bacteria and plants, cannot make their own methionine (Met). Thus, in humans and animals, Met is an essential amino acid that is provided in the form of proteins ingested as food. In our digestive tract dietary proteins are hydrolyzed to amino acids. Met released from dietary proteins is taken up by the epithelium of the digestive tract and transported in the blood to cells of various organs. In every cell of the body Met is metabolized by two major pathways (Fig. 1.1): (1) as a building block to make new proteins in the ribosomal protein biosynthetic apparatus and (2) as a precursor of *S*-adenosylmethionine (AdoMet), a universal donor that provides *methyl groups* for biological methylation reactions and *propyl groups* for polyamine biosynthesis (both derived from Met). In metabolic pathways (1) and (2), Met is activated by reactions with ATP, albeit in a pathway-specific manner: the carboxyl group of Met is activated in pathway (1), while the thioether sulfur atom is activated in pathway (2).

It is the Met utilization pathway (2) that eventually leads to Hcy [20] (Fig. 1.1). As a result of the transfer of its methyl group to an acceptor, AdoMet is converted to *S*-adenosylhomocysteine (AdoHcy). *The reversible enzymatic hydrolysis of AdoHcy is the only known source of Hcy in the human or animal body.* Levels of Hcy are regulated by remethylation to Met, catalyzed by the enzyme MS, and a two-step transsulfuration to cysteine, the first step of which is catalyzed by the enzyme CBS, while the second step is catalyzed by cystathionine γ -lyase (CSE). The remethylation catalyzed by MS requires vitamin B₁₂ and 5,10-methyltetrahydrofolate (CH₃-THF), generated by MTHFR [31] (Fig. 1.1). An alternative remethylation pathway is catalyzed by betaine-Hcy methyltransferase (BHMT) [80]. The transsulfuration requires vitamin B₆. While remethylation by MS occurs in every organ of the body, remethylation by BHMT and transsulfuration by CBS are limited to the liver and kidneys. Hcy can also react oxidatively with other thiols, mainly sulfhydryl groups of extracellular proteins, to form mixed disulfides (*S*-Hcy-protein) [78, 79, 81].

A fraction of Hcy is also metabolized by methionyl-tRNA synthetase (MetRS in Fig. 1.1) to the thioester Hcy-thiolactone [68, 69, 82, 83]. The flow through the Hcy-thiolactone pathway is increased by a high-Met diet (the ultimate precursor of

Hcy), inadequate supply of $\text{CH}_3\text{-THF}$, or impairment of remethylation or transsulfuration reactions by genetic alterations of enzymes, such as CBS, MS, or MTHFR. Hcy-thiolactone is neutral at physiological pH ($\text{p}K_{\text{a}} = 6.67$, [84]) and thus accumulates mostly in the extracellular fluids.

Hcy-thiolactone is metabolized by two pathways: (1) a hydrolytic pathway that affords Hcy—this pathway is catalyzed by intracellular and extracellular Hcy-thiolactonases, otherwise known as bleomycin hydrolase (Blmh) [85] and paraoxonase 1 (Pon1) [81], respectively; and (2) a synthetic pathway in which Hcy-thiolactone reacts chemically with protein lysine residues, forming *N*-Hcy-protein [78, 79, 81] (Fig. 1.1).

Proteolytic degradation of *N*-Hcy-protein affords *Ne*-Hcy-Lys (Fig. 1.1), first discovered in a biological system when *N*-Hcy-hemoglobin was incubated with liver extracts [72]. The isopeptide *Ne*-Hcy-Lys is present in human and mouse plasma. Its levels increase in renal disease and CBS deficiency in humans. Genetic deficiencies in folate and Hcy metabolism and a hyperhomocysteinemic high-Met diet cause elevation of *Ne*-Hcy-Lys in mice. The plasma levels of *Ne*-Hcy-Lys are positively correlated with the nitric oxide synthase inhibitor asymmetric dimethylarginine [86], which is consistent with their common origin as products of protein turnover [72].

2.1 Homocysteine Metabolite Levels

In addition to the free thiol (reduced) form, i.e., free Hcy-SH, several other Hcy species are present in human and animal plasma (Table 2.1) [87]. These include the disulfide homocystine Hcy-S-S-Hcy identified in the urine of patients with homocystinuria [88]; a mixed disulfide of Hcy and Cys, Hcy-S-S-Cys, first described in patients with cystinuria [89] and then in patients with homocystinuria [90]; and a mixed disulfide of Hcy with plasma protein, *S*-Hcy-protein [91, 92], as well as species with substituted carboxyl groups, such as Hcy-thiolactone [64, 76, 93–95], *N*-Hcy-protein [76, 79, 96], and *Ne*-Hcy-Lys [72]. Other known Hcy metabolites include AdoHcy, cystathionine [97, 98], homocysteine sulfinic acid, and homocysteic acid (Table 2.1) [20, 99].

S-Nitroso-Hcy is a potential metabolite that has been first detected in bovine aortic endothelial cells incubated with exogenous Hcy [100]. Treatment of these cells with the nitric oxide synthase inhibitor *N*-nitro-L-Arg prevents nitric oxide generation and the formation of *S*-nitroso-Hcy. Increasing nitric oxide generation by overexpression of the inducible nitric oxide synthase in endothelial cells results in a significant increase in the formation of *S*-nitroso-Hcy [101]. That human endothelial cells produce *S*-nitroso-Hcy has also been inferred from its ability to mediate translational incorporation of Hcy into protein [75] that is observed in these cells [68, 76, 83]. However, the presence of *S*-nitroso-Hcy in humans or animals remains to be documented.

Table 2.1 Concentrations of Hcy metabolites in normal human and mouse plasma and urine

Hcy metabolite	Concentration (nM) in human		Concentration (nM) in mouse	
	Plasma	Urine	Plasma	Urine
tHcy	12,000	2,500	3,000	45,000
Hcy	250			
Hcy-S-S-Hcy + Hcy-S-S-Cys	1,940			
S-Hcy-protein	9,810			
Hcy-thiolactone	0.2	168	3.7	136
N-Hcy-protein	490		1,900	
Ne-Hcy-Lys	<100	<100	400	<100
AdoHcy	15	490		
Homocysteic acid	186			
Homocysteine sulfinic acid	677			
Cystathionine	126	350–49,900	2,479	

Concentration values are from references discussed in the text

2.1.1 “Total Homocysteine”

The sum of free thiol (reduced) and disulfide-bound Hcy (oxidized) species, obtained by the treatment of a sample with a reducing agent, is called “total Hcy” (tHcy) and serves as a plasma marker in clinical studies of relationships between Hcy metabolism and human disease [102]. Unfortunately, the term “total Hcy” is a misnomer because it does not include a host of important Hcy congeners (discussed in the following sections). Normal tHcy levels of about 10 μM increase to several hundred μM in genetic deficiencies in Hcy, folate, or vitamin B₁₂ metabolism, both in mice and humans. In normal human plasma, S-Hcy-protein comprises ~80 % of tHcy, homocystine Hcy-S-S-Hcy and homocysteine-cysteine mixed disulfide Hcy-S-S-Cys comprise 20 %, while free thiol Hcy comprises just ~1 % of tHcy (Table 2.1) [87].

In healthy humans, tHcy concentration in plasma (~10 μM) is ~twofold higher than in urine [95]. In mice, however, plasma tHcy (3.5 μM) is 15-fold lower than urinary tHcy (Table 2.1) [93]. While in humans urinary tHcy clearance is insignificant (~1 %), in mice a significant fraction of tHcy (~38 %) is eliminated by urinary excretion [93]. It should be noted, however, that because the reduction of the disulfide bonds in the commonly used tHcy assays is carried out at alkaline pH, one of them—Hcy-thiolactone—most likely contributes to the tHcy pool.

2.1.2 S-Homocysteinyl-Protein

Plasma protein S-linked Hcy is carried on albumin [103] and γ -globulin [79] and in smaller quantities on transthyretin [104, 105], α_1 -acid glycoprotein, and high-density lipoprotein (HDL) [106]. Each of those proteins, except ApoA1 in HDL,

possesses a cysteine residue with free –SH group that is capable of forming a disulfide bond with a low molecular thiol.

In addition to *S*-linked Hcy, albumin, γ -globulin [107–109], transthyretin [104, 105, 110], α_1 -acid glycoprotein, and HDL [106] are known to carry *S*-linked cysteine, CysGly, and glutathione (GSH) *in vivo*. In normal human plasma the concentration of protein *S*-linked Hcy (10 μ M) is lower than the concentration of protein *S*-linked Cys (165 μ M) and CysGly (17 μ M), but higher than the concentration of protein *S*-linked GSH (1.5 μ M) [111]. In erythrocytes the bulk of blood *S*-GSH-protein occurs as *S*-GSH-hemoglobin, which, with a concentration of 130 μ M, comprises 14 % of erythrocyte GSH content [112].

The presence of *S*-Hcy-protein has also been reported in the liver, kidney, and brain tissues from a patient with MTHFR deficiency at autopsy, but not in tissues from three subjects who died of unrelated causes [91]. Much higher levels of *S*-Hcy-protein accumulate in the brain (403.1 pmol/mg protein) than in the liver (76.1 pmol/mg protein) and kidney (55.2 pmol/mg protein) of the MTHFR-deficient patient. The level of liver *S*-Hcy-protein in the MTHFR-deficient patient (76.1 pmol/mg protein) [91] is lower than the level of liver tHcy in *Mthfr*^{-/-} mice (184 \pm 71 μ M, $n = 7$) [113].

In rodents, tHcy concentrations in tissues and plasma are similar, in the micromolar range [114]. Significant pools of Hcy bound to intracellular proteins by disulfide linkages (*S*-Hcy-protein) exist in rodent tissues and plasma [114]. For example, *S*-Hcy-protein comprises ~42 % of tHcy in rat liver, kidney, heart, and lung. In rat cerebrum and cerebellum *S*-Hcy-protein constitutes 30.4 % and 5.3 %, respectively, of tHcy.

2.1.3 Homocysteine-Thiolactone

In normal humans and mice, plasma Hcy-thiolactone concentrations are in the subnanomolar to low nanomolar range, whereas urinary Hcy-thiolactone concentrations are ~100-fold higher (Table 2.1) [93–95]; >95 % of the filtered plasma Hcy-thiolactone is cleared by the kidney [93, 95]. Plasma Hcy-thiolactone is elevated 59- to 237- and 72-fold in human MTHFR and CBS deficiency, respectively, and 14-fold in mice fed with a high methionine diet.

2.1.4 N-Homocysteinyl-Protein

N-linked Hcy is carried on all blood proteins that have been examined, including hemoglobin, albumin, γ -globulin, fibrinogen, transferrin, antitrypsin, LDL, and HDL [79]. In normal human and mouse blood, *N*-Hcy-protein concentrations are in the submicromolar to low micromolar range (Table 2.1) and increase 10–20-fold in genetic or dietary hyperhomocysteinemia [79, 113, 115]. The levels of *N*-Hcy-protein

in mouse liver are 50–160 pmol/mg protein and increase 4- and 12-fold in *Pcft*^{-/-} and *Cbs*^{-/-} animals [113].

2.1.5 Nε-Homocysteinyl-Lysine

The isopeptide *Nε*-Hcy-Lys, discovered in vitro as a product of a facile reaction of Hcy-thiolactone with lysine [73], forms in vivo during proteolytic turnover of *N*-Hcy-protein [72]. *Nε*-Hcy-Lys is undetectable in normal human plasma (<0.1 μM) and increases to 0.17 and 0.42 μM in patients with renal disease and CBS deficiency, respectively. In normal mouse plasma, *Nε*-Hcy-Lys level is 0.4 μM (Table 2.1) and increase up to tenfold in hyperhomocysteinemic animals.

2.1.6 S-Adenosylhomocysteine

AdoHcy, an immediate precursor of Hcy (Fig. 1.1), occurs in human cells at micromolar concentrations, while in plasma, it is present at nanomolar concentrations (Table 2.1) [116, 117]. AdoHcy concentrations are 33-fold higher in human urine than in plasma, consistent with its significant fractional excretion (39 %) [117].

2.1.7 Cystathionine

Normal human plasma level of cystathionine, an intermediate in the transsulfuration pathway converting Hcy to Cys, is 126 nM. Cystathionine concentrations are much higher in urine, reaching millimolar range (Table 2.1). The urinary clearance of cystathionine is 50.9 % of the clearance of creatinine [98]. In mice, normal plasma cystathionine concentration is 2,479 nM [118], 20-fold higher than in normal human plasma.

2.1.8 Homocysteic Acid and Homocysteine Sulfinic Acid

Other oxidized Hcy metabolites have been reported in humans and experimental animals: homocysteine sulfinic acid (HSA) and homocysteic acid (HCA). However, the mechanism of biological formation of HSA and HCA is not known. Normal human plasma concentration is 677 ± 210 nM for HSA and 186 ± 38 nM for HCA (Table 2.1) [99]. Elevation of Hcy and HCA occurs in cerebrospinal fluid of

children after methotrexate treatment [119]. HSA and HCA are both identified in urine from CBS-deficient patients but not in urine from normal individuals [120].

Extremely high HCA concentrations are reported to be present in plasma (up to 23 μM) and in urine (up to 25 mM) of Alzheimer's disease patients, whereas in control individuals, the HCA levels are somewhat lower (by 40 %) [121]. Such HCA concentrations are 100–10,000-fold higher than HCA values reported by other investigators. Unfortunately, Hasegawa et al. [121] do not discuss these discrepancies and give only a very limited experimental detail for their assay, which prevents any rational explanation of their data.

In rats, oral administration of Hcy increases plasma HCA from an undetectable level to 2.0 μM [122]. Methotrexate treatment elevates both HSA and HCA in rat cerebrospinal fluid [123]. HCA is also reported to be present in mouse brain and urine, at 2.3 μM and 22.5 μM , respectively [124].

HCA has been reported to arise by spontaneous oxidation of Hcy [125]. It can also form by the radiolytic degradation of methionine and methionine-containing peptides [126] and from photooxidation of methionine peptides induced by hydrogen peroxide and UV laser light [127]. Analysis of archived samples from a previously unreported 1958 Stanley Miller's origin of life experiment shows that HCA and other sulfur amino acids are generated in spark discharge experiments designed to imitate primordial environments [128]. Prebiotic formation of methionine in spark discharges in a simulated primitive earth atmosphere containing CH_4 , N_2 , NH_3 , H_2O , and H_2S or CH_3SH has been reported in 1972 [129].

2.2 Toxicity of Homocysteine Metabolites

Acute exposure of living cells and organisms to excess Hcy is known to cause cellular toxicity [7, 68]. The presence of multiple molecular Hcy species raises a question regarding whether any of those species could be more harmful than the other. Numerous clinical and animal studies have established that chronic elevation of plasma tHcy is associated with cardiovascular and neurological abnormalities [34, 36, 37], most severely manifested in genetic deficiencies in Hcy (CBS) [20], folate (MTHFR, PCFT) [31, 130], and cobalamin (cblC) [131, 132] metabolism. However, it should be noted that tHcy is a composite marker, comprised of at least five different Hcy species [87, 102], each of which could exert a distinct biological effect. Moreover, tHcy does not encompass other Hcy metabolites present in the human blood, such as Hcy-thiolactone [94, 95], *N*-Hcy-protein [79, 115], *Ne*-Hcy-Lys [72], AdoHcy, cystathionine, and homocysteic acid [68]. Thus, a contribution of an individual Hcy species to cardiovascular risk or mortality is likely to be obscured by using tHcy as a marker [133]. Indeed, in a few studies that addressed this issue, plasma AdoHcy [116] and anti-*N*-Hcy-protein autoantibodies [134, 135] turned out to be much more sensitive indicators of human cardiovascular disease than plasma tHcy.

2.2.1 *Free Reduced Homocysteine*

There is some evidence suggesting that the free thiol Hcy (reduced form) is more harmful than the disulfide Hcy species (oxidized forms). For example, in two studies that examined the toxicity of individual Hcy species, the free thiol Hcy was associated with endothelial dysfunction in humans, whereas much more abundant disulfide Hcy species were not [136, 137]. The toxicity of free thiol Hcy most likely results from its metabolic conversion to Hcy-thiolactone, which occurs in cultured human and rodent cells [68, 73, 77, 138, 139] and in human [64, 76, 94, 95] and mouse bodies [93, 113]. Furthermore, Hcy-thiolactone is known to be more toxic than Hcy to cultured human endothelial cells [61] and to mice [140, 141]. That the metabolic conversion of Hcy to Hcy-thiolactone is responsible for Hcy toxicity is further supported by studies with rat embryos, which show that L-Hcy-thiolactone, D-Hcy-thiolactone, and L-Hcy are toxic, whereas metabolically inactive D-Hcy (which is not recognized by methionyl-tRNA synthetase and thus cannot be metabolized to Hcy-thiolactone) is not [142]. Plasma levels of the free thiol Hcy are maintained low by its oxidation to disulfides, mostly with the major plasma proteins albumin [81, 103] and γ -globulins [79, 106].

2.2.2 *S-Homocysteinyl-Protein*

There is no evidence that any of the disulfide species of Hcy that occur in the plasma is harmful to the human body [143]. In fact, only free reduced Hcy, comprising 1–2 % of tHcy, but not any of the more abundant disulfide forms of Hcy, including S-Hcy-protein, comprising 80 % of tHcy, is associated with diminished vascular function as measured by flow-mediated dilatation [136, 137]. However, that some S-Hcy-proteins may be harmful is suggested by findings showing that treatments of human endothelial cells with in vitro-prepared S-Hcy-ApoB-100 reduce cell proliferation and viability [144].

In a mouse model of dietary hyperhomocysteinemia, Hcy appears to inhibit vascular fibrinolysis in vivo by forming a disulfide bond with annexin A2 thiol [145]. Annexin A2, an endothelial cell surface co-receptor for plasminogen and tissue plasminogen activator, accelerates the catalytic activation of plasmin, the major fibrinolytic agent in mammals. Thus, derivatizing annexin A2 by Hcy contributes to prothrombotic effects of hyperhomocysteinemia [145].

Whether the formation of *intracellular* S-Hcy-protein in humans could be harmful has been addressed in an ex vivo study, which suggests that Hcy binding to metallothionein, an intracellular zinc-binding protein, causes elevation of intracellular free zinc levels and oxidative stress in cultured human endothelial cells treated with exogenous Hcy [146]. Unfortunately, whether the proposed Hcy binding involves a disulfide bond formation with metallothionein has not been confirmed with purified protein. Although these effects were ascribed to the formation of a putative S-Hcy-metallothionein disulfide, the authors' observations that

Hcy binding is not affected by 10 mM glutathione and that cysteine does not form a disulfide with metallothionein [146] suggest that Hcy may bind to metallothionein by another mechanism, possibly *N*-homocysteinylation. In fact, Hcy-thiolactone and protein *N*-linked Hcy are major Hcy species formed in human endothelial cells [74]. Similar to other proteins [78], metallothionein contains numerous lysine residues and is expected to be a target for *N*-homocysteinylation by Hcy-thiolactone.

2.2.3 Homocysteine-Thiolactone

Because of its high solubility, relative stability, and odorless character, Hcy-thiolactone has been often used instead of Hcy to produce experimental hyperhomocysteinemia in animal models. Early studies, beginning in 1974, well before biological significance of Hcy-thiolactone was established, have shown that *chronic* treatments of animals with Hcy-thiolactone cause pathophysiological changes akin to those observed in human genetic hyperhomocysteinemia. For example, continuous Hcy-thiolactone infusions in baboons for 3 months produced patchy desquamation of vascular endothelium, appearance of circulating endothelial cells, and arterial thrombosis [24]. All Hcy-thiolactone-infused animals developed typical arteriosclerotic or preatherosclerotic intimal lesions composed of proliferating smooth muscle cells averaging 10–15 cell layers surrounded by large amounts of collagen, elastic fibers, glycosaminoglycans, and sometimes lipid [147]. (Note: That Hcy-thiolactone has been used in Harker et al.'s experiments [24, 147] is clarified in Mudd et al. [148].) More recent experiments show that Hcy-thiolactone-supplemented diet for 7 weeks produces atherosclerosis in rats [149].

In contrast, rabbits are resistant to the detrimental effects of Hcy-thiolactone infusions [150, 151]. The inability to generate atherosclerosis in rabbits is most likely due to their high levels of serum Hcy-thiolactonase/PON1, ~tenfold higher than in humans or other animals. Thus, rabbits turn over serum Hcy-thiolactone much more efficiently than other animals [81, 152, 153]. Hcy-thiolactone infused into rabbits is quickly cleared from the blood (within <15 min) [150].

Chronic treatments with Hcy-thiolactone cause developmental abnormalities in chick embryos [154]. Remarkably, these abnormalities include optic lens dislocation [155] that is identical to the ocular phenotype (ectopia lentis) prevalent in human CBS deficiency [20, 29, 30]. This finding suggests that ectopia lentis is caused by elevations of Hcy-thiolactone that are in fact observed in CBS-deficient patients [93].

Acute treatments with Hcy-thiolactone are also known to cause toxicity in experimental animals. For example, intraperitoneal infusions of Hcy-thiolactone into mice or rats, which are used as a model to study mechanisms of epilepsy, cause seizures and death within minutes [156–159]. Exposure of mouse [160] or rat [142] embryos to Hcy-thiolactone causes lethality, growth retardation, and

developmental abnormalities. In one study Hcy-thiolactone was reported to be non-teratogenic in mouse embryos, but the maximum dose used in that study [160] was lower than those used in other studies, so that a teratogenic dose has not been reached.

Rigorous studies in mice using the intraperitoneal injection model show that plasma Hcy-thiolactone is cleared with a half-life of 5.0 min [140, 141]. Studies with *Blmh*^{-/-} and *Pon1*^{-/-} mouse models that have diminished ability to hydrolyze Hcy-thiolactone led to a conclusion that bleomycin hydrolase (*Blmh*) and paraoxonase 1 (*Pon1*) protect the animals against neurotoxicity induced by intraperitoneal injections of L-Hcy-thiolactone [140, 141]. Similar to other harmful products of normal metabolism, endogenous Hcy-thiolactone is also eliminated by urinary excretion, as demonstrated both in humans and mice [93, 95].

Treatments with Hcy-thiolactone inhibit proliferation and can be toxic to cultured human and animal cells [143]. For instance, short-term pretreatment (10 min) of cultured rat hepatoma cells with Hcy-thiolactone leads to the inhibition of insulin signaling by preventing tyrosine phosphorylation of the β -subunit of the insulin receptor and its substrates IRS-1 and Sam68 [161]. Furthermore, pretreatment with Hcy-thiolactone inhibits the interactions of the insulin receptor β -subunit and its substrates with the regulatory subunit p85 of phosphatidylinositol 3-kinase, which in turn inhibits the kinase and blocks the insulin-stimulated glycogen synthesis [161]. Hcy-thiolactone also prevents phosphorylation of GSK-3 and p70S6K catalyzed by mitogen-activated protein kinase, as well as insulin-mediated growth and proliferation [162]. The addition of GSH 5 min before the pretreatment with Hcy-thiolactone restores insulin signaling, suggesting that Hcy-thiolactone-induced oxidative stress might be involved [161, 162]. Much longer (24 h) treatments with higher Hcy concentrations (0.1–1 mM) induce insulin resistance by reducing tyrosine phosphorylation of insulin receptor and IRS-1 in rat adipocytes [163]. Treatments with 0.3–1 mM Hcy (lower concentration is ineffective) also induce resistin, a peptide hormone linked to insulin resistance, after 8–24 h (no induction after 4 h) [163]. Taken together, these findings suggest that Hcy-thiolactone is more effective than Hcy in inducing insulin resistance in cultured cells and thus is likely to contribute of insulin resistance associated with hyperhomocysteinemia in humans and experimental animals.

Hcy-thiolactone is also known to induce endoplasmic reticulum (ER) stress and unfolded protein response (UPR) in retinal epithelial cells [60], as well as apoptotic death in cultured human vascular endothelial cells [61, 164], promyeloid cells [165], and placental trophoblasts [166]. For example, human umbilical vein endothelial cells (HUVECs) treated with 50–200 μ M D,L-Hcy-thiolactone for 24 h show 15–40 % apoptotic cell death quantified after labeling with the fluorescent probe DiOC6(3) and flow cytometry analysis (Table 2.2) [154]. The magnitude of apoptosis in HUVECs treated with 200 μ M D,L-Hcy-thiolactone corresponds to about 2/3 of apoptosis observed in the cells treated with 5 μ g/mL staurosporine or serum-free medium as positive controls (Table 2.2). In contrast to apoptosis induced by staurosporine, apoptotic cell death induced by Hcy-thiolactone in HUVECs is not accompanied by the induction of caspase activity and is not prevented by caspase

Table 2.2 Hcy-thiolactone induces apoptosis in human endothelial cells (adapted from [154])

Treatment (24 h, 37 °C)	Apoptotic cells (%)
D,L-Hcy-thiolactone (200 μM)	30 ± 5
D,L-Homocysteine (200 μM)	1 ± 2
D,L-Homocystine (200 μM)	3 ± 4
L-Cysteine (200 μM)	4 ± 2
Staurosporine (5 μg/mL) (positive control)	58 ± 20

Confluent human umbilical vein endothelial cells (HUVECs) in complete M199 growth medium are treated with indicated thiocompounds or staurosporine. The cells are labeled with the fluorescent probe DiOC₆(3) (10 μg/mL) and analyzed by flow cytometry to quantify apoptotic cells

inhibitors. However, the cell death induced by Hcy-thiolactone is accompanied by phosphatidylserine exposure in cell membranes, characteristic of apoptosis [154]. Control experiments show that 200 μM D,L-Hcy, D,L-homocystine, or L-Cys do not induce apoptosis in HUVECs (Table 2.2), thus indicating that the induction of apoptosis is specific to D,L-Hcy-thiolactone. However, Hcy-thiolactone does not induce apoptosis in transformed cell lines such as HL60 leukemic cells and EA.hy 926 endothelial cells, indicating that the sensitivity to Hcy-thiolactone is cell type dependent [154].

Although the treatment with Hcy, similar to the treatment with Hcy-thiolactone, induces apoptosis, much higher Hcy concentrations are required [58, 61], suggesting that Hcy-thiolactone is more potent than Hcy in causing apoptotic cell death [60, 61, 164]. These findings confirm early studies in which treatments with Hcy-thiolactone caused greater cytotoxicity to endothelial cells than treatments with Hcy [167]. In those studies the toxicity of Hcy-thiolactone is manifested as gross changes in endothelial cell morphology and lysis of 42 % cells during a 16-h exposure. Similar exposure to Hcy produces no changes in cell morphology and only 2 % cell lysis [167].

2.2.4 N-Homocysteinyl-Protein

Plasma N-Hcy-protein levels are elevated in patients with CBS or MTHFR deficiency [115], or coronary artery disease (CAD) patients, compared with normal healthy individuals [168]. Preponderance of evidence links N-Hcy-protein with the pathology of these diseases. As will be discussed in a greater detail in the following sections of this book, N-Hcy-protein is harmful because of its ability to induce inflammation [169], cell death [170, 171], and an autoimmune response [134, 135, 172, 173] and to interfere with blood clotting [174, 175].

2.2.5 *Nε-Homocysteinyl-Lysine*

There is no direct evidence that *Nε*-Hcy-Lys is toxic. However, similar to other Hcy metabolites, *Nε*-Hcy-Lys levels are elevated under pathological conditions, such as human CBS deficiency, renal disease, cardiovascular disease, as well as in *Cbs*^{-/-} and *Mthfr*^{-/-} mice [72, 86]. Plasma *Nε*-Hcy-Lys levels are higher in mice than in humans, most likely reflecting higher Hcy-thiolactone [93] and protein *N*-linked Hcy [113] levels in mice compared with humans.

2.2.6 *S-Adenosylhomocysteine*

Experimental evidence suggests that the accumulation of AdoHcy could be harmful. For example, treatments with Hcy and adenosine deaminase inhibitors elevate intracellular AdoHcy and inhibit cell growth in cultured human endothelial cells [176]. Human uremic patients have hyperhomocysteinemia and elevated AdoHcy levels. The elevated AdoHcy exerts epigenetic effects on gene expression by interfering with cellular methylation reactions and changing DNA methylation patterns in peripheral mononuclear cells [177]. Folate therapy, a common method to reduce hyperhomocysteinemia, lowers AdoHcy, restores DNA methylation to normal levels, and corrects the patterns of gene expression. Plasma AdoHcy is highly correlated with plasma tHcy, whereas increased plasma and lymphocyte AdoHcy levels are associated with decreased DNA methylation [177, 178]. Furthermore, an increase in plasma AdoHcy is a much more sensitive indicator of human cardiovascular disease than an increase in plasma tHcy [116].

In mice, effects of elevated AdoHcy on DNA methylation appear to be tissue specific. *Cbs*^{+/-} mice fed with a high-methionine diet develop hyperhomocysteinemia, elevated levels of AdoHcy, and lower AdoMet/AdoHcy ratios ($p < 0.001$) in the liver and brain [179]. Plasma tHcy correlates positively with AdoHcy in most tissues, except the kidney [180], and negatively with DNA methylation, as one would expect, in the liver. On the other hand, paradoxical *increases* in DNA methylation occur in the brain and the aorta of hyperhomocysteinemic animals [179].

Methylation patterns of the imprinted genes H19 and insulin-like growth factor 2 (Igf2), important for their regulation, are affected by hyperhomocysteinemia in a tissue-specific manner. For example, hyperhomocysteinemic *Cbs*^{+/-} mice have decreased H19 methylation in the liver, whereas in the brain increased H19 methylation and decreased ratios of H19/Igf2 transcripts are observed. In the aorta, hyperhomocysteinemia produces an increase in H19 methylation and a 2.5-fold increase in expression of H19 transcripts. Levels of H19 transcripts in aorta correlate positively with plasma tHcy concentration. These findings suggest that factors other than the methylation capacity can influence DNA methylation patterns.

2.2.7 *Cystathionine*

There is no indication that cystathionine is toxic [20]. Although it accumulates under pathological conditions, such as cystathionase deficiency or cancer, cystathionine seems to be benign. However, the *lack* of cystathionine synthesis has been shown to be responsible for liver steatosis and kidney injury in mouse models [181].

2.2.8 *Homocysteic Acid*

HCA is an analog of the neurotransmitter glutamate. Because of this, HCA is a selective agonist of glutamate receptors [182]. In tissue cultures, supplementation with HCA is toxic to human [183] and animal [184] neuronal cells.

Elevation of HCA from undetectable levels to $119 \pm 20 \mu\text{M}$ that occurs in cerebrospinal fluid of children after methotrexate treatment is associated with neurological toxicity [119]. Persistent cognitive deficits in rats are induced by intrathecal methotrexate treatment and are associated with elevated concentrations of HCA (and HSA) in the cerebrospinal fluid [123]. These deficits are reversed by intraperitoneal injections of dextromethorphan, a noncompetitive antagonist of the *N*-methyl-D-aspartate receptor (NMDA). These findings are consistent with a known agonist role of HCA at glutamate receptors. Overstimulation of the NMDA receptor by HCA has been suggested to contribute to the central nervous system pathology observed in patients with homocystinuria [185]. Consistent with this suggestion, HCA is present in homocystinuric patients (at $\sim 7 \mu\text{M}$ in plasma [186] and in urine [120]). However, it is not known whether HCA accumulates in CNS of these patients.

Chapter 3

Homocysteine-Thiolactone

3.1 Chemical Synthesis

3.1.1 Demethylation of Methionine

Hcy-thiolactone was discovered by serendipity in 1934 as a by-product of an early assay for the quantification of methionine in proteins [187]. The assay involves boiling with hydriodic acid (128 °C, 3 h). This causes demethylation of methionine with the formation of methyl iodide, whose quantitative recovery ($99.5 \pm 2.0 \%$) by absorption in alcoholic solution of silver nitrate was the basis of the methionine assay. The residue from methionine that remains in the acid has been identified by elemental analysis as Hcy-thiolactone. The recovery of Hcy-thiolactone from methionine digestion is also quantitative ($97.0 \pm 2.1 \%$) [187].

Recent studies have found that during hydriodic acid digestion, L-methionine is racemized to D,L-Hcy-thiolactone (Reaction 3.1 and Fig. 3.1). Although no longer used as a methionine assay, the hydriodic acid digestion procedure became a convenient method for the preparation of D,L-[³⁵S]Hcy-thiolactone for biological studies [188]. Enzymatic digestion with bleomycin hydrolase (which exhibits essentially absolute stereoselectivity for L-Hcy-thiolactone) [85] resolves racemic D,L-[³⁵S]Hcy-thiolactone to L-[³⁵S]Hcy and D-[³⁵S]Hcy-thiolactone (Fig. 3.1) [188].

In contrast to hydriodic acid, the digestion with hydrochloric acid is ineffective in demethylation of methionine [3]. For example, during incubation with 6 N HCl at 135 or 120 °C, the rate of conversion of methionine to Hcy-thiolactone is 1,000- and 10,000-fold slower than that observed with hydriodic acid [79]. Concentrated sulfuric acid (18 N) also causes demethylation of methionine at 125–135 °C. However, due to oxidative properties of sulfuric acid, homocystine (in 42.5 % yield) is obtained in this case [3].

Reaction 3.1 The hydriodic acid-dependent conversion of methionine to Hcy-thiolactone (Reprinted from [68])

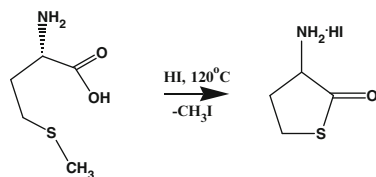
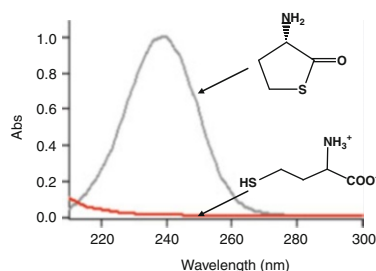


Fig. 3.1 Absorption spectra of L-Hcy-thiolactone-HCl (0.2 mM in water, 25 °C). D,L-Hcy (0.2 mM), shown for comparison, does not appreciably absorb UV light above 220 nm (Reproduced from [68])



3.1.2 Acid-Dependent Cyclization of Homocysteine

In the presence of hydrochloric acid, L-Hcy undergoes intramolecular condensation to L-Hcy-thiolactone (Reaction 3.2) [4]. The rate of ring closure depends on the acid concentration and temperature. For example, in 0.1 N, 0.6 N, or 6 N hydrochloric acid at 100 °C, 50 % of ring closure condensation occurs in 3 h, 15 min, or <5 min, respectively [68]. Because Hcy-thiolactone, in contrast to Hcy, absorbs ultraviolet light (Fig. 3.2), the conversion to Hcy-thiolactone has been exploited in the first spectrophotometric assay for Hcy [189]. The acid-dependent conversion to Hcy-thiolactone followed by its quantification by high-performance liquid chromatography (HPLC) is now used as a convenient procedure for the determination of Hcy in biological samples [64, 79, 93–95, 190].

3.2 Physicochemical Properties

3.2.1 UV Spectrum

Differences in physicochemical properties of Hcy-thiolactone and Hcy are highlighted in Table 3.1. Similar to other thioesters, Hcy-thiolactone absorbs ultraviolet light with a maximum at 240 nm and $\epsilon = 5,000 \text{ M}^{-1}\text{cm}^{-1}$ in water (Fig. 3.2) [68]. The ability to absorb at 240 nm is also a characteristic property of a deprotonated sulfhydryl group [191, 192]. Monitoring absorbance at 240 nm facilitates studies of nucleophilic [73] and electrophilic [84] reactions involving Hcy-thiolactone as well as quantification of Hcy-thiolactone in biological samples [64, 67, 190, 193, 194].

Reaction 3.2 The hydrochloric acid-dependent conversion of Hcy to Hcy-thiolactone (Reprinted from [68])

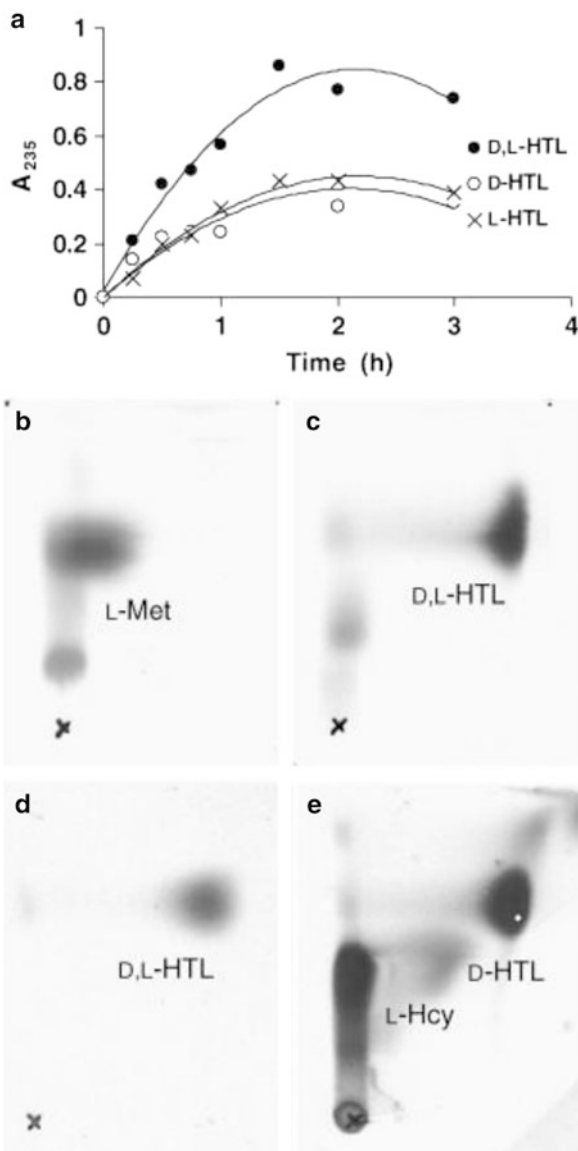
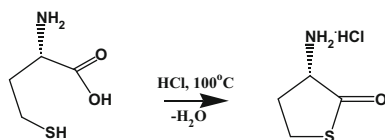
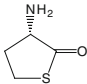
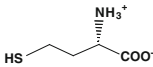


Fig. 3.2 Synthesis of D,L-Hcy-thiolactone and its enantiomeric resolution (with HTL representing Hcy-thiolactone in the figure). (a) Time course of the synthesis of D,L-Hcy-thiolactone from L-Met. Here 30- μ l aliquots of 0.1 M L-Met in 57 % hydriodic acid/1 % hypophosphorous acid

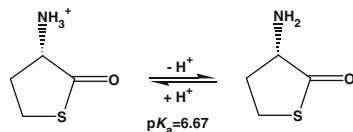
Table 3.1 Physical–chemical properties of L-Hcy-thiolactone and L-Hcy [68]

Property	L-Hcy-thiolactone 	L-Hcy 
Chemical character	Aminoacyl-thioester	Mercapto amino acid
UV spectrum	Yes, $\lambda_{\max} = 240 \text{ nm}$, $\epsilon = 5,000 \text{ M}^{-1} \text{ cm}^{-1}$	No significant absorption at $\lambda > 220 \text{ nm}$
Stability at 37 °C, $t_{0.5}$		
Phosphate-saline	~30 h	~2 h
Human serum	~1 h	~2 h
pK_a of amino group	6.67 ^a	9.04, 9.71 ^b 9.02, 9.69 (thiol group) ^b
Chemical reactivity	<ul style="list-style-type: none"> – Acylates amino groups of protein lysine residues^c – Reacts with aldehydes to afford tetrahydrothiazines^a – Resistant to oxidation – Base-hydrolyzed to Hcy 	<ul style="list-style-type: none"> – Condenses to form Hcy-thiolactone – Reacts with aldehydes to afford tetrahydrothiazines^a – Oxidized to disulfides – Reacts with nitric oxide to afford S-nitroso-Hcy^d

^a[84]^b[463]^c[73, 78]^d[75–77]

Fig. 3.2 (continued) (Sigma-Aldrich) were incubated in 1-ml ampoules (Wheaton) at 128 °C. Reaction mixtures were lyophilized and dissolved in 0.15 mL of 0.15 M K_2HPO_4 , and Hcy-thiolactone was extracted with 5 volumes of a chloroform/methanol (2:1, v/v) mixture. Hcy-thiolactone, recovered from the organic phase (0.6 mL) by re-extraction with 0.15 mL of 0.1 N HCl, was lyophilized and dissolved in 80 μL of water. An 8- μL aliquot of each sample was buffered with 3 μL of 0.5 M Na_2HPO_4 and treated with bleomycin hydrolase (1 μL of 100 μM solution) for 30 min at 25 °C. Bleomycin hydrolase-treated and bleomycin hydrolase-untreated samples were diluted with 0.5 mL of water, and Hcy-thiolactone was quantified by measuring absorbance at 235 nm (*filled circle*). L-Hcy-thiolactone (*open circle*) and D-Hcy-thiolactone (*multiplication sign*) stereoisomers were distinguished by their susceptibility and resistance, respectively, to enzymatic hydrolysis by bleomycin hydrolase. **(b–e)** two-dimensional thin-layer chromatography analyses of the L-[³⁵S]Met/hydriodic acid digestion mixtures. **(b)** L-[³⁵S]Met before digestion. **(c)** Crude D,L-[³⁵S]Hcy-thiolactone obtained by digestion of L-[³⁵S]Met (4 h, 128 °C). **(d)** Purified D,L-[³⁵S]Hcy-thiolactone preparation. **(e)** Treatment with bleomycin hydrolase resolves D,L-[³⁵S]Hcy-thiolactone to L-[³⁵S]Hcy and D-[³⁵S]Hcy-thiolactone. Autoradiograms of the two-dimensional thin-layer chromatography plates (6.7 cm × 5.0 cm) are shown. Origin (marked with *multiplication sign*) is at the *lower left corner*, the first dimension is from bottom to top, and the second dimension is from left to right (Reproduced from [188])

Reaction 3.3 Acid and base forms of Hcy-thiolactone
(Reprinted from [84])



3.2.2 pK_a value

The α -amino group of Hcy-thiolactone has an unusually low pK_a value of 6.67 [84], much lower than a corresponding value for Hcy ($pK_a = 9.04$ and 9.71) (Table 3.1) [192]. The lowering of pK_a of an α -amino group upon esterification of a carboxyl group is a characteristic property of other α -amino acid esters such as leucine methyl ester, leucyl-tRNA ($pK_a = 7.8$, [195]), or valyl-tRNA ($pK_a = 7.5$, [196]), but the magnitude of the effect is less than that observed for Hcy-thiolactone.

Under physiological conditions Hcy-thiolactone exists as a neutral base form (Reaction 3.3), while α -amino group of Hcy exists in a positively charged acid form. Because of this Hcy-thiolactone can freely diffuse through cell membranes. In fact, in cell cultures, most of Hcy-thiolactone produced inside cells is found extracellularly in culture media [63, 64, 67, 73, 74, 138, 190, 193, 194, 197], while in humans and mice, most of Hcy-thiolactone produced in tissues accumulates in the urine [93, 95].

3.2.3 Stability

The hydrochloric acid salt of Hcy-thiolactone is odorless and stable; it can be stored at room temperature essentially indefinitely. In contrast, Hcy has a pungent sulfhydryl odor, is less stable, and has to be stored in a freezer at -20 °C. In solutions at physiological conditions (pH 7.4, 37 °C), the intramolecular thioester Hcy-thiolactone has a half-life of ~ 25 h [73, 198] and is substantially more stable than intermolecular aminoacyl-thioesters, such as methionyl-S-CoA, which hydrolyzes with a half-life of 2.25 h [199]. The hydrolysis of Hcy-thiolactone to Hcy is much faster in alkaline solutions. For example, in 0.1 M NaOH, Hcy-thiolactone hydrolysis is completed in 15 min at room temperature [75, 200].

The rate of Hcy-thiolactone hydrolysis depends on the ionization status of its α -amino group (Fig. 3.3a) [84]. The positively charged acid form of Hcy-thiolactone is hydrolyzed 186 times faster than the neutral base form (Table 3.2). Different susceptibilities to hydrolysis of different ionic forms are characteristic of other esters: for instance, the fully protonated form of valyl-tRNA is hydrolyzed 90 times faster than the un-protonated form [196].

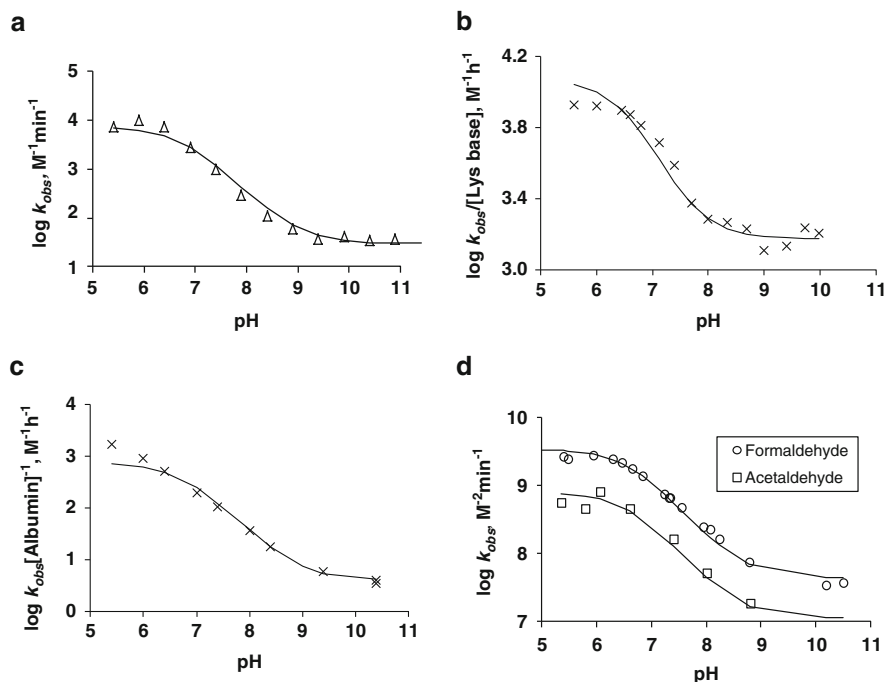


Fig. 3.3 Effects of pH on reactions of Hcy-thiolactone with electrophiles and nucleophiles. Panel (a), pH dependence of the second-order rate constant for the hydrolysis of Hcy-thiolactone ($k = k_{obs}[\text{OH}^-]^{-1}$). Panel (b), pH dependence of the pseudo-first-order rate constant for the reaction of Hcy-thiolactone with lysine ($k = k_{obs}[\text{Lys base}]^{-1}$). Panel (c), pH dependence of the pseudo-first-order rate constant for the reaction of Hcy-thiolactone with human serum albumin ($k = k_{obs}[\text{Albumin}]^{-1}$). Panel (d): pH dependences of the third-order rate constants ($k = k_{obs}[\text{OH}^-]^{-1}[\text{aldehyde}]^{-1}$) of the reactions of HTL with formaldehyde (*open circle*) and acetaldehyde (*open square*). The *solid lines* in each panel are theoretical lines for the reactions of acid and base Hcy-thiolactone forms calculated from the equation $k = (k_{HTL^+})(1-\alpha) + (k_{HTL^0})\alpha$, where α is the fraction of Hcy-thiolactone in the base form, calculated at indicated pH using a $pK_a = 6.67$. Panels (a) and (d)—reproduced with permission from [84]; panels (b) and (c)—H. Jakubowski, unpublished data

Table 3.2 Apparent rate constants, k , for reactions of base (HTL^0) and acid (HTL^+) forms of Hcy-thiolactone with aldehydes, hydroxide anion [84], free lysine base, and human serum albumin (H. Jakubowski, unpublished data)

Reactants	k_{HTL^0}	k_{HTL^+}
HCHO, OH^-	$44 \times 10^6 \text{ M}^{-2} \text{ min}^{-1}$	$3.5 \times 10^9 \text{ M}^{-2} \text{ min}^{-1}$
CH_3CHO , OH^-	$11 \times 10^6 \text{ M}^{-2} \text{ min}^{-1}$	$0.8 \times 10^9 \text{ M}^{-2} \text{ min}^{-1}$
OH^-	$37 \text{ M}^{-1} \text{ min}^{-1}$	$6.9 \times 10^3 \text{ M}^{-1} \text{ min}^{-1}$
Lysine base	$1,500 \text{ M}^{-1} \text{ min}^{-1}$	$11,900 \text{ M}^{-1} \text{ min}^{-1}$
Albumin	$4 \text{ M}^{-1} \text{ min}^{-1}$	$765 \text{ M}^{-1} \text{ min}^{-1}$

Kinetics of the reactions with lysine and albumin are linear, whereas nonlinear kinetics are observed for the reactions with aldehydes

3.2.4 Reactivity Toward Amino Groups

Well before biological relevance of Hcy-thiolactone has been established, it was recognized that “the S-C bond of homocysteine thiolactone is that of a thioester, and its reactivity, particularly in the peptide bond formation, deserves investigation” [201]. Early studies have shown that at alkaline pH values, Hcy-thiolactone in concentrated solutions (0.1–1 M) reacts with itself to form *N*-homocysteinyl-Hcy-thiolactone, which then converts to diketopiperazine of homocysteine, which in turn oxidizes to insoluble polymeric adducts [202]. (These reactions do not occur in diluted Hcy-thiolactone solutions.) To prevent these reactions, Hcy-thiolactone was acetylated with acetic acid anhydride, and the resulting *N*-acetyl-Hcy-thiolactone was used in studies of its reactivity toward amines. In 1956 it was found that *N*-acetyl-Hcy-thiolactone can react with amines and amino acids in alkaline solutions (pH > 9) with the formation of a peptide bond [203]. In 1960s, a few studies examined the reactivity of *N*-acetyl-Hcy-thiolactone with a goal of introducing sulfhydryl groups into proteins [204]. However, because *N*-acetyl-Hcy-thiolactone is much less reactive than Hcy-thiolactone, these studies required long reaction times, relatively high pH [205], or the presence of silver ions as a catalyst [205, 206]. Nevertheless, *N*-acetyl-Hcy-thiolactone has been used to introduce a thiol functionality into small molecules and macromolecules, including aminoglycosides, amino lipids, muramyl dipeptide, cell-surface carbohydrates, human serum albumin, lactoglobulin, enzymes, and oligonucleotides for a variety of applications [207]. Another Hcy-thiolactone congener, γ -thiobutyrolactone, is used in the synthesis of pH-responsive polymeric hydrogels for biomedical applications [208].

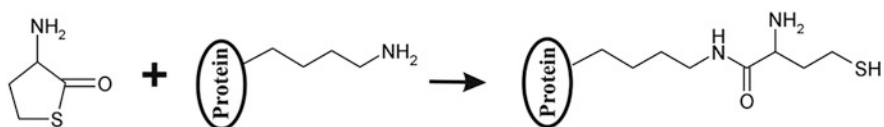
For example, a report published in 1991 describes the modification with *N*-acetyl-Hcy-thiolactone as a facile method to introduce a thiol group at the 5'-end of an oligonucleotide, which, in contrast to other methods, does not require the deprotection step [209]. An oligonucleotide is synthesized using the phosphoramidite method, and an amino group is introduced using the amino modifier II. The oligo is purified and reacted with 5 mg of *N*-acetyl-Hcy-thiolactone in 0.5 mL pH 8 phosphate buffer for 3 h, after which the reaction is >95 % complete. The thiol-substituted oligonucleotide is then labeled with a thiol-specific reagent, such as *N*-(4-dimethylaminoazobenzene-4')-iodoacetamide or fluorescent *N*-(3-prenyl)-maleimide. In this way, oligonucleotides containing a desired dye are prepared. The presence of the dye attached to an oligonucleotide is confirmed by UV/vis and fluorescence spectral analyses [209].

Strong incentives to examine the reactions of Hcy-thiolactone with proteins under physiological conditions appeared in 1990s after Hcy-thiolactone has been discovered in living cells and the mechanism of its biological formation elucidated [63, 138, 197, 210] and when elevated Hcy has been recognized as a risk factor for cardiovascular and neurodegenerative diseases [211]. Subsequent studies demonstrate that the thioester bond of Hcy-thiolactone is highly susceptible to reactions with nucleophiles under physiological conditions, particularly with the side chain amino group of protein lysine residues (Table 3.3). For example, at pH 7.4 and

Table 3.3 Second-order rate constants, k , for reactions of Hcy-thiolactone with proteins and lysine derivatives (pH 7.4)

Protein (kDa) or lysine derivative	k at 25 °C ($M^{-1} h^{-1}$)	k at 37 °C ($M^{-1} h^{-1}$)
α_2 -Macroglobulin (725)	400	
Low-density lipoprotein (500)	150	
Fibrinogen (340)	101	
γ -Globulin (140)	112	
Transferrin (80)	150	560
Albumin (68)	128	466
Hemoglobin (64)	84	600
MetRS (64)	60	
α -Crystallin (36)	10	
DNase I (37)	9	
Trypsin (24)	9	
Myoglobin (16)	40	
Cytochrome c (12.5)	36	150
RNase A (12.5)	3	
Poly-Lys (150)		6,700
LysLys		26
LysAla		3
Lysine	1	5
α - <i>N</i> -acetyl-lysine		3.8
ϵ - <i>N</i> -acetyl-lysine		1.2

Linear kinetics observed in a wide range of reagent concentrations (compiled from [78, 84])

**Reaction 3.4** Chemical modification of a protein lysine residue by Hcy-thiolactone (Reprinted from [68])

temperature 37 °C, Hcy-thiolactone modifies proteins by forming *N*-Hcy-protein adducts, in which Hcy is *N*-linked to the ϵ -amino group of protein lysine residues as shown in Reaction 3.4 [68, 73, 78]. Other amino acid side chain groups in protein do not appreciably react with Hcy-thiolactone. Indeed, *N*-linked Hcy is found in albumin [78, 96, 212, 213], hemoglobin [214], fibrinogen [116, 215], and cytochrome c [136] only on lysine residues. In proteins, the reactivity of side chain lysine ϵ -amino residues is much greater than the reactivity of the *N*-terminal amino group [78]. In free lysine, the ϵ -amino group exhibits threefold greater reactivity with Hcy-thiolactone than the α -amino group of lysine (second-order rate constants, $k_{\text{obs}}/[\text{Lys}]$, are $3.8 M^{-1} h^{-1}$ and $1.2 M^{-1} h^{-1}$, respectively, at pH 7.4; Table 3.3). These studies were facilitated by the availability of radiolabeled [^{35}S]Hcy-thiolactone of high specific activity [78], prepared as illustrated in Fig. 3.2.

The characteristic UV absorption at 240 nm disappears during the reaction of Hcy-thiolactone with amines, which facilitates studies of the *N*-homocysteinylation reaction. The rate of Hcy-thiolactone reaction with lysine at pH 7.4, measured spectroscopically at 240 nm, is first order with respect to both Hcy-thiolactone and lysine. The rate increases with increasing pH, consistent with the lysine base form (with uncharged amino groups) being the reacting species. The second-order rate constant's dependence on pH (Fig. 3.3b) is consistent with ionization of Hcy-thiolactone with $pK_a = 6.67$ and suggests that the positively charged acid form of Hcy-thiolactone is more reactive with lysine ($k_{\text{obs}}/[\text{Lys base}] = 11,870 \text{ M}^{-1} \text{ h}^{-1}$) than the neutral base form ($k_{\text{obs}}/[\text{Lys base}] = 1,500 \text{ M}^{-1} \text{ h}^{-1}$) (Table 3.2). The reaction of Hcy-thiolactone with purified human serum albumin exhibits similar pH dependence (Fig. 3.3c) and indicates that the acid form of Hcy-thiolactone is 191-fold more reactive with the protein than the base form (764.0 vs. $4.0 \text{ M}^{-1} \text{ h}^{-1}$, Table 3.2).

3.2.5 Reactivity Toward Carbonyl Compounds

The α -amino group of Hcy-thiolactone is highly reactive toward electrophiles, such as formaldehyde, acetaldehyde, pyridoxal phosphate, *o*-phthalaldehyde, or streptomycin (Tables 3.2 and 3.4) [68, 84]. Corresponding 1,3-tetrahydrothiazine-4-carboxylic acids are formed as products of these reactions (Reaction 3.5) [84]. The rate of condensation of Hcy-thiolactone with a large molar excess of formaldehyde or acetaldehyde, measured spectrophotometrically at 240 nm, is first order with respect to Hcy-thiolactone. The dependence of the pseudo-first-order rate constant on aldehyde concentration is more complex: at low concentration of aldehyde, the rate constant increases linearly with the aldehyde concentration, but at high concentrations, the rates level off and are less dependent on aldehyde concentration. Such kinetic behavior indicates formation of an intermediate (Reaction 3.5). A similar reaction between the α -amino group of Hcy-thiolactone and the tyrosylquinone cofactor of lysine oxidase in vitro causes irreversible inactivation of the enzyme [216].

Changes in pH affect the ionization status of the α -amino group of Hcy-thiolactone and the rate of its reaction with aldehydes (Fig. 3.3d). For example, the positively charged acid form of Hcy-thiolactone reacts with formaldehyde and acetaldehyde 79 and 73 times faster, respectively (Table 3.2), than the neutral base form (structures of the acid and base forms are shown in Reaction 3.3) [84]. At physiological pH = 7.4, second-order rate constants for the reaction with aldehydes are $1,200\text{--}8,648 \text{ M}^{-1} \text{ h}^{-1}$ (Table 3.4) more than 200 times faster than for the reaction of Hcy-thiolactone with lysine (Table 3.3).

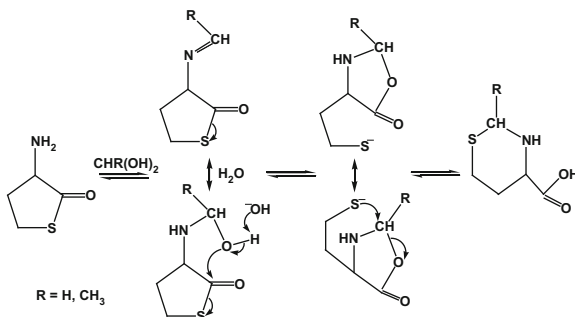
The facile formation of tetrahydrothiazines from Hcy-thiolactone and aldehydes (Reaction 3.5) raises an interesting possibility that the endogenous Hcy-thiolactone formed in the human body may be inactivated and disposed of in the form of

Table 3.4 Second-order rate constants, k , for reactions of Hcy-thiolactone with aldehydes

Aldehyde	k at 25 °C ($M^{-1} h^{-1}$)
Formaldehyde ^a	8,648
Acetaldehyde ^a	2,496
Streptomycin ^b	1,200 (2,000 at 37 °C)

^aData recalculated from [84]. Nonlinear kinetics observed suggest the formation of an intermediate

^bH. Jakubowski, unpublished data



Reaction 3.5 The mechanism for the formation of 1,4-tetrahydrothiazine from Hcy-thiolactone and formaldehyde ($R=H$) or acetaldehyde ($R=CH_3$). The initial product of the reaction of Hcy-thiolactone with aldehydes is carbinolamine in a chemical equilibrium with imine. The formation of the carbinolamine greatly destabilizes the thioester bond by facilitating anchimeric assistance by the carbinolamine group, which makes possible an intramolecular attack of the oxygen on the thioester bond to form a five-membered lactone. This leads to the liberation of the thiolate group. Subsequent attack of the thiolate on an aldehyde-derived carbon leads to rapid formation of the six-membered ring of the tetrahydrothiazine and lysis of the lactone (Reprinted from [84])

metabolically inactive tetrahydrothiazine via the kidneys. This possibility is supported by findings showing that acetaldehyde [217] and other aldehydes are formed in the human body [218] and that in rats injected intraperitoneally with radiolabeled 1,3-tetrahydrothiazine-4-carboxylic acid, 55 % of the administered compound is excreted in the urine and only 6 % is expired as carbon dioxide [219]. However, to what extent the formation of tetrahydrothiazines contributes to metabolic flows of sulfur-containing amino acids in animals and humans remains to be examined.

The reaction of Hcy-thiolactone with *o*-phthalaldehyde (OPA), generating a fluorescent adduct, is exploited in sensitive assays for Hcy-thiolactone quantification. For example, Hcy-thiolactone separated by HPLC on a cation exchange column is quantified by monitoring fluorescence after post-column derivatization with OPA/NaOH [93–95]. An alternative method involves HPLC on a reversed-phase C18 column, on-column derivatization using an OPA-containing solvent, and quantification by fluorescence [220] (see the following section).

3.3 Quantification Methods

3.3.1 Assays Based on Radiolabeling

The discovery that Hcy-thiolactone is formed biologically in living cells relied on the use of radiolabeled precursors such as [³⁵S]sulfate [63], [³⁵S]cysteine [197], [³⁵S]methionine [73, 138], and [³⁵S]homocysteine [73, 74] as tracers. After incubating cultured cells with any of those precursors, the labeled media and cells are collected separately. The labeled cells are extracted with formic acid. [³⁵S]Hcy-thiolactone is separated from other [³⁵S]-labeled metabolites present in cell extracts and culture media by two-dimensional thin-layer chromatography (TLC) using as little as 5 μ L sample and cellulose or silica gel plates as small as 5 cm \times 4 cm. The first-dimension solvent is butanol/acetic acid/water (4/1/1, v/v), while isopropanol/ethyl acetate/water/ammonia (12/12/1/0.12, v/v) is the second-dimension solvent. [³⁵S]Hcy-thiolactone is visualized by autoradiography using Kodak BioMax X-ray film and quantified by scintillation counting. An illustration of the two-dimensional TLC separation of the radiolabeled Hcy-thiolactone is shown in Fig. 3.1. The radiolabeling methods have an excellent reproducibility and sensitivity (allowing detection of <100 femtomoles of Hcy-thiolactone) and have been used extensively to elucidate Hcy-thiolactone metabolic pathways in microorganisms such as *Escherichia coli* [193, 197] and the yeast *Saccharomyces cerevisiae* [63, 221], plants [190], as well as in a variety of cultured human and rodent cells [73, 74, 138].

3.3.2 Assays Based on Direct UV Monitoring

Similar to other thioesters [189], Hcy-thiolactone absorbs ultraviolet light with the maximum at 240 nm and $\epsilon = 5,000 \text{ L mol}^{-1} \text{ cm}^{-1}$ in water [68]. Spectral monitoring at 240 nm has been used for direct quantification of Hcy-thiolactone in bacterial cultures [193, 194]. Because of its limited sensitivity (the limit of detection is 0.1 mM), the use of this method is limited to experimental systems in which high concentrations of Hcy-thiolactone are generated.

3.3.3 High-Performance Liquid Chromatography-Based Assays

Nonradioactive HPLC-based assays have subsequently been developed and are available for Hcy-thiolactone quantification in biological samples, including plasma, urine, and tissues. The assays are based on HPLC coupled with UV absorbance or fluorescence detection.

3.3.3.1 High-Performance Liquid Chromatography with UV Detection

The first HPLC-based method for the determination of Hcy-thiolactone in biological samples exploited the ability of Hcy-thiolactone to absorb in UV [64]. Sample preparation procedures for HPLC analyses of Hcy-thiolactone levels in bacterial or yeast cultures are fast and simple: after removal of cells by short centrifugation, culture media are injected into an HPLC column. Sample preparation for the human plasma Hcy-thiolactone assay requires deproteinization by centrifugation in Millipore 10-kDa cutoff ultrafilters and extraction with charcoal or chloroform/methanol, followed by lyophilization. In order to monitor recovery, radiolabeled [³⁵S]Hcy-thiolactone is included in plasma samples as a tracer. Chromatographic separation is achieved on a reversed-phase C18 or a cation exchange polysulfoethylaspartamide (PSEA) HPLC column, and the quantification is by monitoring UV absorption at 240 nm, the wavelength at which the Hcy-thiolactone spectrum has a maximum (Fig. 3.1). The method allows detection of 5 pmol Hcy-thiolactone with 6 % reproducibility. The procedure works well for Hcy-thiolactone determinations in diverse cell cultures, including the bacteria *E. coli* and *Mycobacterium smegmatis*, the yeast *Saccharomyces cerevisiae* [64], the plants [190], and human vascular endothelial cells [64]. This assay allowed the discovery of Hcy-thiolactone in human plasma [64], which provided the first evidence that the metabolic conversion of Hcy to Hcy-thiolactone—Hcy editing—is conserved in evolution from bacteria to man.

3.3.3.2 High-Performance Liquid Chromatography with Fluorescence Detection

That thiols can be quantified by a reaction with OPA was first reported in 1966, when it was found that a reaction of glutathione with OPA generates a fluorescent product. This finding allowed the development of a highly sensitive and specific assay for reduced glutathione when carried out at pH 9–12 [222]. Similar reactions have been described subsequently for Hcy and Hcy-thiolactone and shown to yield maximal fluorescence when carried out at pH \geq 13 [223]. The fluorescence due to glutathione is greatly diminished at pH \geq 13, while Hcy and Hcy-thiolactone give strong fluorescence signals. These findings provide basis for the development of fluorescent Hcy-thiolactone and Hcy assay [223]. The assay utilizes a C30 reversed-phase HPLC column, post-column derivatization with OPA/NaOH, and fluorescence detection. In alkaline solutions (pH \geq 13), Hcy-thiolactone is quickly hydrolyzed to Hcy, which reacts with OPA to form a relatively stable fluorescent derivative, quantified by using excitation at 370 nm and emission at 480 nm. The assay has a sensitivity of 0.2 pmol for Hcy-thiolactone and 0.1 pmol for Hcy but so far has had very limited application, being used only for Hcy-thiolactone and Hcy quantification in Hep G2 cell cultures [223] and for in assays of Hcy-thiolactonase activity of Pon1 [224].

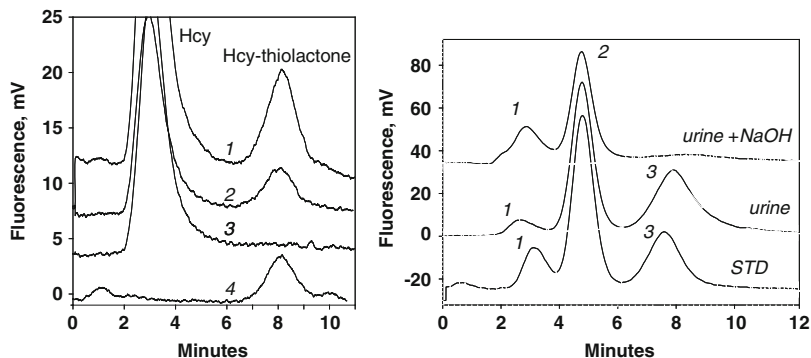


Fig. 3.4 Determination of Hcy-thiolactone by cation exchange HPLC. Detection is by fluorescence emission at 480 nm (excitation at 370 nm) after post-column derivatization with OPA. *Left panel:* plasma Hcy-thiolactone. Analyses of samples prepared from human plasma containing 6.7 and 2.8 nM Hcy-thiolactone are illustrated by trace 1 and trace 2, respectively. Hcy-thiolactone is absent in plasma samples treated with NaOH before HPLC analysis (trace 3). Hcy-thiolactone standard (100 fmol) elutes at 8 min (trace 4). A peak eluting in a void volume is due to Hcy present in plasma samples. *Right panel:* urinary Hcy-thiolactone. Samples prepared from human urine (containing 538 nM Hcy-thiolactone) before (middle trace) and after 5-min treatment with 0.1 M NaOH (top trace). Lower trace (labeled STD) was obtained with a standard sample containing 0.5 pmol Hcy (peak 1), 200 pmol histidine (peak 2), 1 pmol Hcy-thiolactone (peak 3) (Reproduced from [94, 95])

The first universal HPLC assay that allows analysis of Hcy-thiolactone in any biological samples, including human and mouse plasma [94], urine [95], and tissues [140, 141], has been developed by using a cation exchange PSEA column, post-column derivatization with OPA, and fluorescence detection (excitation at 370 nm, emission at 480 nm). The plasma Hcy-thiolactone assay involves ultrafiltration on Millipore 10-kDa cutoff device to remove protein followed by selective extraction of Hcy-thiolactone from the deproteinized sample. A crucial step in sample preparation is chloroform/methanol extraction, which is more selective than the charcoal extraction [64] for plasma samples. Further purification and quantification are achieved by HPLC on a cation exchange PSEA column and fluorescence detection after post-column derivatization with OPA/NaOH. The limit of detection is 0.36 nM. As little as 25 fmol Hcy-thiolactone in a sample can be detected and quantified [94, 95]. Examples of HPLC analyses of human plasma and urinary Hcy-thiolactone are shown in Fig. 3.4. Using this assay, Hcy-thiolactone concentrations in plasma from normal healthy human subjects ($n = 60$) were found to vary from <0.1 to 34.8 nM, with an average of 2.82 ± 6.13 nM. In 29 of the 60 human plasma samples analyzed, Hcy-thiolactone levels were below the detection limit. This method has also been successfully used in the first studies of human urinary Hcy-thiolactone excretion, which found that the bulk of Hcy-thiolactone formed in the human body is cleared by the kidney [95]. Charcoal extraction is a crucial step in the determination of urinary Hcy-thiolactone. Hcy-thiolactone concentrations in human urine (11–485 nM; $n = 19$) are 100-fold higher than in plasma

(<0.1–22.6 nM; $n = 20$) and are negatively correlated with urinary pH. This assay is now routinely used in studies of the role of Hcy-thiolactone in human [93], mouse [93, 113, 140, 141], and bacterial [67] physiology.

An alternative method for urinary Hcy-thiolactone determination utilizes a solid-phase extraction on C18 cartridges, an on-column derivatization with OPA, and fluorescence detection [220]. The on-column derivatization results in narrower peaks and shorter run times (3 min), compared with the post-column derivatization method. The limit of quantification is 20 nM. Using the on-column derivatization, Hcy-thiolactone concentrations in human urine from 15 subjects were found to vary from 25 to 297 nM (mean 103 ± 89 nM), similar to the values reported previously using the post-column derivatization method [95].

3.3.4 Gas Chromatography/Mass Spectrometry Assay

Plasma Hcy-thiolactone can also be assayed by a gas chromatography/mass spectrometry (GC–MS) method with deuterated d_4 -Hcy-thiolactone as an internal standard [225]. Hcy-thiolactone is extracted from the plasma using silica solid-phase and then derivatized with heptafluorobutyric anhydride. The derivatized sample is analyzed by GC–MS in NCI mode with methane as the reagent gas and Hcy-thiolactone ion $[M(-)[\text{bond}]HF]$ and the d_4 -Hcy-thiolactone standard are quantified in a single-ion monitoring mode. The calibration line shows a dynamic linear range up to 40 nM. Within-day precision ($n = 20$, nominal concentration 5.2 nM) was 0.96 %, and between-day precision was 3.9 %, with a detection limit of 1.7 nM and quantification limit of 5.2 nM. This procedure has had a very limited application, being used with only two human plasma samples, in which Hcy-thiolactone concentration was found to be 18 and 25 nM.

3.3.5 Gold Nanoparticle Homocysteine-Thiolactone Sensor

Gold nanoparticles are known to interact with thiols [226, 227], including Hcy [228], which results in appearance of new absorption maxima at 610–660 nm. This principle has been exploited to develop a method for detection and quantification of Hcy-thiolactone. For this purpose fluorosurfactant (FSN)-capped gold nanoparticles (AuNPs) are used as aminothiols removers [227] and as sensors [229]. Hcy-thiolactone does not bind to the surface of the FSN-AuNPs in the pH range of 4.0–10.0. In contrast, under these pH conditions, the FSN-AuNPs are aggregated by Hcy and cysteine. Thus, FSN-AuNPs are effective sorbent materials for Hcy and cysteine, but not for Hcy-thiolactone. When added to a solution containing thiols and Hcy-thiolactone, FSN-AuNPs bind >98 % Hcy and >99 % cysteine. Subsequent removal of FSN-AuNPs particles by centrifugation leaves Hcy-thiolactone in the supernatant. Treatment of the supernatant with NaOH

converts Hcy-thiolactone to Hcy, which is then detected by its ability to induce aggregation of the FSN-AuNPs, quantified by measurements of absorption ratios at 610 and 550 nm, A_{610}/A_{550} . The selectivity of the gold nanoparticle probe is significantly higher for Hcy-thiolactone than for aminothiols. The sensitivity of FSN-AuNPs toward Hcy-thiolactone can be further improved by optimizing the AuNPs concentration. The lowest detectable concentration of HTL is 100 nM. This approach has been validated by quantification of Hcy-thiolactone in human urine samples [229].

3.4 Biosynthesis

3.4.1 *The Involvement of Methionyl-tRNA Synthetase*

The first indication that Hcy-thiolactone is likely to form biologically in living organisms came with the 1981 discovery of the enzymatic conversion of Hcy to Hcy-thiolactone in error-editing reactions of aminoacyl-tRNA synthetases (AARSs) [210]. AARSs are responsible for quality control [65] in the flow of information from a gene to protein and carry out two basic functions in protein biosynthesis: (a) provide chemically activated amino acids (in the form of aminoacyl-tRNA) and (b) mediate the transfer of genetic information [6]. The chemical activation involves a reaction with ATP, generating a high-energy intermediate, AARS•AA-AMP (Reaction 3.6), which subsequently reacts with tRNA to form a high-energy ester bond between the carboxyl group of an amino acid and a hydroxyl of the 3'-terminal ribose of tRNA (Reaction 3.7).

The genetic information transfer involves matching amino acids with corresponding tRNAs according to the rules of the genetic code. This in effect translates the words from the nucleic acid language into the words in the protein language. Thus, each of the twenty canonical AARSs translates its own set of nucleic acid words (triplets of bases) into a protein word (amino acid). For example, methionyl-tRNA synthetase (MetRS) translates the word “AUG” in the nucleic acid language as “methionine” in the protein language. Similarly, CysRS assures that words “UGU” and “UGC” in the nucleic acid language mean “cysteine” in the protein language.

High accuracy of an AARS in the tRNA aminoacylation reaction is achieved by preferential binding of a cognate amino acid and a quality control step in which non-cognate amino acids are edited [6, 230]. Editing is used to achieve high selectivity when the differences in binding energies of amino acids to AARSs are inadequate [65, 231].

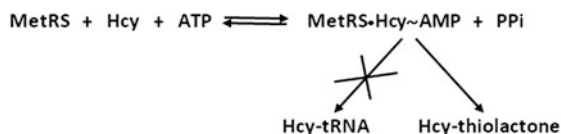
Because of its similarity to the protein amino acid methionine, during protein biosynthesis, the nonprotein amino acid Hcy is often incorrectly selected in place of methionine by MetRS. (The major role of MetRS is, of course, to catalyze the synthesis of methionyl-tRNA^{Met}, with Met-AMP as an intermediate.) Thus, in the



Reaction 3.6 The formation of aminoacyl adenylate catalyzed by AARS



Reaction 3.7 The aminoacylation of tRNA by AARS



Reaction 3.8 The formation of Hcy-thiolactone catalyzed by MetRS

presence of Hcy and ATP, MetRS catalyzes the formation of homocysteinyl-adenylate (Hcy-AMP).

That Hcy is a substrate for MetRS was first found in *in vitro* studies with purified *E. coli* and *Bacillus stearothermophilus* enzymes [232, 233]. However, in contrast to the cognate methionine which is transferred from Met-AMP to tRNA^{Met}, the misactivated Hcy is *not* transferred from Hcy-AMP to tRNA^{Met} [233].

Instead, Hcy-AMP is edited by the conversion to Hcy-thiolactone in an intramolecular reaction in which the side chain thiolate of Hcy displaces the AMP group from the carboxylate of the misactivated Hcy (Reaction 3.8) [210]. Thin-layer chromatography (TLC) shows that a new compound forms when MetRS is incubated with Hcy and ATP but is absent in incomplete reaction mixtures missing any of the three components. This new compound is identified as Hcy-thiolactone. It separates from Hcy on cellulose or silica gel TLC plates and is visualized under UV and by staining with ninhydrin. It cochromatographs with an authentic Hcy-thiolactone standard, absorbs UV light, and gives the same yellow color with ninhydrin as the standard [210]. Two pages from the author's laboratory notebook describing the original experiment in which the formation of Hcy-thiolactone during Hcy editing by MetRS has been discovered are shown in Fig. 3.5.

In the Hcy editing reaction, 1.03 mol ATP is hydrolyzed per mol of Hcy-thiolactone formed, which indicates that the cyclization by intramolecular thioester bond formation, rather than hydrolysis, is a favored reaction of Hcy-AMP [234]. The Hcy editing reaction is not affected by tRNA^{Met} [210].

The Hcy-thiolactone formation reaction corrects an error in amino acid selection, prevents Hcy from accessing the genetic code for methionine [6, 7], and is conserved in evolution from bacteria to human beings [64, 93, 197]. Hcy editing, one of a few error-correcting reactions that can be *directly* examined in living organisms, is a textbook paradigm of *in vivo* editing reactions in the translation of the genetic code [235, 236].

The involvement of MetRS in the biosynthesis of Hcy-thiolactone *in vivo* was first reported in microorganisms, such as *E. coli* [197] and the yeast *Saccharomyces*

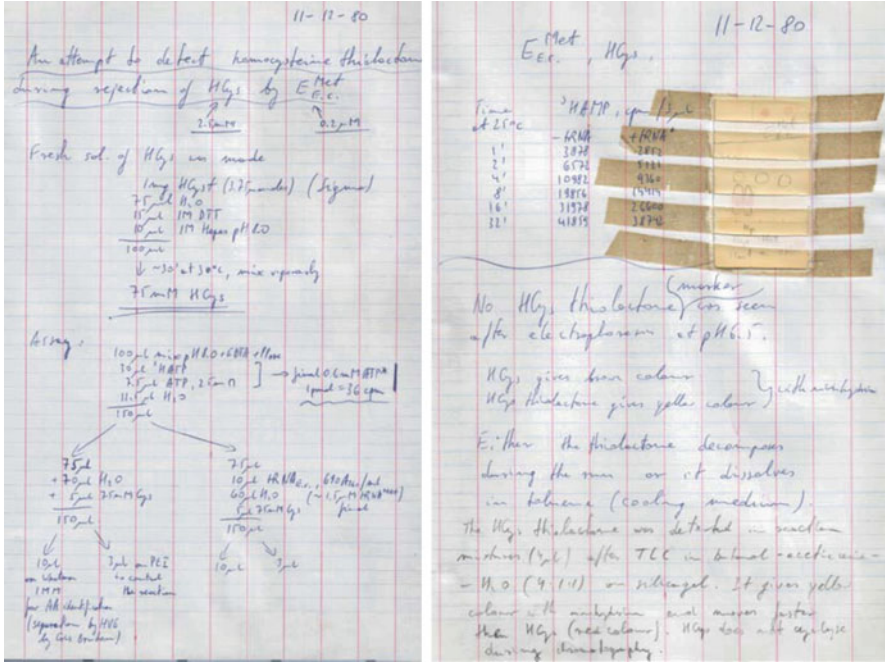


Fig. 3.5 Pages from the author’s laboratory notebook describing the discovery of Hcy-thiolactone formation during Hcy editing by MetRS (December 11, 1980). Hcy-thiolactone, formed in the reaction mixtures containing Hcy, [¹⁴C]ATP (the radiolabeled form is used as tracer to follow ATP hydrolysis to AMP during Hcy editing), tRNA, and MetRS, is separated from Hcy by thin-layer chromatography on a silica plate and detected by staining with ninhydrin (yellow). The original TLC plate is Scotch-taped in the upper right of the second page. The staining has faded since then, but the round pencil traces outlining the Hcy-thiolactone spots are visible in the middle of the plate. The slower migrating elongated spot is Hcy (originally stained red with ninhydrin)

cerevisiae [63]. The evidence that MetRS is responsible for Hcy-thiolactone biosynthesis in mammalian cells, including human, came from studies of Hcy-thiolactone metabolism in cultured human cervical carcinoma (HeLa), mouse adenocarcinoma (RAG), and Chinese hamster ovary (CHO) cells [138]. Subsequent studies have demonstrated that the rice *Oryza sativa* MetRS expressed in *E. coli* has the ability to catalyze the conversion of Hcy to Hcy-thiolactone and that MetRS is involved in Hcy-thiolactone biosynthesis in the plant *Lupinus luteus* [190].

Extensive cell culture and whole organism studies have established that Hcy-thiolactone formation during Hcy editing catalyzed by MetRS is universal and occurs in all organisms and cell types investigated from bacteria [64, 193, 194, 197], yeast [63, 64], and plants [190] to mice [93] and humans [64, 93–95]. Hcy-thiolactone synthesis during the Hcy editing reaction is also catalyzed by *E. coli* leucyl-tRNA and isoleucyl-tRNA synthetases, both in vitro [210] and in vivo [193].

The evidence that Hcy editing is part of MetRS-catalyzed tRNA aminoacylation with Met in living organisms is summarized below. Also discussed below is the

Table 3.5 Hcy-thiolactone levels in cultures of wild-type and temperature-sensitive aminoacyl-tRNA synthetase mutants of Chinese hamster ovary (CHO) cells (data from [138])

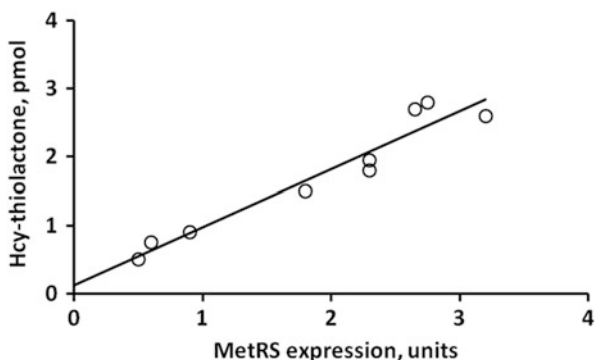
CHO cell line	Hcy-thiolactone, pmol/10 ⁷ cells	
	34 °C	39.5 °C
Wild type	2.0	3.7
	1.6	16.4
Met-1	0.3	<0.1
	0.5	<0.1
Arg-1	3.0	5.8
	7.6	21.3

Hcy-thiolactone levels were measured at 34 °C and 39.5 °C after 6 h and 12 h of labeling with 10 μM [³⁵S]methionine (0.1 mCi mL⁻¹, 10⁴ Ci mol⁻¹; 1 Ci = 37 GBq) in αMEM medium supplemented with 5 % fetal bovine serum, 10 μg mL⁻¹ adenosine, and 10 μg mL⁻¹ deoxythymidine

evidence showing that enhanced Hcy-thiolactone biosynthesis is linked to pathological conditions.

- (a) Cells expressing MetRS variants defective in the Met-binding site of the enzyme are also defective in Hcy-thiolactone synthesis as shown in Chinese hamster ovary (CHO) cells [138], the yeast *Saccharomyces cerevisiae* [63], and *E. coli* [197]. For example, Met-1 CHO cells expressing a temperature-sensitive (*ts*) MetRS variant do not produce Hcy-thiolactone at the nonpermissive temperature (39.5 °C), while they support Hcy-thiolactone biosynthesis at the permissive temperature (34 °C), albeit to a lesser extent than wild-type cells (Table 3.5) [138]. Control experiment with Arg-1 CHO cells expressing a *ts* ArgRS variant shows that a mutation in unrelated aminoacyl-tRNA synthetase does not prevent Hcy-thiolactone synthesis.
- (b) Conversely, increasing the expression of MetRS in growing cells also leads to proportional increases in Hcy-thiolactone synthesis as demonstrated for *E. coli* [197], yeast [63], and rice [190] enzymes. A relationship between cellular MetRS levels and the rate of Hcy-thiolactone synthesis in *E. coli* is illustrated in Fig. 3.6.
- (c) Biosynthesis of Hcy-thiolactone in human endothelial cells is directly proportional to Hcy concentration in culture media and inversely proportional to Met concentration (Fig. 3.7), consistent with the involvement of MetRS. Supplementation with folic acid decreases Hcy-thiolactone biosynthesis by lowering Hcy and increasing Met concentrations in endothelial cells [74].
- (d) Hyperhomocysteinemia caused by genetic or nutritional deficiencies in Hcy or folate metabolism in all studied organisms, including human [93], mouse [93, 113], plant [190], yeast [63], and *E. coli* [197], leads to greatly increased biosynthesis of Hcy-thiolactone. Comparisons of plasma Hcy-thiolactone levels between cystathionine β-synthase (CBS)-deficient or methylenetetrahydrofolate reductase (MTHFR)-deficient patients and unaffected control individuals [93] are illustrated in Tables 3.6 and 3.12.

Fig. 3.6 A relationship between the cellular levels of MetRS and Hcy-thiolactone synthesis in *E. coli* cells. Different cellular MetRS levels are produced by manipulating the expression of the MetRS gene cloned in a plasmid under the control of β -galactosidase promoter (Reproduced from [197])



Similarly, treatments with the antifolate drug aminopterin (which prevents remethylation of Hcy to Met by Met synthase) cause hyperhomocysteinemia and increase Hcy-thiolactone levels in cultured human cells and in the plant *Lupinus luteus* [63].

Experiments with mouse renal adenocarcinoma cells [138], human breast cancer cells [73], and oncogenically transformed human endothelial cells [64] show that oncogenic transformation increases Hcy levels and leads to increased Hcy-thiolactone biosynthesis [237].

- (e) Supplementation of growth media with methionine, the natural substrate of MetRS, competes Hcy out of the MetRS active site and completely abolishes the biosynthesis of Hcy-thiolactone in *E. coli* [197] and yeast [63]. Supplementation with other amino acids does not affect Hcy-thiolactone biosynthesis. Similar inhibition by methionine of Hcy-thiolactone biosynthesis catalyzed by MetRS has been recapitulated in vitro [210]. Supplementation with Met inhibits Hcy-thiolactone biosynthesis also in human endothelial cells [74].

Taken together, these findings provide genetic evidence that MetRS is involved in Hcy-thiolactone biosynthesis, establish a substrate–product relationship between Hcy and Hcy-thiolactone in ex vivo cultured cells and in vivo in intact organisms, suggest that Hcy editing occurs at the active site (whose major role is providing Met-tRNA for protein biosynthesis), and show that Hcy editing is universally conserved from the bacteria to humans and is greatly enhanced under pathological conditions in humans and experimental animals.

3.4.2 Molecular Mechanism

3.4.2.1 The Synthetic/Editing Active Site of Methionyl-tRNA Synthetase

Although studied in several biological systems, molecular mechanism of Hcy editing is best understood for *E. coli* MetRS. The Hcy editing reaction occurs in

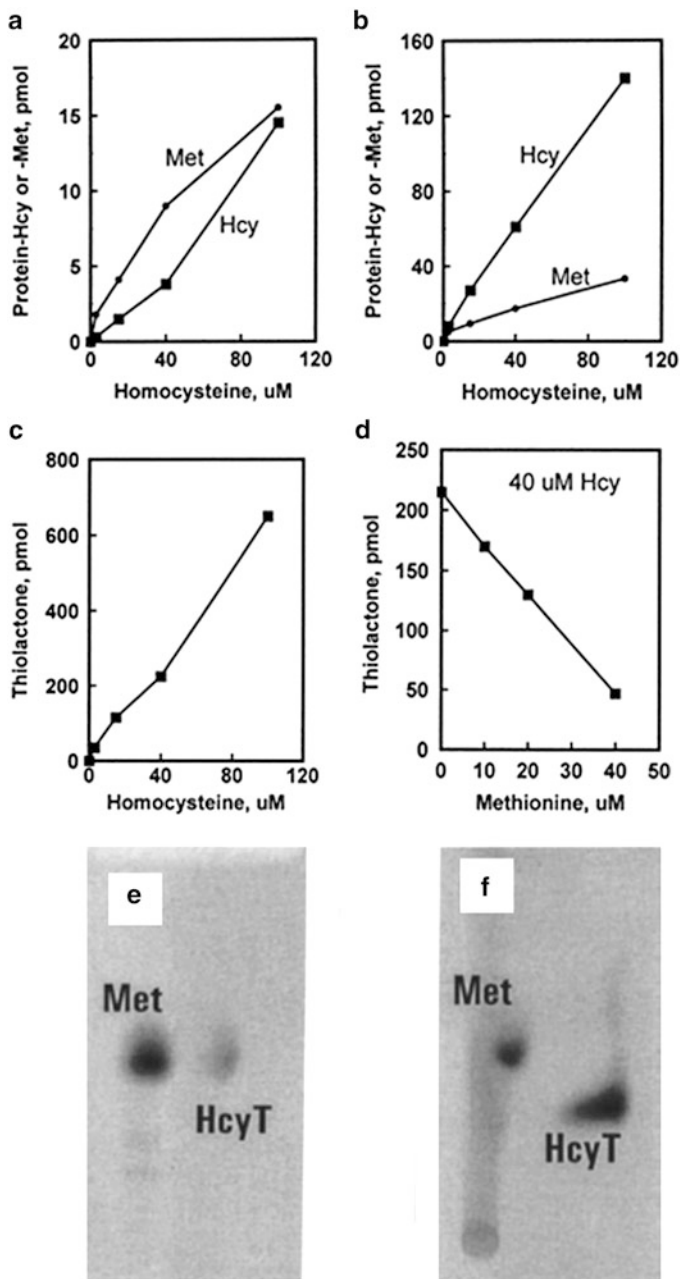


Fig. 3.7 Hcy-thiolactone and *N*-Hcy-protein formation in cultured human endothelial cells. Confluent cultures of human umbilical vein cells are labeled with [³⁵S]Hcy (330 to 5,000 Ci mol⁻¹) for 48 h. Panels (a) and (b): Levels of *N*-Hcy- protein (filled square) and protein-Met (filled circle) in intracellular (a) and extracellular (b) proteins as a function of [³⁵S]Hcy concentration. Panels (c) and (d): levels of Hcy-thiolactone as a function of [³⁵S]Hcy (c) and Met (d). Panels (e) and (f): Autoradiograms of two-dimensional TLC separations of [³⁵S]amino acids liberated by acid

Table 3.6 Plasma Hcy-thiolactone levels are elevated in human genetic hyperhomocysteinemia (Data from [93])

Patient genotype (<i>n</i>)	Hcy-thiolactone (nM)		Hcy (μ M)	
	Mean \pm SD	Range	Mean \pm SD	Range
Unaffected (9)	0.2 \pm 0.14	0.1–0.4	7.2 \pm 0.9	6.0–8.6
<i>CBS</i> ^{-/-} (14)	14.4 \pm 30.4	0.1–100.8	36.1 \pm 25.8	15–93
<i>MTHFR</i> ^{-/-} (4)	11.8 \pm 8.8	2.9–22.2	50.1 \pm 15.1	23–68
<i>MTHFR</i> ^{+/-} (6)	0.5 \pm 0.3	0.1–1.0	7.8 \pm 2.8	5.2–12.2

the synthetic/editing active site [238], whose major function is to carry out the synthesis of methionyl-tRNA for protein biosynthesis [239]. Whether methionine or Hcy completes the synthetic or editing pathway, respectively, is determined by the partitioning of its side chain between the specificity and thiol-binding subsites of the synthetic/editing active site [240]. A subsite that binds carboxyl and α -amino groups of methionine or Hcy does not appear to contribute to specificity [238]. Methionine completes the synthetic pathway because its side chain is firmly bound by the hydrophobic and hydrogen bonding interactions with the specificity subsite (Fig. 3.8, top panel).

The crystal structure of *E. coli* MetRS•Met complex reveals that hydrophobic interactions involve side chains of Tyr15, Trp253, Pro257, and Tyr260; Trp305 closes the bottom of the hydrophobic pocket but is not in the contact with the methyl group of the substrate methionine. The sulfur atom of the substrate methionine makes two hydrogen bonds: one with the hydroxyl of Tyr260 and the other with the backbone amide of Leu13 [239]. Crystal structures of *E. coli* MetRS complexed with analogs of methionine and methionyl adenylate show that residues Tyr15 and Trp253 play key roles in the strength of the binding of methionine and of its analogs and thus determine the specificity of the enzyme for methionine. Full motions of these residues are required to recover the maximum in free energy of binding: in the closed conformation (MetRS•Met complex), Tyr15 interacts with the amino nitrogen of the methionine substrate by forming a π - π bond, and Trp253 maintains hydrophobic interaction with methionine (assisted by a π - π bond between Trp253 and Phe300) [241], whereas in the open conformation (free MetRS), Tyr15 and Trp253 flip over to the other side of the active site pocket. Residue Tyr15 also controls the size of the hydrophobic pocket where the amino acid side chain interacts. In addition, His301 appears to participate to the specific recognition of the sulfur atom of methionine [242].

The active site residues Trp253 and Tyr15 that control the conformational flexibility of MetRS are highly conserved in the MetRS sequence of all species,

←
Fig. 3.7 (continued) hydrolysis from dithiothreitol (DTT)-treated cellular (e) and extracellular (f) proteins from HUVEC cultures labeled with [³⁵S]Hcy are shown. N-linked Hcy liberated from proteins during acid hydrolysis is converted to Hcy-thiolactone (HcyT in the figure) (Reproduced from [74] and [139])

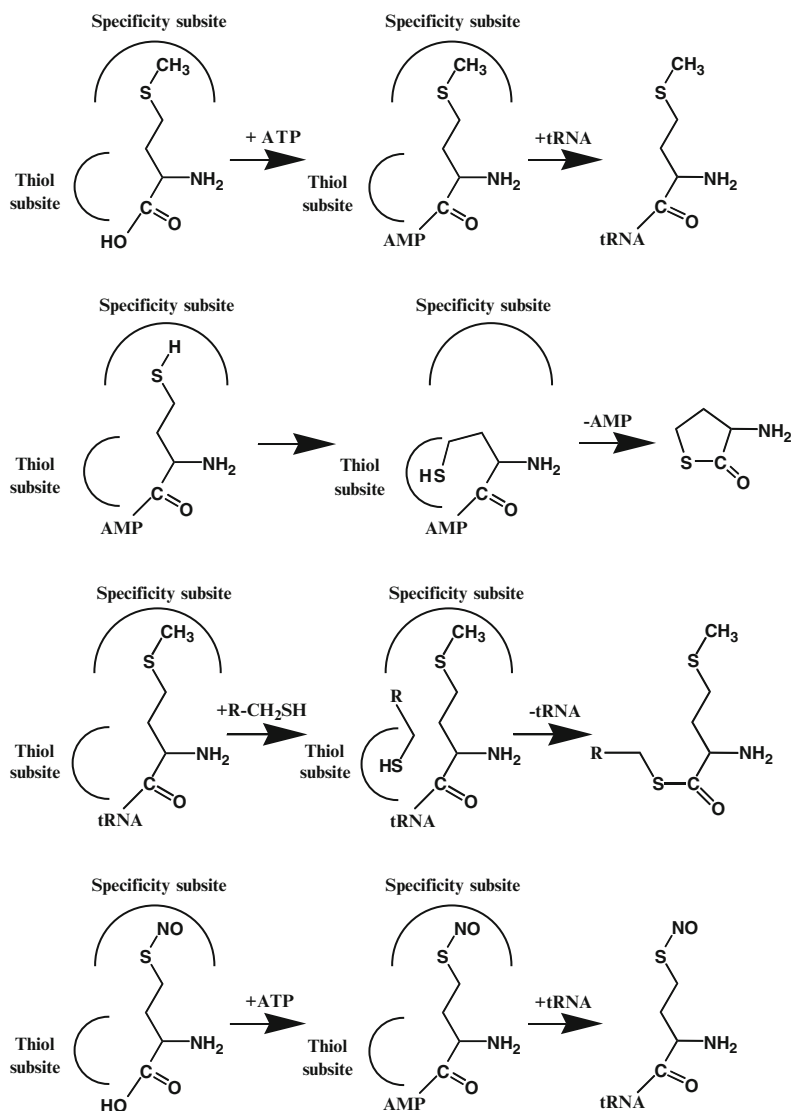


Fig. 3.8 Reactions catalyzed by MetRS. From *top to bottom*: the aminoacylation of tRNA with Met, the synthesis of Hcy-thiolactone during Hcy editing, the synthesis of methionyl thioesters, the aminoacylation of tRNA with S-NO-Hcy (Reproduced from [76])

including human [241]. Similarly, Asp52, which is responsible for the recognition of the amino nitrogen of the methionine substrate, is also conserved in the protein sequence of all species. Along with these, Tyr260 is also conserved in the primary structure of all species. The variations in the MetRS active site residues among different species are shown in Table 3.7.

Table 3.7 Comparison of active site residues of MetRS from different organisms (Adapted from [241])

Organism	Residue number							
	12	13	14	257	259	260	297	301
<i>Homo sapiens</i>	Ala	Leu	Pro	Thr	Gly	Tyr	Asn	His
<i>Saccharomyces cerevisiae</i>	Ala	Leu	Pro	Thr	Gly	Tyr	Asn	His
<i>Escherichia coli</i>	Ala	Leu	Pro	Pro	Gly	Tyr	Ile	His
<i>Pyrococcus furiosus</i>	Ala	Leu	Pro	Pro	Gly	Tyr	Asn	His
<i>Methanocaldococcus jannaschii</i>	Ala	Leu	Ala	Pro	Gly	Tyr	Ile	His
<i>Thermus thermophilus</i>	Pro	Ile	Tyr	Leu	Asn	Tyr	Ile	His
<i>Mycobacterium smegmatis</i>	Pro	Ile	Ala	Leu	Asn	Tyr	Ile	His

The non-cognate substrate Hcy, missing the methyl group of methionine, cannot interact with the specificity subsite as effectively as the cognate methionine does. This allows the side chain of Hcy to move to the thiol-binding subsite, which promotes the synthesis of the thioester bond during editing (Fig. 3.8, middle panel). Mutations of Tyr15 and Trp305 affect the ability of MetRS to discriminate between Hcy and methionine [238]. The active site residue Asp52, which forms a hydrogen bond with the α -amino group of the substrate methionine, deduced from the crystal structure of the MetRS•Met complex [239], is involved in the catalysis of both synthetic and editing reactions but does not contribute to substrate specificity of the enzyme. The substitution Asp52Ala inactivates both the synthetic and editing functions of MetRS [75, 238, 240].

3.4.2.2 The Thiol-Binding Subsite of Methionyl-tRNA Synthetase

The thiol-binding subsite is responsible for the ability of MetRS to catalyze the thioester bond formation between a thiol and the cognate methionine (Fig. 3.8, middle panel). The *intermolecular* thioester bond formation reaction mimics the *intramolecular* thioester bond formation reaction during Hcy editing and is dubbed *editing in trans* [243]. With CoA-SH or cysteine as a thiol substrate, MetRS catalyzes the formation of Met-S-CoA thioesters [199] and Met-Cys dipeptides [240], respectively, while the reaction with pantetheine generates Met-S-pantetheine thioester. The formation of Met-Cys dipeptide proceeds via a Met-S-Cys thioester intermediate, which spontaneously rearranges to the Met-Cys dipeptide. The formation of Met-Cys dipeptide as a result of *editing in trans* is as fast as the formation of Hcy-thiolactone during Hcy editing.

Although MetRS (as well as IleRS, ValRS, and LysRS) uses the thiol-binding site for Hcy editing, such site also appears to be present in aminoacyl-tRNA synthetases that do not edit Hcy but catalyze the aminoacylation of thiols, such as ArgRS, AspRS, and SerRS [199, 234, 244, 245]. The thiol aminoacylation reactions are analogous to pantetheine thiol aminoacylation by the multienzyme complexes responsible for nonribosomal peptide synthesis. This analogy suggests that the two

fundamentally different peptide-synthesizing systems have a common evolutionary origin. This suggestion is further supported by findings showing that several bacterial species express SerRS homologs that aminoacylate phosphopantetheine prosthetic group of carrier protein with glycine or alanine but do not aminoacylate tRNA [246]. These SerRS homologs and the thiol-aminoacylating ability of aminoacyl-tRNA synthetases may represent molecular fossils linking coded ribosomal protein synthesis with noncoded nonribosomal peptide synthesis [199].

3.4.2.3 *S*-NO-Hcy Is Transferred to tRNA and Participates in Protein Biosynthesis

In the model of the synthetic/editing site of MetRS [240], the side chain of the cognate substrate methionine is bound exclusively in the specificity subsite (Fig. 3.8, top panel), while the side chain of the non-cognate substrate Hcy partitions between the specificity subsite and the thiol-binding subsite of MetRS (Fig. 3.8, middle panel). This is due to 88-fold weaker interaction of Hcy, relative to methionine, with the specificity subsite (Table 3.8). Thus, by enhancing the binding of the side chain of Hcy in the specificity subsite, one could prevent editing and allow Hcy transfer to tRNA^{Met}. This, in fact, has been achieved by exploiting nitrosothiol chemistry in vitro and in vivo in *E. coli* [75] and can occur naturally in nitric oxide (NO)-producing cells, such as human endothelial cells [76].

Hcy is quantitatively converted to *S*-NO-Hcy using equimolar amounts of NaNO₂ in 0.1 M HCl [188]. It is found that *S*-NO-Hcy is a better substrate for MetRS than Hcy in the aminoacyl adenylate formation reaction, mostly due to 14.3-fold lower K_m value [75]. The k_{cat}/K_m value for *S*-NO-Hcy is 6.7-fold higher than for Hcy, indicating stronger binding of *S*-NO-Hcy to the specificity subsite (Table 3.8). This stronger binding to the specificity subsite essentially prevents binding to the editing subsite. As a result, *S*-NO-Hcy is not edited, but, instead, is transferred to tRNA^{Met} forming *S*-NO-Hcy-tRNA^{Met} (Fig. 3.8, bottom panel) at a significant rate (Table 3.8) [75].

S-NO-Hcy-tRNA^{Met} is as stable as Met-tRNA^{Met}—both are deacylated with a half-life of 26 min. In contrast, Hcy-tRNA^{Met} (prepared by de-nitrosylation of *S*-NO-Hcy-tRNA^{Met}) is the least stable aminoacyl-tRNA known (deacylation half-life of 15 s). Hcy-thiolactone and free tRNA^{Met} are the products of deacylation of Hcy-tRNA^{Met} [75].

S-NO-Hcy-tRNA^{Met}, similar to Met-tRNA^{Met}, is a substrate for ribosomal protein biosynthesis [75]. For example, *E. coli* cells unable to metabolize Hcy to Met due to the inactivation of the *metE* gene utilize *S*-NO-Hcy for protein biosynthesis. When cultures of *E. coli metE* mutant cells expressing mouse dihydrofolate reductase (Dhfr) protein are supplemented with *S*-NO-Hcy, the synthesized Dhfr protein is found to contain Hcy. Globin and luciferase produced in an in vitro mRNA-programmed rabbit reticulocyte protein synthesis system supplemented with *S*-NO-Hcy-tRNA^{Met} contain Hcy at positions normally occupied by methionine [75].

Table 3.8 Relative binding, editing, and tRNA aminoacylation under steady-state conditions by *E. coli* MetRS (Compiled from [65, 75, 210])

Amino acid	Binding	Rate of editing	Rate of tRNA aminoacylation
Methionine	100	1	100
S-nitroso-Hcy	7.63	<1	1.2
Homocysteine	1.13	60	<0.0001 ^a

^aHcy is not transferred to tRNA

Table 3.9 Translational and posttranslational incorporation of Hcy into protein in cultured human endothelial cells (Data from [76])

Labeling conditions	Translational		Posttranslational
	[³⁵ S]Hcy-protein (%)	[³⁵ S]Met-protein (%)	<i>N</i> -[³⁵ S]Hcy-protein (%)
[³⁵ S]Hcy, 80 μM	57	19	24
[³⁵ S]Hcy, 40 μM	47	20	33
[³⁵ S]Hcy, 10 μM	37	25	38
[³⁵ S]Hcy, 10 μM + folate, 10 μM	<1	>98	<1
[³⁵ S]Hcy, 10 μM + Met, 20 μM	12	76	12
[³⁵ S]Hcy, 10 μM + HDL, 1 mg mL ⁻¹	68	25	7
Control, <i>eN</i> -[³⁵ S]Hcy-Lys-protein	<4	0	>96

Human umbilical vein endothelial cells (HUVECs) are maintained on Met-free M199 culture medium, supplemented with dialyzed 15 % fetal bovine serum, bovine endothelial cell growth factor, heparin, and indicated concentration of [³⁵S]Hcy (50 μCi mL⁻¹), in the absence and presence of exogenous folate, HDL or Met. [³⁵S]Met-protein and protein-[³⁵S]Hcy (total incorporation of Hcy into protein) are determined by acid hydrolysis of extracellular proteins followed by thin-layer chromatography. [³⁵S]Hcy-protein (translationally incorporated Hcy) and *N*-[³⁵S]Hcy-protein (posttranslationally incorporated Hcy) are distinguished the susceptibility to Edman degradation: *N*-[³⁵S]Hcy-protein is sensitive to Edman degradation, while [³⁵S]Hcy-protein and [³⁵S]Met-protein are resistant. Relative distribution (%) of the [³⁵S]radioactivity among indicated chemical species observed under each experimental condition is shown

Hcy-containing Dhfr, globin, and luciferase are indistinguishable from the native Met-containing proteins on SDS-PAGE gels [75]. This shows that Hcy incorporation into protein in place of Met does not lead to breakage of peptide bonds and that Hcy is compatible with protein structure. Other studies have shown that Hcy can be incorporated in place of cysteine by chemical synthesis into peptides such as the hormone oxytocin [247] and the isopenicillin precursor δ-L-α-amino adipoyl-L-homocysteinyl-D-valine (AhCV) [248]. Resulting Hcy-containing peptides are chemically stable. While Hcy-oxytocin is devoid of biological activity of normal oxytocin [247], AhCV is a substrate for isopenicillin synthase, which oxidizes AhCV to a δ-lactam, a higher homolog of the γ-lactam arising from the oxidation of the natural cysteine-containing precursor [248].

Translational incorporation of Hcy into protein occurs in cultured human vascular endothelial cells (Table 3.9) [76, 83] that are known to produce nitric oxide and

S-NO-Hcy [100]. NO is generated by endothelial nitric oxide synthase and regulates diverse functions in the endothelium, including ion channel activity, anti-oxidative, anti-apoptotic, and anti-inflammatory responses. NO diffuses from the endothelial cells to the vascular smooth muscle cells, where it mediates vasorelaxation. These functions are mediated by protein *S*-nitrosylation [249]. Overexpression of the inducible nitric oxide synthase by transfection of endothelial cells with an adenovirus vector carrying the iNOS gene increases nitric oxide generation and results in a significant increase in the formation of *S*-NO-Hcy [101]. While the biological activities of NO are well established, the role of *S*-NO-Hcy is unclear, but, by becoming a constituent of proteins, it can cause protein damage and thus contribute to the pathophysiology of hyperhomocysteinemia.

Incubation of human umbilical vein endothelial cells (HUVEC) with [³⁵S]Hcy results in incorporation of the radiolabel into cellular proteins [76]. Compositional analysis shows that ³⁵S-protein from HUVEC + 10 μM [³⁵S]Hcy contains 75 % [³⁵S]Hcy and 25 % [³⁵S]Met (third row, Table 3.9). Because the transsulfuration pathway is absent in endothelial cells, no radioactivity is found in cysteine. When the endothelial cell ³⁵S-protein is subjected to one cycle of Edman degradation, 38 % of ³⁵S is released as a phenyl-thiohydantoin (PTH) derivative of Hcy. Edman degradation of *N*-[³⁵S]Hcy-albumin (positive control; prepared by the modification of human serum albumin with [³⁵S]Hcy-thiolactone—see Sects. 3.2.4. and 5.1.) shows that >96 % of posttranslationally incorporated Hcy is released as a PTH-Hcy (last row, Table 3.9). These results suggest that posttranslationally incorporated Hcy (*N*-[³⁵S]Hcy-protein) represents about a half (38 %) of total protein *N*-linked [³⁵S]Hcy (75 %, third row). Of the 62 % of ³⁵S-protein resistant to Edman degradation, translationally incorporated Hcy ([³⁵S]Hcy-protein) represents 37 % (25 % is [³⁵S]Met-protein). The fraction of [³⁵S]Hcy-protein increases (second column in Table 3.9), and the fraction of [³⁵S]Met-protein decreases (third column) with increasing Hcy in culture media (row 1 and 2). This suggests that the translational incorporation is more important at higher Hcy concentrations.

In cultures supplemented with folic acid, all [³⁵S] recovered by acid hydrolysis of protein is associated only with Met (forth row in Table 3.9). This is due to facilitation by folic acid of the remethylation of Hcy to Met catalyzed by Met synthase, which uses methyltetrahydrofolate as a cofactor (Fig. 1.1). Supplementation with Met, which competes with Hcy and *S*-NO-Hcy for the active site of MetRS and thus prevents both the formation of *S*-NO-Hcy-tRNA and the conversion of Hcy to Hcy-thiolactone, decreases the incorporation of Hcy into protein (5th row). However, the supplementation with HDL does not inhibit translational incorporation of Hcy into protein but inhibits the posttranslational incorporation because of Hcy-thiolactone-hydrolyzing activity of the PON1 protein carried on HDL (see Sect. 3.5.1.).

Taken together, these findings indicate that Hcy can gain an access to the genetic code by *S*-nitrosylation-mediated invasion of the methionine-coding pathway. However, whether *S*-nitroso-Hcy is generated in mammalian organisms and is a component of human or animal proteins remains to be investigated.

3.5 Turnover

Early experiments show that Hcy-thiolactone infused into rabbits is cleared from the blood within <15 min [150]. In wild-type mice, intraperitoneally injected Hcy-thiolactone is quickly hydrolyzed to Hcy, and only a small fraction (6.3 % of the injected dose) shows up in the plasma [141]. The mouse plasma Hcy-thiolactone is cleared with a half-life of 5 min [140, 141]. Elevated plasma Hcy-thiolactone in mice fed with a high-methionine diet is normalized to a basal level after the animals are shifted to a standard chow diet [113]. Hcy-thiolactone is cleared from the tissues and blood by specific enzymes and by urinary excretion.

3.5.1 Enzymatic Turnover

Two enzymes are known to hydrolyze Hcy-thiolactone in humans and animals. Extracellular hydrolysis is catalyzed by paraoxonase 1 (Pon1) [81, 152, 250], while intracellular hydrolysis is catalyzed by bleomycin hydrolase (Blmh) [85, 141, 251]. Recent data show that Pon1 and Blmh contribute to Hcy-thiolactone hydrolysis in the mouse brain [140, 141]. Enzymatic hydrolysis of Hcy-thiolactone to Hcy facilitates its removal by the classical remethylation and transsulfuration pathways.

3.5.1.1 Paraoxonase 1

Pon1, named for its ability to hydrolyze the organophosphate paraoxon, is a 45-kD calcium-dependent enzyme synthesized exclusively in the liver and carried on high-density lipoprotein (HDL) in the blood, although recent studies suggest a wider expression pattern, including the brain [252]. Pon1 protects against high-fat diet-induced atherosclerosis in mice [253] and humans [254, 255]. Pon1-deficient mice are more susceptible to high-fat diet-induced atherosclerosis than wild-type littermates but do not develop atherosclerosis on a control chow diet [253]. Pon1 is also involved in and affected by Hcy metabolism and thus provides a link between metabolism of lipids and Hcy [256, 257].

In humans, PON1 is also implicated in Alzheimer's disease. For example, low serum PON1 activity is a risk factor for dementia [258] and Alzheimer's disease [259, 260]. Hcy, a risk factor for Alzheimer's disease [56, 57], is a negative determinant of PON1 activity [261, 262].

In vitro, human HDL and the purified PON1 protein have the ability to hydrolyze Hcy-thiolactone [81] and to protect against protein *N*-homocysteinylation in serum [152] and cultured human endothelial cells [74]. The in vivo levels of *N*-Hcy-protein in human serum are inversely correlated with Hcy-thiolactonase activity of PON1 [250]. This relationship is recapitulated in in vitro *N*-homocysteinylation experiments with [³⁵S]-Hcy-thiolactone. In Chinese patients with type

2 diabetes, plasma Hcy-thiolactone concentrations are negatively correlated with HDL levels ($r = -0.223$, $P = 0.037$) [362], consistent with the ability of HDL-associated PON1 protein to hydrolyze Hcy-thiolactone [81]. Taken together, these results provide evidence that PON1 has the ability to protect proteins against *N*-homocysteinylolation both in vitro and in vivo in humans.

PON1 is the only enzyme known to metabolize Hcy-thiolactone in human and other mammalian sera, with the highest levels observed in rabbits, which have six times higher Hcy-thiolactonase/PON1 activity than that present in an average human serum [153]. However, serum Hcy-thiolactonase activity is absent in birds, including chicken [81, 153], which makes chicken embryos particularly sensitive to Hcy-thiolactone toxicity [154, 155].

Substrate specificity studies of purified human serum Hcy-thiolactonase/PON1 show that *L*-Hcy-thiolactone is a preferred natural substrate [81]. *D*-Hcy-thiolactone and γ -thiobutyrolactone are hydrolyzed at a rate fourfold slower and 5.5-fold faster, respectively, than *L*-Hcy-thiolactone by the enzyme [85]. The artificial substrates phenyl acetate and paraoxon (hydrolyzed 2,800 and 3.3 times faster than *L*-Hcy-thiolactone) are noncompetitive inhibitors of the Hcy-thiolactonase activity suggesting that Hcy-thiolactone, phenyl acetate, and paraoxon are hydrolyzed at different sites of the enzyme [81]. This suggestion is supported by structure/function studies showing that specific active sites mutations have different effects on arylesterase, paraoxonase, and lactonase activities of the PON1 protein [263, 264]. Other inhibitors of the Hcy-thiolactonase activity such as isoleucine and penicillamine are also noncompetitive, suggesting the presence of a distinct amino acid-binding effector site on PON1 [81]. Hcy-thiolactonase and paraoxonase activities are strongly correlated in various populations [152, 250, 261], indicating that the artificial paraoxonase activity is a good surrogate for the natural Hcy-thiolactonase activity of the PON1 protein.

Hcy-thiolactone metabolism is impaired in *Pon1*^{-/-} mice. For example, serum Hcy-thiolactonase activity is absent in *Pon1*^{-/-} mice [81, 140, 153]. *Pon1*^{-/-} mice have significantly elevated brain Hcy-thiolactone and excrete more Hcy-thiolactone in urine compared with *Pon1*^{+/+} littermates [140]. Furthermore, significantly less plasma Hcy is generated from intraperitoneally injected Hcy-thiolactone in *Pon1*^{-/-} mice than in *Pon1*^{+/+} animals.

Pon1^{-/-} mice are more susceptible than wild-type littermates to neurotoxicity induced by intraperitoneal injections of Hcy-thiolactone (Table 3.10) [140]. Following intraperitoneal injections of *Pon1*^{-/-} mice and *Pon1*^{+/+} littermates with convulsant doses of *L*-Hcy-thiolactone (3,700 nmol g⁻¹ body weight), all mice become somnolescent within 5–10 min. Convulsions, characterized by spontaneous tonic-clonic, grand mal seizures (kangaroo position, extension of fore and hind limbs and tail, status epilepticus), and running fits, occur within 50 min [140]. The incidence of seizures is significantly increased in *Pon1*^{-/-} mice compared with *Pon1*^{+/+} animals (52.8 vs. 29.5 %, $P < 0.042$) (Table 3.10). Seizure latency (i.e., time to first seizure) is significantly decreased for *Pon1*^{-/-} mice compared with *Pon1*^{+/+} animals (33.8 min vs. 41.2 min, $P = 0.019$). While only one mouse out of the 44 *Pon1*^{+/+} mice (2.3 %) dies (at 61 min) after *L*-Hcy-thiolactone injection,

Table 3.10 *Blmh*^{-/-} and *Pon1*^{-/-} mice are more susceptible to Hcy-thiolactone neurotoxicity than wild-type littermates. The mice are injected intraperitoneally with L-Hcy-thiolactone (3,700 nmol g⁻¹ body weight) and monitored for neurological manifestations for 90 min (Adapted from [140, 141])

Genotype (n)	Incidence of seizures, % (n)	Incidence of death, % (n)	Seizure latency period, min	Death latency period, min
<i>Blmh</i> ^{-/-} (32)	93.8 (30)*	46.9 (15)*	33.1 ± 10.1***	46.6 ± 15.1
<i>Pon1</i> ^{-/-} (36)	52.8 (19)**	8.3 (3)	31.8 ± 11.6****	50 ± 30
Wild type (44)	29.5 (13)	2.3 (1)	41.2 ± 10.8	61

*, **, ***, ****Significantly different from wild type—Fisher exact test **P* < 0.001, ***P* = 0.042 vs. wild type; *T* test ****P* = 0.012, *****P* = 0.019 vs. wild type

the incidence of death is somewhat increased for *Pon1*^{-/-} mice (to 3 out of 36 *Pon1*^{-/-} mice, 8.3 %). *Pon1*^{-/-} mice have elevated postinjection levels of *N*-Hcy-protein in the brain, compared with wild-type *Pon1*^{+/+} littermates, which suggest that the mechanism of Hcy-thiolactone-induced neurotoxicity involves *N*-homocysteinylation of brain proteins. Although in this experimental model Hcy is also generated, postinjection Hcy levels are not significantly different in *Pon1*^{-/-} and *Pon1*^{+/+} mice and thus do not explain the increased toxicity in *Pon1*^{-/-} animals. Taken together, the experiments with *Pon1*-null mouse model provide the first direct evidence that Hcy-thiolactone, rather than Hcy itself, is neurotoxic in vivo [140].

Human *PON1* has genetic polymorphisms, e.g., *PON1-M55L* and *PON1-R192Q*, which affect PON1 function [265, 266], including Hcy-thiolactonase activity [152, 261]. For example, high Hcy-thiolactonase activity is associated with *PON1-L55* and *PON1-R192* alleles, whereas low Hcy-thiolactonase activity is associated with *PON1-M55* and *PON1-Q192* alleles [152, 261]. Purified serum PON1-R192 allozyme has 2.5-fold higher Hcy-thiolactonase activity than the PON1-Q192 allozyme [267], which explains the association of high activity with *PON1-R192* allele.

However, several studies have found that PON1 phenotype (Hcy-thiolactonase or paraoxonase activity) is a predictor of cardiovascular disease, but the *PON1-R192Q* or *PON1-M55L* genotypes are not [255, 265, 266, 268, 269]. For example, Hcy-thiolactonase activity is found to be significantly lower in a group of 128 coronary artery disease patients with angiographically confirmed atherosclerotic lesions, compared to a control group of 142 individuals who have no lesions [255]. A negative correlation is found between the severity of atherosclerotic lesions and Hcy-thiolactonase activity in the patients. Moreover, the natural Hcy-thiolactonase activity is a more significant predictor of the disease than the artificial paraoxonase activity [255].

Furthermore, Hcy is a negative regulator of *Pon1* expression in mice [270], whereas Hcy-thiolactonase activity of PON1 is negatively correlated with plasma Hcy in humans [261]. Negative effects of Hcy on PON1 expression or activity most likely contribute to the proatherogenic role of Hcy [256, 257].

3.5.1.2 Bleomycin Hydrolase

Blmh, named for its ability to hydrolyze the anticancer drug bleomycin, is ubiquitously expressed in mammalian tissues, but its expression level is tissue dependent, as shown in mice [271, 272], rats [273, 274], rabbits [271, 275, 276], and humans [277], and is also present in other species [278, 279]. Blmh is studied in the context of Hcy toxicity [85, 251], cancer therapy [277, 280], Alzheimer's disease [281–284], Huntington's disease [285], keratinization disorders [286], and protein breakdown [285, 287]. The human genetic polymorphism *BLMH-Ile443Val* is associated with an increased risk for Alzheimer's disease [282].

Human and yeast Blmh have almost identical molecular structures, similar to the 20S proteasome, and belong to a family of self-compartmentalizing intracellular cysteine proteases [278, 288]. Its evolutionary conservation and wide distribution suggests that Blmh has a conserved cellular function.

Its physiological function was unknown until 2006 when it was shown that Blmh is a major Hcy-thiolactonase in humans and yeast and that it protects against Hcy toxicity in yeast [85]. Recombinant human and yeast Blmh proteins, expressed in *E. coli*, exhibit Hcy-thiolactonase activities similar to those of native purified enzymes. Active site mutations, C73A for the human Blmh and H369A for the yeast Blmh, inactivate the Hcy-thiolactonase activity. Furthermore, yeast *Blmh*-null strains are deficient in Hcy-thiolactonase activity, produce more Hcy-thiolactone, and exhibit greater sensitivity to Hcy toxicity than wild-type yeast. These results show that Blmh protects cells against Hcy toxicity by hydrolyzing Hcy-thiolactone [85].

Substrate specificity studies of purified human Blmh show that the enzyme exhibits absolute stereospecificity for L-Hcy-thiolactone, the preferred natural substrate [85]. Methyl esters of L-Cys and L-Met, but not of other L-amino acids, are also hydrolyzed. However, D-Hcy-thiolactone, D-Met methyl ester, γ -thiobutyrolactone, and L-homoserine lactone are not hydrolyzed by Blmh [85].

Hcy-thiolactonase activity of Blmh is significantly reduced in brains from Alzheimer's disease patients compared with unaffected brains [251]. This finding suggests that diminished functional Blmh activity could contribute to the pathology of the disease.

Blmh is highly stereoselective and hydrolyzes the L-stereoisomer of Hcy-thiolactone, while the D-stereoisomer is not hydrolyzed (Fig. 3.2) [85]. Comparative studies of D-Hcy-thiolactone vs. L-Hcy-thiolactone clearances in mice suggest that Blmh participates in Hcy-thiolactone clearance in vivo [141]. For example, when wild-type mice are intraperitoneally injected with D-, or D,L-Hcy-thiolactone, 88 % and 47 % of the injected dose of D- and D,L-Hcy-thiolactone, respectively, is recovered in mouse plasma (Table 3.11). The amounts of recovered D- and D,L-Hcy-thiolactone are 14- and 7-fold higher, respectively, than the amount L-Hcy-thiolactone of recovered in mice injected with the L-stereoisomer (6.3 % of the injected dose). However, half-lives of plasma D-, D,L-, or L-Hcy-thiolactone are similar (Table 3.11). These findings provide evidence that stereoselective

Table 3.11 Turnover of *D*-, *D,L*-, and *L*-Hcy-thiolactone in the mouse

Hcy-thiolactone stereoisomer	HTL recovered in plasma, % injected dose	Plasma HTL $t_{0.5}$, min
<i>L</i> -	6.3 ± 0.2	5.0 ± 0.9
<i>D</i> -	88 ± 3	5.7 ± 0.3
<i>D,L</i> -	47 ± 4	5.5 ± 0.2

Wild-type C57BL/6J mice are injected intraperitoneally with *L*- ($n = 6$), *D*- ($n = 3$), or *D,L*- stereoisomers ($n = 6$) of Hcy-thiolactone at a dose of 150 nmol g⁻¹ body weight. Plasma Hcy-thiolactone (HTL) levels are assayed at time points up to 30-min postinjection. Plasma concentrations at time zero (HTL⁰) and half-lives ($t_{0.5} = 0.69/k$) are calculated from plasma concentrations at time t (HTL ^{t}) according to the equation [HTL ^{t}] = [HTL⁰]·e^{- k t} , where k is a first-order rate constant. Hcy-thiolactone recovery calculations are based on assumptions that the i.p.-injected Hcy-thiolactone, being mostly neutral ($pK_a = 6.67$), distributes uniformly throughout the body and that blood constitutes 8 % of the mouse body weight (Data from [141])

Hcy-thiolactone-hydrolyzing enzyme(s), such as *Blmh*, is responsible for the metabolism of Hcy-thiolactone during its transition from the intraperitoneal cavity to the bloodstream in mice. In contrast, clearance of Hcy-thiolactone from the bloodstream is non-stereospecific [141].

To study the physiological role of *Blmh*, a mouse model with inactivated *Blmh* gene has been generated [272]. *Blmh*^{-/-} mice are found to be more sensitive to bleomycin toxicity than wild-type littermates, as expected. In addition, *Blmh*^{-/-} mice have somewhat lower body weight (by ~10 %), produce fewer pups in a litter (60 % compared to wild type), and are prone to tail dermatitis [272].

The *Blmh*-null mouse model facilitated examination of the role *Blmh* in Hcy-thiolactone metabolism and in the pathology caused by acute hyperhomocysteinemia. It was found that metabolic conversion of Hcy-thiolactone to Hcy is impaired in *Blmh*-null mice. For example, *Blmh*^{-/-} mice have elevated brain and kidney Hcy-thiolactone levels and excrete more Hcy-thiolactone in urine, compared with wild-type *Blmh*^{+/+} littermates [141]. These findings suggest that the kidneys and the brain are major sources of increased urinary Hcy-thiolactone excretion in *Blmh*^{-/-} mice.

Furthermore, significantly more of intraperitoneally injected *L*-Hcy-thiolactone is recovered in the plasma of *Blmh*^{-/-} mice relative to wild-type animals (14.4 % vs. 5.9 %, $P < 0.0001$). This means that, during its transit from the intraperitoneal cavity to the bloodstream, *L*-Hcy-thiolactone is metabolized less efficiently in *Blmh*^{-/-} mice compared with *Blmh*^{+/+} animals. The i.p.-injected Hcy-thiolactone is hydrolyzed to Hcy, which accumulates in the blood immediately after injection, but is subsequently cleared with a half-life of about 30 min. However, less Hcy is generated in *Blmh*^{-/-} mice, compared with wild-type *Blmh*^{+/+} littermates [141].

Blmh^{-/-} mice are also found to be more susceptible to Hcy-thiolactone neurotoxicity than wild-type littermates [141]. For example, when *Blmh*^{-/-} and *Blmh*^{+/+} mice are i.p. injected with convulsant doses of *L*-Hcy-thiolactone (3,700 nmol g⁻¹ body weight), seizures occur within 50 min. The incidence of seizures is significantly increased in *Blmh*^{-/-} mice compared with *Blmh*^{+/+} animals (93.8 % vs. 29.5 %, $P < 0.001$) (Table 3.10). Seizure latency (i.e., time to first seizure) is

significantly decreased for *Blmh*^{-/-} mice compared with *Blmh*^{+/+} animals (33.1 min vs. 41.2 min, *P* = 0.012). While only one mouse out of 44 *Blmh*^{+/+} mice (2.3 %) dies (at 61 min) after *L*-Hcy-thiolactone injection, the incidence of death is significantly increased for *Blmh*^{-/-} mice (to 46.9 %, *P* < 0.001) (Table 3.10) [141]. Although in the i.p. injection experimental model Hcy is also generated, Hcy levels are *decreased* by the inactivation of the *Blmh* gene. Thus, in this model, neurotoxicity can be assigned to Hcy-thiolactone, but not to Hcy. Taken together, the experiments with *Blmh*-null mouse model provide direct evidence that Hcy-thiolactone, rather than Hcy itself, is neurotoxic in vivo [141].

3.5.2 Urinary Excretion

In humans and mice endogenous Hcy-thiolactone is also eliminated by urinary excretion [93, 95]. Hcy-thiolactone concentrations in urine vary from 11 nM to 485 nM and are 100-fold higher than in plasma. Urinary Hcy-thiolactone accounts for 2.5–28 % of urinary tHcy. Relative renal clearance of Hcy-thiolactone is 0.2–7.0 of creatinine clearance, while clearance of tHcy is only about 0.001–0.003 [95]. Efficient urinary elimination of Hcy-thiolactone is typical for the waste or toxic products of normal human metabolism.

Calculations based on a normal human glomerular filtration rate of 180 L/day and a free plasma Hcy concentrations of 3 μM indicate that 99 % of filtered tHcy is reabsorbed [289]. A similar calculation for Hcy-thiolactone (0.12–2.4 nM in plasma and 286–415 nmol/day eliminated with urine) indicates that only 0.4–3.8 % is reabsorbed and >95 % of filtered Hcy-thiolactone was excreted in humans [95].

Urinary Hcy-thiolactone levels are negatively correlated to urinary pH (Fig. 3.9a). In contrast, urinary pH is not correlated to urinary tHcy levels (Fig. 3.9b). A possible mechanism facilitating the accumulation of Hcy-thiolactone in urine and explaining the pH dependence of urinary elimination of Hcy-thiolactone involves a gain of positive charge by Hcy thiolactone, which prevents its reabsorption by the renal tubules. Hcy-thiolactone has a *pK*_a = 6.67 [84] and exists in the positively charged acid form and the neutral base form (Reaction 3.3). Thus, at pH 7.4 in the blood, Hcy-thiolactone exists in the mostly neutral base form, whereas at pH 5–6 in the urine, the positively charged form predominates. Urinary acidification apparently maintains low fractional concentration of the uncharged base form of Hcy-thiolactone inside tubular lumen. This sustains continuous Hcy-thiolactone diffusion from the tubular cells (with high fractional concentration of the base form) into the lumen (with low fractional concentration of the base form).

In mice fed a normal chow diet, urinary Hcy-thiolactone concentration is 140 nM [93], similar to urinary Hcy-thiolactone value in humans [95]. However, in mice fed a hyperhomocysteinemic high-Met diet, urinary Hcy-thiolactone increases 25-fold, compared to mice fed a normal diet. The distributions of Hcy-thiolactone between plasma and urine in mice fed a normal diet and humans are

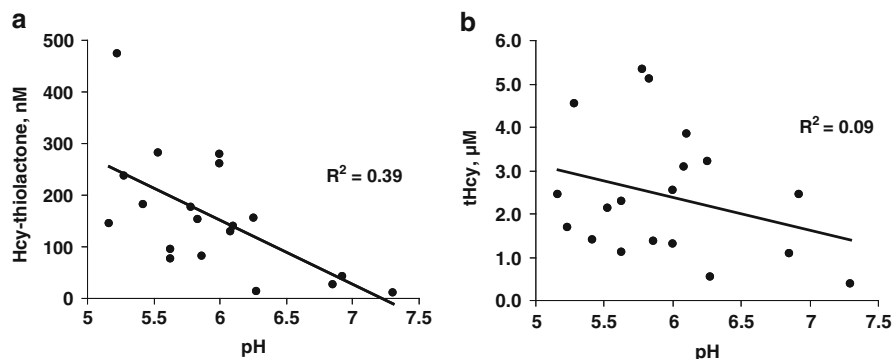


Fig. 3.9 Urinary concentrations of Hcy-thiolactone (a), but not tHcy (b), are negatively correlated with urinary pH (Reproduced from [95])

similar: much higher Hcy-thiolactone concentrations accumulate in urine than in plasma (the urinary/plasma Hcy-thiolactone ratio is 37 in mice [93] and 100 in humans [95]). This shows that urinary clearances of Hcy-thiolactone in mice and humans are similar and that in mice, similar to humans [95], >95 % of the filtered Hcy-thiolactone is excreted in the urine. Furthermore, significantly higher urinary/plasma Hcy-thiolactone ratios are found in mice fed hyperhomocysteinemic high-Met diet than in the animals fed a normal diet, which suggests that efficiency of urinary Hcy-thiolactone clearance increases in hyperhomocysteinemia.

Renal excretion removes a large fraction of Hcy-thiolactone [95] that would otherwise cause protein *N*-homocysteinylation and damage. Thus, urinary excretion is an important route of Hcy-thiolactone elimination, and intact renal function is important for Hcy-thiolactone detoxification in humans and mice.

3.6 Clinical Significance

As discussed in Sect. 2.2.3, numerous *ex vivo* studies with model cellular systems show that Hcy-thiolactone is cytotoxic, much more than Hcy itself (e.g., Table 2.2). Other studies have found that Hcy-thiolactone is associated with pathological conditions. For example, plasma Hcy-thiolactone is elevated under conditions predisposing to atherosclerosis and neurodegenerative diseases, such as caused by genetic CBS or MTHFR deficiencies in humans [93]. A basal Hcy-thiolactone level of 0.2 nM in unaffected individuals increases to 14.4 nM and 11.8 nM in *CBS*^{-/-} and *MTHFR*^{-/-} patients, respectively (Table 3.6). Although in these patients tHcy and *N*-Hcy-protein are elevated as well, the relative increase in Hcy-thiolactone significantly exceeds the increases in other Hcy metabolites (Table 3.12).

Table 3.12 Human genetic hyperhomocysteinemia: Mutations in *MTHFR* or *CBS* gene increase plasma Hcy-thiolactone and N-Hcy-protein (Recalculated from [93, 115])

Genotype (<i>n</i>)	Fold increase relative to unaffected individuals		
	N-Hcy-protein	Hcy-thiolactone	tHcy
<i>MTHFR</i> ^{-/-} , before therapy (1)	31.4	237	31.0
<i>MTHFR</i> ^{-/-a} (4)	9.0	59	7.5
<i>MTHFR</i> ^{+/-} (6)	2.2	2.5	1.2
Unaffected (9)	1 (0.49 ± 0.08 μM)	1 (0.2 ± 0.14 nM)	1 (6.7 ± 1.9 μM)
<i>CBS</i> ^{-/-a} (29)	6.2	72	7.2
<i>CBS</i> ^{-/-} , noncompliant (1)	24.7		43.9

^a*MTHFR*^{-/-} and *CBS*^{-/-} patients were on an Hcy-lowering therapy

In a study of 120 Chinese patients with type 2 diabetes and 40 healthy controls, tHcy and Hcy-thiolactone levels are associated with the development and progression of diabetic macrovasculopathy (MAVP) [362]. Plasma tHcy and Hcy-thiolactone are found to be significantly elevated in the patients (tHcy [25th and 75th quartiles]: 9.28 [7.51–11.82] vs. 5.64 [5.17–8.00] μM, $P = 0.01$; Hcy-thiolactone: 3.38 [2.94–4.73] vs. 2.91 [2.77–3.08] nM, $P < 0.05$). Plasma tHcy and Hcy-thiolactone levels in patients with MAVP are significantly higher compared with patients without MAVP (Hcy: 10.36 [7.67–12.45] vs. 7.85 [6.76–10.52] μM, $P < 0.05$; Hcy-thiolactone: 4.27 [3.02–5.11] vs. 3.12 [2.63–3.77] nM, $P < 0.05$).

Furthermore, plasma Hcy-thiolactone concentrations are positively correlated with urinary excretion of albumin/creatinine (Alb/Cr; $r = 0.285$, $P = 0.007$), duration of diabetes ($r = 0.249$, $P = 0.019$), age ($r = 0.233$, $P = 0.028$), and fibrinogen levels ($r = 0.289$, $P = 0.034$). However, plasma Hcy-thiolactone concentrations are negatively correlated with HDL levels ($r = -0.223$, $P = 0.037$) [362], consistent with the ability of HDL-associated PON1 protein to hydrolyze Hcy-thiolactone [81]. Binary logistic regression shows that Hcy-thiolactone, tHcy, smoking, serum triglyceride, and urinary Alb/Cr are significantly associated with the risk of diabetic MAVP ($P < 0.05$) [362]. Taken together, these findings suggest that Hcy-thiolactone provides a plausible chemical mechanism for explaining the toxicity of hyperhomocysteinemia to the human vascular endothelium discussed in a greater detail in Chapter 6).

An ongoing study under the direction of the author of this book is examining determinants of Hcy-thiolactone excretion in human urine in patients with coronary artery disease, with a major goal to evaluate the prognostic effect of urinary Hcy-thiolactone on the risk of subsequent myocardial infarction and mortality. The study is using urine samples from the Western Norway B Vitamin Intervention Trial (WENBIT) [55]. Another goal is to analyze how urinary Hcy-thiolactone levels are affected by B-vitamin supplementation. Also being analyzed are associations of Hcy-thiolactone levels with subsequent myocardial infarction (cardiovascular death, nonfatal myocardial infarction) and mortality. The usefulness of Hcy-thiolactone as a predictor of these outcomes will be determined. Associations of Hcy-thiolactone with CVD history, gender, smoking, hypertension, diabetes,

microalbuminuria, MTHFR 677C->T polymorphism, plasma B vitamins, betaine, tHcy, glomerular filtration rate (GFR), and circulating inflammation markers (CRP, neopterin, and KTR (kynurenine/ tryptophan ratio)) are also being investigated.

When completed, these studies will generate new information regarding the link between Hcy-thiolactone and CVD. The expected results will provide new diagnostic tools and will lead to new insights into the prevention and/or treatment of CVD.

Chapter 4

Discoveries of Protein S- and N-Homocysteinylation

In early studies, Hcy was identified in plasma and urine from patients with CBS or MTHFR deficiency [290, 291], but was undetectable in normal individuals. What was surprising in those studies was the inability to detect Hcy in tissues from CBS- or MTHFR-deficient patients [292, 293]. This suggested that a significant quantity of Hcy must have escaped detection by the conventional methods of amino acid analysis [294], possibly because Hcy was bound to protein via disulfide bonds and removed during the deproteinization step.

Indeed, a simple treatment with the disulfide-reducing agent 2-mercaptoethanol led to the discovery of Hcy in normal individuals and revealed that most plasma and tissue Hcy is linked to protein via disulfide bonds [91]. It was also demonstrated that exogenous Hcy added to plasma quickly becomes protein bound and can be quantitatively released by the 2-mercaptoethanol treatment. These findings provided the first evidence for a redox reaction of Hcy with plasma proteins that is now called protein S-homocysteinylation [41, 295]. Subsequent studies have identified albumin [103] and IgG [79] as the major carriers of S-linked Hcy in plasma. Albumin also carries most of plasma Cys [111], which forms a disulfide bond with the conserved Cys34 thiol [108, 296].

Protein N-homocysteinylation was first discovered in studies of Hcy-thiolactone metabolism in cultured human cells using [³⁵S]Met and [³⁵S]Hcy as tracers. Those studies demonstrated that fibroblasts from CBS-deficient patients and the oncogenically transformed cells from breast cancer patients produce more Hcy-thiolactone and N-Hcy-protein than normal cells from unaffected individuals [73]. The treatment of cells with the antifolate drug aminopterin increases N-Hcy-protein levels, in addition to increasing Hcy-thiolactone and Hcy. In human endothelial cells, the extent of protein N-homocysteinylation increases with

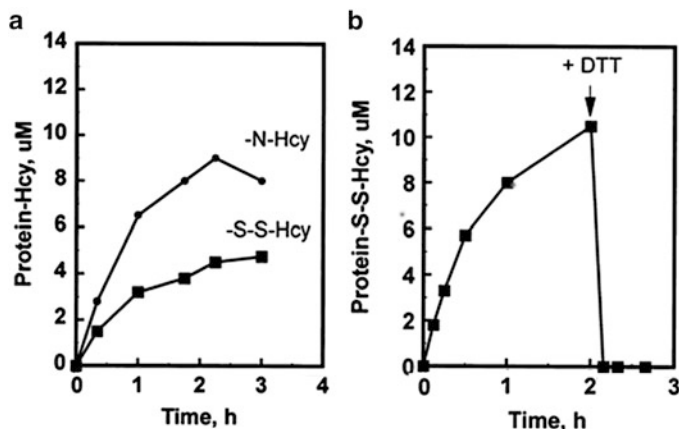


Fig. 4.1 Reactions of Hcy-thiolactone and Hcy in human serum. (a) Kinetics of protein *N*-homocysteinylation (filled circles) and protein *S*-homocysteinylation (filled squares) in the presence of 12 μM [³⁵S]Hcy-thiolactone. (b) Kinetics of protein *S*-homocysteinylation (filled squares) with 12 μM [³⁵S]Hcy. At the point indicated by an arrow, 10 mM DTT was added (Reproduced from [81])

increasing Hcy concentration (Fig. 3.7) and decreases with increasing levels of folic acid (which lowers Hcy levels) and HDL (which hydrolyzes Hcy-thiolactone) (Table 3.9) [74].

Subsequent studies have revealed that the incubation of human serum with [³⁵S]Hcy-thiolactone results in a progressive incorporation of the [³⁵S] radiolabel into protein (Fig. 4.1a). At 3 h, most of the [³⁵S] becomes protein bound and is precipitable by trichloroacetic acid. Treatment with dithiothreitol (DTT) of the [³⁵S]Hcy-thiolactone-modified serum protein releases only ~30 % of the incorporated [³⁵S] as free [³⁵S]Hcy, which suggests two modes of Hcy binding to protein [78, 81]. [³⁵S]Hcy in the DTT-resistant fraction of the [³⁵S]-protein adducts is bound to a side chain amino groups of protein lysine residues [78, 96]. Similar fractions of *N*-[³⁵S]Hcy-protein and *S*-[³⁵S]Hcy-protein adducts are obtained with [³⁵S]Hcy-thiolactone concentrations ranging from 10 nM to 1 mM [78].

Control experiments, with separately prepared *S*-[³⁵S]Hcy-protein, confirm that DTT treatment releases all disulfide-bound Hcy from the protein. For example, incubation of exogenous [³⁵S]Hcy with human serum results in a progressive formation of *S*-[³⁵S]Hcy-protein adducts that are precipitable with trichloroacetic acid. The treatment with DTT renders essentially all [³⁵S]Hcy from the *S*-[³⁵S]Hcy-protein adducts trichloroacetic acid soluble (Fig. 4.1b). Polyacrylamide gel electrophoresis under nonreducing conditions demonstrates that *S*-[³⁵S]Hcy-albumin represents most (>95 %) of *S*-[³⁵S]Hcy-protein in human serum [81].

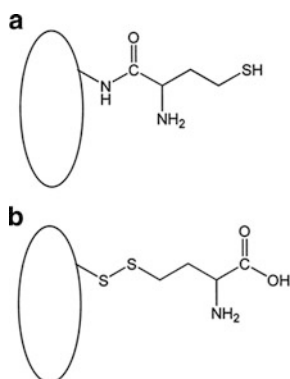


Fig. 4.2 Schematic structures of *N*-Hcy-protein and *S*-Hcy-protein adducts. (a) *N*-Hcy-protein: the carboxyl group of Hcy forms an amide bond with the side chain amino group of a protein lysine residue (Lys525 in human serum albumin). (b) *S*-Hcy-protein: the thiol of Hcy forms a disulfide bond with the side chain thiol of a protein cysteine residue (Cys34 in human serum albumin). The ovals represent protein molecules (Reproduced from [81])

These findings demonstrate that Hcy-thiolactone undergoes two major reactions in serum: (1) protein *N*-homocysteinylation and (2) enzymatic hydrolysis to Hcy, followed by protein *S*-homocysteinylation. The enzymatic hydrolysis to Hcy is catalyzed by serum Hcy-thiolactonase/PON1 [81]. Structures of *N*-Hcy-protein and *S*-Hcy-protein adducts are illustrated in Fig. 4.2a, b, respectively.

Chapter 5

N-Homocysteinyl-Proteins

5.1 Synthesis In Vitro

During Hcy-thiolactone biosynthesis, a high-energy bond of ATP is conserved in the thioester bond of Hcy-thiolactone (Reactions 3.7 and 3.8). This high-energy thioester bond is responsible for the chemical reactivity of Hcy-thiolactone toward amino groups in proteins [73, 78, 139].

When [³⁵S]Hcy-thiolactone is added to human plasma, it disappears with a half-life of ~1 h at 37 °C [78], 25-fold faster than expected from the rate of spontaneous Hcy-thiolactone hydrolysis [73]. After 3 h most of the radioactivity from [³⁵S]Hcy-thiolactone is incorporated covalently into protein [73, 78]. Reduction with DTT releases 30 % of the incorporated [³⁵S] radiolabel as free reduced [³⁵S]Hcy. The DTT-resistant fraction of the [³⁵S]Hcy-protein adducts is also resistant to treatments with reagents or enzymes that destroy ester or anhydride bonds, such as NaOH, hydroxylamine, or rabbit esterase. These findings indicate that protein amino groups form stable adducts with Hcy-thiolactone while protein hydroxyl and carboxyl groups are not involved. That protein lysine residues are involved is supported by the finding that Hcy-thiolactone reacts preferentially with free lysine forming an *N*-Hcy-Lys adduct that can be separated from unreacted lysine and Hcy-thiolactone by thin-layer chromatography [73]. Subsequent NMR studies have established that the adduct's structure is that of the isopeptide *Ne*-Hcy-Lys [72].

In vitro reactions of Hcy-thiolactone with lysine (Fig. 3.3b) and serum albumin (Fig. 3.3c) exhibit similar dependences on pH, which suggests that a similar mechanism is involved in both reactions. Furthermore, of the two ionic species of Hcy-thiolactone (Reaction 3.3), the positively charged acid form, less abundant at physiological pH = 7.4, is much more reactive than the more abundant neutral base form, both toward free lysine and protein lysine (Table 3.2).

Polyacrylamide gel electrophoretic analyses under reducing conditions show that in serum incubated with [³⁵S]Hcy-thiolactone, each serum protein becomes ³⁵S labeled. Bands corresponding to major serum proteins, such as albumin (67 kDa), γ -globulin (50 and 25 kDa), fibrinogen (47, 56, and 67 kDa), transferrin (80 kDa),

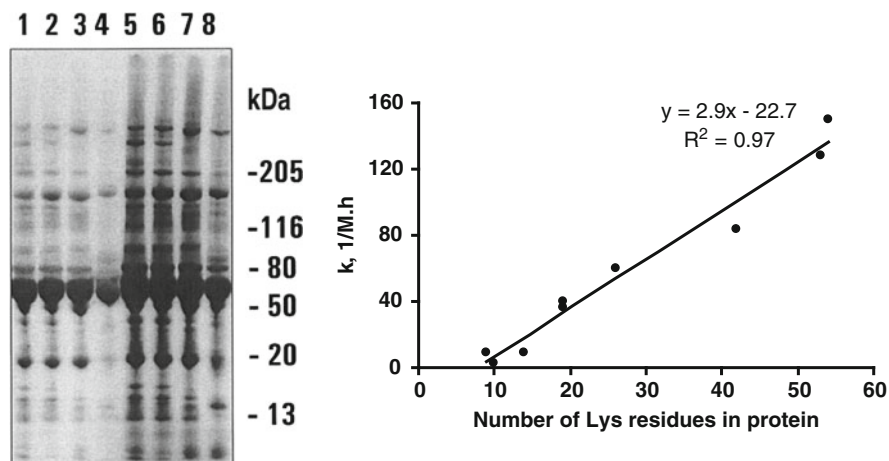


Fig. 5.1 The concentration of a protein and its lysine residues content are major determinants of *N*-homocysteinylation. *Left panel:* Individual proteins present in serum are susceptible to *N*-homocysteinylation. Human sera from three donors (lanes 1–3 and 5–7) and rabbit serum (lanes 4 and 8) are incubated with 10 μ M (lanes 1–4) or 100 μ M (lanes 5–8) [35 S]Hcy-thiolactone for 4 h at 37 $^{\circ}$ C and analyzed by SDS-PAGE on 4–20 % gels under reducing conditions. After electrophoresis, the gel was stained with *Coomassie Blue*, dried, and autoradiographed using Kodak BioMax MR X-ray film. The patterns of *Coomassie blue*-stained protein bands and 35 S-labeled bands are identical. An autoradiograph of the gel is shown. *Right panel:* A relationship between lysine residues content and protein's reactivity with Hcy-thiolactone. Second-order rate constants measured at 25 $^{\circ}$ C are plotted as a function of a number of lysine residues per mole of the following proteins: trypsin, RNase A, DNase I, cytochrome *c*, myoglobin, MetRS, hemoglobin, serum albumin, and transferrin (Reproduced from [78])

and α_2 -macroglobulin (189 kDa), are the most heavily 35 S labeled [78]. Overall, each serum protein is *N*-homocysteinylylated proportionally to its abundance (Fig. 5.1, left panel).

Individual *N*-Hcy-proteins are prepared *in vitro* by incubating a desired protein with Hcy-thiolactone at physiological pH and temperature. The *N*-homocysteinylation reaction is completed in 4 h at 37 $^{\circ}$ C; the reaction is ten times slower at 25 $^{\circ}$ C [78, 139]. Second-order rate constants for reactions of Hcy-thiolactone with individual purified proteins are listed in Table 3.3.

The number of lysine residues is the major determinant of protein's reactivity toward Hcy-thiolactone. For proteins that vary in size from 104 to 698 amino acid residues, there is a very good correlation ($r = 0.97$) between protein's lysine content and its reactivity with Hcy-thiolactone (Fig. 5.1, right panel) [78, 139]. Larger proteins, such as fibrinogen (3,588 amino acid residues) and low-density lipoproteins (LDL) (~5,000 amino acid residues), react with Hcy-thiolactone ~six-fold less efficiently than expected from their lysine contents (Table 3.3), suggesting great differences in lysine residues reactivities, possibly due to their different exposures to the solvent. Indeed, subsequent mass spectroscopic studies show that protein lysine residues exhibit different reactivities toward Hcy-thiolactone.

For example, Lys525 is a predominant site of *N*-homocysteinylation in human serum albumin [96], while in human fibrinogen α -Lys562, β -Lys344, and γ -Lys385 are predominant sites for *N*-homocysteinylation [215].

Studies with human serum albumin show that the rate of protein *N*-homocysteinylation is first order with respect to Hcy-thiolactone and protein concentration. The pH dependence of pseudo-first-order rate constant of *N*-homocysteinylation (Fig. 3.3c) is consistent with the ionization of Hcy-thiolactone with $pK_a = 6.67$ (Reaction 3.3) and suggests that the positively charged acid form of Hcy-thiolactone is more reactive with protein ($k = 764$ M/h) than the neutral base form ($k = 4$ M/h) (Table 3.2). The structures of the acid and base forms of Hcy-thiolactone are illustrated in Reaction 3.3. The reaction of Hcy-thiolactone with free lysine exhibits similar pH dependence (Fig. 3.3b).

Hcy is quantitatively recovered (as Hcy-thiolactone in the presence of a reducing agent) from *N*-Hcy proteins only by acid hydrolysis [78, 79]. In fact, this principle is a basis for quantification of *N*-linked Hcy content in proteins [297].

Analysis by Edman degradation of a sample of *N*-homocysteinylation human serum albumin, containing 3 mol Hcy/mol protein, shows that two major products are released in the first cycle (as a phenylthiohydantoin, PTH, derivative): PTH-Hcy and PTH-Asp. This outcome indicates that a free amino group is present on *N*-linked Hcy and that the α -amino group of N-terminal aspartic acid residue is not susceptible to *N*-homocysteinylation; if free amino groups were absent, no PTH-Hcy and PTH-Asp derivatives would have been recovered [78].

Mass spectrometric analyses have also identified that only ϵ -amino groups of *internal* lysine residues, but not α -amino group of the N-terminal amino acid, are targets for Hcy-thiolactone modification in human serum albumin [96, 212, 213], hemoglobin [68, 214], cytochrome *c* [298], fibrinogen [175, 215], and dynein [299].

So far, specific lysine residues susceptible to *N*-homocysteinylation are known for several proteins. In addition to the predominant Lys525 residue [96], six other lysine residues in human serum albumin are susceptible to the modification by Hcy-thiolactone in vitro: Lys4, Lys12, Lys137, Lys159, Lys205, and Lys212 [212, 213]. Seventeen lysine residues in human fibrinogen susceptible to the modification by Hcy-thiolactone have been identified [215]: five in α -subunit [Lys562 and Lys52 (major), Lys70, Lys81, and Lys129 (minor)], five in β -subunit [Lys344 and Lys396 (major), Lys148, Lys217, and Lys298 (minor)], and seven in γ -subunit [Lys385, Lys266, and Lys373 (major), Lys85, Lys95, Lys170, and Lys273 (minor)]. Three of these residues, α -subunit Lys52 and Lys129 and β -subunit Lys298, have originally been found to be susceptible to *N*-homocysteinylation in vitro by other investigators [175]. Fourteen sites in hemoglobin susceptible to the modification by Hcy-thiolactone have been identified [214]: seven in α -subunit (Lys7, 11, 16, 56, 90, 99, and 139) and seven in β -subunit (Lys8, 17, 59, 61, 66, 82, 95, 120, and 144). In cytochrome *c*, 4 lysine residues (Lys8 or -13, Lys86 or -87, Lys99, and Lys100) are susceptible to *N*-homocysteinylation in vitro [298].

5.2 Biological Formation

Biological formation of *N*-Hcy-protein has originally been discovered in tissue cultures of human cells (Fig. 3.7) [73, 74] and subsequently demonstrated to occur in humans [115] and mice [113]. The biological mechanism involves two steps. In the first step, Hcy is metabolically converted to Hcy-thiolactone by methionyl-tRNA synthetase (Reactions 3.7 and 3.8). In the second step, Hcy-thiolactone reacts with protein lysine residues, affording *N*-Hcy-protein (Reaction 3.4). These reactions have also been demonstrated in in vitro studies with purified components. Evidence supporting this mechanism includes precursor–product relationships between Hcy, Hcy-thiolactone, and *N*-Hcy-protein, observed both in ex vivo tissue culture studies and in vivo in humans and mice. The observations that mutations in genes encoding enzymes that participate in Hcy metabolism lead to increases in *N*-Hcy-protein levels add further support for this mechanism. Additional supporting evidence comes from the identification of specific *N*-Hcy-lysine residues in human serum albumin [96, 212, 213] and fibrinogen [215] in vivo.

5.2.1 *N*-Hcy-Protein Levels In Vivo

The demonstration that protein *N*-homocysteinylation occurs in intact organisms in vivo came with the discovery of *N*-linked Hcy in human plasma proteins, first reported in 2000 [139]. Subsequent studies have confirmed this finding and established that normal human plasma contains $0.49 \pm 0.08 \mu\text{M}$ [79, 115, 220], $0.51 \pm 0.11 \mu\text{M}$ [300], and $0.35 \pm 0.13 \mu\text{M}$ [301] protein *N*-linked Hcy. Several genetic and dietary factors that affect the levels of *N*-Hcy-protein in humans and mice have been identified. In humans, these include mutations in the *CBS* and *MTHFR* genes, polymorphic variations in the *PON1* gene. In mice, known determinants of *N*-Hcy-protein include *Cbs*, *Mthfr*, *Pcft*, *Pon1*, and *Blmh* genes, as well as the diet.

Protein *N*-linked Hcy increases significantly in hyperhomocysteinemia. For example, in *CBS*- and *MTHFR*-deficient patients, plasma protein *N*-linked Hcy levels are elevated up to 31.4-fold (Table 3.12). Furthermore, *CBS*-deficient patients have also up to ninefold higher plasma levels of prothrombotic *N*-Hcy-fibrinogen than normal subjects [115].

Genetic or nutritional disorders in Hcy or folate metabolism increase protein *N*-homocysteinylation also in experimental animals [113]. For example, the inactivation of *Cbs*, *Mthfr*, or the proton-coupled folate transporter (*Pcft*) gene causes 10–30-fold increase in plasma *N*-Hcy-protein levels (Tables 5.1 and 5.2). Liver *N*-Hcy-protein is elevated 3.4-fold in severely hyperhomocysteinemic *Cbs*-deficient mice, 11-fold in extremely hyperhomocysteinemic *Cbs*-deficient mice, and 3.6-fold in severely hyperhomocysteinemic *Pcft*-null mice. However, liver *N*-Hcy-protein levels are similar in *Mthfr*-null mice ($49.8 \pm 38.2 \text{ pmol/mg protein}$)

Table 5.1 Mouse genetic hyperhomocysteinemia: inactivation of folate (*Mthfr*, *Pcft*) or Hcy (*Cbs*) metabolism genes increases *N*-Hcy-protein levels (Recalculated from [113])

Genotype (<i>n</i>)	Fold increase relative to wild-type littermates			
	<i>N</i> -Hcy-protein		tHcy	
	Plasma	Liver	Plasma	Liver
<i>Mthfr</i> ^{-/-} (7)	6.3	1.4	8.6	1.1
<i>Pcft</i> ^{-/-} (4)	24.7	3.6	75.0	5.1
<i>Cbs</i> ^{-/-} (4)	8.1		58.3	
<i>Tg-S466L Cbs</i> ^{-/-} (4)	12.6		60.9	
<i>Tg-I287T Cbs</i> ^{-/-} (4)	10.4	11.3	143.2	75.7
<i>Tg-hCBS Cbs</i> ^{-/-} (4)	4.2	3.4	27.4	3.8

Table 5.2 Tissue levels of *N*-Hcy-protein and tHcy in *Pcft*^{-/-} mice and wild-type *Pcft*^{+/+} littermates

Organ	<i>Pcft</i> genotype	<i>N</i> -Hcy, pmol/1 mg protein	<i>N</i> -Hcy, fold increase in <i>Pcft</i> ^{-/-} vs. <i>Pcft</i> ^{+/+}	tHcy, pmol/1 mg protein	tHcy, fold increase in <i>Pcft</i> ^{-/-} vs. <i>Pcft</i> ^{+/+}
Brain ^a	+/+	47 ± 10	1.2	113 ± 13	1.2
	-/-	58 ± 8		138 ± 59	
Heart ^b	+/+	112 ± 22	2.8	166 ± 33	4.3
	-/-	318 ± 98		703 ± 267	
Lungs ^b	+/+	229 ± 70	1.6	348 ± 92	2.8
	-/-	362 ± 113		969 ± 524	
Liver ^{b,c}	+/+	87 ± 32	3.7	299 ± 92	5.1
	-/-	318 ± 98		1,529 ± 391	
Kidney ^b	+/+	126 ± 49	1.8	499 ± 194	2.2
	-/-	228 ± 38		1,109 ± 152	
Plasma ^c	+/+	46 ± 12	24.8	36 ± 11	75.3
	-/-	1,132 ± 264		2,696 ± 566	

Jakubowski and Perla-Kajan, unpublished data

^a*p* = 0.14–0.22

^b*p* < 0.005 for the differences in *N*-Hcy-protein or tHcy between *Pcft*^{-/-} and *Pcft*^{+/+} mice

^cData from [113]

and wild-type littermates (34.7 ± 12.7 pmol/mg protein). In folate metabolism deficiencies (*Mthfr*, *Pcft*), *N*-Hcy-protein levels increase much more in the plasma than in the liver or other organs, while in Hcy metabolism deficiency (*Cbs*), similar increases in *N*-Hcy-protein are observed in both the plasma and the liver (Tables 5.1 and 5.2).

Protein *N*-homocysteinylolation is reversibly modifiable by a diet (Table 5.3). For example, plasma *N*-Hcy-protein increases 11.6-fold in mice fed a high-methionine diet for 2 weeks, compared with animals fed a normal chow diet [113]. The increase in *N*-Hcy-protein reflects 36-fold and 14-fold increases in plasma tHcy and Hcy-thiolactone levels, respectively. After replacing the high-methionine diet with a normal chow diet, plasma *N*-Hcy-protein decreases sixfold after 2 weeks but remains twofold elevated compared with mice fed

Table 5.3 Plasma *N*-Hcy-protein, Hcy-thiolactone, and tHcy are reversibly modified by a diet in wild-type C57BL/6 J mice (Data from [113])

Diet (eight mice/group)	<i>N</i> -Hcy-protein (μM)	Hcy-thiolactone (nM)	tHcy (μM)
Control, 0 weeks	1.89 ± 0.70	5.74 ± 2.42	3.45 ± 0.30
High-Met, 2 weeks	22.1 ± 13.5	79.4 ± 11.9	126 ± 76
High-Met, 2 weeks control, 4 weeks	3.60 ± 1.11	4.47 ± 0.97	5.47 ± 2.83

only a normal chow diet. At the same time plasma tHcy and Hcy-thiolactone return to normal values. These findings are consistent with much slower turnover of *N*-Hcy-protein (half-life 10.2 h) compared with the turnover of tHcy (half-life 26.2 min) and Hcy-thiolactone (half-life 5.0 min) in the mouse (Fig. 5.4) [140, 141].

The discovery that PON1 has the ability to hydrolyze Hcy-thiolactone led to a hypothesis that PON1 protects against protein *N*-homocysteinylation [81]. Support for this hypothesis came from findings showing that when serum is supplemented with Hcy-thiolactone, much less *N*-Hcy-protein accumulates in the serum from human donors with high Hcy-thiolactonase/PON1 activity compared with donors with low Hcy-thiolactonase/PON1 activity [152]. The lowest extent of protein *N*-homocysteinylation is observed in rabbit serum [152] which has the highest Hcy-thiolactonase/PON1 activity (six times that of an average human serum) [153]. Thus, high Hcy-thiolactonase activity affords better protection against protein *N*-homocysteinylation in vitro than the low activity. This inverse relationship between the levels of *N*-Hcy-protein and Hcy-thiolactonase activity of PON1 is also observed in vivo in humans. In fact, plasma *N*-Hcy-protein is negatively correlated with serum Hcy-thiolactonase activity ($r = -0.43$, $P = 0.01$) in CBS-deficient patients [250]. However, in contrast to the activity of PON1 measured with the natural substrate Hcy-thiolactone, enzymatic activities of the PON1 protein measured with artificial substrates correlate less strongly ($r = -0.36$, $P = 0.025$ for paraoxonase activity) or do not correlate at all (phenyl acetate hydrolase and γ -thiobutyrolactone hydrolase activities) with plasma *N*-Hcy-protein. Furthermore, the inverse in vivo relationship between Hcy-thiolactonase activity and *N*-Hcy-protein is recapitulated in separate in vitro *N*-homocysteinylation experiments with [^{35}S]Hcy-thiolactone and sera from CBS-deficient subjects. Taken together, these findings provide evidence that the Hcy-thiolactonase activity of PON1 is a major determinant of plasma *N*-Hcy-protein levels in vivo in humans [250].

In related experiments, the level of *N*-linked Hcy in plasma proteins has been found to increase in rats in response to lowering serum Hcy-thiolactonase activity of PON1 by treatment with the lipid metabolism-regulating hormone leptin. As leptin administration has no effect on plasma total Hcy, it has been suggested that the decreased capacity to metabolize Hcy-thiolactone and concomitant increase in protein *N*-homocysteinylation contribute to the pro-atherogenic effect of chronic hyperleptinemia [302].

Table 5.4 Levels of *N*-linked Hcy in different proteins (Compiled from [79, 297])

Specie	Protein (Mw, kDa)	<i>N</i> -Hcy/protein, mol/mol \times 1,000
Human	Ferritin (443)	470 \pm 20
	Hemoglobin (64)	14.1 \pm 4.1
	Albumin (68)	3.6
	γ -Globulin (150)	3.6
	Fibrinogen (340)	1.0
	LDL (500)	1.0
	Transferrin (80)	0.8
	Antitrypsin (51)	0.7
Horse	HDL (150)	0.4
	Ferritin (443)	515 \pm 75
	Apoferritin (443)	480 \pm 70
	Catalase (250)	9.0
	Myoglobin (17.1)	1.44 \pm 0.04
	Cytochrome <i>c</i> (11.8)	1.07 \pm 0.17
	Aldolase (25.3)	2.1
Bovine	Thyroglobulin (669)	25.3 \pm 2.0
	α -Crystallin (36)	2.6 \pm 1.3
	Histone (15)	0.33 \pm 0.05
	Carbonic anhydrase (29)	0.2
Pig	Esterase (60)	13.0 \pm 2.5
	Elastase (26.4)	4.16 \pm 1.12
	Acylase (45)	2.85 \pm 0.00
Chicken	Ovalbumin (45)	3.82 \pm 1.80
	Lysozyme (17)	0.06

5.2.1.1 Cellular Proteins

Commercially available purified proteins each contain *N*-linked Hcy, at levels as high as 0.470 and 0.515 mol Hcy/mol protein for human and equine ferritins, respectively, to as low as 0.00006 mol Hcy/mol protein for chicken lysozyme (Table 5.4). Similar levels of *N*-linked Hcy are found in iron-loaded ferritin and iron-free apoferritin (Table 5.4), indicating that the presence of iron does not interfere with the assay used. Most proteins contain intermediate levels of *N*-linked Hcy, from about 0.001 mol Hcy/mol protein for cytochrome *c* and myoglobin to 0.01–0.025 mol Hcy/mol protein for catalase, esterase, and thyroglobulin.

5.2.1.2 Blood Proteins

Examination of purified human blood proteins demonstrates that normal human hemoglobin, serum albumin, and γ -globulins contain 0.0036–0.0060 mol *N*-Hcy/mol protein, while fibrinogen, LDL, HDL, transferrin, and antitrypsin contain lower levels, 0.0004–0.0010 mol *N*-Hcy/mol protein [79]. Recalculation of these values (by taking into account normal levels of individual blood proteins) shows that the

Table 5.5 Concentrations of Hcy carried on proteins in normal human blood (Recalculated from the data of [79])

Protein	Protein <i>N</i> -linked Hcy (nM)	Protein <i>S</i> -linked Hcy (nM)
Hemoglobin ^a	27,800	3,300
Albumin ^b	2,800	7,300
γ -Globulin ^b	700	3,500
Fibrinogen ^b	14	<19
Transferrin ^b	28	<5
Antitrypsin ^b	24	7
HDL ^b	23	47
LDL ^b	17	9

^aConcentrations in erythrocytes^bPlasma concentrations**Table 5.6** *N*-homocysteinylation at Lys525 of albumin is increased in human CBS deficiency (Data from [213])

Genotype (<i>n</i>)	<i>N</i> -Hcy-Lys525 peptide (%)
<i>CBS</i> ^{+/+} (29)	1.02 ± 1.21
<i>CBS</i> ^{-/-} (15)	3.99 ± 2.60*

**P* = 0.0007

concentration of *N*-linked Hcy carried on hemoglobin in erythrocytes is 27.8 μ M (Table 5.5), exceeding the concentration of plasma tHcy. Similar recalculation shows that albumin and γ -globulin carry micromolar concentrations of *N*-linked Hcy, whereas fibrinogen, transferrin, antitrypsin, HDL, and LDL carry nanomolar concentrations of *N*-linked Hcy.

The value calculated for *N*-Hcy-albumin (0.36 mol% = 2.8 μ M in plasma, Table 5.4) is higher than the value of *N*-Hcy-protein measured directly with normal human plasma (0.51 μ M) and closer to the mean values measured in plasma from hyperhomocysteinemic CBS- and MTHFR-deficient patients on a Hcy-lowering therapy (3.02 μ M and 4.4 μ M, respectively) [115]. The relatively high content of *N*-linked Hcy in the commercial albumin preparations may possibly be due to demethylation of methionine residues of albumin during its purification from plasma. The values obtained for *N*-Hcy-albumin using a chemical assay [115] are similar to the values obtained with the LC-MS assay, which shows that *N*-Hcy-Lys525-albumin constitutes 1.0 % and 4.0 % of plasma total albumin in healthy controls and CBS-deficient patients, respectively (Table 5.6) [213].

The value calculated for *N*-Hcy-fibrinogen (0.1 mol% = 14 nM, Table 5.4) is consistent with direct assays of fibrinogen isolated from human subjects, which show that in normal plasma, *N*-Hcy-fibrinogen levels are 35.8 ± 14.3 nM [115]. The *N*-linked Hcy carried on *N*-Hcy-fibrinogen constitutes about 10 % of total *N*-linked Hcy present in normal plasma protein (0.35 ± 0.13 to 0.51 ± 0.11 μ M [79, 115, 300, 301]).

The value calculated for *N*-Hcy-HDL (0.04 mol% = 23 nM) is much smaller than that obtained by a semiquantitative Western blot immunoassay of *N*-Hcy-ApoAI in HDL isolated from human plasma (0.46–5.2 μ M or 1.0–7.4 % of total ApoAI) [303]. Possible reasons for the discrepancy are discussed in Sect. 5.5.4 of this book.

Table 5.7 Levels of *N*-linked Hcy in albumin and hemoglobin from different species (Data from [297])

Specie	<i>N</i> -Hcy/albumin, mol/mol \times 1,000	<i>N</i> -Hcy/hemoglobin, mol/mol \times 1,000
Human	2.65	14.1 \pm 4.1
Baboon		12.7 \pm 0.4
Bovine	3.17 \pm 1.56	30.7 \pm 0.8
Pig	3.41 \pm 1.51	16.8 \pm 5.5
Rat	4.86 \pm 1.61	82.8 \pm 29.1
Mouse	8.61 \pm 0.05	

Protein *N*-linked Hcy occurs in serum albumin from various organisms, including human, sheep, pig, rabbit, rat, mouse, and chicken [79]. Comparisons across the species show that the rodent proteins contain more *N*-linked Hcy than the primate proteins. For example, more *N*-linked Hcy is present in albumins from the rat (0.00486 mol/mol) and the mouse (0.00861 mol/mol) than in human albumin (0.00265 mol/mol) [297]. Rat hemoglobin contains more *N*-linked Hcy than human and baboon hemoglobins (0.0828 mol/mol vs. 0.0141 mol/mol and 0.0127 mol/mol, respectively) (Table 5.7). This could reflect a higher relative concentration of free Hcy in rodents as compared to humans [304]. However, human and pig albumins contain similar levels of *N*-linked Hcy, as does human and pig hemoglobins [297], indicating that human and pigs are alike in this regard (Table 5.7).

About 5–15 times more *N*-linked Hcy is present in hemoglobin than in serum albumin (0.013–0.083 vs. 0.0027–0.008 mol/mol, Table 5.7) from each species examined, from human to rat [297]. As the *in vitro* rates of the modification with Hcy-thiolactone are similar for the two proteins [78], this finding can be explained by much slower turnover of hemoglobin compared to albumin (103 days for hemoglobin vs. 19 days for albumin in humans). Taking the blood hemoglobin concentration as 2.2 mM (150 mg/mL), one can calculate that the concentration of *N*-Hcy-hemoglobin is 28.7–183.1 μ M, i.e., much higher than the concentration of tHcy (4–8 μ M) in the normal mammalian blood. These data extend to other mammalian species the original finding that a significant fraction of Hcy present in human blood is circulating as *N*-Hcy-hemoglobin [79].

Of almost three dozen individual proteins examined, only one, human transthyretin, has been reported not to contain *N*-linked Hcy [104]. However, the detection limit of the LC–MS method used in that study was 1 % relative to total transthyretin [104], i.e., several orders of magnitude less sensitive than that of the HPLC with fluorescence detection method, which allows quantification of as little as 0.00006 mol *N*-linked Hcy/mol protein [297]. Thus, the inability to detect protein *N*-linked Hcy in transthyretin is most likely due to inadequate sensitivity of the method.

5.2.1.3 Collagen

Severely hyperhomocysteinemic *Tg-I278T Cbs^{-/-}* mice (plasma tHcy = 272 \pm 50 μ M vs. 1.9 \pm 1.6 μ M in wild-type *Tg-I278T Cbs^{+/+}* littermates) [305] have elevated plasma *N*-Hcy-protein (16.6 \pm 4.1 μ M vs. 1.9 \pm 1.6 μ M in wild type) [113] and

Table 5.8 *N*-linked Hcy and *S*-linked Hcy levels in human hair keratin [308]

Gender (<i>n</i>)	<i>N</i> -Hcy, pmol/mg hair	<i>S</i> -Hcy, pmol/mg hair	<i>N</i> -Hcy/(<i>N</i> -Hcy + <i>S</i> - Hcy)	SDS-soluble <i>N</i> -Hcy fraction
Female (11)	95 ± 39	126 ± 41	0.36 ± 0.10	0.38 ± 0.08
Male (7)	82 ± 41	181 ± 64	0.31 ± 0.11	0.49 ± 0.09

exhibit connective tissue abnormalities similar to those observed in CBS-deficient human patients [46]. Collagen prepared from the skin of these mice using the acetic acid extraction method shows protein bands characteristic of type I collagen on SDS-PAGE gels. Analysis of *N*-linked Hcy content in these collagen preparations shows that *Tg-I278T Cbs*^{-/-} mice have 18-fold higher skin *N*-Hcy-collagen levels than *Tg-I278T Cbs*^{+/+} littermates (89.9 ± 25.1 vs. 5.0 ± 2.4 pmol/mg skin) [306]. Similar elevation in *N*-linked Hcy in the *Cbs*-deficient mice is observed in bone collagen. These findings demonstrate that collagen is a target for *N*-homocysteinylation in vivo in mice [306].

5.2.1.4 Milk Protein

The *N*-linked protein Hcy has also been discovered in other biological fluids. For example, commercial cow milk contains 1.09 ± 0.01 μM protein *N*-linked Hcy and 3.45 ± 0.25 μM tHcy, whereas cow whey contains 1.51 ± 0.34 μM protein *N*-linked Hcy and 5.4 ± 2.5 μM tHcy [297]. Human milk contains 0.28 ± 0.09 μM (*n* = 3) protein *N*-linked Hcy and 2.3 μM tHcy. The presence of protein *N*-linked Hcy has not been previously described in milk or other foodstuffs, but the levels of tHcy in milk are comparable to tHcy levels reported for other foodstuffs examined thus far (Roquefort cheese, white bread, tuna, and pig liver; [307]).

5.2.1.5 Hair Keratin

Human and animal hair keratin contains significant amounts of *N*-linked Hcy [308]. Normal human hair contains 82–95 pmol *N*-Hcy/mg hair (Table 5.8). *N*-linked Hcy comprises 31–36 % of all Hcy content in human hair keratin, while the remaining 64–69 % is *S*-linked. Similar levels of *N*-Hcy-keratin are present in mouse pelage hair (Table 5.9). Other mammalian species examined, such as the rat, the rabbit, the dog, the cat, the goat, the sheep, and the horse, all contain *N*-Hcy-keratin in their hair. *N*-Hcy-keratin is also present in feathers of birds, such as chicken, pigeons, and sea gulls.

More *N*-Hcy-keratin accumulates in pelage hair from hyperhomocysteinemic mice [308]. For example, *N*-Hcy-keratin is elevated 12-, 6.3-, or 2.7-fold in pelage from *Cbs*^{-/-}, *Cse*^{-/-}, or *Mthfr*^{-/-} mice, compared with wild-type animals, respectively (Table 5.9). The increase in *N*-linked Hcy content is associated with diminished solubility of hair keratin in 2 % SDS, most pronounced in *Cbs*^{-/-} mice, in

Table 5.9 *N*-linked Hcy and *S*-linked Hcy levels in mouse pelage keratin [308]

Genotype (<i>n</i>)	<i>N</i> -Hcy, pmol/mg hair	<i>S</i> -Hcy, pmol/mg hair	<i>N</i> -Hcy/(<i>N</i> -Hcy + <i>S</i> - Hcy)	SDS-soluble <i>N</i> -Hcy fraction
Wild type (12)	87 ± 10	127 ± 10	0.59 ± 0.05	0.25 ± 0.05
<i>Cbs</i> ^{-/-} (9)	1,056 ± 104	2,138 ± 360	0.33 ± 0.03	0.04 ± 0.00
<i>Cse</i> ^{-/-} (5)	546 ± 41	682 ± 129	0.55 ± 0.03	0.14 ± 0.01
<i>Mthfr</i> ^{-/-} (4)	237 ± 23	356 ± 74	0.40 ± 0.06	0.21 ± 0.03

which only 4 % is SDS soluble, compared with 25 % SDS-soluble *N*-Hcy-keratin in wild-type animals. These findings suggest that *N*-homocysteinylation causes keratin damage.

In vitro studies have shown that *N*-homocysteinylation causes protein damage (Fig. 5.11). The findings that increased keratin *N*-homocysteinylation in hyperhomocysteinemic mice decreases its solubility provide the first evidence that protein damage induced by *N*-homocysteinylation occurs in vivo. The defect in keratin solubility associated with *N*-homocysteinylation [308] can explain pelage abnormalities observed in *Cbs*^{-/-} mice [309].

5.2.2 Site-Specific *N*-Homocysteinylation In Vivo

Identification of specific *N*-Hcy-Lys residues in proteins in vivo provides direct support for a conclusion that protein *N*-homocysteinylation in humans occurs by a mechanism involving the reaction of Hcy-thiolactone with protein lysine residues (Reaction 3.4). So far, site-specific *N*-homocysteinylation in vivo has been analyzed for human serum albumin [212, 213], fibrinogen [215], and dynein [299].

Three albumin residues, Lys525, 137, and 212, are found to be *N*-homocysteinylation in vivo in human plasma from CBS-deficient patients and unaffected individuals, with Lys525 being the predominant in vivo-modified site (Fig. 5.2). Albumin peptide containing *N*-Hcy-Lys525 is identified in essentially all analyzed plasma samples (43 out of 44), including those that had the lowest tHcy concentration (9.9 μM), whereas peptides containing *N*-Hcy-Lys137 and *N*-Hcy-Lys212 are identified in albumin from CBS-deficient patients whose plasma tHcy concentration was elevated, at least 34.9 ± 11.0 μM and 131 ± 21 μM, respectively [212].

Three lysine residues carry *N*-linked Hcy in fibrinogen isolated from CBS-deficient patients, one in each subunit: Lys562 in α-subunit, Lys344 in β-subunit, and Lys385 in γ-subunit (Fig. 5.3). These three in vivo *N*-homocysteinylation sites are also predominant sites for fibrinogen *N*-homocysteinylation in vitro [215].

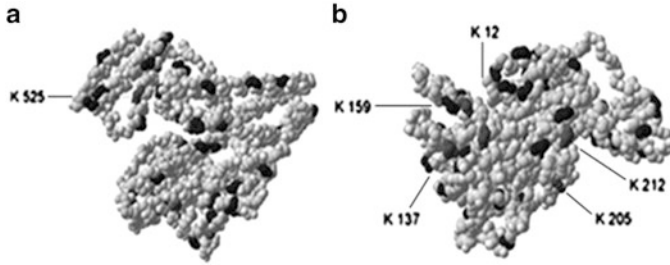


Fig. 5.2 A model of the crystallographic structure of human serum albumin based on 1 bm0.pdb. Lysine and *N*-Hcy-lysine residues are highlighted with *black* and *dark gray* color, respectively. (a) Front view. (b) A Back view. This pdb structure is missing Lys4. Lys residues 525, 205, and 137 are found to be *N*-homocysteinylated in vivo (Reproduced from [212])



Fig. 5.3 Schematic representation of polypeptide chain composition and independently folded domains (boxed) in fibrinogen. Lysine residues *N*-homocysteinylated in vivo and in vitro are indicated by *dark-blue circles*, while residues susceptible to *N*-homocysteinylation in vitro are indicated by *red circles* [215]

In rat hippocampal neuronal cells cultured in folate-deficient media, motor proteins kinesin and dynein become *N*-homocysteinylated, which leads to protein aggregation and reduced interactions with tubulin [299]. Similar changes occur when neuronal cells are treated with Hcy-thiolactone, suggesting that kinesin and dynein *N*-homocysteinylation cause protein aggregation and prevent their physiological interactions with tubulin. LC-MS analyses identify Lys1218 in the microtubule-binding domain of dynein as being *N*-homocysteinylated, which could account for the diminished interaction with tubulin [299].

These findings strongly support a conclusion that *N*-Hcy-proteins are formed in mammalian organisms as a result of posttranslational modification of proteins by Hcy-thiolactone.

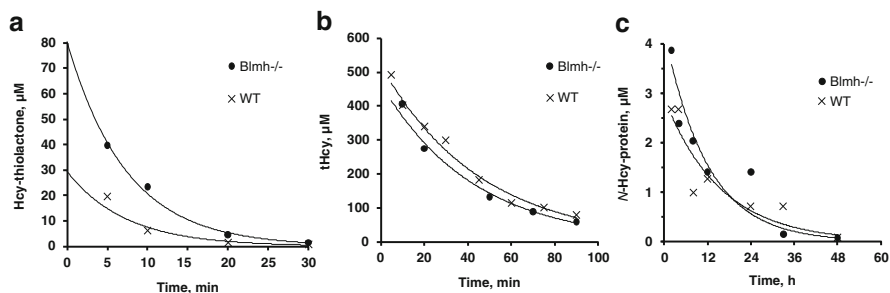


Fig. 5.4 Kinetics of plasma Hcy-thiolactone (a), total Hcy (b), and *N*-Hcy-protein (c) turnover in mice. For Hcy-thiolactone (a) and total Hcy (b) turnover experiments, mice have been injected i.p. with 600 nmol L-Hcy-thiolactone/g body weight. For *N*-Hcy-protein (c) turnover experiments, 2,850 nmol L-Hcy-thiolactone/g body weight L-Hcy-thiolactone was used. Metabolites were analyzed at indicated times post-injection and data points were fitted to an exponential equation $[A^t] = [A^0]e^{-k \cdot t}$, where k is a first-order rate constant, $[A^t]$ is metabolite concentration measured at time t , and $[A^0]$ is metabolite concentration extrapolated to time zero. Representative kinetics obtained for individual knockout *Blmh*^{-/-} (filled circle) and wild-type *Blmh*^{+/+} (multiplication sign) mice are shown (Reproduced from [141])

5.3 Turnover

An indirect evidence for the proteolytic degradation of *N*-Hcy-protein is provided by the discovery of anti-*N*-Hcy-protein IgG autoantibodies [172, 310], which specifically recognize *Ne*-Hcy-Lys epitopes and whose formation can only be initiated by proteolytic degradation of *N*-Hcy-protein to antigenic peptides that are then displayed on the cell surface. First direct evidence for *N*-Hcy-protein turnover came from mouse studies. Wild-type mice fed with a high-Met diet accumulate up to 22 μ M *N*-Hcy-protein in plasma [113]. These mice have also elevated plasma Hcy-thiolactone (from 6 to 80 nM) and tHcy levels (from 3.5 to 126 μ M). Shifting the mice from high-Met to normal chow diet normalizes Hcy-thiolactone and tHcy levels and lowers *N*-Hcy-protein to 3.6 μ M, indicating that *N*-Hcy-proteins are turned over. Direct kinetic measurements indicate that *N*-Hcy-protein turns over with a half-life of 10.2 ± 1.4 h in the mouse plasma [141] (Fig. 5.4). The clearance of plasma *N*-Hcy-protein is 24-fold slower than the clearance of plasma Hcy (half-life of 26.2 min) and 120-fold slower than the clearance of plasma Hcy-thiolactone (half-life of 5.1 min) (Fig. 5.4) [140, 141]. *N*-Hcy-protein is turned over by proteolytic degradation with the liberation of the isopeptide *Ne*-Hcy-Lys (Fig. 5.5) [72].

5.3.1 *Ne*-Homocysteinyl-Lysine

5.3.1.1 Chemical Synthesis

Ne-Hcy-Lys isopeptide has been originally identified in vitro on TLC plates as a product of facile reaction of Hcy-thiolactone with lysine [73, 139]. This reaction

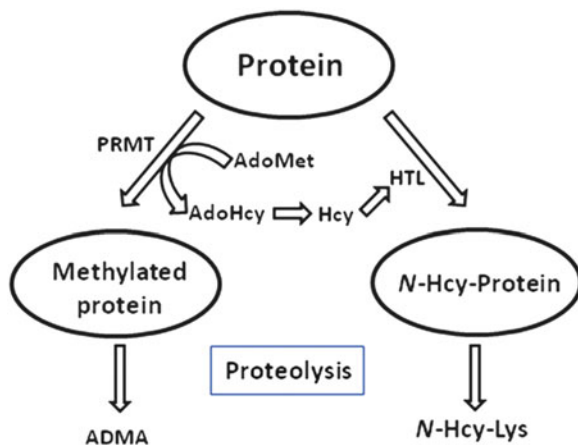
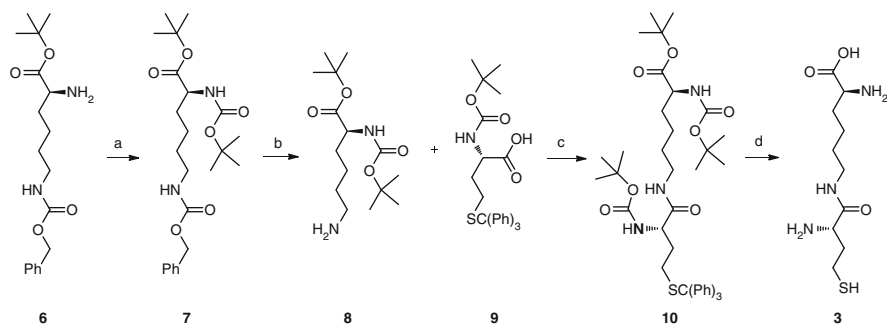


Fig. 5.5 *N*-Hcy-Lys and asymmetric dimethylarginine (ADMA) are derived from the proteolysis of modified proteins. Arginine residues in proteins are methylated by protein arginine methyltransferase (PRMT), which uses *S*-adenosylmethionine (AdoMet) as a methyl donor and produces *S*-adenosylhomocysteine (AdoHcy). Hcy derived from the enzymatic hydrolysis of AdoHcy is converted by methionyl-tRNA synthetase to Hcy-thiolactone (HTL), which modifies protein lysine residues, affording *N*-Hcy-protein. Subsequent proteolytic degradation of *N*-Hcy-protein affords the isopeptide *N*-Hcy-Lys (Reprinted from [86])

has been utilized to synthesize *Ne*-Hcy-Lys isopeptide on a preparative scale [72]. *D,L*-Hcy-thiolactone hydrochloride (5 mmol) is incubated with *L*-lysine (5 mmol) in 100 mL 0.2 M sodium phosphate buffer, pH 7.4, 0.2 mM EDTA (24 h, room temperature). The rate of *Ne*-Hcy-Lys formation increases about twofold when pH increases from 6.0 to 7.4 and does not significantly change between pH 7.4 and 9.0. The yield increases 1.7-fold and 1.4-fold at pH 8.0 and 9.0, respectively, relative to the yield at pH 6.0. The reaction product, *Ne*-Hcy-Lys, is purified by preparative HPLC using a reversed-phase X Bridge Prep C18 column (19 × 100 mm, 5 μm, from Waters). Fractions containing *Ne*-Hcy-Lys isopeptide, a predominant product eluting at 2 min, are collected dried out under vacuum to afford a white powder. The isopeptide structure is confirmed by ¹H NMR (300 MHz, D₂O): δ = 4.10 (*t*, *J* = 6.6 Hz, 1H, CHNH₂), 4.04 (*t*, *J* = 6.6 Hz, 1H, CHNH₂), 3.32–3.17 (m, 2H, CH₂NHC(O)), 2.61 (dt, *J* = 7.2 Hz, *J* = 2.4 Hz, 2H, CH₂SH), 2.24–2.11 (m, 2H, CH₂CH₂SH), 2.03–1.85 (m, 2H, HOOCCH(NH₂)CH₂), 1.64–1.55 (m, 3H, CH₂CH₂NHC(O)), SH), and 1.51–1.36 (m, 2H, CH₂CH₂CH₂NHC(O)) (chemical shifts δ in ppm, coupling constants *J* in Hz) [72].

Ne-Hcy-Lys (**3**) has also been synthesized in a solution phase using common procedures for peptide synthesis (Reaction 5.1) starting from commercially available lysine derivative (*ε*-*N*-Cbz-Lys-O-*t*Bu) (**6**) [311]. The α-NH- group in **6** is protected by introducing the Boc-protecting group (**7**). The carbobenzyoxy group from the ε-NH is selectively removed by catalytic hydrogenation using 10 % Pd/C to obtain α-*N*-Boc-Lys-O-*t*Bu (**8**). The fully protected isopeptide **10** is synthesized via amide bond formation between the free ε-NH- of **8** and the activated



Reaction 5.1 Synthesis of *Ne*-Hcy-Lys isopeptide (**3**). Reaction conditions: (a) Ar, (Boc)₂O, NaHCO₃, CHCl₃, reflux/1.5 h, 95 %. (b) H₂, 10 % Pd/C, EtOH, rt/16 h, 97 %. (c) Et₃N/HOBT/DMAP/EDCI, DMF, rt/24 h, 90 %. (d) Ar, TFA:H₂O:TIS:Phenol 88:5:2:5, rt/4 h, 95 % (Reprinted from [311])

hydroxybenzotriazole ester of α -N-Boc-S-Trityl-Hcy-OH (**9**), using DMAP/EDCI as the coupling reagents. Removal of trityl- and Boc-protecting groups is achieved in one step using a mixture TFA:H₂O:TIS:phenol 88:5:2:5 under argon atmosphere. The target *Ne*-Hcy-Lys isopeptide (**3**) is isolated as a white solid in 79 % overall yield and purity >96 % as determined by HPLC. ¹H NMR, ¹³C NMR, and mass spectrometry data are consistent with the expected structure [311].

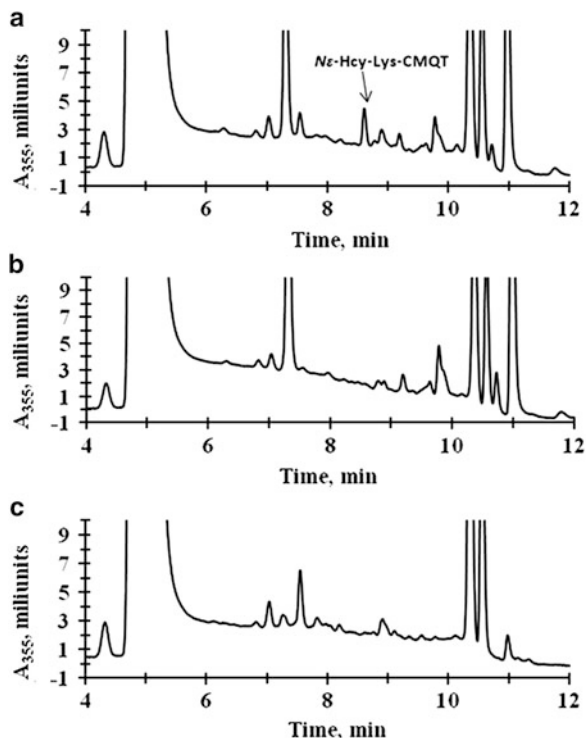
5.3.1.2 Physicochemical Properties

The isopeptide *Ne*-Hcy-Lys is a solid, white powder, easily dissolving in water. Acidified aqueous solution of the isopeptide (0.1 M) is stable at least 2 weeks at +4 °C. The thiol group of *Ne*-Hcy-Lys oxidizes reversibly to a disulfide form, which does not move from the origin of the thin-layer chromatography plate [73]. The bulk of plasma *Ne*-Hcy-Lys exists in the disulfide form [72]. Similar to other low molecular thiols, *Ne*-Hcy-Lys shows affinity to nucleophilic substitution reaction with 2-haloquinolinium or 2-halolepidinium salts [72]. 2-chloro-1-methylquinolinium tetrafluoroborate (CMQT) undergoes facile reaction with *Ne*-Hcy-Lys to give a stable thioether with a characteristic UV spectrum with an absorption maximum at 355 nm. The reactivity of its sulfhydryl was exploited to develop an *Ne*-Hcy-Lys plasma assay [72, 86].

5.3.1.3 Biological Formation

Metabolic pathway leading to *Ne*-Hcy-Lys is initiated by the conversion of Hcy to Hcy-thiolactone catalyzed by MetRS. Hcy-thiolactone spontaneously reacts with protein lysine residues generating *N*-Hcy-protein. That proteolytic degradation of *N*-Hcy-protein affords *Ne*-Hcy-Lys was shown by incubation of *N*-Hcy-hemoglobin with mouse liver extracts. *Ne*-Hcy-Lys is formed only in complete incubation

Fig. 5.6 Reversed-phase HPLC analyses of *N*-Hcy-hemoglobin degradation in mouse liver extracts. Shown are HPLC traces obtained with (a), complete reaction mixture containing *N*-Hcy-hemoglobin and mouse liver extract; (b), *N*-Hcy-hemoglobin; and (c), mouse liver extract. *Ne*-Hcy-Lys, eluting at 8.6 min, is present only in complete reaction mixture, indicated by an arrow in panel (a) (Reproduced from [72])



mixtures and absent when liver extracts and *N*-Hcy-hemoglobin are incubated separately (Fig. 5.6). The isopeptide *Ne*-Hcy-Lys is present in humans and mice, and its levels increase in hyperhomocysteinemic subjects or mice.

5.3.1.4 Quantification

The *Ne*-Hcy-Lys plasma assay [72] is based on the procedure used previously for the determination of plasma thiols [312]. Plasma (50 μ L), phosphate buffer (pH 7.4, 0.2 M, 100 μ L), and tris(2-carboxyethyl)phosphine (TCEP, 0.25 M, 10 μ L) in phosphate buffer (pH 7.4, 0.2 M) are incubated for 10 min, and 10 μ L of 0.1 M 2-chloro-1-methylquinolinium tetrafluoroborate (CMQT) was added. After 3 min, 50 μ L of 3 M perchloric acid is added to precipitate protein, which was removed by centrifugation (10 min, 12,000 \times *g*). The supernatant is transferred to a vial, and 10 μ L is injected into a reversed-phase C18 HPLC column (Agilent, Zorbax SB-C18 4.6 \times 150 mm, 5 μ m). The detection and quantification is by UV absorbance at 355 nm. The C18 column separates the *Ne*-Hcy-Lys-CMQT derivative from CMQT excess, other aminothiols, and unidentified matrix components. The detection (LLD) and quantification (LLQ) limits for *Ne*-Hcy-Lys were 0.08 and 0.1 μ M, respectively. This assay has been used to establish biological significance of *Ne*-Hcy-Lys in humans and mice.

5.3.1.5 Clinical Significance

Nε-Hcy-Lys levels are elevated under pathological conditions such as human renal disease, peripheral artery disease, and CBS deficiency, as well as mouse *Cbs* or *Mthfr* deficiency, suggesting increased turnover of *N*-Hcy-protein in these pathologies. Plasma *Nε*-Hcy-Lys comprises 0.7–1.2 and 0.7–4.4 % of plasma tHcy or 15.5–17.5 and 8.5–35 % of plasma protein *N*-linked Hcy in humans (renal disease or CBS-deficient patients) and mice, respectively. In healthy human subjects *Nε*-Hcy-Lys comprises <1.2 % of plasma tHcy or <12.7 % of plasma protein *N*-linked Hcy. Thus, plasma *Nε*-Hcy-Lys levels are higher in mice than in humans, most likely reflecting higher Hcy-thiolactone [93] and protein *N*-linked Hcy [113] levels in mice compared with humans.

Nε-Hcy-Lys is significantly elevated in acute myocardial infarction patients compared with controls [86]. Its formation is linked with the nitric oxide synthase inhibitor asymmetric dimethylarginine (ADMA), consistent with the origin of both *Nε*-Hcy-Lys and ADMA as products of protein turnover (Fig. 5.5). Surprisingly, the isopeptide *Nε*-Hcy-Lys levels are not associated with plasma tHcy or vitamin B₁₂ and folate. Moreover, *Nε*-Hcy-Lys levels show no correlation with titers of anti-*N*-Hcy-protein autoantibodies or with IL-6-mediated inflammation, oxidative stress, and thrombin generation. These findings suggest that *Nε*-Hcy-Lys is a new marker of acute myocardial infarction independently of Hcy-related metabolites and cofactors [86].

Nε-Hcy-Lys isopeptide is associated with progression of peripheral artery disease in patients treated with folic acid for 12 months [313]. Folic acid administration decreases plasma tHcy by 70.5 %. However, despite decrease in tHcy, serum *Nε*-Hcy-Lys is still detectable in 28 (21.4 %) of those patients on folic acid who were current smokers and survivors of ischemic stroke ($p < 0.001$).

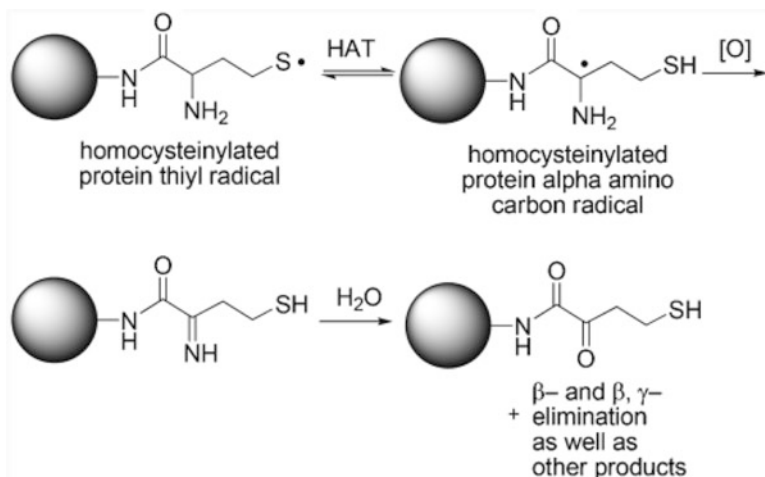
Nε-Hcy-Lys is detected in 17.3 % of patients on long-term hemodialysis, but not in control subjects [314]. Hemodialysis patients have 3.1-fold lower PON1 activity measured with paraoxon ($p < 0.0001$), 20 % higher ADMA ($p < 0.0001$), 30 % higher PAI-1 ($p < 0.0001$), and 10 % lower total cholesterol ($p = 0.001$) and LDL-cholesterol ($p < 0.0001$), together with 20 % lower triglycerides ($p < 0.0001$) compared with subjects without detectable *Nε*-Hcy-Lys. In hemodialysis patients *Nε*-Hcy-Lys levels correlate with paraoxonase 1 activity ($r = -0.62$, $p < 0.0001$), ADMA ($r = 0.58$, $p < 0.0001$), and PAI-1 ($r = 0.59$, $p < 0.0001$). These findings suggest that in hemodialysis patients, *Nε*-Hcy-Lys is associated with lipid profile, endothelial dysfunction, and impaired fibrinolysis [314].

5.4 Structural and Functional Consequences

The first indication that the incorporation of Hcy into peptide bonds can be detrimental to biological function came from now classical structure/function studies of oxytocin, the first peptide hormone to be sequenced and synthesized [315]. Oxytocin is secreted from the pituitary gland and acts as a neuromodulator in the brain. As one of the two known hormones released by the human posterior pituitary gland that act at a distance (the second is vasopressin), oxytocin is important in sexual reproduction, induces uterine contractions and stimulates milk production, and plays a key role in social attachment and affiliation in nonhuman mammals. Intranasal administration of oxytocin causes a substantial increase in trust among humans, thereby greatly increasing the benefits from social interactions [316]. Administration of oxytocin has also been shown to modulate emotion processing in healthy male volunteers, which may contribute to the emerging role of the neuropeptide in promoting affiliative and approach behaviors by reducing the salience of potentially ambiguous and threatening social stimuli [317].

Oxytocin is a 1,007 Da cyclic nanopeptide **CysTyrIleGlnAsnCysProLeuGlyNH₂** [315] composed of a disulfide-bonded cyclic hexapeptide amide-linked to a tripeptide amide. Cysteine residues 1 and 6 form an intrachain disulfide bond. Cys1 residue possesses a free amino group and is joined to the rest of the cyclic portion of the molecule through its carboxyl group, while Cys6 residue is connected through its amino group to the rest of the cyclic portion of the molecule and through its carboxyl group to the tripeptide ProLeuGly-NH₂. Its structure has been determined by classical peptide chemistry methods and confirmed by chemical synthesis. Chemically synthesized oxytocin has full biological activity of the natural oxytocin isolated from the posterior pituitary gland [315]. The ability to prepare synthetic oxytocin allowed elucidation of relationships of molecular structure to biological function of the hormone.

One of the analogs prepared is Hcy-oxytocin in which Cys1 residue is replaced by Hcy [247]. This substitution introduces one additional methylene (-CH₂-) group and generates an analog with a 21-membered disulfide ring, in contrast to oxytocin, which possesses a 20-membered ring. This change in structure led to a loss of characteristic pharmacological properties of oxytocin. The Hcy-oxytocin does not exhibit avian depressor and rat pressor activity and has only a very low oxytocic activity, less than 0.2 % of that possessed by oxytocin [247]. Loss of activity in Hcy-oxytocin is caused by the increase in size of the ring and not by the change in position of the free amino group relative to the disulfide bond. This was shown by synthesis and functional examination of 1- γ -mercaptobutyric acid-oxytocin, a deaminated analog of Hcy-oxytocin, which turned out to have no detectable avian depressor activity and 0.8 % of oxytocic activity [318]. 1 β -Mercaptopropionic-oxytocin, a deaminated analog of oxytocin, is highly potent and has enhanced avian depressor, oxytocic and rat antidiuretic activities, a decreased rat pressor activity, and an unaltered milk-ejecting activity in lactating rabbits [319].



Reaction 5.2 Kinetically favored intramolecular hydrogen atom transfer (HAT) process involving *N*-Hcy-protein promotes carbonyl formation and multiple fragmentation products including NH₃, H₂S, ethylene, and α,β -unsaturated amides, analogous to the chemistry of free Hcy. Captodative stabilization of the thiol radical renders the alpha C–H bond weaker than the S–H bond by ca. 4 Kcal/mol (Reprinted from [311])

The incorporation of Hcy into protein in the *N*-homocysteinylation reaction results in substitution of the ϵ -amino group of a protein lysine residue with an Hcy residue containing a free thiol group. This leads to a decrease of the net positive charge on a protein, due to the fact that a highly basic ϵ -amino group of a protein lysine residue ($pK_a = 10.5$) is replaced by a less basic α -amino group of *N*-linked Hcy (estimated $pK_a \sim 7$). Furthermore, the introduced free thiol is susceptible to redox reactions, which generate disulfide bonds [298] or oxidative damage [96].

Oxidative damage induced by *N*-homocysteinylation has been originally demonstrated for human serum albumin [96] and hemoglobin [68]. Subsequent studies have shown that protein oxidation occurs via kinetically favored intramolecular hydrogen atom transfer from α -carbon to a thiol radical (Reaction 5.2) [311]. The α -carbon-centered radical is detected using methyl viologen as a probe, which turns blue in the presence of *N*-Hcy-albumin due to the appearance of viologen radical. Another probe, fluorone black, affords an increase in the A₅₁₂ absorbance signal in the presence of *N*-Hcy-albumin, which indicates the presence of α -carbon radicals [311]. The α -carbon radicals react with oxygen to form superoxide and protein carbonyls (Reaction 5.2). The formation of protein carbonyls in *N*-Hcy-albumin is detected with a colorimetric reaction with 2,4-dinitrophenyl hydrazine, which shows a 60 % increase in the carbonyl content of *N*-Hcy-albumin (containing 7–8 mol *N*-linked Hcy/mol protein; prepared in vitro by incubation of human serum albumin with Hcy-thiolactone) compared with unmodified native albumin [311].

Such chemical alterations affect structure and biological function of Hcy-thiolactone-modified proteins. For example, early *in vitro* studies have shown that *N*-homocysteinylation of trypsin and methionyl-tRNA synthetase causes progressive loss of their enzymatic activity with increasing degree of *N*-homocysteinylation [78]. *N*-Hcy-proteins are prone to oxidative damage [96, 311] and aggregation [78, 96, 171] and are cytotoxic [170, 171] and immunogenic [134, 135, 172]. Subsequent studies have shown that *in vitro* *N*-homocysteinylation inactivates paraoxonase 1 activity in human HDL [320] and RNase activity of human serum albumin [321]. Although studied with several proteins, the structural and functional consequences of *N*-homocysteinylation are best understood for albumin and fibrinogen, the known targets for the modification by Hcy-thiolactone in the human body.

N-Hcy-proteins are novel examples of modified proteins that expand the known repertoire of nonenzymatic protein modifications [322] by other metabolites, such as glucose, products of lipid peroxidation, or certain drugs, such as penicillin or aspirin [78]. These protein modification reactions share two common aspects: (i) each involves protein lysine residues as sites of modifications and (ii) are linked to human pathology, such as cardiovascular disease, Alzheimer's disease, diabetes, and drug allergy or intolerance [78].

5.4.1 *N*-Homocysteinylation and Redox Function

5.4.1.1 *N*-Hcy-Albumin

Human serum albumin is the most abundant multifunctional plasma protein present at a mean concentration of 0.63 mM. Albumin, a globular protein of 66.5 kDa molecular weight, is composed of 585 amino acid residues, including 56 lysine residues and 35 cysteine residues, 34 of which form 17 disulfide bonds and one, Cys-34, has a free thiol [323]. It is synthesized in the liver and has a half-life of ~19 days in the circulation.

The first detailed studies of structural and functional alterations in a protein caused by *N*-homocysteinylation have been carried out with human serum albumin [96], in which Lys-525 is a predominant site for *N*-homocysteinylation both *in vitro* and *in vivo* in the human body [79]. These studies have led to the discovery of a novel molecular form of albumin and provided a paradigm illustrating how the function of a protein thiol can be affected by *N*-homocysteinylation of a protein lysine residue.

Of the two major physiological forms of human serum albumin (Fig. 5.7), albumin-Cys³⁴-S-S-Cys (containing cysteine in a disulfide linkage with Cys³⁴ of albumin) reacts with Hcy-thiolactone faster than albumin-Cys³⁴-SH (mercaptoalbumin, containing Cys³⁴ with a free thiol). The reactivity of Lys⁵²⁵ residue, a predominant site of *N*-homocysteinylation, is about twofold greater in albumin-Cys³⁴-S-S-Cys than in mercaptoalbumin. The *N*-homocysteinylation of

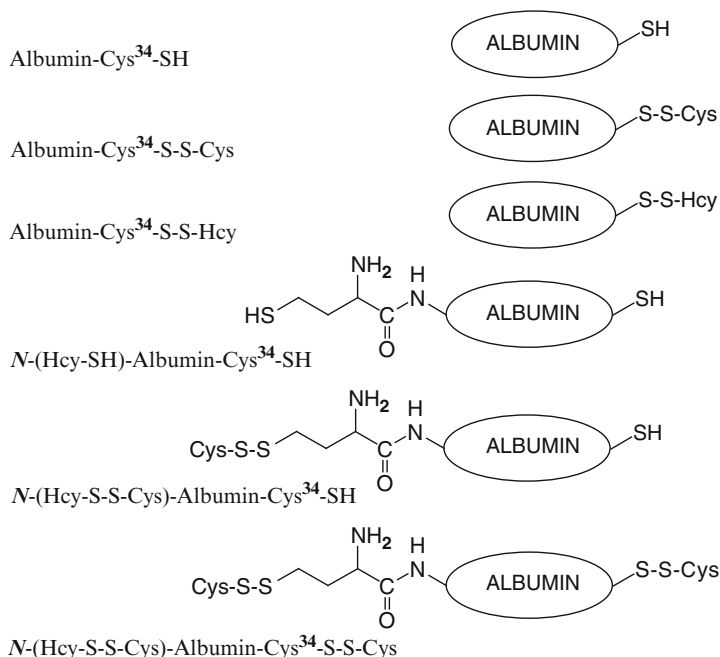


Fig. 5.7 Structures of the different forms of human serum albumin. Reproduced from [96]

albumin is chromatographically separated from unmodified albumin by anion exchange HPLC (Fig. 5.8). The different susceptibilities of albumin-Cys³⁴-S-S-Cys and albumin-Cys³⁴-SH to the modification by Hcy-thiolactone are consistent with a structural transition in albumin dependent on the status of the Cys³⁴ residue [324].

The reactions of albumin-Cys³⁴-S-S-Cys and albumin-Cys³⁴-SH with Hcy-thiolactone yield two different primary products, *N*-(Hcy-SH)-albumin-Cys³⁴-S-S-Cys (Reaction 5.3) and *N*-(Hcy-SH)-albumin-Cys³⁴-SH (Reaction 5.4), respectively (Fig. 5.9). However, these primary products are not observed due to fast thiol–disulfide exchange reactions that result in the formation of a single product, *N*-(Hcy-S-S-Cys)-albumin-Cys³⁴-SH (Fig. 5.9), which is observed on an anion exchange column (Fig. 5.8).

The thiol–disulfide exchange reactions occur in trans between different molecules of *N*-(Hcy-SH)-albumin-Cys³⁴-S-S-Cys or between *N*-(Hcy-SH)-albumin-Cys³⁴-SH and albumin-Cys³⁴-S-S-Cys. The equilibrium is strongly shifted toward *N*-(Hcy-S-S-Cys)-albumin-Cys³⁴-SH because the Cys-34 thiolate anion has unusually low pK_a of ~ 5 [323] and thus is more thermodynamically stable than Hcy thiolate anion (pK_a of ~ 10) [191, 192]. The low pK_a of the Cys-34 thiolate also makes the thiol–disulfide exchange of *N*-(Hcy-SH)-albumin-Cys³⁴-SH with albumin-Cys³⁴-S-S-Cys thermodynamically more favored than with cysteine.

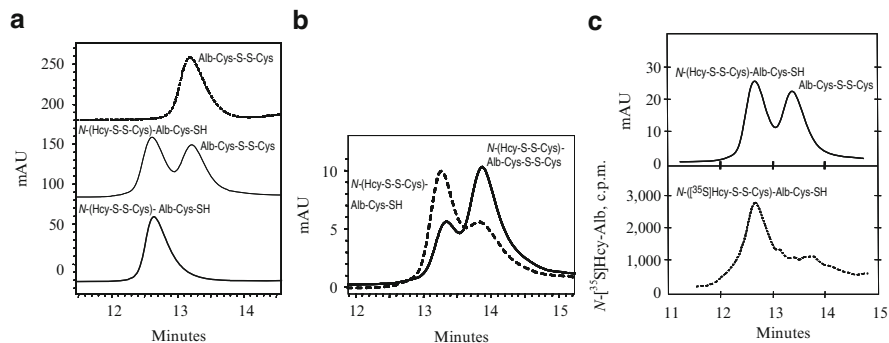
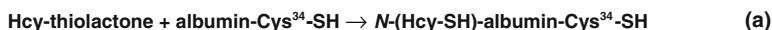


Fig. 5.8 Anion exchange HPLC analysis of Hcy-thiolactone-modified albumin-Cys³⁴-S-S-Cys. Albumin-Cys³⁴-S-S-Cys was modified with Hcy-thiolactone or [³⁵S]Hcy-thiolactone at 37 °C and analyzed by anion exchange HPLC. Panel (a), protein profiles after 0-h (*top trace*), 4-h (*middle trace*), and 22-h (*bottom trace*) modification with Hcy-thiolactone. Panel (b) shows protein profiles of the 10-h reaction with Hcy-thiolactone after an overnight incubation without (*dotted line*) and with a twofold molar excess of cysteine (*solid line*). Panel (c), protein (*upper panel*) and ³⁵S (*lower panel*) profiles after 4 h of modification with [³⁵S]Hcy-thiolactone (Reproduced from [96])



Reaction 5.3 Mechanism of *N*-homocysteinylation of albumin-Cys³⁴-S-S-Cys



Reaction 5.4 Mechanism of *N*-homocysteinylation of mercaptoalbumin (albumin-Cys³⁴-SH)

The formation of a mixed disulfide bond between Cys and *N*-linked Hcy induces substantial structural changes that lead to increased sensitivity of *N*-(Hcy-S-S-Cys)-albumin-Cys³⁴-SH, compared with *N*-(Hcy-SH)-albumin-Cys³⁴-SH, to proteolysis by trypsin or chymotrypsin [96].

Other plasma *N*-Hcy-proteins also undergo facile thiol–disulfide exchange with albumin-Cys³⁴-S-S-Cys. For example, when equimolar amounts of *N*-Hcy-transferrin and albumin-Cys³⁴-S-S-Cys are incubated together, albumin-Cys³⁴-S-S-Cys is quantitatively converted to albumin-Cys³⁴-SH (Reaction 5.5). Unmodified transferrin does not induce this reaction. *N*-homocysteinylation of fibrinogen, antitrypsin, hemoglobin, myoglobin, and cytochrome *c*, but not unmodified native proteins, also removed cysteine from the albumin-Cys³⁴-S-S-Cys disulfide with the liberation of albumin-Cys³⁴-SH. The equilibrium of those reactions is strongly shifted toward *N*-(Hcy-S-S-Cys)-protein and albumin-Cys³⁴-SH [96].



Reaction 5.5 Thiol–disulfide exchange between *N*-Hcy-transferrin and albumin-Cys³⁴-S-S-Cys. Similar reactions occur with other *N*-Hcy-proteins, such as *N*-Hcy-fibrinogen, *N*-Hcy-antitrypsin, *N*-Hcy-hemoglobin, *N*-Hcy-myoglobin, and *N*-Hcy-cytochrome *c*

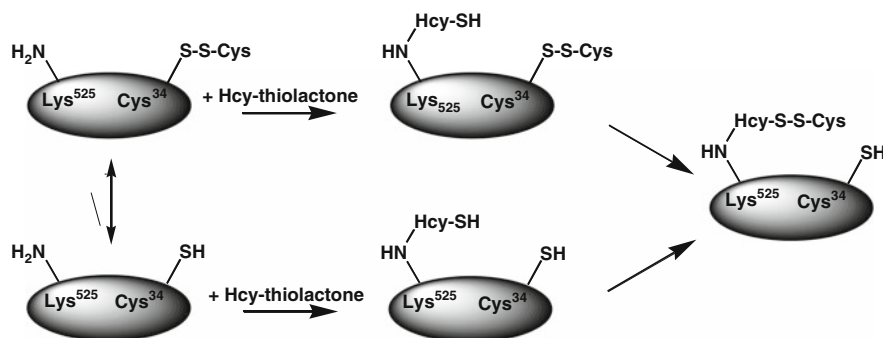


Fig. 5.9 *N*-Homocysteinylation of Lys⁵²⁵ prevents the structural transition in albumin dependent on the status of the conserved Cys³⁴ residue (Reproduced from [69])

Of the seven lysine residues of human albumin (Lys⁴, Lys¹², Lys¹³⁷, Lys¹⁵⁹, Lys²⁰⁵, Lys²¹², and Lys⁵²⁵) identified as targets for *N*-homocysteinylation by Hcy-thiolactone in vitro, Lys⁵²⁵ is a predominant site of *N*-homocysteinylation, while Lys¹³⁷ and Lys²¹² are minor sites, both in vitro and in vivo (Fig. 5.2) [212, 213]. Taken together, these results provide evidence for a novel form of albumin, *N*-(Hcy-S-S-Cys)-albumin-Cys³⁴-SH (Figs. 5.7 and 5.9), and suggest that a disulfide at Cys³⁴, a conserved residue in albumins from various organisms, promotes the conversion of *N*-(Hcy-SH)-albumin-Cys³⁴-SH to a more proteolytically sensitive form *N*-(Hcy-S-S-Cys)-albumin-Cys³⁴-SH, which would facilitate clearance of the *N*-homocysteinylated form of mercaptoalbumin. These data also suggest that, by rendering Cys³⁴ reduced, *N*-homocysteinylation prevents the structural transition in albumin dependent on the status of the conserved Cys³⁴ residue (Fig. 5.9).

N-Hcy-albumin becomes more susceptible than native albumin to aggregation [78] and oxidative damage by hydrogen peroxide [96]. Exposure to *N*-Hcy-albumin increases monocyte adhesion to the endothelial monolayers in a co-culture model [169]. Unmodified albumin does not have any effect on monocyte adhesion. The increased adhesion is observed only when *N*-Hcy-albumin is used at concentration observed in hyperhomocysteinemic subjects, but not when the concentration corresponds to that observed in normal individuals. The increased cell adhesion is accompanied by upregulation of genes involved in the inflammatory response (ICAM-1, VCAM-1) and vascular remodeling (ADAM17, MCP1, Hsp60) in both endothelial cells and monocytes. *N*-Hcy-albumin also induces release of Tnf- α from endothelial cells to the medium. As these responses are observed at relatively low concentration of *N*-Hcy-albumin, these findings suggest that *N*-Hcy-protein rather

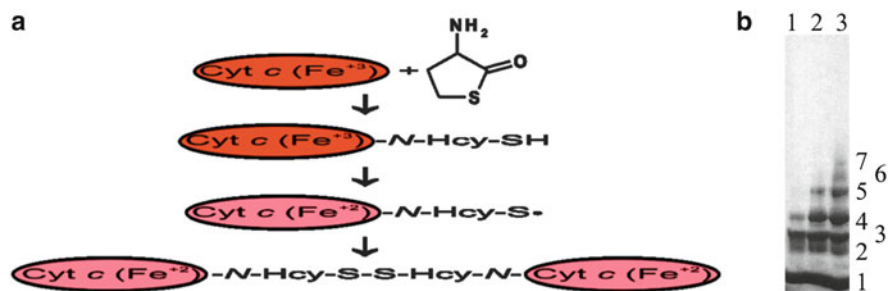


Fig. 5.10 *N*-Homocysteinylation of cytochrome *c* renders it reduced and leads to oligomerization. *Left panel*: Schematic illustration of the mechanism of the modification of cytochrome *c* with Hcy-thiolactone. Oxidized and reduced forms of cytochrome *c* are shown as red and green ovals, respectively. *Right panel*: SDS-PAGE analysis of *N*-Hcy-cytochrome *c* oligomers on 4–20 % gels. Bovine cytochrome *c* (10 mg/mL) was modified for 24 h at 25 °C with 30 μM (lane 1), 600 μM (lane 2), and 2.5 mM (lane 3) [³⁵S]Hcy thiolactone. The samples were denatured in the absence of 2-mercaptoethanol and subjected to SDS-PAGE. An autoradiogram of the gel is shown. The patterns of ³⁵S-labeled bands are identical to the patterns of red cytochrome *c* bands (not shown). Unmodified cytochrome *c* migrates as a single band (not shown). Numbers from 1 to 7 next to the bands indicate cytochrome *c* monomers, dimers, trimers, etc., respectively, as determined by comparison with migration of protein molecular mass standards (Reproduced from [78] and [298])

than Hcy itself induces cellular responses leading to chronic upregulation of inflammatory chemokines/cytokines, which are involved in atherosclerotic lesion formation [169].

5.4.1.2 *N*-Hcy-Cytochrome *c*

Studies of the modification of cytochrome *c* by Hcy-thiolactone provide a paradigm illustrating how the function of a heme-containing protein can be affected by *N*-homocysteinylation [298]. Four lysine residues of cytochrome *c*, Lys8 or 13, Lys86 or 87, Lys99 and Lys100, are preferential sites for the modification by Hcy-thiolactone in vitro. *N*-homocysteinylation of ferricytochrome *c* results in its conversion to a ferrous form, which is manifested as a change in the color of the solution from red to green. Experimental data are consistent with the following mechanism (Fig. 5.10). Reaction of Hcy-thiolactone with any of the four susceptible lysine residues of ferricytochrome *c* affords *N*-(Hcy-SH)-Cyt *c*(Fe⁺³). The heme iron in the product undergoes reduction by the thiolate of *N*-linked Hcy to afford modified ferrocyanochrome *c*, *N*-(Hcy-S·)-Cyt *c*(Fe⁺²). The reduction occurs in trans between different molecules of *N*-(Hcy-SH)-Cyt *c*(Fe⁺³) and can also occur with other *N*-Hcy-proteins. For example, a similar reduction of heme-Fe⁺³ was also observed during incubation of ferricytochrome *c* with *N*-(Hcy-SH)-albumin [298]. An intramolecular reduction is unlikely, because the sites of *N*-homocysteinylation are located too far from the heme iron. Dimerization of the thiyl radicals in different molecules of the modified ferrocyanochrome *c*, *N*-(Hcy-S·)-Cyt *c*(Fe⁺²), leads to the

formation of multimeric forms of *N*-Hcy-cytochrome *c* (Fig. 5.10) that are observed on nonreducing SDS-PAGE gels [78]. Multimers of *N*-Hcy-cytochrome *c* can also be separated by capillary electrophoresis [325]. Furthermore, *N*-Hcy-cytochrome *c* becomes more resistant than the native cytochrome *c* to proteolytic degradation. Thus, *N*-homocysteinylation of susceptible lysine residues in cytochrome *c* has important structural and functional consequences, manifested by increased resistance to proteolysis and change in iron redox state. A thiol of the *N*-linked Hcy introduced by *N*-homocysteinylation changes the redox state of the heme ligand of cytochrome *c* by rendering it reduced (Fig. 5.10) [298].

5.4.2 *N*-Hcy-Fibrinogen and Fibrin Clot Properties

In vitro studies show that the modification by Hcy-thiolactone interferes with the function of fibrinogen, a major blood clotting protein. Fibrinogen is a dimer of three polypeptides, A α , B β , C γ , linked by 29 disulfide bonds. During coagulation fibrinogen is converted to an insoluble fibrin by thrombin-catalyzed removal of fibrinopeptides from the A α and B β chains. Although fibrinogen does not have a free thiol, and thus cannot bind Hcy by a disulfide linkage, the protein is known to be susceptible to *N*-homocysteinylation by Hcy-thiolactone in vitro (Table 3.3) [78, 139] and, like other circulating proteins, carry *N*-linked Hcy in vivo in the human blood (Tables 5.4 and 5.5) [79].

Because lysine residues are important for the binding of fibrinolytic enzymes to fibrin, their modification by Hcy-thiolactone is likely to impair fibrinolysis and lead to increased thrombogenesis. Indeed, fibrin clots formed from in vitro-prepared *N*-Hcy-fibrinogen have more compact structure and lyse slower than clots from unmodified control fibrinogen [175]. For example, the half lysis time of the clots formed from *N*-Hcy-fibrinogen is significantly increased, compared to the clots formed from the control fibrinogen (15.5 ± 3.5 min vs. 11.7 ± 2.1 min, $P < 0.001$). The decreased susceptibility to lysis is caused by less efficient activation of plasminogen on clots formed from *N*-Hcy-fibrinogen. Although tPA binding is increased, the binding of plasminogen to *N*-Hcy-fibrin is not affected relative to control fibrin [175]. In addition, *N*-Hcy-fibrinogen acquires the ability to form disulfide-linked complexes with albumin. However, fibrin clots generated from albumin-containing complexes of *N*-Hcy-fibrinogen have half lysis time not different from those for clots from *N*-Hcy-fibrinogen [326].

The in vitro prothrombotic effects of *N*-Hcy-fibrinogen are similar to the prothrombotic effects of fibrinogen mutations in humans, which introduce a cysteine thiol group, e.g., A α Arg16 \rightarrow Cys, Arg554 \rightarrow Cys, Ser532 \rightarrow Cys; B β Arg14 \rightarrow Cys, Arg44 \rightarrow Cys, Arg255 \rightarrow Cys; and C γ Arg275 \rightarrow Cys, Tyr354 \rightarrow Cys [327–330] (human fibrinogen database is available at <http://www.geht.org>).

Confocal microscopy of fibrin clots formed from in vitro-prepared *N*-Hcy-fibrinogen demonstrates a denser structure with increased branching compared to control [331]. Consistent with their denser clot structure, lysis of fibrin clots formed

Table 5.10 Plasma *N*-Hcy-fibrinogen, total fibrinogen, and the ratio of *N*-Hcy-fibrinogen/total fibrinogen in CBS-deficient patients and unaffected individuals (Data from [115])

Genotype (<i>n</i>)	<i>N</i> -Hcy-fibrinogen (nM)	Total fibrinogen (μM)	<i>N</i> -Hcy-fibrinogen/total fibrinogen (%)
<i>CBS</i> ^{+/+} (7)	35.8 ± 14.3	6.56 ± 1.98	0.61 ± 0.21
<i>CBS</i> ^{-/-a} (27)	72.5 ± 58.1*	6.95 ± 1.65 [#]	1.00 ± 0.64*
<i>CBS</i> ^{-/-a} , noncompliant (1)	314.8	8.30	3.78

^a*CBS*^{-/-} patients were on an Hcy-lowering therapy

*P = 0.01

[#]P = 0.32 for *CBS*^{-/-} vs. *CBS*^{+/+}

from *N*-Hcy-fibrinogen is 1.3 times slower compared to control fibrin. Fibrinogen purified from human plasma obtained from patients with hyperhomocysteinemia has higher content of *N*-linked Hcy compared to fibrinogen from control subjects. The purified fibrinogen with high in vivo *N*-linked Hcy content (2.38 μM) produces fibrin clots with a denser structure and a 1.2-fold longer lysis time, compared with fibrin clots with low in vivo *N*-linked Hcy content (0.34 μM) [331].

Plasma levels of the prothrombotic *N*-Hcy-fibrinogen are elevated up to tenfold in CBS-deficient patients (Table 5.10) [115] who are known to be prone to atherothrombosis [46]. Mass spectrometric analyses identify three lysine residues that carry *N*-linked Hcy in fibrinogen isolated from CBS-deficient patients, one in each subunit: Lys562 in α-subunit, Lys344 in β-subunit, and Lys385 in γ-subunit (Fig. 5.3) [215]. These three in vivo *N*-homocysteinylation sites are also predominant sites for fibrinogen *N*-homocysteinylation in vitro. The α-subunit Lys562 site of *N*-homocysteinylation is located in an unstructured region of the αC domain known to be involved in tPA and plasminogen binding (α392-610), which can explain abnormal characteristics of clots formed from *N*-Hcy-fibrinogen [175]. *N*-Hcy-Lys562 is close to the sites of two mutations Ser532->Cys and Arg554-Cys that are associated with thrombosis [328, 329]. Thus, it is likely that at least *N*-Hcy-Lys562 contributes to prothrombotic properties of *N*-Hcy-fibrinogen in CBS-deficient patients. Taken together, these findings suggest that fibrinogen *N*-homocysteinylation contributes to the pro-coagulant phenotype observed in hyperhomocysteinemic patients.

5.4.3 *N*-Homocysteinylation and LDL Function

Low-density lipoprotein, the major cholesterol transport protein in plasma, enters cells by binding to specific surface receptors that mediate its cellular uptake and transport to lysosomes [332]. Lysine residues are involved in the LDL receptor interaction [333]. LDL is susceptible to *N*-homocysteinylation by Hcy-thiolactone in vitro [78, 139] and native LDL carries small amounts of *N*-linked Hcy in the circulation (Tables 5.4 and 5.5) [79].

Chemical modification of 15–20 % of the lysine residues of LDL by carbamylation with cyanate or by acetoacetylation with diketene prevents the LDL from competitively displacing unmodified ¹²⁵I-LDL from the high-affinity

receptor sites or from directly binding to the receptor [334]. *N*-Hcy-LDL containing from 5 to 50 *N*-Hcy residues per protein molecule can be prepared by incubation with Hcy-thiolactone [335]. At modification level of >9 *N*-Hcy residues per LDL molecule (>2.5 % lysine residues modified), some aggregation occurs, but is reversed by DTT, suggesting that it is caused by disulfide bond formation. At 8 *N*-Hcy residues per LDL molecule, *N*-Hcy-LDL exhibited the same mobility on paper electrophoresis, gel filtration elution pattern, and particle size (20 nm) as native LDL. At this extent of modification, the affinity of *N*-Hcy-LDL for LDL receptors and subsequent internalization by L_2C lymphocytes is identical to that of native LDL.

Higher extent of *N*-homocysteinylation causes increase in density, faster electrophoretic mobility, and aggregation and precipitation of *N*-Hcy-LDL [336]. Such highly modified *N*-Hcy-LDL is taken up and degraded faster than native LDL and causes increased cholesterol accumulation in human macrophages. Degradation of *N*-Hcy-LDL and native LDL by macrophages is inhibited 75.6 % and 11.4 %, respectively, by cytochalasin B, suggesting increased uptake of aggregated *N*-Hcy-LDL by phagocytosis. Highly modified *N*-Hcy-LDL, containing about 90 *N*-Hcy residues per LDL molecule (25 % lysine residues modified), exhibits decreased binding, internalization, and degradation by normal human fibroblasts.

A more recent study shows that *N*-Hcy-LDL containing about 25 *N*-Hcy residues per LDL molecule has fluorescence characteristics and levels of lipid hydroperoxides similar to those of native LDL, suggesting that *N*-homocysteinylation does not significantly affect its structure and does not cause oxidative damage [170]. Treatment with *N*-Hcy-LDL, but not with native LDL, induces significant increase in the levels of hydroperoxides in human aortic endothelial cells, suggesting that *N*-Hcy-LDL induces oxidative damage in these cells. At the same time, a significant decrease in cell viability in *N*-Hcy-LDL-treated cells, but not in native LDL-treated cells, is observed [170]. Furthermore, incubation of endothelial cells with *N*-Hcy-LDL causes a significant increase in cytoplasmic calcium levels and peroxynitrite production and a decrease in Na^+/K^+ -ATPase and nitric oxide production in these cells, compared with cell incubated with control LDL. In addition, a positive correlation is observed between Na^+/K^+ -ATPase activity and cytoplasmic Ca^{2+} content and between peroxynitrite activity and cytoplasmic Ca^{2+} content. These findings show that *N*-Hcy-LDL induces alterations in functional properties and nitric acid metabolism of human endothelial cells [337].

5.4.4 *N*-Homocysteinylation and HDL Function

High-density lipoprotein plays a central role in reverse cholesterol transport and has anti-inflammatory and antioxidant properties. These activities are responsible for atheroprotective roles of HDL. In addition to lipids, HDL contains ApoA1 as a major protein component and Hcy-thiolactonase/PON1 as a minor protein component. Human HDL carries small amounts of *N*-linked Hcy (Tables 5.4 and 5.5) [79, 303] and is susceptible to *N*-homocysteinylation by Hcy-thiolactone in vitro [320].

Under physiological conditions *in vivo*, one or two lysine residues, out of the 21 lysine residues present in ApoA1 are *N*-homocysteinylylated [303]. *In vitro*, however, 5 or 6 lysine residues can be *N*-homocysteinylylated using high concentrations of Hcy-thiolactone. The susceptibility of HDL to *N*-homocysteinylylation by Hcy-thiolactone *in vitro* is negatively correlated with the paraoxonase activity [320] (which reflects the native Hcy-thiolactonase activity of PON1). Similar protection against *N*-homocysteinylylation by high activity of Hcy-thiolactonase/PON1 is observed for total serum protein not only *in vitro* but also *in vivo* in humans [152, 250].

N-Homocysteinylylation causes an increase in the intensity and a blue shift of the intrinsic Trp fluorescence of HDL [320]. Similar changes are observed in the external fluorescent lipophilic probe Lourdan that binds at the lipid–water interface of HDL. This indicates that *N*-homocysteinylylation induces structural changes in the environment of Trp residues as well as in the Lourdan binding site of HDL [320]. *N*-Hcy HDL has a significantly decreased paraoxonase activity relative to native untreated HDL. These results indicate that the modification by Hcy-thiolactone affects structure and function of HDL.

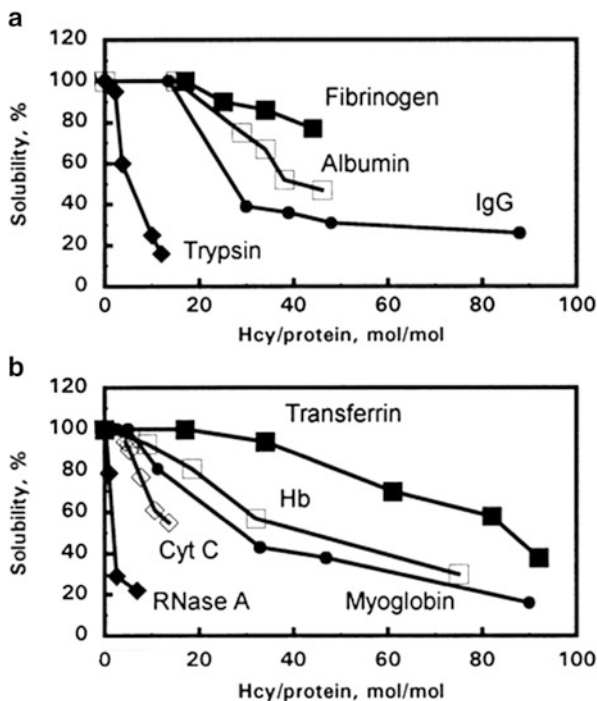
5.4.5 *N*-Homocysteinylylation Induces Protein Aggregation and Amyloid Conversion

Early studies of protein modification by Hcy-thiolactone have shown that *N*-Hcy-proteins have a tendency to aggregate and precipitate from solutions [78]. Some proteins, such as RNaseA, trypsin, and cytochrome *c*, aggregate and precipitate when the extent of *N*-homocysteinylylation is low, 1–2 mol *N*-Hcy/mol protein (Fig. 5.11). Other proteins, such as fibrinogen, albumin, IgG, and transferrin, are fully soluble even when the extent of *N*-homocysteinylylation is as high as 20 mol *N*-Hcy/mol protein but eventually begin to precipitate when the extent of modification is higher. Other proteins, such as hemoglobin and myoglobin, exhibited intermediate sensitivity to *N*-homocysteinylylation (Fig. 5.11). Subsequent studies have shown that protein aggregation elicited by *N*-homocysteinylylation involves amyloid conversion even in proteins with mostly helical structures, such as albumin.

5.4.5.1 *N*-Hcy-Albumin

Serum albumin is an inherently stable globular protein with mostly α -helical structure. Incubation of albumin in diluted solutions for several weeks at 37 °C does not lead to protein aggregation. However, incubation over extended periods of time (7 days or longer) of serum albumin modified with Hcy-thiolactone confers on the protein the ability to bind thioflavin T which induces fluorescence (a positive test for the presence of β -sheet structures characteristic of amyloids). This reveals

Fig. 5.11 *N*-homocysteinylation affects protein solubility. Proteins are modified with [³⁵S]Hcy-thiolactone to achieve indicated extents of *N*-homocysteinylation. The soluble and insoluble protein fractions are separated by high-speed microcentrifugation. Relationships between protein *N*-linked Hcy content solubility are shown for: (a) fibrinogen (filled square), albumin (open square), γ -globulin (filled circle), and trypsin (filled diamond); (b), transferrin (filled square), hemoglobin (open square), myoglobin (filled circle), cytochrome *c* (open diamond), and RNase A (filled diamond) (Reproduced from [78])



the propensity of *N*-Hcy-albumin to undergo the conversion to a structure with amyloid-like properties [171].

The dynamic light scattering (DLS) analysis shows a predominant peak with a radius of 3.7 nm of native albumin in the control sample, as well as a minor peak corresponding to particles with a radius of 150–200 nm, indicating a very low tendency of untreated albumin to aggregate. Similar analysis of the *N*-Hcy-albumin sample reveals that large aggregates with particle size of 170 nm are formed during this extended incubation and that a peak with a radius of 3.7 nm of native albumin is absent. Control experiments show that incubation in the presence of 10 mM Hcy does not lead to albumin aggregation. Thus, albumin *N*-homocysteinylation induces mild conformational changes leading to the formation of native-like aggregates, which evolve over time to amyloid-like structures. These aggregates are toxic to cells [171].

Other experiments show that *N*-Hcy-albumin serves as a seed and induces aggregation of native albumin. This is demonstrated by “seeding” experiments in which a small volume of *N*-Hcy-albumin solution containing aggregates (72 nm in radius) is added to a large volume of native albumin solution (Fig. 5.12). After 18-day incubation the DLS analyses reveal large aggregates with a radius of 500 nm, while native albumin molecules with a radius of 3.7 nm are absent (Fig. 5.12, panel d). In contrast, the control sample seeded with untreated

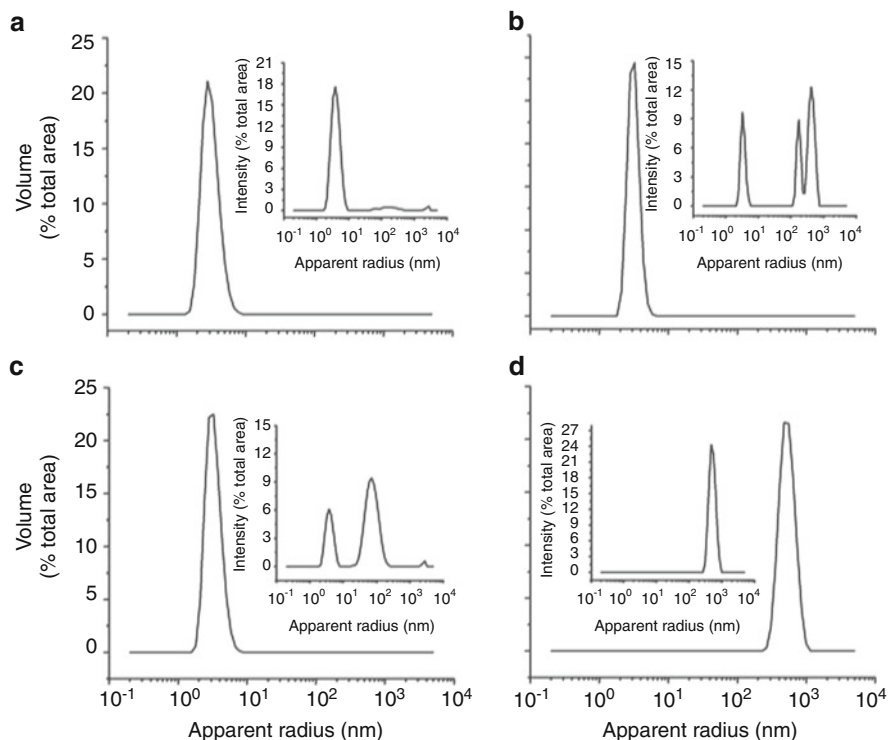


Fig. 5.12 Seeding experiment: *N*-Hcy-albumin induces aggregation of native unmodified albumin. The aggregation state of sample was monitored by DLS. A sample of untreated albumin (900 μ L) is seeded with *N*-Hcy-albumin (100 μ L). Untreated albumin is used as a control. Samples are incubated at 37 $^{\circ}$ C. Time 0: control experiment (a), seeded sample (c). After 18 days: control experiment (b), seeded sample (d) (Reproduced from [171])

albumin contains native molecules and only a small amount of large particles (Fig. 5.12, panel b) [171].

N-Homocysteinylation initiates albumin aggregation process under physiological-like conditions generating large protein complexes formed by native albumin molecules that precipitate from the solution. The precipitated aggregates, but not the soluble *N*-Hcy-albumin monomers, exhibit properties characteristic of amyloid structures: they become fluorescent when treated with thioflavin T and bind Congo red, a dye usually used to monitor the formation of amyloid structures. In circular dichroism (CD) spectral analyses, the aggregates show a reduction of the signals at both 208 and 222 nm, characteristic of amyloid structures. The aggregation does not involve disulfide bond formation but hydrophobic interactions facilitated by local protein unfolding. The early aggregates are cytotoxic and induce apoptosis in cultured mammalian cells. Furthermore, early aggregates of *N*-Hcy-albumin can

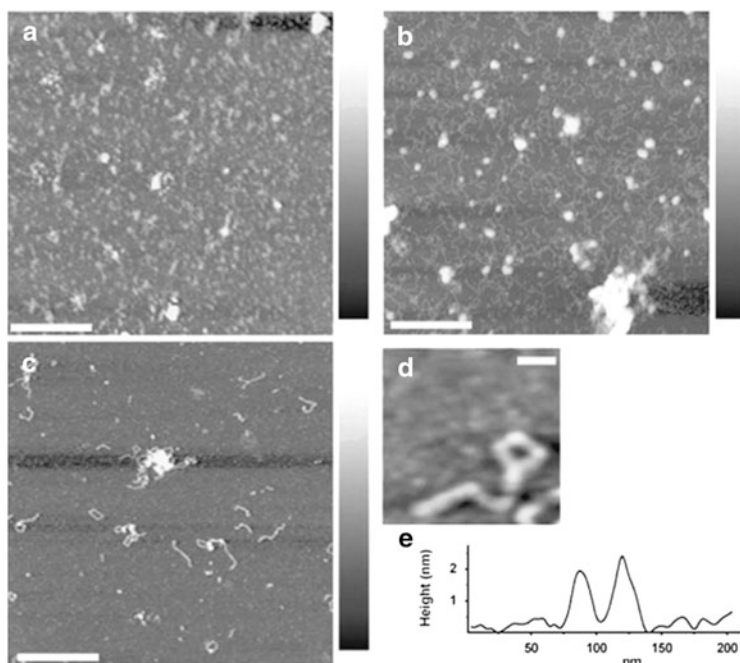


Fig. 5.13 Atomic force microscopy images of 30-day-old albumin samples. Control albumin (a), *N*-Hcy-albumin (b), *N*-Hcy-albumin diluted 50-fold with bidistilled water (c), zoom of (c) on an annular shape of protein aggregates (d). Image size of (a)–(c) is $2\ \mu\text{m} \times 2\ \mu\text{m}$; the scale bar represents 50 nm. Color scale range of (a) 9 nm, (b) 40 nm, and (c) 9.7 nm. Image size of (d), $185\ \text{nm} \times 185\ \text{nm}$. The scale bar represents 40 nm. Line profile (e) of the annular aggregate shown in (d); the height of the protein aggregate is about 2 nm, and the diameter of the annular aggregate is 54 nm (Reproduced from [171])

act as a seed, stimulating the conversion of native albumin to molecular forms with greater propensity to aggregate [171].

Atomic force microscopy and transmission electron microscopy analyses show that aggregated *N*-Hcy-albumin undergoes time-dependent structural reorganization. After 7 days, *N*-Hcy-albumin aggregates show no specific morphology and the absence of well-ordered structures [171]. However, after longer time (30 days) the aggregates show the presence of curly protofibrils and circular structures similar to amyloid pores (Fig. 5.13).

Importantly, the levels of protein *N*-homocysteinylation that induce aggregation and toxicity are close to those observed in albumin from patients with hyperhomocysteinemia due to CBS deficiency [338]. Taken together, these findings identify a mechanism that may explain the role of Hcy in neurological abnormalities observed in CBS- [46] or *MTHFR*-deficient patients [339], as well as in cognitive impairment and Alzheimer's disease in the general population [56].

5.4.5.2 *N*-Hcy-Insulin

Insulin, a glucose-regulating polypeptide hormone, is composed of two polypeptide chains of 21 and 30 amino acid residues linked together by two interchain disulfide bonds. It is associated with diabetes and is known to form amyloid fibrils. The fibrillation of insulin, induced by elevated temperature, low pH, organic solvents, or sheer stress, is a serious biomedical problem.

Early studies have shown *N*-homocysteinylation of amino groups of insulin impairs its biological function, while methionylation or leucylation does not [340]. For example, treatment with *N*-acetyl-Hcy-thiolactone at pH 8.0, 25 °C for 24 h, results in incorporation of 1.7 moles of *N*-acetyl-Hcy residues per mol insulin. Anion exchange chromatography on a DEAE-cellulose column separates *N*-acetyl-Hcy-insulin (containing two moles of *N*-acetyl-Hcy residues per mol) from the unmodified protein. The modified insulin loses its activity in the mouse-convulsion test and does not compete with native insulin in the binding to anti-insulin antiserum [340]. These effects suggest that *N*-homocysteinylation causes profound changes in the insulin structure. In contrast, when methionyl groups (2.5 mol/mol insulin) are introduced on the free amino groups of insulin, the methionylated insulin retains >50 % of its original activity. Similarly, little impairment do biological activity is observed when leucine residues are introduced on the amino groups of insulin. The results obtained with *N*-acetyl-Hcy-thiolactone suggest that insulin might be prone to inactivation by a more physiologically relevant reaction with Hcy-thiolactone.

Recent studies show that *N*-homocysteinylation with Hcy-thiolactone induces gross structural alterations and aggregation of insulin in a dose-dependent manner [341]. For example, incubation of insulin (350 μM) with Hcy-thiolactone (200 μM) at pH 7.4, 37 °C for 24–144 h, accelerates unfolding, which is accompanied by structural transition from α-helical to β-sheet structures, as revealed by CD spectroscopy [342]. This structural transition is manifested by reduction in the intrinsic tyrosine fluorescence, suggesting a more polar environment of Tyr residues in *N*-Hcy-insulin. Increases in 1-anilino-8-naphthalene sulfonate and thioflavin T fluorescence are also observed, indicating greater exposure of hydrophobic surfaces and formation of amyloid fibrils, respectively, in *N*-Hcy-insulin. Unfolding of insulin following *N*-homocysteinylation is accompanied by the transition from α-helix to β-sheet structures and exposure of insulin hydrophobic surfaces to the aqueous environment that leads to the formation of insulin fibrils. These *N*-Hcy-insulin fibrils have been shown to be toxic to cultured cancer cells [342].

Although the sites of *N*-homocysteinylation in *N*-Hcy-insulin are not known, a single lysine residue at position 29 in β-chain and N-terminal β-Phe1 and α-Gly1 residues are likely candidates. Consistent with this suggestion, N-terminal β-Phe1 and α-Gly1 residues are found to be the sites of the modification by glucose in human insulin [343], and the principal sites of glycation are found to be located in the β-chain of bovine insulin in peptides β1-13 and β22-30 generated by endoproteinase Glu C digestion [344].

5.4.5.3 *N*-Hcy-Prion

Misfolding of the natively α -helical prion protein (PrP^C) into a β -sheet-rich isoform (PrP^{Sc}) and the formation of amyloid aggregates are believed to be the causes of neurodegenerative diseases such as scrapie in sheep, bovine spongiform encephalopathy, and hereditary Creutzfeldt–Jakob disease and Gerstmann–Strausler–Scheinker-like syndrome in humans. The form of disease is determined by two prion types, which differ in their stabilities against denaturing agents, have different proteinase K cleavage sites, and form different prion aggregate deposits [345]. Multiple factors, including genetic variation, physicochemical environment, and posttranslational modifications (such as glycation) [346] determine the propensity of PrP^C to form aggregates.

A recent study suggests that *N*-homocysteinylation contributes to the conversion of PrP^C to PrP^{Sc} [347]. Incubation of ovine PrP^C with Hcy-thiolactone leads to *N*-homocysteinylation of the residues Lys197 and Lys207 and the formation of prion multimers, detected on nonreducing SDS-PAGE gels. The DLS measurements reveal large *N*-Hcy-PrP^{Sc} aggregates that enhance thioflavin T fluorescence and are resistant to proteinase K digestion. Epifluorescence microscopy in the presence of thioflavin T shows that these aggregates have cluster-like structure. Infrared spectroscopy reveals increased content of β -sheet structures in *N*-Hcy-PrP^{Sc} relative to unmodified PrP^C. Taken together, these findings show that *N*-homocysteinylation accelerates amyloid-like transformation of PrP^C [347].

5.4.5.4 *N*-Hcy-Amyloid β -Peptide

Genetic hyperhomocysteinemia causes neurological abnormalities in humans, manifested by seizures and mental retardation [20]. In a general population, elevated plasma Hcy level is associated with neurodegenerative diseases such as dementia and Alzheimer's disease [56].

Amyloid β -peptide (A β) is a normal product of cellular metabolism, and aggregation of A β plays central role in mediating neurotoxicity in Alzheimer's disease. A β is natively unfolded in the monomeric state. In vitro modification of A β _{1–42} with Hcy-thiolactone decreases its propensity to form amyloid fibrils [348]. CD spectroscopy reveals attenuated changes in the signal at 218 nm obtained with *N*-Hcy-A β _{1–42}, suggesting that *N*-homocysteinylation inhibits β -sheet formation. *N*-Hcy-A β _{1–42} becomes more toxic and induces cell death in PC12 cells to a greater extent than unmodified A β _{1–42} does. These data suggest that the diminished propensity of *N*-Hcy-A β _{1–42} to form β -sheet structures decreases oligomer elongation and fibril formation and leads to new protofibrils with low self-assembly and high toxicity [348].

5.4.5.5 *N*-Hcy-Tau

Tau, an essential component of neuronal cytoskeleton, binds and stabilizes microtubule proteins (MTP), regulates nucleation and assembly of tubuli, is important for neuronal integrity, and plays a role in Alzheimer's disease. The MTP network is highly dynamic and regulates cell division and intracellular transport [349]. Tau exists in six alternatively spliced isoforms. Highly conserved 31 amino acid repeats in the C-terminal domain of the tau protein constitute the MTP binding region of tau [350]. The C-terminal domain of tau contains three or four (3R and 4R) contiguous microtubule-binding repeats. Tau isoform 4R stabilizes MTP more efficiently than 3R and is overexpressed in Alzheimer's disease [351]. The positively charged lysine residues in the MTB binding regions of tau interact with the negative C terminus of tubulin in a sequence-specific fashion [352].

Interactions of *N*-Hcy-tau containing 1.6, 7.2, and 25.2 mol *N*-Hcy/mol protein with MTP and tubulin were studied by ultracentrifugation and SDS-PAGE analyses [353]. After ultracentrifugation of mixtures containing MTP and *N*-Hcy-tau or control unmodified tau, *N*-Hcy-tau is found predominantly in the supernatant, while control tau is found in the pellet. The extent of tau binding to MTP is inversely related to the extent of tau *N*-homocysteinylation. These results suggest that *N*-homocysteinylation reduces tau's affinity for the MTP.

In addition to binding to MTP, tau regulates nucleation and assembly of tubulin. Tau increases the rate of MTP elongation by decreasing tubulin dissociation during assembly. This lowers the critical concentration for elongation. In the presence of *N*-Hcy-tau, critical concentration of tubulin *increases* from $1.95 \pm 0.18 \mu\text{M}$ to $2.42 \pm 0.31 \mu\text{M}$. Thus, *N*-Hcy-tau fails to decrease tubulin dissociation, and the extent of tubulin assembly is reduced as the extent of tau *N*-homocysteinylation increases [353].

5.4.5.6 *N*-Hcy-Caseins

Bovine α (S1)-, β -, and κ -caseins are intrinsically unstructured proteins with different aggregation and micelle formation propensities. Collectively, the caseins make up about 80 % of the total milk protein (30–35 g/L). The caseins can coagulate into curds and separate from other proteins, mostly lactoglobulins, which remain soluble at 3 g/L in the whey. The milk protein carries small amounts of *N*-linked Hcy: $1.09 \pm 0.01 \mu\text{M}$ in total milk (which also contains $3.45 \pm 0.25 \mu\text{M}$ tHcy) and $1.51 \pm 0.34 \mu\text{M}$ in whey (which also contains $5.4 \pm 2.5 \mu\text{M}$ tHcy) [297].

The modification of individual caseins with Hcy-thiolactone generates proteins containing 1.5, 2.1, and 1.3 *N*-linked Hcy residues per one β -, α (S1)-, and κ -casein molecule, respectively [354]. Studies of the fluorescence of Trp residues, thioflavin T, and 1-anilino-8-naphthalene sulfonate, as well as CD spectroscopy studies, show that *N*-homocysteinylation causes increase in β -sheet structures. Furthermore, *N*-Hcy-caseins acquire increased propensity to aggregate. The sizes of aggregates

and aggregation rates depend on the extent of *N*-homocysteinylation and temperature. The DLS and microscopic studies reveal the formation of large aggregates of *N*-Hcy-caseins (1–3 μm). *N*-Homocysteinylation of α (S1)- and β -caseins results in the formation of regular spheres, whereas *N*-homocysteinylated κ -casein forms thin unbranched fibrils about 400–800 nm long. Amyloid character of *N*-Hcy- κ -casein fibrils is further confirmed by the changes in Congo red spectra. These data indicate that *N*-homocysteinylation of intrinsically unstructured proteins restricts their structure to the β -sheet conformation, which facilitates amyloidal transformation of native caseins structures [354].

5.4.5.7 *N*-Hcy-Crystallin

Preponderance of evidence indicates that hyperhomocysteinemia is often associated with various diseases of the eye. For example, in humans one of the manifestations of severe hyperhomocysteinemia due to CBS deficiency is the dislocated optic lens, ectopia lentis [46]. However, the molecular basis of pathology of the visual system induced by elevated Hcy is not known. Lens protein modifications are often underlying problems, becoming more prevalent with age. Thus, it is likely that lens protein modification by *N*-homocysteinylation might contribute to pathological consequences of hyperhomocysteinemia affecting the eye. Indeed, bovine α -crystallin, a major component of lens protein pool, is known to be susceptible to *N*-homocysteinylation in vitro (Table 3.3) [78] and to carry a small amount of *N*-linked Hcy in vivo (Table 5.4) [297]. The molecular consequences of bovine lens protein *N*-homocysteinylation have been examined in a recent study using spectroscopic techniques, SDS-PAGE, and Western blot analysis [355]. Similar to other proteins [78], *N*-homocysteinylation induces lens protein aggregation, which, if it were to occur in the eye, would cause vision problems. Lens protein aggregates undergo fibrillation, which is detected by increases in Congo red absorption and thioflavin T fluorescence. SDS-PAGE and Western blotting of *N*-homocysteinylated lens proteins show that essentially all detectable eye lens crystallins become prone to aggregation after the modification, with *N*-Hcy- α -crystallin comprising the major portion of lens protein aggregate. These findings suggest that lens protein *N*-homocysteinylation is a possible mechanism accounting for the association of hyperhomocysteinemia with impairments of the visual system [355].

5.4.5.8 *N*-Hcy-Dynein

Folate deficiency markedly affects hippocampal cell proliferation, migration, differentiation, survival, vesicular transport, and synaptic plasticity [299]. This occurs through alterations in signaling, impaired expression of proteins involved in elongation and stabilization of axons and dendrites, defect in cell polarity and

trafficking, and increased *N*-homocysteinylation of key proteins important for synapse formation, function, and plasticity.

Kinesin and dynein are motor proteins involved in vesicular transport along the microtubules from one part of neuronal cell to another. In rat hippocampal neuronal cells cultured in folate-deficient medium that induces hyperhomocysteinemia, kinesin and dynein become *N*-homocysteinylated, which leads to protein aggregation and reduced interaction with tubulin [299]. The colocalization of Hcy with kinesin and dynein and the occurrence of cellular protein aggregates are demonstrated by immunohistochemistry using antibodies against kinesin, tubulin, and Hcy-glutaraldehyde-BSA conjugates. These interactions are also confirmed by immunoprecipitation and Western blotting and quantified by the proximity ligation assay in which a pair of oligonucleotide-labeled secondary antibodies generates a signal only when the two probes are bound in close proximity. The signal from each interacting pair is visualized as an individual fluorescent dot; the number of dots is quantified by counting and assigned to a specific subcellular location on microscopy images. The proximity ligation assay shows that *N*-homocysteinylation of kinesin and dynein increases 29- and 37-fold, respectively, in the folate-deficient cells, compared with folate-replete cells. At the same time the interactions of kinesin and dynein with tubulin decrease 3.2- and 3.6-fold, respectively, in the folate-deficient cells. Similar changes occur when the rat neuronal cells are treated with Hcy-thiolactone, supporting a conclusion that *N*-homocysteinylation of kinesin and dynein causes aggregation and prevents their interactions with tubulin. LC-MS/MS analyses identify Lys1218 residue in dynein as being *N*-homocysteinylated [299].

5.5 Quantification of *N*-Hcy-Protein

The discovery that *N*-Hcy-protein is formed biologically in living cells relied on the use of radiolabeled [³⁵S]methionine and [³⁵S]homocysteine as precursors [73, 74]. In those experiments confluent cultures of human cells in 3.5-cm dishes are labeled for 24–48 h with 0.1 mCi/mL [³⁵S]methionine or [³⁵S]homocysteine (5–100 μM) in methionine-free medium supplemented with fetal bovine serum and other requirements. Streptomycin is not used in these experiments because it reacts with Hcy-thiolactone (Table 3.4) [74]. Extracellular and cellular proteins are treated with DTT to remove free and disulfide-linked Hcy. Covalently incorporated [³⁵S]Hcy and [³⁵S]Met are released from the radiolabeled protein by hydrolysis with 6 N HCl, 25 mM DTT (1 h, 120 °C); under these conditions protein *N*-linked Hcy is converted to [³⁵S]Hcy-thiolactone [139]. [³⁵S]Hcy-thiolactone is separated from [³⁵S]Met by two-dimensional TLC on 5 cm × 4 cm cellulose or silica gel plates using as little as 5 μL acid-hydrolyzed sample (Fig. 3.7e, f). The first-dimension solvent is butanol/acetic acid/water (4/1/1, v/v), and the second-dimension solvent is isopropanol/ethyl acetate/water/ammonia (12/12/1/0.12, v/v). [³⁵S]Hcy-thiolactone is visualized by autoradiography using Kodak BioMax X-ray film

and quantified by scintillation counting. The radiolabeling method has been used to provide the first evidence that protein *N*-homocysteinylation occurs in cultured human umbilical vein endothelial cells (Fig. 3.7) and normal human fibroblasts and that the accumulation of *N*-Hcy-protein increases in CBS-deficient fibroblasts and breast cancer cells [73, 74]. This method has also been instrumental in the demonstration that protein *N*-homocysteinylation is universal in mammalian cells and occurs in another kingdom of life, the plants [190].

Subsequently, to facilitate studies of *N*-Hcy-protein in humans and experimental animals, HPLC-based assays have been developed. Liquid chromatography/mass spectrometry assays are now used for monitoring site-specific *N*-homocysteinylation. Immunoassays with rabbit polyclonal anti-*N*-Hcy-protein IgG antibodies are also used for monitoring *N*-Hcy-protein. Methods are also being developed for the detection of *N*-Hcy-protein by exploiting their selective reactions with aldehydes.

5.5.1 High-Performance Liquid Chromatography Assay with UV Detection

In the first HPLC assay developed for the determination of *N*-linked Hcy content in proteins, *N*-Hcy-protein is subjected to acid hydrolysis under reducing conditions. Under these conditions the liberated Hcy is converted to Hcy-thiolactone, which is then quantified by cation exchange HPLC with UV detection [79].

The assay requires 200 μ L human plasma or 10 mg protein sample. Free and disulfide-bound Hcy are removed by treatments with 5 mM dithiothreitol (DTT) in phosphate-buffered saline and ultrafiltration on Millipore 10-kDa cutoff devices at 4 °C (repeated six times). The completeness of the treatments is verified by assaying Hcy in the last filtrate. Protein sample is then transferred from the ultrafiltration device to a 1-mL glass ampoule, supplemented with DTT to 25 mM and HCl to 6 M, frozen at -80 °C, sealed under vacuum, and hydrolyzed at 120 °C for 1 h. The hydrolysate is lyophilized, dissolved in 2 M ammonium bicarbonate, 1 M dipotassium phosphate, supplemented with [³⁵S]Hcy-thiolactone (18,000 cpm, 40,000 Ci/mol) as a tracer to monitor recovery. Hcy-thiolactone is extracted with chloroform/methanol (2:1, v/v) followed by re-extraction of the organic layer with 0.1 M HCl. The acid extracts are lyophilized, taken up in water, and further purified by two-dimensional thin-layer chromatography on cellulose or silica gel plates (6.7 cm \times 5 cm). The first dimension solvent is butanol/acetic acid/water (4/1/1, v/v), while isopropanol/ethyl acetate/water/ammonia (12/12/1/0.12, v/v) is used as the second-dimension solvent. The [³⁵S]Hcy-thiolactone spot is visualized by autoradiography using Kodak BioMax X-ray film, scraped off the plate, and Hcy-thiolactone is eluted with cold 2 mM HCl (60 μ L, on ice). Final purification and quantification is by cation exchange HPLC on a polysulfoethylaspartamide column (PSEA, 2.1 \times 200 mm, 5 μ , 300 Å, from PolyLC, Inc.) using NaCl gradient from

50 to 160 mM in 10 mM sodium monophosphate for 6-min and 3-min re-equilibration time and a flow rate of 0.5 mL/min. The effluent is monitored in UV at 240 nm, λ_{\max} for Hcy-thiolactone [68].

Using this assay, *N*-linked Hcy has been discovered in individual human blood proteins, with highest amounts found in albumin and hemoglobin. Lower amounts of protein *N*-linked Hcy are found in human fibrinogen, transferrin, antitrypsin, IgG, LDL, and HDL. *N*-linked Hcy is also present in albumins from other species, including sheep, pig, rabbit, chicken, rat, and mouse. This study also demonstrated for the first time that protein *N*-linked Hcy is a significant component of human plasma. The plasma concentrations of *N*-Hcy-protein vary between different individuals from 0.5 to 13 μM , which represent from 0.3 to 23 % of plasma tHcy. Plasma *N*-Hcy-protein is positively correlated with plasma tHcy [79].

5.5.2 *High-Performance Liquid Chromatography Assays with Fluorescence Detection*

5.5.2.1 Derivatization with OPA

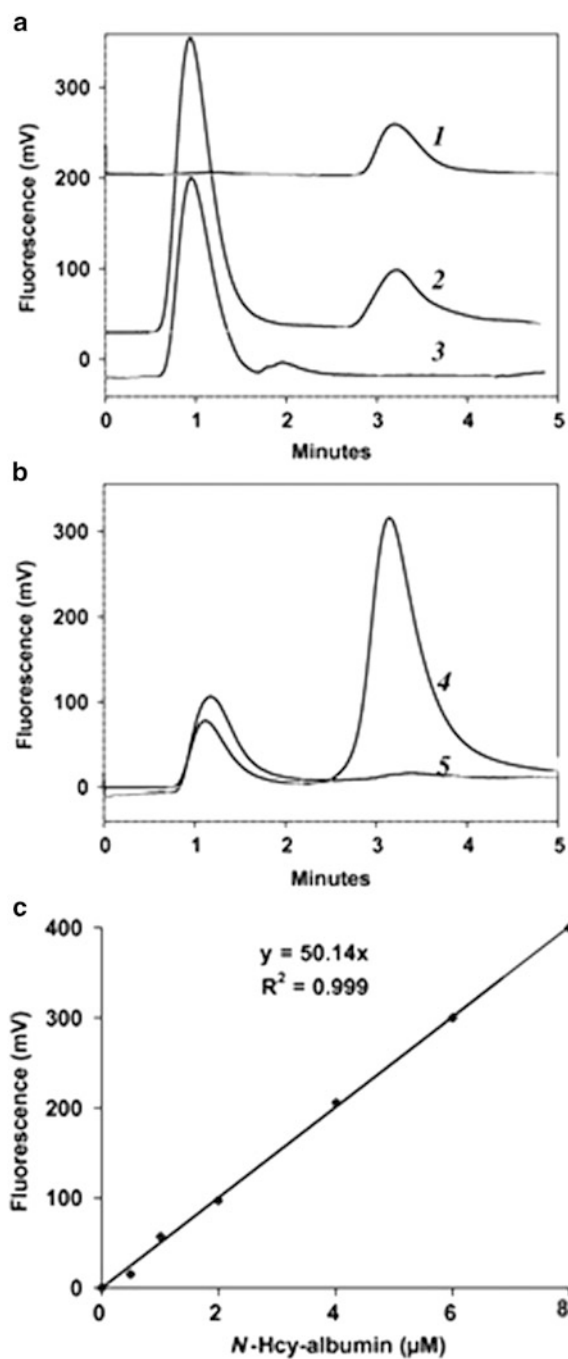
The original protein *N*-linked Hcy assay has been modified to increase the sensitivity and allow analyses of much smaller samples [297]. The new assay requires only 5 μL plasma or 0.1 mg purified protein and uses post-column derivatization with alkaline OPA followed by fluorescence detection.

After removal of free and disulfide-bound Hcy by treatments with DTT and ultrafiltration on Millipore 10-kDa cutoff devices, protein is hydrolyzed with 6 M HCl, 25 mM DTT. The hydrolysates are lyophilized, dissolved in 10 μL water containing 20,000 cpm [^{35}S]Hcy-thiolactone (40,000 Ci/mol) as a tracer to monitor recovery, and the liberated Hcy-thiolactone is purified by two-dimensional TLC on cellulose or silica gel plates (5 cm \times 4 cm). The [^{35}S]Hcy-thiolactone spot is localized by autoradiography and scraped off the plate, and Hcy-thiolactone is recovered by elution with 60 μL cold 2 mM HCl.

The recovered Hcy-thiolactone is quantified by HPLC on a cation exchange PSEA column (2 mm \times 35 mm) eluted isocratically with 10 mM sodium phosphate, pH 6.6, and 20 mM NaCl at a flow rate of 0.36 mL/min for 5 min. The effluent is mixed in a three-way tee with 2.5 mM OPA and 0.25 M NaOH, delivered at a flow rate of 0.18 mL/min. The mixture passes through Teflon tubing reaction coil (0.3 mm i.d. \times 3 m) and is monitored with a Jasco 1,520 fluorescence detector using excitation at 370 nm and emission at 480 nm.

The assay is calibrated with in vitro-prepared *N*-Hcy-albumin standard containing 0.027 mol *N*-linked Hcy/mol protein (Fig. 5.14). The sensitivity of this assay allows detection of as little as 0.00006 mol Hcy/mol protein. With this assay, *N*-linked Hcy in individual proteins was found to vary from as high as 0.470–0.515 mol/mol protein for human and equine ferritins to as low as 0.00006 mol/mol protein for chicken lysozyme. An example of HPLC

Fig. 5.14 Determination of protein *N*-linked Hcy by cation exchange HPLC. Protein *N*-linked Hcy is converted to Hcy-thiolactone, which is then quantified by HPLC. (a) Hcy-thiolactone standard (5 pmol) elutes at 3.2 min (trace 1). Analysis of a sample prepared from 6 μM *N*-[^{35}S]Hcy-HSA standard is illustrated by trace 2. Trace 3 is a control showing a baseline obtained with 2 mM HCl eluate of cellulose scrapings from the TLC plate. (b) Analyses of samples prepared from ferritin hydrolysate (20 μg) before (trace 4) and after (trace 5) treatment with NaOH. Detection was by fluorescence emission at 480 nm (excitation at 370 nm) after post-column derivatization with OPA. *Bottom panel:* calibration line for the *N*-Hcy-albumin standard (Reproduced from [297])



determination of *N*-linked Hcy in ferritin is illustrated in Fig. 5.14b. Hemoglobins from a variety of species (baboon, bovine, horse, pig, rat, mouse, and chicken) contain more protein *N*-linked Hcy than did corresponding albumins (0.0127–0.0828 vs. 0.0027–0.0086 mol/mol). Normal human plasma and milk were found to contain sub-micromolar concentrations of protein *N*-linked Hcy, whereas cow milk and whey contained micromolar concentrations of protein *N*-linked Hcy. This assay has been extensively used in the studies of plasma and tissue *N*-Hcy-protein in genetic deficiencies in folate and Hcy metabolism in humans [115] and mice [113] as well as in studies of physiological roles of paraoxonase 1 and bleomycin hydrolase using *Pon1*-null [140] and *Blmh*-null [141] mice.

An alternative HPLC assay for protein *N*-linked Hcy uses tris(2-carboxyethyl) phosphine (TCEP) for S-linked Hcy reduction and removal and on-column derivatization with alkaline OPA and fluorescence detection [220]. The method's limit of quantification for protein *N*-linked Hcy is 0.25 μM . The utility of the method was demonstrated with plasma samples from 18 subjects, in whom protein *N*-linked Hcy varied from 1.6 to 3.3 μM (mean = 2.52 μM) and tHcy concentrations varied from 7.7 to 134 μM .

5.5.2.2 Derivatization with 4-Fluoro-7-sulfamoyl-benzofurazan

Two other *N*-Hcy-protein assays rely on pre-column derivatization with other fluorescent thiol reagents. In one assay, thiols in plasma protein are derivatized with 4-fluoro-7-sulfamoyl-benzofurazan. The derivatized proteins are then acid-hydrolyzed, and the liberated derivatized Hcy is quantified by C18 reversed-phase HPLC and fluorescence detection [300]. The method was applied to 35 plasma samples from 20 healthy adults and 15 hemodialysis patients. The mean concentrations for control group were $0.51 \pm 0.11 \mu\text{M}$ for protein *N*-linked Hcy and $13.9 \pm 5.8 \mu\text{M}$ for tHcy. In 15 hemodialysis patients, the mean concentrations were $0.74 \pm 0.20 \mu\text{M}$ for protein *N*-linked Hcy and $47.2 \pm 26.1 \mu\text{M}$ for tHcy. The peptide fraction containing protein *N*-linked Hcy accounts for 4.2 % of tHcy in healthy adults and 2.0 % in hemodialysis patients.

5.5.2.3 Derivatization with 7-Fluorobenzo-2-Oxa-1,3-Diazole-4-Sulfonate

In another assay [301], plasma protein *N*-linked Hcy is quantified by HPLC after sample reduction with tri-*n*-butyl-phosphine, gel filtration, derivatization with ammonium 7-fluorobenzo-2-oxa-1,3-diazole-4-sulfonate, and acid hydrolysis. Using this assay, it is found that protein *N*-linked Hcy and S-linked Hcy in uremics are significantly elevated relative to control subjects. The protein *N*-linked Hcy and tHcy concentrations in uremic patients were $0.86 \pm 0.14 \mu\text{M}$ and $69.38 \pm 15.15 \mu\text{M}$, respectively. After folate therapy, protein *N*-linked Hcy in uremic patients is normalized to the levels observed in healthy subjects ($0.40 \pm 0.06 \mu\text{M}$), whereas S-linked Hcy is lowered (to $26.01 \pm 3.80 \mu\text{M}$) but remains elevated relative to control subjects ($11.35 \pm 1.03 \mu\text{M}$).

5.5.3 *Immunoassays with Rabbit Polyclonal Anti-N-Hcy-Protein Antibodies*

N-Hcy-proteins were first found to be immunogenic in 1998 when anti-*N*-Hcy-protein IgG antibodies were generated by immunizing rabbits with homologous low-density lipoprotein modified with Hcy-thiolactone [356]. Similar antibodies were subsequently prepared by immunizing rabbits with Hcy-thiolactone-modified keyhole limpet hemocyanin (KLH) [172] and rabbit serum albumin [168].

Rabbit polyclonal anti-*N*-Hcy-protein antibodies, generated with rabbit serum *N*-Hcy-albumin as an antigen, were used in clinical studies of plasma *N*-Hcy-protein as a risk factor for coronary heart disease in a group of 254 patients and 308 controls [168]. For an *N*-Hcy-protein ELISA immunoassay, tested plasma is mixed with anti-*N*-Hcy-protein antiserum and added to wells of microtiter plates coated with *N*-Hcy-albumin. Bound antiserum is detected with anti-rabbit IgG secondary antibody conjugated with HRP by reading A₄₉₂ after reaction with OPD solution. The plasma level of *N*-Hcy-protein adducts was significantly higher in coronary heart disease patients than in controls (40.65 ± 10.87 units/mL vs. 30.58 ± 10.20 units/mL, $P < 0.01$), with odds ratio of 7.34 (95 % confidence interval 4.020–13.406, $P < 0.01$), and increased according to the number of atherosclerotic coronary arteries: 35.59 ± 10.34 units/mL ($n = 76$), 41.88 ± 8.83 ($n = 70$), and 43.13 ± 11.47 ($n = 108$) in subjects with 1, 2, and 3 affected arteries, respectively ($r = 0.174$, $P < 0.01$).

Rabbit polyclonal anti-*N*-Hcy-protein IgG antibodies, generated with *N*-Hcy-KLH as an antigen [172], are useful for the immunohistochemical detection of *N*-Hcy-protein in human and mouse tissues with good sensitivity and specificity [357]. This antibody detects *N*-Hcy-protein in a dot blot assay with the signal depending on the amount of the antigen, but the magnitude of the signal is protein dependent. The rabbit anti-*N*-Hcy-protein IgG specifically detects *N* ϵ -Hcy-Lys epitopes in human tissues, as shown by positive immunohistochemical staining of myocardium and aorta samples from cardiac surgery patients, and a lack of staining when the antibody was pre-adsorbed with *N*-Hcy-albumin. An increased immunohistochemical staining for *N*-Hcy-protein is also observed in aortic lesions from *ApoE*^{-/-} mice, and the staining is increased in *ApoE*^{-/-} animals that are fed with a hyperhomocysteinemic high-methionine diet [357].

5.5.4 *Western Blot Immunoassay for N-Hcy-ApoAI*

N-homocysteinylation introduces a free thiol group into a protein. Such thiol group can be easily detected in proteins that do not contain cysteine residues with a free thiol group. This principle has been exploited for the detection and quantification of *N*-Hcy-ApoAI [303], a major protein component of HDL particles that does not contain free cysteine residue thiols. The (*N*-Hcy-SH)-ApoAI in serum or HDL is

treated with cysteamine $\text{HS-CH}_2\text{CH}_2\text{-NH}_2$. This generates an adduct (*N*-Hcy-S-S- $\text{CH}_2\text{CH}_2\text{-NH}_2$)-ApoAI, in which cysteamine is bound via a disulfide bond to the *N*-linked Hcy residue and introduces a free amino group into the *N*-homocysteinylated protein. The additional amino group changes the protein's isoelectric point, which allows separation of the more basic (*N*-Hcy-S-S- $\text{CH}_2\text{CH}_2\text{-NH}_2$)-ApoAI adduct from unmodified ApoAI by isoelectric focusing on polyacrylamide gels. Separated modified and unmodified forms of ApoAI are detected by Western blotting and staining with an antihuman ApoAI polyclonal antibody (goat). The stained bands are quantified by digital scanning and the ratio of *N*-Hcy-ApoAI/total ApoAI is calculated. The results are corrected for an occasional nonspecific band by subtracting the ratio obtained without cysteamine treatment from that with cysteamine treatment [303].

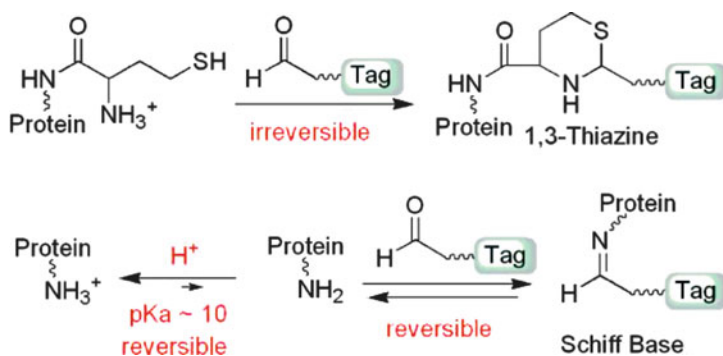
The reproducibility of this semiquantitative method is 19.1 %. In a population of 27 healthy subjects, the concentration of *N*-Hcy-ApoAI varies from 1.2 to 14.5 mg/dL, whereas the ratio of *N*-Hcy-ApoAI/total ApoAI varies from 1 to 7.4 % (ApoAI concentration varies from 110 to 200 mg/dL). *N*-Hcy-ApoAI was significantly correlated with total ApoAI ($r = 0.673$, $p = 0.001$). However, *N*-Hcy-ApoAI is not correlated with tHcy, which varied in the normal range from 5 to 15 μM .

The *N*-Hcy-ApoAI values of 1.2 to 14.5 mg/dL correspond to 0.57 μM to 6.9 μM *N*-Hcy-ApoAI in plasma. However, such high *N*-Hcy-ApoAI concentrations are unrealistic because total *N*-Hcy-protein levels in plasma are known to be about 0.5 μM , most of which is due to *N*-Hcy-albumin [78, 115, 300, 358].

5.5.5 Detection of Protein *N*-Homocysteinylolation by Selective Reactions with Aldehydes

Hcy and Hcy-thiolactone are known to react with aldehydes to yield 1,3-tetrahydrothiazine-4-carboxylic acid derivatives (Table 3.1) (Reaction 3.5) [84]. These reactions are being explored for the detection of free Hcy in biological samples [227, 359, 360] and *N*-Hcy-proteins [214].

The condensation reaction between an aldehyde tag and γ -thiol and α -amino groups of *N*-linked Hcy residue in *N*-Hcy-protein yields 1,3-thiazine adduct (Reaction 5.6). Under acidic conditions ($\text{pH} = 3$), the reaction of the aldehyde with *N*-linked protein Hcy is irreversible, while a possible competing Schiff base formation with the protein amino groups is reversible and favors the protonated free amines (Reaction 5.6). For example, rhodamine aldehyde selectively reacts with *N*-Hcy-myoglobin (containing 0.4 *N*-Hcy/mol protein) to form a fluorescent 1,3-thiazine adduct [214]. Mass spectrometric analyses show that *N*-linked Hcy in myoglobin is quantitatively converted to a corresponding 1,3-thiazine derivative and that the reaction is completed in 3 h. Selectivity is demonstrated by LC-ESI-MS, which shows no detectable formation of a Schiff base under acidic ($\text{pH} = 3$) conditions. Quantification of the fluorescence associated with the band of



Reaction 5.6 In reactions of aldehydes with *N*-Hcy-protein, 1,3-thiazine formation is favored over Schiff base formation under acidic conditions (Reprinted from [214])

N-Hcy-myoglobin-rhodamine aldehyde adduct (excitation at 450 nm, emission at 520 nm) after separation on SDS-PAGE gels shows that the assay is linear from 160 ng to 2.5 μ g modified myoglobin. The detection limit is 80 ng *N*-Hcy-myoglobin [214], corresponding to 1.8 pmol *N*-linked Hcy in myoglobin.

The rhodamine aldehyde tagging assay detects protein *N*-homocysteinylation in biological samples. For example, normal human serum, which is known to contain small amounts of *N*-Hcy-albumin [96], is labeled with rhodamine aldehyde and *N*-Hcy-myoglobin is added as a standard. After separation on SDS-PAGE gels, the fluorescence signal is detected in the albumin band, in addition to the band of *N*-Hcy-myoglobin used as a positive control [214].

Using this approach but with a different tag, biotinylated aldehyde, increases the sensitivity and allows detection of *N*-linked Hcy in human and rat proteins [214]. After incubation with biotinylated aldehyde (pH 3.0, 25 °C, 8 h), proteins are separated by SDS-PAGE, subjected to Western blotting, and detected by chemiluminescence using streptavidin-horseradish peroxidase, SuperSignal West Pico chemiluminescence substrate, and FluoroChem Imager SP. In this assay, the extent of *N*-homocysteinylation is found to be greater in rat hemoglobin than that observed in human hemoglobin. The biotin aldehyde labeling assay also demonstrates higher levels of *N*-homocysteinylation in rat serum proteins, compared with human serum proteins [214]. These results are consistent with previous assays of *N*-linked Hcy in hemoglobin and albumin from different species (Table 5.7) using an HPLC-based method [297] and provide a validation for the biotin aldehyde labeling approach.

Selective reactions with aldehydes can also be used for affinity enrichment of *N*-Hcy-proteins or *N*-Hcy-peptides, usually present at low abundance, to increase sensitivity of their detection [214]. For this purpose aldehyde resins are used. Tryptic peptides obtained from *N*-Hcy-proteins are passed through the Self Pack POROS 20 AL resin functionalized with an aliphatic aldehyde. After washing unbound peptides, the bound *N*-Hcy-peptides are eluted by three treatments with *O*-methylhydroxylamine. The combined eluted fractions are concentrated and

analyzed by mass spectroscopy. Using this approach, over a dozen of *N*-homocysteinylation sites have been identified in in vitro-prepared human *N*-Hcy hemoglobin [214].

5.5.6 Liquid Chromatography/Mass Spectrometry Analysis of the Site-Specific Protein *N*-Homocysteinylation In Vivo

Site-specific *N*-homocysteinylation is assayed by using a liquid chromatography/mass spectrometry (LC–MS) method. So far, site-specific *N*-homocysteinylation in vivo has been analyzed for human serum albumin [212, 213] and fibrinogen [215]. The sites of *N*-homocysteinylation identified in these proteins in vivo correspond to lysine residues that are the most reactive with Hcy-thiolactone in vitro.

5.5.6.1 *N*-Hcy-Albumin

The LC–MS method was first used in 2004 to demonstrate that Lys525 in human serum albumin is a predominant site of the modification by Hcy-thiolactone in vitro and in vivo [96]. This has been achieved by the identification of ⁵²⁵K*QTALVELVK⁵³⁴ peptide carrying *N*-linked Hcy at lysine-525 (⁵²⁵K*) in albumin modified with Hcy-thiolactone in vitro (used at 1:1 molar ratio) as well as in native albumin isolated from individuals with elevated plasma Hcy levels (40–80 μM). At that time, the analyses of site-specific *N*-homocysteinylation in vivo required extensive sample workup and enrichment procedures [96], which precluded their routine use.

To overcome these limitations, a new LC–MS method for monitoring site-specific albumin *N*-homocysteinylation directly in human plasma samples has been developed [212, 213]. To be able to detect site-specific *N*-homocysteinylation in vivo, it is important to know which lysine residues in the protein are susceptible to the modification with Hcy-thiolactone in vitro and which peptides containing *N*-Hcy-Lys residues can be detected. For this purpose, *N*-Hcy-albumin containing 6 moles Hcy/mol albumin is prepared by an overnight incubation of human serum albumin (10 mg/mL) with 10 mM L-Hcy-thiolactone-HCl in 0.1 M sodium phosphate buffer, pH 7.4, 0.1 mM EDTA at 22 °C [78, 139]. One nanomole of *N*-Hcy-albumin is then reduced with 45 mM DTT in 0.1 M ammonium bicarbonate, alkylated with 0.1 M iodoacetate, and digested with trypsin at a trypsin:protein ratio of 1:50 37 °C for 17 h. Tryptic peptides are fractionated on a C18 microcolumn (ZipTip, Millipore) using 10, 30, 50, and 100 % acetonitrile [298] or on a C18 HPLC column. Each fraction is applied on the Prespotted Anchorchip and analyzed on a MALDI-TOF Autoflex instrument (Bruker Daltonics). Peptide identification is performed by MASCOT, allowing for a mass increase of 57 Da due to carbamidomethylation and of 174 Da due to *N*-homocysteinylation and carbamidomethylation. These analyses show that K4

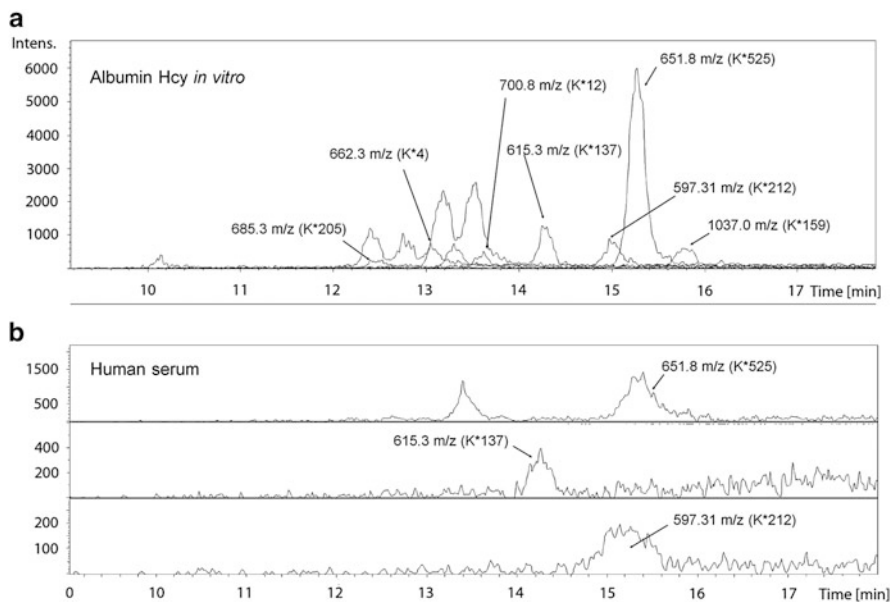


Fig. 5.15 Mass spectrometric identification of *N*-Hcy-Lys residues in *N*-homocysteinylated albumin. LC-ESI-MS chromatograms of selected ions of *N*-Hcy-Lys-peptides obtained by the digestion with trypsin of *in vitro* *N*-homocysteinylation of human serum albumin (panel **a**) and *N*-Hcy-Lys-peptides of albumin from tryptic digests of human serum from a CBS-deficient hyperhomocysteinemic subject (panel **b**) (Reproduced from [212])

($^1\text{DAHK}^*\text{SEVAHR}^{10}$, 1,323.6 m/z), K12 ($^{11}\text{FK}^*\text{DLGEENFK}^{20}$, 1,400.7 m/z), K137 ($^{137}\text{K}^*\text{YLYEIAR}^{144}$, 1,229.7 m/z), K159 ($^{146}\text{HPYFYAPELLFFA K}^*\text{R}^{160}$, 2,073.1 m/z), K205 ($^{200}\text{CASLQK}^*\text{FGER}^{209}$, 1,369.6 m/z), and K212 ($^{210}\text{AFK}^*\text{AWAVAR}^{218}$, 1,193.6 m/z), in addition to previously identified K525 ($^{525}\text{K}^*\text{QTALVELVK}^{534}$, 1,302.8 m/z) [96] in human serum albumin, are susceptible to the modification by Hcy-thiolactone *in vitro*.

The identity of *N*-homocysteinylation sites in human serum albumin is confirmed by additional tandem mass spectrometric analyses using LC/ESI-MS/MS system consisting of nano-LC chromatograph hyphenated to q-ToF hybrid mass spectrometer. Identification of the seven *N*-Hcy-Lys-peptides in tryptic digest of *N*-Hcy-albumin is achieved in a single analysis in this system (Fig. 5.15). From the recorded mass spectra, it is possible to deduce sequences of all seven consecutively eluted *N*-Hcy-Lys-peptides. Retention times of peptides together with CID MS/MS spectra for the four most abundant *N*-Hcy-Lys-peptides unequivocally confirmed their structures [212].

Knowing the masses of Hcy-containing peptides derived from the *in vitro*-prepared *N*-Hcy-albumin, we can determine whether these peptides are present in samples prepared from native human serum. For this purpose, human serum is diluted 60-fold with 50 mM NH_4HCO_3 and reduced with 1 mM DTT at 95 °C for 5 min. Thiol groups are blocked with 4 mM iodoacetamide at 22 °C in the dark for 20 min, and the serum protein is digested with sequencing grade trypsin. Tryptic

digests were subjected to LC–MS analysis using a nanoscale liquid chromatography system (EASY-nLC, Proxeon) coupled to a quadrupole-time-of-flight mass spectrometer (microTOF-Q™, Bruker Daltonics). Samples (10 µL) are loaded on a C18 pre-column (5 µm i.d., Nano Separations) and separated on a C18 column (100 µm i.d., 150 mm, Nano Separations) using 0–54 % acetonitrile gradient in 0.1 % formic acid for 30 min. Data are analyzed using Data Analysis and Bio Tools software (Bruker Daltonics).

Three albumin residues, Lys525, 137, and 212, are found to be *N*-homocysteinylated *in vivo* in human plasma from CBS-deficient patients and unaffected individuals, with Lys525 being the predominant *in vivo*-modified site (Fig. 5.15). Albumin peptide containing *N*-Hcy-Lys-525 is present in essentially all analyzed plasma samples (43 out of 44), including those which had the lowest tHcy concentration (9.9 µM), whereas peptides containing *N*-Hcy-Lys-137 and *N*-Hcy-Lys-212 are present in CBS-deficient patients whose plasma tHcy concentration was elevated, at least 34.9 ± 11.0 µM and 131 ± 21 µM, respectively [212].

To determine whether the amount of 525 K*QTALVELVK 534 peptide reflects the extent of total serum protein *N*-homocysteinylolation, the 651.3 *m/z* peptide is quantified in tryptic digests of plasma samples from healthy individuals, who have low levels of *N*-Hcy-protein, and from CBS-deficient patients, who have elevated levels of *N*-Hcy-protein [115]. For quantification purposes, signal intensity of the 651.3 *m/z* peptide is normalized to signal intensity of a major albumin peptide 42 LVNEVTEFAK 51 (575.3 *m/z*).

For peptides containing *N*-Hcy-Lys525 and *N*-Hcy-Lys137, intra-assay variability is ≤ 10 %. Inter-assay variability determined from duplicate assays of 20 human plasma samples on two different days is 43 %. Other *N*-Hcy-peptides are present in low abundance, have low signal/noise ratios, and cannot be reliably quantified.

Normalized levels of the 651.3 *m/z* peptide (containing *N*-Hcy-Lys525) are significantly higher in CBS-deficient patients ($n = 15$), compared with healthy individuals ($n = 29$) (0.0399 ± 0.0260 vs. 0.0102 ± 0.0121 , $P = 0.0007$) (Table 5.6).

These values suggest that about 1 % and 4 % albumin molecules are *N*-homocysteinylated at Lys525 in healthy individuals and CBS-deficient patients, respectively. The higher levels of *N*-homocysteinylolation at Lys525 in albumin from CBS-deficient patients reflect elevated total Hcy and *N*-Hcy-protein levels in these patients [115] measured using chemical assays [297]. There is a significant correlation between the albumin *N*-Hcy-Lys525 peptide and plasma tHcy ($r = 0.49$, $p < 0.001$) [213].

5.5.6.2 *N*-Hcy-Fibrinogen

Analysis of sites that are *N*-homocysteinylated in fibrinogen *in vivo* requires purification of the protein from human plasma using the glycine precipitation method [115, 361]. Purified fibrinogen is acetamidated, digested with trypsin, and

subjected to LC–MS analyses. Three *N*-Hcy-Lys-peptides containing α -Lys562, β -Lys344, and γ -Lys385 are identified in fibrinogen isolated from CBS-deficient patients [215]. These three *in vivo* *N*-homocysteinylation sites are the predominant sites for fibrinogen *N*-homocysteinylation *in vitro* (Fig. 5.3).

Chapter 6

Pathophysiological Consequences of Protein *N*-Homocysteinylation

Elevated Hcy-thiolactone and *N*-Hcy-protein levels are found to be associated with pathological conditions. For example, plasma Hcy-thiolactone and *N*-Hcy-protein are elevated under conditions predisposing to atherothrombosis and neurological abnormalities, such as caused by CBS or MTHFR deficiencies in humans [115] and mice [113]. In humans, plasma Hcy-thiolactone levels are also associated with the development and progression of vascular complications in diabetic patients [362], whereas elevated *N*-Hcy-protein levels are associated with an increased risk of heart disease [168]. Furthermore, Hcy-thiolactonase activity of PON1, which protects against protein *N*-homocysteinylation in CBS-deficient patients [250], also predicts cardiovascular disease in humans [269].

The sensitivity of mammalian cells and organisms to hyperhomocysteinemia raises a broader question of mechanistic basis. On a molecular level, hyperhomocysteinemia is known to activate the expression of genes that are under control of signaling pathways that respond to a load in the endoplasmic reticulum (ER). These include the Bip/GRP78 gene, encoding an ER chaperone [363]; CHOP/GADD153, encoding a transcription factor implicated in cellular responses to ER stress [364, 365]; and HERP, encoding a protein that may be involved in degradation of misfolded ER proteins [366]. The cellular response to ER stress is known as the unfolded protein response (UPR) and includes a conserved transcriptional adaptation by which cell adjusts the biosynthesis of proteins involved in ER function to the physiological demand. The UPR involves signaling pathways that monitor the folding environment of the ER and transduce signals across the membrane to the cytoplasm and nucleus [367, 368].

Relatively high (millimolar) concentrations of Hcy are required to activate the UPR in *ex vivo* cultured cells. However, the activation of CHOP/GADD153 gene expression increases in the liver of mice with diet-induced hyperhomocysteinemia [369]. These findings suggest that ER dysfunction and UPR have a role in the pathophysiology of hyperhomocysteinemia in intact organisms *in vivo*.

During the folding process, proteins form their globular native states in a manner determined by their primary amino acid sequence [231, 370]. Thus, small changes in amino acid sequence caused by Hcy incorporation into protein have a potential to

create misfolded protein aggregates. The appearance of misfolded/aggregated proteins in the lumen of the ER activates the UPR that, when overwhelmed, leads to cell death via apoptosis; protein aggregates are known to be inherently toxic to cells [371].

The molecular basis for the impairment in ER function by hyperhomocysteinemia is not known but may include protein *N*-homocysteinylation by Hcy-thiolactone (Reaction 3.4) that can cause protein misfolding and induce ER stress. As discussed in the following sections, protein modification by Hcy-thiolactone can also create altered proteins with newly acquired interactions or impaired function and can lead to induction of autoimmune responses.

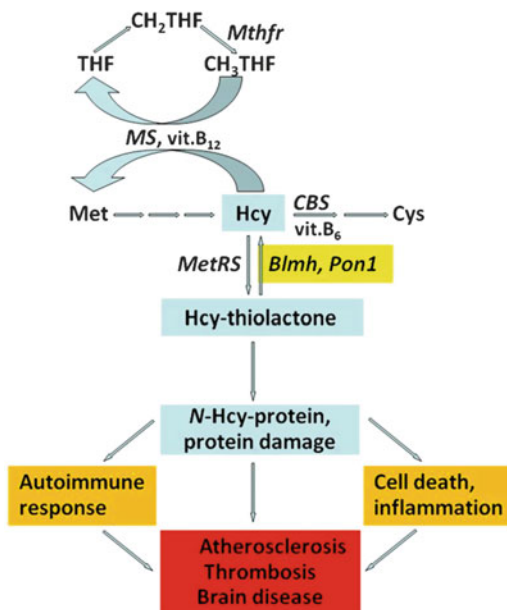
The findings that *N*-Hcy-proteins have the propensity to aggregate [78, 139, 153, 336] and induce cell death in cultured cells, first demonstrated for *N*-Hcy-LDL and human endothelial cells [170], are consistent with this concept. In addition to its propensity to aggregate, *N*-Hcy-albumin [78], which accumulates in hyperhomocysteinemia [213], forms amyloid-like protofibrils that are toxic to cells [171]. Recent findings show that *N*-homocysteinylation induces amyloidal transformation in several other proteins, further discussed in Sect. 5.4 of this book. It should be noted that ER stress and UPR in cultured human endothelial cells and in mice are induced by hyperhomocysteinemia [18, 58, 59, 369], which also elevates plasma Hcy-thiolactone [64, 74, 93] and *N*-Hcy-protein levels [78, 113].

Furthermore, treatments with Hcy-thiolactone are more effective than treatments with Hcy in inducing ER stress and UPR in retinal epithelial cells [60] and apoptotic death in cultured human vascular endothelial cells [61, 164]. The greater sensitivity of cells to Hcy-thiolactone suggests that protein modification by Hcy-thiolactone leads to the UPR and induction of the apoptotic pathway. Consistent with this scenario, cellular levels of *N*-Hcy-protein are elevated under conditions of hyperhomocysteinemia-induced ER stress both in cultured cells [74] and in the mouse liver [113]. *N*-Hcy-proteins are known to undergo major structural changes [78, 96] which cause misfolding and formation of toxic amyloid aggregates [171]. Recent studies show that folic acid limitation increases cellular Hcy levels, induces *N*-homocysteinylation of the motor protein dynein, and induces the formation of *N*-Hcy-protein aggregates in rat neuronal cells [299]. Proteolytic degradation of *N*-Hcy-protein can generate antigenic peptides, which can be displayed on cell surface and induce an autoimmune response.

6.1 The Hcy-Thiolactone Hypothesis

Studies of Hcy-thiolactone metabolism shed light on a mechanism underlying pathological consequences of elevated Hcy levels. The Hcy-thiolactone hypothesis (Fig. 6.1), originally formulated in 1997 [62], states that the metabolic conversion of Hcy to Hcy-thiolactone followed by the nonenzymatic protein modification by Hcy-thiolactone—protein *N*-homocysteinylation—is an underlying biochemical mechanism that contributes to the pathology of hyperhomocysteinemia, such as

Fig. 6.1 The pathology of hyperhomocysteinemia: the Hcy-thiolactone hypothesis (Adapted from [93])



observed in cardiovascular and neurodegenerative diseases [69, 73, 74, 78, 134]. The thioester chemistry of Hcy-thiolactone underlies its ability to form stable isopeptide bonds with protein lysine residues, which impairs or alters the protein's function. Major pathophysiologic consequences linked to the accumulation of *N*-Hcy-protein include inflammation [169], cell death [170, 171], an autoimmune response [134, 135, 172, 173], and interference with blood clotting (Fig. 6.1) [174, 175].

The verification of Hcy-thiolactone hypothesis became possible with the development of sensitive chemical [79] and immunological assays [168, 357] for detection and quantification of Hcy-thiolactone [94, 95] and protein *N*-linked Hcy in humans [115, 297] and mice [93, 113]. Evidence supporting the Hcy-thiolactone hypothesis is discussed in a greater detail in the following sections.

6.1.1 *Hcy-Thiolactone Levels in Hyperhomocysteinemia*

The Hcy-thiolactone hypothesis predicts that Hcy-thiolactone will be elevated under conditions predisposing to cardiovascular or neurodegenerative disease, such as hyperhomocysteinemia due to mutations in genes encoding Hcy or folate-metabolizing enzymes. This prediction has been confirmed *in vivo* in humans and mice. For example, CBS-deficient patients have greatly elevated Hcy-thiolactone levels [93]: mean plasma Hcy-thiolactone concentration in CBS^{-/-} patients (14.4 nM) is 72-fold higher than in unaffected CBS^{+/+} individuals (Table 3.12).

This finding is consistent with *ex vivo* observations that cultured human CBS-deficient fibroblasts synthesize much more Hcy-thiolactone than normal fibroblasts [73].

Moreover, 5-methyltetrahydrofolate deficiency, secondary to a mutation in the *MTHFR* gene, leads to elevation of Hcy-thiolactone levels in humans [93]: plasma Hcy-thiolactone in *MTHFR*-deficient patients (11.8 nM) is 24- or 59-fold higher than in *MTHFR* heterozygous or normal individuals, respectively (Table 3.12). This *in vivo* finding is consistent with *ex vivo* observations showing that limited availability of folic acid greatly enhances Hcy-thiolactone synthesis in human fibroblasts [73] and vascular endothelial cells [74]. It should be noted that because *MTHFR*^{-/-} patients, like *CBS*^{-/-} patients, were on Hcy-lowering therapy, their Hcy-thiolactone concentrations represent minimal values. In fact, in one *MTHFR*^{-/-} patient for whom samples were obtained before therapy, the therapy resulted in lowering plasma Hcy-thiolactone from 47.3 to 16.6 nM (tHcy was lowered from 208 μM before therapy to 66.2 μM after therapy) [93].

A high-Met diet causes elevation of Hcy levels in humans and animals and is often used as a model of experimental hyperhomocysteinemia [44, 48]. Feeding a high methionine diet to mice for 6 weeks also increases plasma and urinary Hcy-thiolactone levels, 3.7- and 25-fold, respectively, compared to mice fed a normal chow diet. Normal plasma and urinary Hcy-thiolactone levels in mice are 3.7 nM and 140 nM [93].

Taken together, these findings show that genetic or dietary hyperhomocysteinemia increases Hcy-thiolactone levels in human and mice, as predicted by the Hcy-thiolactone hypothesis (Fig. 6.1). A clinical study showing that plasma Hcy-thiolactone levels are associated with the development and progression of vascular complications in diabetic patients [362] provides additional support for the Hcy-thiolactone hypothesis.

6.1.2 Protein N-Linked Hcy in Hyperhomocysteinemia

The Hcy-thiolactone hypothesis [93] predicts that protein *N*-homocysteinylation will be elevated under conditions conducive to atherosclerothrombotic diseases, such as hyperhomocysteinemia. Indeed, as predicted by the Hcy-thiolactone hypothesis, protein *N*-linked Hcy [76, 79, 96, 139] is elevated in human subjects with hyperhomocysteinemia due to mutations in *CBS* or *MTHFR* gene (Tables 3.12 and 5.1) [115].

To explain the link between hyperhomocysteinemia and higher cardiovascular risk and mortality observed in uremic patients, protein *N*-homocysteinylation was examined [372]. Significantly higher protein *N*-linked Hcy levels are found in uremic patients on hemodialysis than in control subjects [300, 301]. Interestingly, the ratio of protein *N*-linked Hcy to tHcy is lower in hemodialysis patients than in control subjects [300, 301]. Similarly, the ratio of protein *N*-linked Hcy to tHcy in patients with high plasma tHcy (50–120 μM) is lower than in patients with low

plasma tHcy (5–40 μ M) [79]. The lower protein *N*-linked Hcy/tHcy ratios suggest that the Hcy-thiolactone clearance is more effective at high plasma tHcy levels. This suggestion is supported by a finding that in mice fed a hyperhomocysteinemic high-Met or high-Hcy diet, the ratio of urinary to plasma Hcy-thiolactone is sevenfold or fourfold higher, respectively, compared to mice fed a normal diet [93].

Hyperhomocysteinemia is linked to increased mortality in CAD patients [37]. In a clinical study that examined a relationship between Hcy and CAD, plasma protein *N*-linked Hcy levels are significantly higher in coronary heart disease patients than in controls and are associated with the risk of CAD [168]. Furthermore, there is a weak but significant positive correlation between protein *N*-linked Hcy level and the number of diseased coronary arteries: the higher protein *N*-linked Hcy level, the greater the number of afflicted arteries.

Studies using polyclonal rabbit anti-*N*-Hcy-protein IgG antibodies [310] demonstrate that *N*-Hcy-protein is present in diseased human cardiac tissues [357, 373]. A positive immunohistochemical staining of myocardium and aorta samples from cardiac surgery patients is observed. Control experiments demonstrate that the staining is specific for *N*-Hcy-protein. No immunostaining is observed with rabbit preimmune IgG, with iodoacetamide-treated tissues (which destroys the *N* ϵ -Hcy-Lys-protein epitope), or with the antibody pre-adsorbed by preincubation of IgGs with *N*-Hcy-albumin. That immunostaining is specific for Hcy-thiolactone-modified protein is shown by increased intensity of the staining in tissues pretreated with Hcy-thiolactone [357, 373].

Immunohistochemical studies also demonstrate that *N*-Hcy-protein accumulates within atherosclerotic lesions in *ApoE*^{-/-} mice [357]. *ApoE*^{-/-} mice develop atherosclerosis spontaneously on a normal chow, but the process is accelerated by hyperhomocysteinemia caused by a high-Met diet [45]. Chemical assays establish that high-Met diet causes significant elevation also in Hcy-thiolactone and *N*-Hcy-protein levels [93, 115]. Positive staining for *N*-Hcy-protein is observed in aortas of *ApoE*^{-/-} mice fed with a normal chow diet, and the staining increases in animals fed with a hyperhomocysteinemic high-Met diet [357].

These findings show that hyperhomocysteinemia increases levels in human and mice and that elevated *N*-Hcy-protein levels are linked to CAD in humans and to atherosclerosis in mice, as predicted by the Hcy-thiolactone hypothesis (Fig. 6.1).

6.2 *N*-Hcy-Protein and Adaptive Autoimmune Responses

6.2.1 *Atherosclerosis Is an Inflammatory Disease*

Atherosclerosis is now widely recognized as a chronic inflammatory disease [43] that involves innate and adaptive immunity [374–376]. Lipid peroxidation is thought to play a central role in the initiation of both cellular and humeral

responses. Phospholipid peroxidation generates reactive aldehydes, such as malondialdehyde, 4-hydroxynonenal, and 1-palmitoyl-2-(5-oxovaleroyl)-*sn*-glycero-3-phosphocholine that can modify lysine residues in LDL and in other proteins. The resulting oxidized lipid-protein adducts, e.g., malondialdehyde-LDL, carry neo-self epitopes, which are recognized by specific innate and adaptive immune responses. That inflammation is important is supported by studies showing that increased plasma concentration of markers of inflammation, such as C-reactive protein (CRP), interleukin-1, serum amyloid A, and soluble adhesion molecules, is an independent predictor of vascular events [377]. Autoantibodies against modified LDL are elevated in vascular disease patients in some, but not all, studies [378]. As discussed in the following paragraphs, accumulation of *N*-Hcy-protein in hyperhomocysteinemia also leads to autoimmune responses.

6.2.2 *N*-Hcy-Protein Is Immunogenic in Rabbits

Details of the mechanism underlying the role of Hcy in adaptive immune response are beginning to emerge. The modification by Hcy-thiolactone, like other chemical modifications, such as glycation, acetylation, methylation, ethylation, and carbamylation [376], renders LDL highly immunogenic [356]. Furthermore, immunization of rabbits with Hcy-thiolactone-modified keyhole limpet hemocyanin (KHL) leads to the generation of anti-*N*-Hcy-protein antibodies [172, 310]. Of considerable interest are the observations that antisera from such immunizations bind not only to the *N*-Hcy-KHL but also to a variety of other proteins on which the *N*-linked Hcy epitope is present, such as *N*-Hcy-LDL, *N*-Hcy-albumin, *N*-Hcy-hemoglobin, *N*-Hcy-transferrin, and *N*-Hcy-antitrypsin. These data suggest that autoantibodies, once formed *in vivo* in response to *N*-Hcy-LDL or any other *N*-Hcy-protein, would be capable of binding to other endogenous *N*-Hcy-proteins.

6.2.3 *N*-Hcy-Protein Is Autoimmunogenic in Humans

In humans, Hcy incorporation into proteins triggers an adaptive immune response, manifested as the induction of IgG autoantibodies recognizing *Ne*-Hcy-Lys epitopes on *N*-Hcy-proteins. These autoantibodies react with any *N*-Hcy-protein, including *N*-Hcy-hemoglobin, *N*-Hcy-albumin, *N*-Hcy-transferrin, and *N*-Hcy-antitrypsin [172]. The antigen specificity of the human anti-*N*-Hcy-protein autoantibodies is essentially identical to the specificity of rabbit anti-*N*-Hcy-protein antibodies generated by inoculations with *N*-Hcy-LDL [356] or *N*-Hcy-KLH [172, 310] (Fig. 6.2). Plasma levels of anti-*N*-Hcy-protein autoantibodies [135, 172, 173, 310] and protein *N*-linked Hcy [76, 79, 96, 139] vary considerably among individuals and are strongly correlated with plasma Hcy (Fig. 6.3). In contrast, the titers of anti-*N*-Hcy-protein autoantibodies are not correlated with plasma

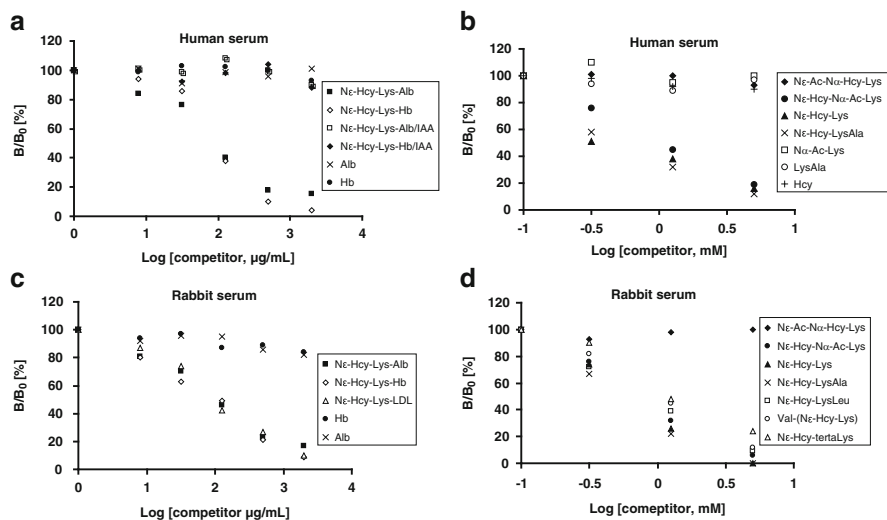


Fig. 6.2 Specificity of binding to *N*-Hcy-hemoglobin of a human anti-*N*-Hcy-protein autoantibody (**a**, **b**) and a rabbit polyclonal anti-*N*-Hcy-protein antibody (**c**, **d**). Microtiter wells are coated with $10 \mu\text{g mL}^{-1}$ human *N*-Hcy-hemoglobin and incubated with a 40-fold dilution of a human serum (**a**, **b**) or 200-fold dilution of rabbit antiserum (**c**, **d**) with or without indicated competitor. Rabbit antiserum is obtained from animals inoculated with *N*-Hcy-keyhole limpet hemocyanin. Results are expressed as B/B_0 , where B is the amount of IgG bound in the presence of competitor and B_0 that without competitor (Reprinted from [172])

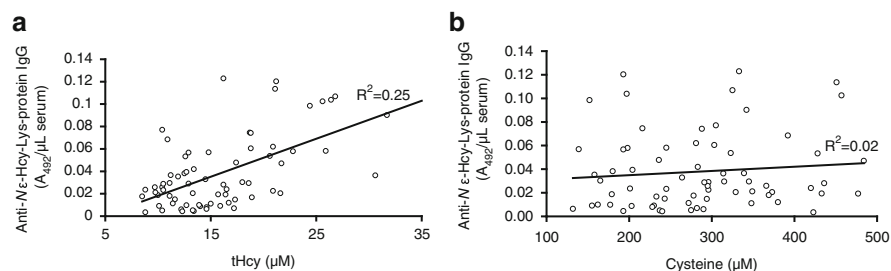


Fig. 6.3 Relationships between serum anti-*N*-Hcy-protein IgG and tHcy (**a**) or cysteine (**b**) in healthy human subjects (Reprinted from [172])

cysteine or methionine [172]. The Hcy-dependent variation in anti-*N*-Hcy-protein autoantibody titers is consistent with the Hcy-thiolactone hypothesis (Fig. 6.1): elevation in Hcy leads to inadvertent elevation in Hcy-thiolactone, observed *ex vivo* in human fibroblasts [73] and endothelial cells [64, 74], and *in vivo* in humans and mice [64, 93–95]. Protein modification by Hcy-thiolactone generates neo-self antigens, *Nε*-Hcy-Lys-protein. Increased accumulation of neo-self *Nε*-Hcy-Lys epitopes in proteins, observed *ex vivo* in cultured human cells treated

with Hcy [64, 73, 74] and in vivo in hyperhomocysteinemia due to CBS-, MTHFR-, or PCFT-deficiency in humans [115] and mice [113], triggers an autoimmune response.

6.2.4 Anti-*N*-Hcy-Protein Autoantibodies in Atherosclerosis

Plasma levels of anti-*N*-Hcy-protein autoantibodies, similar to plasma tHcy levels, are significantly elevated in stroke and CAD patients. For example, 63-year-old male stroke patients ($n = 37$) have higher serum levels of tHcy and anti-*N*-Hcy-protein autoantibodies, compared with age-matched control individuals ($n = 29$) [172]. However, in groups of women stroke patients ($n = 17$) and control individuals ($n = 45$), in whom tHcy levels are similar, the levels of anti-*N*-Hcy-protein autoantibodies are also similar.

In a larger study of patients <50 years old, the seropositivity to anti-*N*-Hcy-protein autoantibodies is fivefold more frequent in male patients ($n = 88$) with angiographically confirmed CAD than in age-matched healthy individuals ($n = 100$) (52 % vs. 10 %, $P < 0.001$) [135]. To examine the clinical usefulness of anti-*N*-Hcy-protein IgG autoantibodies, their predictive value in CAD is analyzed and compared to the predictive value of tHcy and other risk factors [135]. An age-adjusted risk for early CAD in men <50 years old, related to seropositivity for anti-*N*-Hcy-protein IgG autoantibodies, is 9.87 (95 % CI 4.50–21.59, $p < 10^{-5}$). In multivariate logistic regression analysis, only seropositivity to anti-*N*-Hcy-protein IgG autoantibodies (OR 14.92; 95 % CI 4.47–49.19; $p = 0.00002$), smoking (OR 8.84; 95 % CI 2.46–31.72; $p = 0.001$), hypertension (OR 43.45; 95 % CI 7.91–238.7), and HDL cholesterol (OR 0.015; 95 % CI 0.002–0.098; $p = 0.00002$) are independent predictors of early CAD. Interestingly, compared with tHcy, anti-*N*-Hcy-protein IgG autoantibodies are a more sensitive predictor of early CAD in men. A risk for premature CAD is almost 15-fold higher in patients who are seropositive for anti-*N*-Hcy-protein IgG autoantibodies after adjusting for coronary risk factors, Hcy and CRP. These analyses show that elevated levels of anti-*N*-Hcy-protein autoantibodies significantly contribute to the risk of CAD in male patients [135]. Taken together, these studies suggest that an autoimmune response against *N*-Hcy-proteins is a feature of Hcy-linked atherosclerosis [69, 134].

The findings that the levels of *N*-Hcy-protein are elevated in uremic patients on hemodialysis [300, 301] suggest that an autoimmune response against *N*-Hcy-protein might also be enhanced in these patients. This possibility was examined in a group of 43 patients (58.8 years old) who were on maintenance hemodialysis for an average of 50 months and an age- and sex-matched group of 31 apparently healthy individuals [379]. Significantly higher levels of anti-*N*-Hcy-protein IgG autoantibodies are found in the hemodialysis patients, compared with controls. Similar to the studies with stroke patients [172], the levels of anti-*N*-Hcy-protein IgG autoantibodies are strongly correlated with plasma tHcy, both in hemodialysis

patients and in controls, consistent with the etiology of these autoantibodies. Furthermore, a subgroup of hemodialysis patients who survived myocardial infarction ($n = 14$) had significantly higher levels of anti-*N*-Hcy-protein IgG autoantibodies than a subgroup of hemodialysis patients without a history of CAD ($n = 29$) [379]. Taken together, these data suggest that an autoimmune response against *N*-Hcy-proteins contributes to the development of CAD in hemodialysis patients.

In general, antibodies protect against exogenous pathogens and endogenous altered neo-self molecules to maintain homeostasis by neutralization and clearance. Similar to other autoantibodies [376], the anti-*N*-Hcy-protein autoantibodies can be beneficial or deleterious. For example, the clearing of *N*-Hcy-protein from the circulation by anti-*N*-Hcy-protein autoantibodies would be beneficial. On the other hand, binding of the autoantibodies to *N*-Hcy-protein [134, 172, 310] in tissues may contribute to the deleterious effects of hyperhomocysteinemia on many organs [20, 29, 30]. For instance, if the neo-self *Ne*-Hcy-Lys epitopes were present on endothelial cell membrane proteins, anti-*N*-Hcy-protein autoantibodies would form antigen–antibody complexes on the surface of the vascular wall. Endothelial cells coated with anti-*N*-Hcy-protein autoantibodies would be taken up by the macrophage via the Fc receptor, resulting in injury to the vascular surface. Under chronic exposures to elevated Hcy, the neo-self epitopes *Ne*-Hcy-Lys, which initiate the injury, are formed continuously, and the repeating attempts to repair the damaged vascular wall would lead to an atherosclerotic lesion [69, 134].

The involvement of an autoimmune response in CAD is further supported by findings showing that lowering plasma tHcy by folic acid supplementation for 3 and 6 months lowers anti-*N*-Hcy-protein autoantibodies levels in control subjects but not in patients with CAD [173]. These findings show that lowering plasma tHcy normalizes anti-*N*-Hcy-protein IgG autoantibody levels within 3 months, but only in healthy subjects. Plasma tHcy, Hcy-thiolactone, and *N*-Hcy-protein levels are also reversibly modified by the diet in mice [113]. These findings suggest that while primary Hcy-lowering intervention by B-vitamin supplementation is beneficial, secondary intervention may be ineffective and may explain at least in part the failure of B-vitamin therapy [51, 52] to lower cardiovascular events in myocardial infarction patients.

6.3 *N*-Hcy-Protein and Innate Immune Responses

Innate immune responses play an important role in etiology of thrombosis and atherosclerosis [374–376]. These responses are mediated by cytokines and chemokines produced by multiple cell types. Proinflammatory cytokines are typically produced in response to the injury (inflammation) and subsequently induce a variety of target cell to release further cytokines and chemokines in order to mobilize the innate system to promote reparative processes that involve recruitment of circulating leukocytes to the injury site. While acute induction is protective, the

chronic expression of the inflammatory cytokines and chemokines can be harmful and lead to a disease. Numerous studies have established a link between hyperhomocysteinemia and innate immune responses. For example, in humans, TNF- α , a key cytokine in the inflammatory process, is strongly correlated with plasma tHcy ($r = 0.48, p < 0.001$), and in multivariate regression analysis, plasma tHcy is an independent predictor of the plasma TNF- α levels [380].

Other evidence also suggests that Hcy contributes to innate immune responses. Indeed, many human studies, although not all [381–384], have reported associations between Hcy and markers of inflammation. For example, significant associations between plasma tHcy and CRP are observed in the Framingham Heart Study [385] and in the Physician's Health Study [386]. In another study, hyperhomocysteinemia is associated with increased levels of both CRP and interleukin-6 in humans [387]. A similar positive association between Hcy and interleukin-6 is reported in patients with diabetic nephropathy [388]. Importantly, in the Holven et al. study [387], elevated level of interleukin-6 is observed in hyperhomocysteinemic individuals in the absence of hypercholesterolemia. Plasma tHcy is positively associated with soluble tumor necrosis factor (TNF) receptor in the Nurses' Health Study [389]. A positive correlation is also observed between plasma tHcy and neopterin (a marker of Th1 type immune response) in Parkinson's disease patients [390].

Furthermore, dietary hyperhomocysteinemia is known to trigger an innate immune response and enhance vascular inflammation in mice [45]. This is manifested by increased activation of nuclear factor (NF)- κ B in the aorta and kidney, enhanced expression of vascular cell adhesion molecule (VCAM)-1 and receptor for advanced glycation end products in the aorta, and TNF- α in plasma [45]. Elevated Hcy is associated with elevated monocyte chemoattractant protein-1 and increased expression of vascular adhesion molecules in humans [391, 392] and rats [393–395].

Genetic hyperhomocysteinemia in untreated or poorly compliant human CBS-deficient patients leads to chronic induction (3.7- to 72-fold) of multiple proinflammatory cytokines [IL-1 α , IL-6, TNF- α , IL-17, and IL-12(p70)] and chemotactic chemokines (fractalkine, MIP-1 α , and MIP-1 β) compared to the normal age- and gender-matched controls [396]. Hcy-lowering therapy normalizes the levels of proinflammatory cytokines and chemokines, with the exception of TNF- α , which, although reduced 3.4-fold by the therapy, remained tenfold elevated above the normal level.

Similarly, hyperhomocysteinemic *Cbs*^{-/-} mice exhibit a chronic inflammatory state as indicated by measurements of plasma CRP: *Cbs*^{-/-} mice have sevenfold elevated CRP, compared with wild-type littermates. Hcy lowering by betaine treatment significantly reduced plasma CRP levels (by 50 %), although it remained elevated compared with control wild-type mice. In addition, *Cbs*^{-/-} mice have highly elevated proinflammatory cytokines IL-1 α , IL-1 β (three to fourfold), and TNF- α (35-fold). Hcy lowering significantly ameliorated the constitutive expression of proinflammatory cytokines in *Cbs*^{-/-} mice [396].

How excessive accumulation of Hcy triggers an innate immune response is unknown, but accumulating evidence suggests that protein *N*-homocysteinylolation and the resulting protein damage are involved (Fig. 6.1). Hyperhomocysteinemia is known to cause elevation of Hcy-thiolactone [93] and *N*-Hcy-protein levels [79, 113, 115] in humans (Table 3.12) and mice (Table 5.1). Moreover, *N*-Hcy-proteins are susceptible to protein damage (Fig. 5.11) [68, 96] via a thiyl radical mechanism (Reaction 5.2), which leads to the generation of protein carbonyls [311]. In fact, the extent of protein damage assessed by measurements of protein carbonyls is significantly greater in liver proteins from *Cbs*^{-/-} mice compared with wild-type littermates [397]. Protein carbonyls are also elevated in plasma of human CBS-deficient patients, and Hcy-lowering therapy partially prevents protein carbonyl accumulation [398].

N-Hcy-proteins, particularly *N*-Hcy-LDL, are highly immunogenic [356]. *N*-Hcy-LDL is present in the human blood [79] and is taken up by macrophages faster than unmodified LDL [336]. Furthermore, levels of anti-*N*-Hcy-protein autoantibodies are weakly, but significantly, correlated with plasma CRP levels ($r = 0.24$, $p = 0.002$) [135], suggesting that *N*-Hcy-protein is proinflammatory. This suggestion is further supported by recent findings [169] showing that the treatment with *N*-Hcy-albumin increases binding of monocytes to ex vivo cultured endothelial cells and induces expression of proinflammatory chemokines and cytokines such as VCAM1, ICAM-1, and MCP1 in both monocytes and endothelial cells. In addition, the treatment with *N*-Hcy-albumin upregulates numerous genes, including five that are implicated in endothelial cell activation: CCL2, HSPD1, ADAM17, TFP1, and NRP1 [169]. It should be noted that these proinflammatory effects on cell adhesion and gene expression are observed at 1- μ M *N*-Hcy-albumin, an elevated concentration (twofold above normal, see Table 2.1) that is observed in uremic hyperhomocysteinemic patients [301]. Although proinflammatory cytokines can also be induced in human cultured cells by Hcy, much higher concentrations (usually submillimolar or higher) are required [45, 399, 400]. Taken together, these results strongly suggest that *N*-Hcy-protein is involved in the induction of inflammatory response associated with hyperhomocysteinemia (Fig. 6.1).

6.4 *N*-Hcy-Fibrinogen and Thrombosis

Patients with severe hyperhomocysteinemia due to CBS deficiency suffer from life-threatening thromboembolic events by the age of 30 [46]. Mild to moderate hyperhomocysteinemia, more prevalent than severe hyperhomocysteinemia, is also associated with increased risk for myocardial infarction, stroke, and thrombosis [401]. The identification of *N*-homocysteinylolation site at Lys562, located in an unstructured region involved in plasmin and tPA binding (Fig. 5.3), in the prothrombotic *N*-Hcy-fibrinogen that accumulates in the circulation of CBS-deficient patients [79, 115] suggests that the modified fibrinogen can impair fibrinolysis

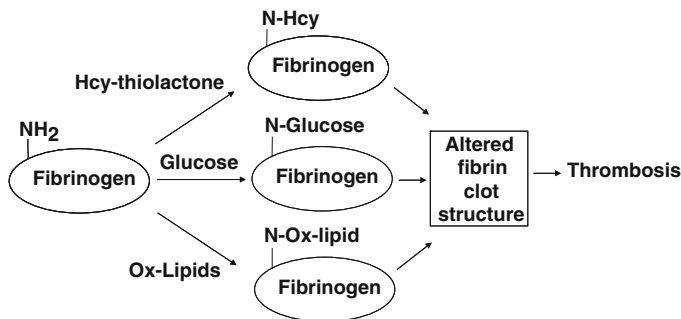


Fig. 6.4 Fibrinogen modifications affect fibrin clot structure and lead to enhanced thrombosis (Reproduced from [143])

in vivo. The in vivo relevance of fibrinogen *N*-homocysteinylation in humans is further supported by findings showing that elevated plasma tHcy decreases permeability, and increases resistance to lysis, of fibrin clots from plasma of coronary artery disease (CAD) patients and healthy subjects [174]. Moreover, fibrin clot structure is more compact and less permeable in CAD patients than in controls. These detrimental effects of elevated plasma tHcy on fibrin clot structure are consistent with a mechanism involving fibrinogen modification by Hcy-thiolactone (Fig. 6.4) [174]. Furthermore, prothrombotic *N*-Hcy-fibrinogen levels are significantly elevated in CBS-deficient patients (Table 5.10) known to have increased susceptibility to thrombosis [115].

In patients with diabetes and hypercholesterolemia, the fibrin clot structure is less permeable and less susceptible to lysis by plasmin, i.e., thrombogenic, compared with CAD patients or healthy subjects. However, the influence of Hcy on the clot structure in patients with diabetes and hypercholesterolemia is obscured by the dominant effects of glucose and cholesterol, respectively. These findings suggest that fibrinogen modifications by glucose and products of lipid oxidation, like the modification by Hcy-thiolactone, are detrimental and that these modifications predominate over the modification by Hcy-thiolactone in patients with diabetes and hypercholesterolemia (Fig. 6.3) [174].

Lowering plasma tHcy by folic acid supplementation improves clot structure (increases permeability and susceptibility to lysis) in asymptomatic human subjects. This finding suggests that Hcy-lowering therapy by vitamin supplementation can have beneficial antithrombotic effects [174]. Taken together, these results support a hypothesis that fibrinogen *N*-homocysteinylation by Hcy-thiolactone leads to abnormal resistance of fibrin clots to lysis in vivo and thus contributes to increased risk of thrombosis [174, 175]. In addition to *N*-homocysteinylation, other fibrinogen modifications, such as those occurring in hypercholesterolemia and hyperglycemia, can also increase the risk of thrombosis (Fig. 6.3) [174].

6.5 *N*-Hcy-Collagen and Connective Tissue Abnormalities

CBS deficiency is characterized clinically by widespread deformities and malfunction of connective tissue including joint, laxity, kyphoscoliosis, pigeon breast, genu valgum, severe osteoporosis, ectopia lentis, and vascular disease in which dilatation of medium-sized arteries occur frequently [20]. Patients with homocystinuria due to CBS deficiency often exhibit skeletal abnormalities resembling the phenotype of patients with Marfan syndrome [20, 46], a connective tissue disease caused by mutations in the fibrillin-1 gene, which affect the delivery of fibrillin-1 and/or its assembly into microfibrils.

Collagen, the most abundant protein in mammals (comprising 25–35 % of the whole-body protein content), is the major component of connective tissues. The unusual mechanical stability of collagen fibrils and collagenous tissues is largely dependent on the formation of covalent intramolecular pyridinoline cross-links between collagen chains [402]. Because lysine residues are involved in the pyridinoline cross-link formation that is essential for proper assembly of collagen fibers and their mechanical properties, *N*-homocysteinylation of these lysine residues by Hcy-thiolactone can prevent normal cross-linking and thus contribute to connective tissues abnormalities observed in severe hyperhomocysteinemia. Relatively low levels of *N*-linked Hcy in collagen can result in a structural defect in the supramolecular organization of the connective tissue.

That skin collagen is defective in hyperhomocysteinemia has been shown by its increased extractability from the skin of CBS-deficient patients: the extraction with 1-M NaCl and 0.5-M acetic acid solubilizes 7.8 % and 10.1 % of dermal collagen from two CBS-deficient patients, whereas only 2.4 % and 2.9 % is extracted from two age-matched control individuals [403]. Furthermore, collagen type I cross-links (assayed by quantification of carboxyterminal telopeptide of collagen type I in plasma) are reduced threefold in nine CBS-deficient patients relative to the 20 control individuals ($1.14 \pm 0.24 \mu\text{g/L}$ vs. $3.29 \pm 0.32 \mu\text{g/L}$) [404]. Because the extent of collagen biosynthesis (assessed by quantification of *C*-terminal propeptide of type I procollagen and of *N*-terminal propeptide of procollagen type III) is the same in patients with homocystinuria and in control subjects, these findings indicate that connective tissue abnormalities in hyperhomocysteinemia are linked to diminished collagen cross-linking, but not biosynthesis [404].

Cbs-deficient mice have skin and bone abnormalities similar to those observed in humans [305, 309, 405]. Analysis of *N*-linked Hcy content in collagen isolated from *Tg-I278T Cbs*^{-/-} mice shows that these mice have 18-fold higher skin *N*-Hcy-collagen content than *Tg-I278T Cbs*^{+/+} littermates (89.9 ± 25.1 vs. 5.0 ± 2.4 pmol/mg skin) [306]. Similar elevation in *N*-linked Hcy in the *Cbs*-deficient mice is observed in bone collagen. These findings show that collagen is *N*-homocysteinylation in vivo in mice. However, it remains to be determined whether *N*-homocysteinylation prevents collagen cross-linking.

Chapter 7

S-Homocysteinylated Proteins

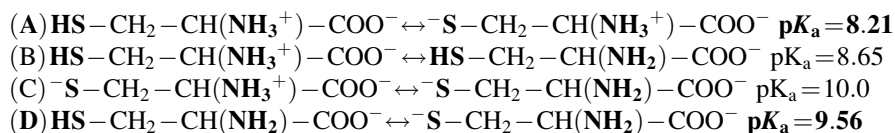
Human proteome includes 214,000 cysteine residues, which constitute 2.26 % of the encoded amino acids [406]. Many proteins contain at least one cysteine residue with a free –SH group as well as more numerous disulfide-bonded cysteine residues. For example, of the 35 cysteine residues present in the structures of albumin and γ -globulin, the most abundant serum proteins, one has a free –SH group and the other 34 are engaged in 17 disulfide bonds [407]. These cysteine residues can engage in thiol–disulfide exchange reactions with low molecular weight thiols or disulfides. Indeed, both albumin [91, 296, 408] and γ -globulin [79, 106] carry S-linked cysteine, Hcy, CysGly, glutathione (GSH), and γ -GluCys. Furthermore, specific cysteine residues, both free and disulfide-bonded, exhibit different reactivities in the thiol–disulfide exchange reactions [409].

There are two different types of disulfides in protein structures that have different functional roles: one type of disulfides stabilizes proteins by cross-linking their polypeptide chains while other disulfides are redox reactive. For example, while cysteamine is able to reduce only five disulfide bonds in γ -globulin, it reduces only one disulfide bond in serum albumin [407]. Thus, biologically important thiols, including Hcy, can potentially interact with specific protein cysteine residues and affect protein's structure and function.

The extent of Hcy binding via disulfide bonds to protein thiols in vivo will depend on their reactivity, the concentration of competing small-molecule thiols, such as GSH and cysteine, and ionization constants (pK_a values) of their sulfhydryl groups. The concentration of major small-molecule thiols in healthy organisms is several orders of magnitude higher than the concentration of Hcy. For example, cellular concentrations of GSH are 5–10 mM, and plasma concentrations of cysteine are about 0.3 mM, whereas total Hcy concentrations in plasma and tissues are about 5–10 μ M.

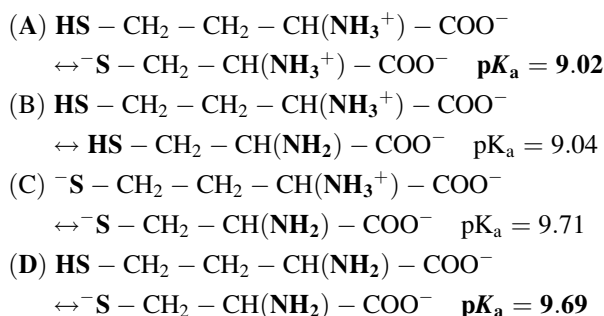
Classical studies of Benesh and Benesh [191] show that four different ionic species of cysteine exist in solution at physiological pH: a form with both thiol and amino groups protonated $\mathbf{HS-CH_2-CH(NH_3^+)-COO^-}$, a form with deprotonated thiol and amino groups $\mathbf{^-S-CH_2-CH(NH_2)-COO^-}$, and forms with either thiol or amino group deprotonated, $\mathbf{^-S-CH_2-CH(NH_3^+)-COO^-}$ and $\mathbf{HS-CH_2-CH}$

(NH₂)–COO[–], respectively. The equilibrium between these forms involves the hydrogen cation transfer that is governed by microscopic pK_a values for the dissociation of each species:

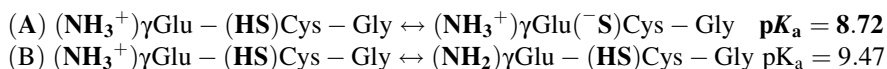


Titration of Cys, Hcy, GSH, and γ GluCys show that half of each thiol is dissociated at pH 8.8, 10.0, 9.2, and 9.9, respectively. At physiological pH = 7.4, the extent of ionization of a thiol group in CysGly, cysteine, Hcy, GSH, and γ GluCys is calculated to be 11 %, 6 %, 1 %, 1 %, and 1 %, respectively [191].

Subsequent studies of Reuben and Bruice [192] show that experimental data for Hcy titration fit a model with four ionizations:



In the case of GSH, the data fit best a single ionization [192]:



These pK_a values indicate that the cysteine thiol is more reactive than the Hcy thiol, which in turn exhibits reactivity similar to the GSH thiol.

A search for potentially redox-active cysteine disulfides by scanning the Protein Data Bank (for structures of proteins in alternate redox states) reveals over 1,134 pairs of proteins, many of which exhibit conformational difference between alternate redox states [409]. The search identifies classes of proteins that exhibit disulfide oxidation following expulsion of metals such as zinc, major reorganization of the polypeptide chains in association with disulfide-redox activity, order/disorder transitions, and changes in quaternary structure. As discussed in a greater detail in the following sections, similar changes in proteins can be experimentally induced by binding of Hcy via a disulfide bond with a protein cysteine residue.

7.1 Plasma S-Homocysteinyl-Proteins

7.1.1 S-Hcy-Albumin

Two major forms of serum albumin exist in the circulation: albumin-Cys³⁴-SH, known as mercaptoalbumin, and albumin-Cys³⁴-S-S-Cys (Fig. 5.7), accounting for about two-thirds (0.45 mM) and one-third (0.15 mM), respectively, of total plasma albumin [323]. Two minor forms, accounting for 1–2 % of total albumin, also exist in the circulation: albumin-Cys³⁴-S-S-Hcy [91, 103] and N-Hcy-albumin (Fig. 5.7) [79]. Albumin carries >80 % of plasma Hcy [103] and Cys [296]. The in vivo ability of albumin to form a disulfide with Hcy has been recapitulated in vitro [78, 81, 91].

Bound Hcy and Cys form a disulfide bond with the conserved residue Cys³⁴ of albumin, which is located in a 10-Å-wide hydrophobic pocket. The Cys³⁴ residue has an unusually low pK_a of 5 and thus exists as a thiolate anion at physiological pH. The oxidation status of Cys³⁴ governs the local structure: *buried* for the reduced thiolate form and *exposed* for the disulfide form [410]. These two structural forms of albumin can be separated on a conventional [323] or HPLC anion exchange columns [96] (Fig. 5.8). Albumin also carries S-linked GSH and CysGly (Fig. 7.1) [106, 408]. S-linked Hcy, Cys, GSH, and CysGly are also carried on globulin (Fig. 7.1), HDL, and α₁-acid glycoprotein, but not on transferrin (which does not possess a cysteine residue with a free thiol) [106]. It is not known whether S-thiolation occurs in the plasma or intracellularly during biogenesis of these proteins.

In vitro studies suggest that albumin-Cys³⁴-S-S-Hcy can form in three thiol–disulfide exchange reactions: (1) between Hcy and albumin-Cys³⁴-S-S-Cys, (2) between mercaptoalbumin (Alb-SH) and Hcy-S-S-Hcy, and (3) between Alb-SH and Hcy-S-S-Cys [411, 412]. The physiological role of the redox transitions in albumin is not understood.

In the presence of excess Hcy, S-linked Cys and CysGly are released from S-thiolated albumin with a half-life of 30 min, and there is a corresponding increase in S-Hcy-albumin. Under the same conditions, release of S-linked Cys and CysGly from α₁-acid glycoprotein is much slower with a half-life of 24 h. Half-maximal increase in Hcy S-linked to α₁-acid glycoprotein requires several hours [106].

Exchange reactions with excess GSH show more rapid displacement of Cys, Hcy, and CysGly from albumin than from α₁-acid glycoprotein. However, exchange reaction with GSH is faster: half-lives are 10 min for the displacement of Cys and CysGly and <10 min for the displacement of Hcy from albumin and about 3 h for thiol displacement from α₁-acid glycoprotein [106]. These findings suggest that GSH is more effective than Hcy in thiol–disulfide exchange reactions.

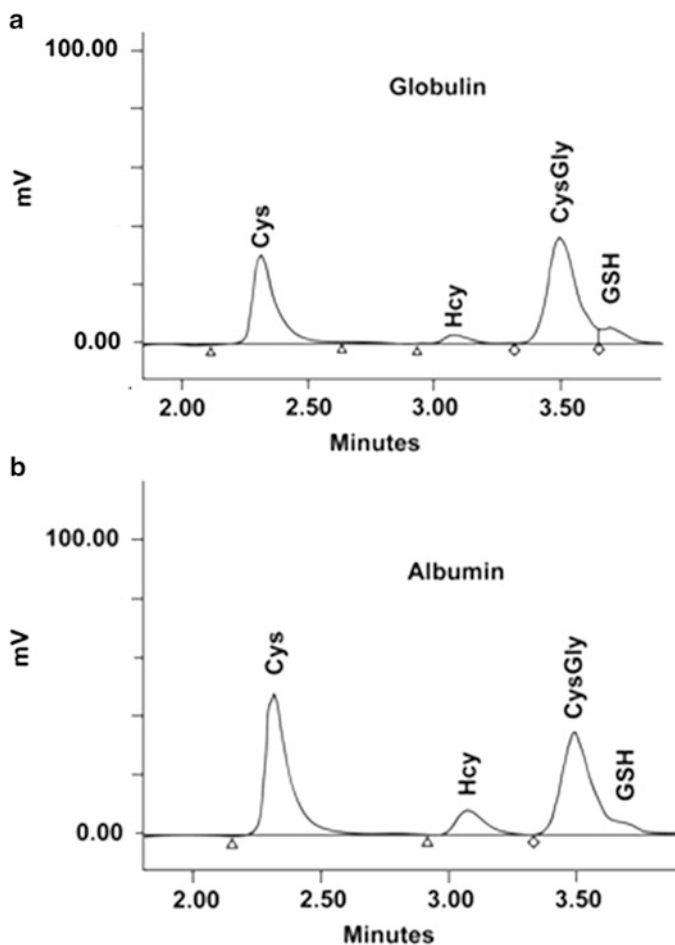


Fig. 7.1 HPLC analysis of thiol-containing amino acids released from globulin (*top panel*) or albumin (*bottom panel*) fractions of serum. Peaks are indicated as Cys (cysteine), Hcy (homocysteine), CysGly (cysteinylglycine), and GSH (glutathione). The *vertical axis* shows fluorescence detector response in millivolts (Reproduced from [106])

7.1.2 S-Hcy-Transferrin

Transferrin (TTR) is a minor plasma protein that occurs at concentrations 0.2–0.4 mg/mL, about 200-fold lower than serum albumin. In human plasma, TTR exists as a homotetramer of 13.8-kDa subunits, each of which has a single Cys¹⁰ residue. TTR transports the hormone thyroxine and the retinol-binding protein–retinol complex [413] and has been linked to the formation of amyloid deposits in familial TTR amyloidosis, senile systemic amyloidosis [414], and familial amyloidotic polyneuropathy [415].

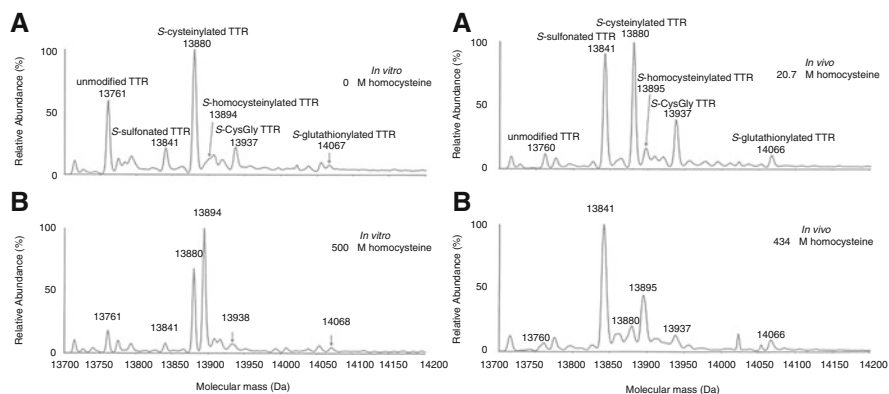


Fig. 7.2 Mass spectrometric analysis of transthyretin *S*-homocysteinylation *in vitro* (left panel) and *in vivo* (right panel). The transthyretin was immunoprecipitated from human plasma, purified by reversed-phase HPLC, and analyzed by ESI-MS (Reproduced from [105])

The single Cys¹⁰ residue of TTR carries *S*-linked Hcy, in addition to cysteine, glutathione, CysGly, and sulfonyl residue [104, 105]. Low levels of *S*-Hcy-TTR, comprising a few percent of total TTR, are detectable by LC-MS in normal human plasma (Fig. 7.2). The low abundance of *S*-Hcy-TTR probably explains why it was not detected in early studies [416]. In plasma from CBS-deficient and cblC/D-deficient patients, *S*-Hcy-TTR levels increase about tenfold to comprise about 20 % of total TTR (Fig. 7.2). TTR in human plasma, as well as purified TTR, is also able to bind Hcy *in vitro* [105]. Higher fraction of *S*-conjugated TTR is observed in patients with symptomatic amyloid disease [417].

Homotetrameric TTR variants, including *S*-Cys-TTR, *S*-GSH-TTR, *S*-CysGly-TTR-, and *S*-sulfo-TTR, chemically synthesized starting with wild-type TTR, are more amyloidogenic than unconjugated wild-type TTR at the higher end of the acidic pH range (pH 4.4–5.0) [418]. The variants are similarly destabilized relative to wild-type TTR toward urea denaturation and exhibit rates of urea-mediated tetramer dissociation (pH 7) and methanol-facilitated fibril formation similar to those of wild-type TTR. Under mildly acidic conditions (pH 4.8), the amyloidogenesis rates of the mixed disulfide TTR variants are much faster than the wild-type rate. *S*-Sulfo-TTR is less amyloidogenic and forms fibrils more slowly than wild type under acidic conditions, yet it exhibits stability and rates of tetramer dissociation similar to those of wild-type TTR when subjected to urea denaturation.

Conversion of the Cys¹⁰ thiol group to a mixed disulfide with the amino acid Cys, the CysGly peptide, or GSH increases amyloidogenicity and the amyloidogenesis rate above pH 4.6, conditions under which TTR probably forms fibrils in humans. Hence, these modifications may play an important role in human amyloidosis [418].

The most prevalent modification, *S*-cysteinylation, renders TTR substantially more amyloidogenic than wild-type TTR at pH 5, which may be a risk factor for the

onset of senile systemic amyloidosis [418]. It is likely that *S*-homocysteinylation similarly increases amyloidogenicity of TTR; this, however, remains to be demonstrated.

It has been stated that *N*-Hcy-transthyretin is undetectable in human plasma [104]. However, the authors acknowledge that their inability to detect *N*-Hcy-transthyretin is due to the interference from a signal corresponding to *S*-Cys-transthyretin and to low sensitivity of their assay: the detection limit of the LC-MS assay used by Sass et al. [104] is 1 % relative to total transthyretin. This limit of detection is several orders of magnitude less sensitive than that of the HPLC with fluorescence detection method, which allows quantification of as little as 0.00006 mol *N*-linked Hcy/mol protein (or 0.006 mol%) [297].

7.1.3 *Apolipoprotein B and Lipoprotein[a]*

ApoB-100, the major protein of LDL, is composed of a single polypeptide chain of 4,563 amino acid residues and contains a site for binding to the cell-surface LDL receptor. Sixteen of the 25 cysteine residues exist in the disulfide form, while nine cysteine residues have free sulfhydryl groups [419]. Each of the low molecular weight thiols present in plasma has been reported to bind to ApoB via disulfide bonds. Thus, ApoB-100 isolated from normal human plasma carries 0.0137 mol *S*-linked Hcy/mol ApoB [420], and the content of *S*-linked Cys, CysGly, GSH, and γ GluCys (in mol/mol ApoB-100) is 0.324, 0.108, 0.0095, and 0.0026, respectively. Plasma tHcy is a major determinant of *S*-Hcy-ApoB-100 levels.

Incubation of ApoB-100 with increasing concentrations of Hcy (up to 0.1 mM) leads to increased binding with saturation at about 0.2 mol *S*-linked Hcy/mol ApoB [144]. Increase of Hcy concentration to 5 mM does not lead to any further increase in Hcy binding. This means that Hcy is able to form disulfide bonds with only a very small fraction (2.2 %) of the 9 cysteine thiols that are present in ApoB-100. The reasons for such an inefficient binding are not clear but raise a possibility that a minor variant of ApoB or a contaminating protein, and not ApoB-100 itself, is responsible for Hcy binding.

The treatment of cultured human endothelial cells with *S*-Hcy-ApoB-100 prepared in vitro led to increased generation of reactive oxygen species, decreased proliferation, and increased cytotoxicity [144]. Whether these effects are specific to *S*-thiolation of ApoB-100 by Hcy and whether *S*-thiolation by other thiols, in particular the much more abundant thiolation with cysteine, affects interactions of ApoB-100 with endothelial cells have not been examined.

S-Hcy-ApoB-100 is reported to be significantly elevated (to 0.024 mol *S*-linked Hcy/mol ApoB) in chronic kidney disease (CKD) patients in comparison with healthy controls [421]. *S*-Cys-ApoB-100 is also significantly elevated in these patients to 0.386 mol *S*-linked Hcy/mol ApoB. In CKD patients, plasma *S*-Hcy-ApoB-100 varies from 0.01 to 0.06 mol *S*-Hcy/mol ApoB while tHcy varies from 8 to 60 μ M. Plasma *S*-Hcy-ApoB is positively correlated with tHcy and creatinine.

However, only creatinine is a positive determinant of *S*-Hcy-ApoB in CKD patients. Lipid-lowering therapy causes a 31 % decrease in *S*-linked ApoB thiols, including a 40 % decrease in *S*-Hcy-ApoB [422]. The decreased levels of protein bound thiols are most likely a consequence of oxidative stress improvement as assessed by measurements of plasma malondialdehyde levels and allantoin/uric acid ratios during the therapy. *S*-Hcy-ApoB-100 and *S*-Cys-ApoB-100 are also significantly elevated in acute myocardial infarction patients [423].

Lipoprotein [a] (Lp[a]) is a lipoprotein that consists of LDL and apolipoprotein [a] (apo[a]), disulfide-linked to the apoB-100 moiety of LDL [419]. Lp[a], in contrast to LDL, does not bind to the LDL receptor, but the reduction and removal of apo[a] restores the affinity of the remaining LDL for the receptor to normal levels [424]. Apo(a) shares remarkable structural homology to plasminogen and binds to plasmin-modified fibrin surface. Its ability to compete with plasminogen for binding sites on fibrin in clots may be responsible for the association of Lp[a] with increased risk for cardiovascular disease [425–428]. Lp[a] colocalizes with fibrin in atherosclerotic lesions and is physically associated with fibrin in the arterial wall [429].

The single disulfide bond between apo[a] and ApoB-100 is susceptible to reduction by Hcy and other sulfhydryls *in vitro*. Incubation of Lp[a] with thiols increases its binding to plasmin-treated fibrin, but not to other proteins [430]. DTT is more effective than Hcy, cysteine, *N*-acetyl-Cys, or GSH in enhancing the binding. The binding is specific to Lp[a], as shown by the inability of Hcy to affect the binding of LDL or plasminogen to fibrin. Although it does not alter the molecular weight of Lp[a] on gel filtration, Hcy partially reduces Lp[a] [430]. Thus, Hcy and other thiols alter the Lp[a] particle and increase the reactivity of the plasminogen-like apo[a] portion of the molecule.

However, it is not known whether Lp[a] is modified by Hcy *in vivo*, in particular in patients with hyperhomocysteinemia. Free apo[a] is elevated in patients with nephrotic syndrome and in patients undergoing peritoneal dialysis, relative to normal control subjects, but there is no relationship between apo[a] and plasma tHcy [428].

7.2 Extracellular Matrix Proteins

7.2.1 *Fibrillins*

Fibrillin-1, fibrillin-2, and fibrillin-3, modular 350-kDa calcium-binding glycoproteins, are major components of 10–12-nm microfibrils in the extracellular matrix [431]. They serve as a scaffold for the deposition of elastin and the formation of the elastic fibers. The structure of fibrillin-1 is dominated by two types of disulfide-rich motifs, the calcium-binding epidermal growth factor-like (cbEGF) and transforming growth factor beta binding protein-like (TB) domains. With its

content of 13.4 % cysteine residues, fibrillin-1 is one of the most-cysteine-rich proteins. Cysteine residues form intradomain disulfide bonds important for the correct folding and structure of each domain. Disruption of the connective tissue structure contributes to the pathogenic mechanisms underlying two inherited diseases with very different etiologies: Marfan syndrome and homocystinuria. Marfan syndrome is a connective tissue disease caused by mutations in the fibrillin-1 gene. Many missense mutations cause fibrillin-1 domain misfolding, which may affect the delivery of fibrillin-1 and/or its assembly into microfibrils. Patients with homocystinuria often exhibit skeletal abnormalities resembling the Marfan syndrome phenotype [20, 46], suggesting that elevated Hcy levels may lead to chemical reduction of disulfide bonds within fibrillin-1 domains resulting in the loss of native structure.

In vitro experiments show that Hcy reduces disulfide bonds of recombinant fibrillin-1 cbEGF domain fragments, which results in structural changes that lead to misfolding of the protein [432]. Mass spectroscopic analyses identify Hcy residues attached via disulfide bonds to fibrillin-1 fragments. Calcium binding protects domain structure of the protein against reduction by Hcy. Circular dichroism spectroscopy reveals moderate changes in the secondary structure of recombinant fragments spanning the entire human fibrillin-1 molecule after treatment with Hcy [433]. S-homocysteinylation affects also functional properties of the fibrillin-1 fragments. For example, calcium binding to S-homocysteinylated fragments is completely abolished, and the fragments containing S-linked Hcy become significantly more susceptible to proteolytic degradation [433].

S-homocysteinylated fibrillin-1 fragments exhibit abnormal self-interaction, reduced multimerization of the C terminus, and impaired coacervation properties [434]. The deposition of the fibrillin-1 network by human dermal fibroblasts is reduced by the treatment of the cells with 1-mM Hcy, but not with 0.3-mM Hcy. These effects are specific to S-homocysteinylation and are not observed after S-cysteinylation. However, binding of fibrillin-1 to heparin through several domains distributed throughout the molecule is inhibited similarly by Hcy and cysteine (each at 0.3 mM) [434].

The cause of connective tissue abnormalities resulting from hyperhomocysteinemia has been studied in an in vivo chick model [19]. Hyperhomocysteinemia was induced by feeding 2-day-old chicks with a high-Met diet for up to 9 weeks. The aortas of the hyperhomocysteinemic chicks show severe histopathology, including pronounced separation of elastic lamellae with marked smooth muscle proliferation and aneurysms. Electron microscopy studies revealed disordered elastic fibers in aorta and absence or disrupted assembly of microfibrils. Immunohistochemical examinations demonstrated a loss of fibrillin-2 in the aortic tissue. Although it has not been examined whether these abnormalities are linked to S-homocysteinylation of any of the connective tissue components, these data provide evidence that elevated Hcy or its metabolites disrupt normal microfibril structure, leading to aberrant elastic fibers [19].

7.2.2 *Fibronectin*

The assembly of fibrillin-1 depends on fibronectin, which exists in two forms: soluble plasma fibronectin, synthesized by hepatocytes, and cellular fibrous form secreted and assembled by mesenchymal cells [435]. Cellular fibronectin is secreted as a disulfide-bonded dimer with >60 cysteine residues, most of which form intrachain disulfides. In addition to fibrillin, fibronectin also assembles other matrix proteins: collagen types I and III, thrombospondin-1, fibulin-1, and LTBP-1.

In vitro experiments show that when human plasma is treated with 0.5-mM [³⁵S] Hcy, plasma fibronectin, in addition to albumin, undergoes *S*-homocysteinylation. Purified fibronectin also binds [³⁵S]Hcy, and the binding is reversed by the treatment with the reducing agent 2-mercaptoethanol [436]. About five Hcy molecules bind per each 440-kDa fibronectin dimer. Mass spectroscopic analyses indicate that *S*-homocysteinylation regions are located in the N- and C-terminal domains, but not in the collagen-binding region [436].

However, the treatment with 0.5 mM [³⁵S]Cys does not lead to fibronectin *S*-cysteinylation (in plasma or purified), which indicates that the binding is specific for Hcy. The incorporation of Hcy via disulfide linkages affects fibronectin function, as shown by the inhibition of *S*-Hcy–fibronectin binding to fibrin. However, the binding to gelatin/collagen, involving a different domain of fibrillin, is not affected by *S*-homocysteinylation [436].

Fibronectin *S*-homocysteinylation compromises its interaction with fibrillin-1 but not with heparin [437]. Hcy, but not cysteine, reduces the fibronectin disulfide-bound dimer to monomers and modifies epitopes for disulfide-dependent binding of monoclonal antifibronectin antibodies.

S-homocysteinylation inhibits *de novo* assembly of fibronectin on cells [437]. For example, the treatment with 1-mM Hcy reduces, while 5-mM Hcy completely abolishes, fibronectin deposition on human dermal fibroblasts. Similar treatments with cysteine do not affect fibronectin assembly while the treatment with DTT completely prevented fibronectin deposition and network formation on fibroblasts.

These results indicate that native disulfide bonds in fibronectin molecule are important for its function and that the disruption of these disulfide bonds impairs normal fibronectin function. It remains to be determined, however, whether *S*-homocysteinylation of fibronectin or other components of the extracellular matrix occurs in CBS-deficient patients or in human hyperhomocysteinemia in general.

7.2.3 *Tropoelastin*

Microfibrils formed by fibrillins serve as a scaffold for the deposition of tropoelastin, which is important for the formation and maintenance of elastic fibers. Properly assembled elastic fibers confer elasticity on tissues such as skin, lung, and aorta. During elastic fiber biogenesis, tropoelastin undergoes maturation and

cross-linking to form an insoluble polymeric elastin [438]. Elastin is responsible for the properties of extensibility and elastic recoil of the extracellular matrix in a variety of tissues.

Tropoelastin contains two cysteine residues that form an intramolecular disulfide bond and are located at the conserved C terminus encoded by exon 36 [439]. Studies of coacervation of a recombinant tropoelastin fragment containing the sole two cysteine residues present in human tropoelastin reveal a statistically significant increase in the coacervation temperature (1.4 °C) after treatment with 0.3-mM Hcy [434]. However, the velocity of coacervation is not affected by Hcy. Treatment with cysteine does not affect the coacervation temperature of the tropoelastin fragment. The coacervation of a control fibrillin-1 peptide that does not contain cysteine residues is not affected by Hcy or cysteine. Although these findings suggest that Hcy could interfere with the biogenesis of elastic fibers, there is no direct evidence that S-homocysteinylated is involved.

7.3 Blood Homeostasis Proteins

7.3.1 Factor Va

During blood clotting, the prothrombinase complex, containing factor Va, is responsible for the conversion of prothrombin to thrombin. Factor V (M wt 330,000 Da) is activated by α -thrombin cleavages at Arg709, Arg1018, and Arg1545. The product, factor Va, is composed of a heavy chain, residues 1–709 (M wt 105,000 Da), derived from the N terminus of factor V and a noncovalently associated light chain, residues 1,546–2,196 (M wt 74,000 Da), derived from the COOH terminus (A3-C1-C2 domains) [440]. Factor Va is proteolytically inactivated by activated protein C [441].

Treatments with Hcy, cysteine, and Hcy-thiolactone have no effect on factor V activation by α -thrombin. However, factor Va derived from Hcy-treated, but not cysteine- or Hcy-thiolactone-treated, factor V is inactivated by activated protein C at a reduced rate [442]. Incubation with [³⁵S]Hcy results in formation of S-[³⁵S] Hcy-factor V, which is prevented by the treatment with β -mercaptoethanol. After cleavage of S-[³⁵S]Hcy-factor V with activated protein C, followed by resolution on nonreducing SDS-PAGE gels, [³⁵S]Hcy is found only in fragments known to contain free sulfhydryl groups: the light chain (Cys1960, Cys2113), the B region (Cys1085), and the 26/28-kDa fragment (residues 507–709) (Cys-539, Cys-585). Treatment with β -mercaptoethanol removes all radiolabel [442].

Impaired inactivation of the prothrombinase complex might explain the thrombotic tendency in CBS-deficient or other hyperhomocysteinemic patients. However, it is unclear whether the inactivation of the prothrombinase complex by Hcy occurs in such patients. Furthermore, there is no evidence for the presence of

S-Hcy-factor Va in the plasma or for the impairment of protein C activation by thrombin in experimental hyperhomocysteinemia in humans or animals [443].

7.3.2 *Annexin A2*

Studies of annexin A2, a calcium-regulated and phospholipid-binding protein, reveal the existence of an antifibrinolytic mechanism involving *S*-homocysteinylation [145]. The annexin A2 complex is the endothelial cell-surface co-receptor for plasminogen and tissue plasminogen activator (TPA) that accelerates the catalytic activation of plasmin, the major fibrinolytic enzyme in mammals. The binding of TPA and plasminogen to annexin A2 increases the catalytic efficiency of TPA-dependent plasmin generation 60-fold [444]. TPA binding is inhibited by the hexapeptide LCKLSL corresponding to residues 7–12 of annexin A2. Hcy decreases the ability of annexin A2 to bind to TPA, while cysteine has no effect [445]. Mass spectroscopic studies have shown that purified annexin A2 incubated *in vitro* with Hcy becomes *S*-homocysteinylated at residue Cys8 [446]. *Ex vivo* studies with endothelial cells labeled with [³⁵S]Hcy show a prominent ³⁵S-labeled 36-kDa band on nonreducing SDS-PAGE gels that corresponds to annexin A2 and disappears on reducing gels. This suggests that Hcy forms a disulfide bond with the residue Cys8 of annexin A2 in cultured endothelial cells. As a result of this posttranslational modification, plasminogen activation on the endothelial cell surface is significantly impaired [446].

Annexin A2 binds Hcy also *in vivo* in a mouse model of hyperhomocysteinemia [145]. When mice are fed with a high-Met, low-folate diet, plasma Hcy levels increase to about 70 μM, and annexin A2 becomes *S*-homocysteinylated, as demonstrated by the immunostaining of lung sections using a polyclonal antibody generated against *S*-homocysteinylated A2 N-terminal peptide. (This antibody is specific for A2 and fails to react with any other protein.)

Annexin A2 isolated from the lung tissue of hyperhomocysteinemic mice fails to bind TPA and does not support plasminogen activation, whereas annexin A2 isolated from control mice was fully active in TPA binding and plasminogen activation. Treatment with 2-mercaptoethanol of annexin A2 isolated from the hyperhomocysteinemic mice restores its activity, which shows that *S*-homocysteinylation impairs normal annexin A2 function *in vivo*. The hyperhomocysteinemic mice exhibit microvascular fibrin accumulation in the kidneys, heart, and lung, as well as diminished angiogenesis [145]. This phenotype of the hyperhomocysteinemic mouse is similar to the phenotype observed in the annexin A2 knockout mouse [447].

In a chemical FeCl₃ vascular injury model of thrombosis, complete occlusion of the carotid artery occurs in six of seven mice on high-Met diet but only in one of seven mice on a control diet. Furthermore, post-injury blood flow in mice on high-Met diet is reduced to 50 %, whereas post-injury blood flow in control mice is essentially not affected. This prothrombotic phenotype is reversed by infusion of

wild-type recombinant annexin A2 into the hyperhomocysteinemic mice. Taken together, these results indicate that the inhibition of annexin A2-dependent fibrinolysis by S-homocysteinylation in vivo generates a prothrombotic phenotype.

If S-homocysteinylation of annexin A2 generates a prothrombotic phenotype, it should be observed in any model of hyperhomocysteinemia, regardless of whether the model is dietary or genetic. Surprisingly, however, a prothrombotic phenotype is not observed in genetic hyperhomocysteinemia. Specifically, severely hyperhomocysteinemic Tg-I278T *Cbs*^{-/-} mice do not display increased susceptibility to arterial or venous thrombosis, measured by several methods, including photochemical injury of the carotid artery, chemical (FeCl₃) injury in the carotid artery and mesenteric arterioles, and ligation of the inferior vena cava [448]. There are no significant differences in hemostatic and hemodynamic parameters between Tg-I278T *Cbs*^{-/-} and control mice. Although the authors [448] do not discuss this, these data suggest that annexin A2 S-homocysteinylation for an unknown reason does not occur in the *Cbs*^{-/-} mice. Another possibility is that other mechanisms of fibrinolysis are enhanced in severely hyperhomocysteinemic mice.

7.4 Intracellular Proteins

7.4.1 Heterogenous Nuclear Ribonucleoprotein E1 (hnRNP-E1)

Folates participate in one carbon metabolism and are essential for the synthesis of DNA and the remethylation of Hcy to methionine. Inadequate folate supply leads to the elevation of Hcy levels. High-affinity folate receptors (FR), discovered in 1981 [449], are critical for the cellular uptake of 5-methylenetetrahydrofolate [450]. In addition to hyperhomocysteinemia, folate deficiency also induces a marked elevation of the cell-surface FR protein, but not FR mRNA, in HeLa cells. The FR expression is regulated posttranslationally by heterologous nuclear ribonucleoprotein E1 (hnRNP-E1), which binds to an 18 base cis-element in the 5'-UTR of FR- α mRNA [451].

The accumulation of intracellular Hcy resulting from folate deficiency has been shown to trigger the interaction of FR- α mRNA cis-element with hnRNP-E1, which then stimulates the biosynthesis and upregulation of FR [452]. Studies with purified components demonstrate that Hcy induces a concentration-dependent increase in the affinity of hnRNP-E1 to FR- α mRNA, which correlates with increase in translation of the FR in vitro and in cultured human cells [453]. Inhibition of hnRNP-E1 synthesis by siRNA reduces both constitutive and Hcy-induced FR biosynthesis.

Mass spectroscopic studies show that Hcy binds to hnRNP-E1 via multiple disulfide bonds within the K-homology domains that are known to interact with FR- α mRNA. To identify the sites of S-homocysteinylation, S-homocysteinylated

hnRNP-E1 is prepared *in vitro* by incubation of recombinant GST-hnRNP-E1 with 50- μ M Hcy. Digestion with trypsin followed by LC-MS/MS analysis shows that *S*-linked Hcy is present at several cysteine residues of hnRNP-E1 (Cys54, Cys109, Cys158, Cys163, and Cys149) [453].

These findings show that the disruption of critical disulfide bonds by *S*-homocysteinylation unmasks an RNA-binding pocket in hnRNP-E1 and optimizes its binding to FR- α mRNA cis-element required for the FR upregulation. Furthermore, these data suggest that hnRNP-E1 may function as a physiologically relevant cellular sensor of folate deficiency [453].

In addition to FR- α mRNA, *S*-homocysteinylated hnRNP-E1 also binds to cis-elements of other mRNAs, including 15-lipoxygenase mRNA, human papillomavirus 16 (HPV16) L2 mRNA, tyrosine hydroxylase mRNA, and the neuronal intermediate neurofilament middle molecular mass (neurofilament-M) mRNA. That these interactions are likely to occur *in vivo* has been demonstrated by increased accumulation of tyrosine hydroxylase and neurofilament-M in the adrenal medulla and the cerebellum, respectively, in brains of murine fetuses (gestation day 17) whose mothers were fed folate-deficient diet prior to and during pregnancy [453]. Other studies have shown that the translation of these mRNAs is also activated by the conventional reducing agent 2-mercaptoethanol or DTT.

Human papillomavirus (HPV) 16 is known to transform epithelial tissues to cancer in the presence of several cofactors, but there is insufficient evidence that poor nutrition (folate deficiency) has any such role. Because physiological folate deficiency leads to *S*-homocysteinylation of hnRNP-E1 and activates a nutrition-sensitive (Hcy-responsive) posttranscriptional RNA operon that includes interaction with HPV16 L2 mRNA, the functional consequences of folate deficiency on HPV16 in immortalized HPV16-harboring human (BC-1-Ep/SL) keratinocytes and HPV16-organotypic rafts have been investigated [454]. In addition to interacting with HPV16 L2 mRNA cis-element, *S*-homocysteinylated hnRNP-E1 also binds (with greater affinity) to another HPV16 57-nucleotide poly(U)-rich cis-element in the early polyadenylation element (upstream of L2L1 genes). These interactions lead to reductions of both L1 and L2 mRNA and proteins (but not HPV16 E6 and E7) *in vitro*, while in cultured keratinocytes, HPV16-low-folate-organotypic rafts develop in physiological low-folate medium. (Intracellular Hcy increases from 7 μ M in high-folate to 20 μ M in low-folate medium.) Furthermore, HPV16-low-folate-organotypic rafts contain fewer HPV16 viral particles, a similar HPV16 DNA viral load, and a much greater extent of integration of HPV16 DNA into genomic DNA, compared with HPV16-high-folate-organotypic rafts. Subcutaneous implantation of 18-day-old HPV16-low-folate-organotypic rafts into folate-replete immunodeficient mice transforms this benign keratinocyte-derived raft tissue into an aggressive HPV16-induced cancer within 12 weeks. Taken together, these results establish a likely molecular linkage between poor folate nutrition and HPV16 and predict that nutritional folate and/or vitamin B₁₂ deficiency, which are both common worldwide, is likely to alter the natural history of HPV16 infections and also warrant serious consideration of B vitamins as reversible cofactors in oncogenic transformation of HPV16-infected tissues to cancer [454].

7.4.2 *Metallothionein*

Metallothionein is a 6-kDa zinc-binding chaperone and superoxide radical scavenger that regulates zinc homeostasis and detoxifies heavy metals. Twenty of the approximately sixty amino acid residues of mammalian metallothioneins are cysteines, whose side chains are the only ligands to the seven zinc atoms in two clusters. Zinc can be released from metallothionein by oxidized thiols including cysteamine disulfide, coenzyme A disulfide, and glutathione disulfide (GS-SG). GS-SG is known to participate in a thiol/disulfide interchange with the solvent-accessible zinc-bound thiolates in metallothionein, which causes the clusters to collapse and release zinc [455].

Treatment of endothelial cells with Hcy also causes increase in free zinc, which is detected by preloading the cells with Zinquin AM [146]. In contrast, similar treatment with cysteine does not induce zinc release. As a direct consequence of free zinc elevation, the expression of early growth response-1 (Egr-1) protein, a zinc finger transcription factor that regulates proinflammatory and procoagulant genes associated with atherothrombosis [456], is transiently elevated in Hcy-treated cells [146]. In addition, the superoxide radical scavenging ability of metallothionein is inhibited after treatment with Hcy, thereby leading to superoxide production and increased oxidative stress.

Experiments with endothelial cells labeled with [³⁵S]Hcy followed by resolution of cell extracts on nonreducing SDS-PAGE gels and detection by autoradiography and Western blotting with anti-metallothionein antibodies suggest that metallothionein is a target for S-homocysteinylation [146]. Autoradiograms show a [³⁵S]-labeled band of 10 kDa that coincides with the metallothionein band detected by Western blotting. The radiolabeled band is absent in a sample that has been reduced with 2-mercaptoethanol. Surprisingly, however, the radiolabeled band is still present in samples reduced with glutathione. These findings suggest a mechanism in which Hcy binding to metallothionein disrupts intracellular redox homeostasis and induces endothelial cell dysfunction. However, the proposed mode of interaction between Hcy and metallothionein remains to be confirmed in *in vitro* studies with purified components.

7.4.3 *Dimethylarginine Dimethylaminohydrolase*

Endothelial dysfunction due to decreased bioavailability of nitric oxide is observed in hyperhomocysteinemia [457]. Asymmetrical dimethylarginine (ADMA), a competitive inhibitor of the enzyme nitric oxide synthase, is an important regulator of vascular function. Increased levels of Hcy are associated with increased levels of ADMA, which suggests that ADMA may mediate Hcy-induced endothelial dysfunction due to reduced nitric oxide production [458]. ADMA is known to be hydrolyzed by the enzyme dimethylarginine dimethylaminohydrolase (DDAH) [459].

In cultured bovine aortic endothelial cells, Hcy induces the accumulation of ADMA and inhibits DDAH activity in cell lysates prepared from cells that had been preincubated with Hcy [460]. Treatment of endothelial cells with the thiol reagent pyrrolidine dithiocarbamate prevents the accumulation of ADMA, suggesting that the DDAH active site thiol is involved. Experiments with recombinant DDAH show that Hcy inhibits the enzyme activity *in vitro*. Biotinylated Hcy (prepared using Pierce Sulfo-NHS-Biotinylation Kit), but not biotinylated methionine or cysteine, bind to recombinant DDAH and the binding is prevented by pyrrolidine dithiocarbamate, again suggesting the involvement of an active site thiol. It remains to be determined whether a putative *S*-Hcy–DDAH adduct can be detected in cell extracts or tissues from hyperhomocysteinemic organisms. However, the formation of such adduct *in vivo* is unlikely in view of the findings showing that plasma ADMA levels are not related to plasma tHcy levels in treated CBS-deficient individuals who have tHcy levels from 14 to 237 μM [461].

That Hcy is not disulfide bonded with the active site cysteine residue is demonstrated by crystallographic studies of the bovine brain DDAH [462]. The structure of the DDAH–Hcy complex indicates that Hcy binds in the active site pocket in the same orientation as citrulline does (a product of ADMA hydrolysis) and that it binds with a closed lid conformation. However, even in the absence of reducing agents, no electron density of a disulfide bond is found between the two sulfur atoms. The distance between the sulfur atoms of Hcy (S δ) and active site Cys (S γ), 3.5 Å observed in the crystallographic structure, is too large to be compatible with the disulfide bond formation. Therefore, these results do not support the formation of a disulfide bond between Hcy and the active site Cys thiol as proposed [460].

References

1. Johnson TB. Sulfur linkages in proteins. *J Biol Chem.* 1911;9:439–48.
2. Mueller JH. A new sulfur-containing amino acid isolated from the hydrolytic products of protein. *J Biol Chem.* 1923;58:157–69.
3. Butz LW, du Vigneaud V. The formation of homologue of cysteine by the decomposition of methionine with sulfuric acid. *J Biol Chem.* 1932;99:135–42.
4. Riegel B, Du Vigneaud V. The isolation of homocysteine and its conversion to a thiolactone. *J Biol Chem.* 1935;112:149–54.
5. Finkelstein JD. Homocysteine: a history in progress. *Nutr Rev.* 2000;58(7):193–204.
6. Jakubowski H. Quality control in tRNA charging. *Wiley Interdiscip Rev RNA.* 2012;3(3):295–310.
7. Jakubowski H. Quality control in tRNA charging—editing of homocysteine. *Acta Biochim Pol.* 2011;58(2):149–63.
8. Refsum H, Ueland PM, Nygard O, Vollset SE. Homocysteine and cardiovascular disease. *Annu Rev Med.* 1998;49:31–62.
9. Maron BA, Loscalzo J. The treatment of hyperhomocysteinemia. *Annu Rev Med.* 2009;60:39–54.
10. Joseph J, Handy DE, Loscalzo J. Quo vadis: whither homocysteine research? *Cardiovasc Toxicol.* 2009;9(2):53–63.
11. Benevenga NJ. Toxicities of methionine and other amino acids. *J Agric Food Chem.* 1974;22(1):2–9.
12. Benevenga NJ, Steele RD. Adverse effects of excessive consumption of amino acids. *Annu Rev Nutr.* 1984;4:157–81.
13. Harper AE, Benevenga NJ, Wohlhueter RM. Effects of ingestion of disproportionate amounts of amino acids. *Physiol Rev.* 1970;50(3):428–558.
14. Dayal S, Lentz SR. Murine models of hyperhomocysteinemia and their vascular phenotypes. *Arterioscler Thromb Vasc Biol.* 2008;28(9):1596–605.
15. Matsueda S, Niiyama Y. The effects of excess amino acids on maintenance of pregnancy and fetal growth in rats. *J Nutr Sci Vitaminol.* 1982;28(5):557–73.
16. Osborne-Pellegrin MJ, Fau D. Effects of chronic absorption of dietary supplements of methionine and cystine on arterial morphology in the rat. *Exp Mol Pathol.* 1992;56(1):49–59.
17. Fau D, Peret J, Hadjiiskiy P. Effects of ingestion of high protein or excess methionine diets by rats for two years. *J Nutr.* 1988;118(1):128–33.
18. Zhou J, Moller J, Danielsen CC, Bentzon J, Ravn HB, Austin RC, et al. Dietary supplementation with methionine and homocysteine promotes early atherosclerosis but not plaque rupture in ApoE-deficient mice. *Arterioscler Thromb Vasc Biol.* 2001;21(9):1470–6.
19. Hill CH, Mecham R, Starcher B. Fibrillin-2 defects impair elastic fiber assembly in a homocysteinemic chick model. *J Nutr.* 2002;132(8):2143–50.

20. Mudd SH, Levy HL, Kraus JP. Disorders of transsulfuration. In: Scriver CR, Beaudet AL, Sly WS, Valle D, Childs B, Kinzler KW, Vogelstein B, editors. *The metabolic and molecular bases of inherited disease*, vol. 2. 8th ed. New York, NY: Mc Graw-Hill; 2001. p. 2007–56.
21. Richie Jr JP, Leutzinger Y, Parthasarathy S, Malloy V, Orentreich N, Zimmerman JA. Methionine restriction increases blood glutathione and longevity in F344 rats. *FASEB J*. 1994;8(15):1302–7.
22. Sanz A, Caro P, Ayala V, Portero-Otin M, Pamplona R, Barja G. Methionine restriction decreases mitochondrial oxygen radical generation and leak as well as oxidative damage to mitochondrial DNA and proteins. *FASEB J*. 2006;20(8):1064–73.
23. Komninou D, Leutzinger Y, Reddy BS, Richie Jr JP. Methionine restriction inhibits colon carcinogenesis. *Nutr Cancer*. 2006;54(2):202–8.
24. Harker LA, Slichter SJ, Scott CR, Ross R. Homocystinemia. Vascular injury and arterial thrombosis. *N Engl J Med*. 1974;291(11):537–43.
25. Thampi P, Stewart BW, Joseph L, Melnyk SB, Hennings LJ, Nagarajan S. Dietary homocysteine promotes atherosclerosis in apoE-deficient mice by inducing scavenger receptors expression. *Atherosclerosis*. 2008;197(2):620–9.
26. Boers G. Moderate hyperhomocysteinaemia and vascular disease: evidence, relevance and the effect of treatment. *Eur J Pediatr*. 1998;157 Suppl 2:S127–30.
27. Krupkova-Meixnerova L, Vesela K, Vitova A, Janosikova B, Andel M, Kozich V. Methionine-loading test: evaluation of adverse effects and safety in an epidemiological study. *Clin Nutr*. 2002;21(2):151–6.
28. Cottington EM, LaMantia C, Stabler SP, Allen RH, Tangerman A, Wagner C, et al. Adverse event associated with methionine loading test: a case report. *Arterioscler Thromb Vasc Biol*. 2002;22(6):1046–50.
29. Kluijtmans LA, Boers GH, Kraus JP, van den Heuvel LP, Cruysberg JR, Trijbels FJ, et al. The molecular basis of cystathionine beta-synthase deficiency in Dutch patients with homocystinuria: effect of CBS genotype on biochemical and clinical phenotype and on response to treatment. *Am J Hum Genet*. 1999;65(1):59–67.
30. Yap S, Boers GH, Wilcken B, Wilcken DE, Brenton DP, Lee PJ, et al. Vascular outcome in patients with homocystinuria due to cystathionine beta-synthase deficiency treated chronically: a multicenter observational study. *Arterioscler Thromb Vasc Biol*. 2001;21(12):2080–5.
31. Rosenblatt D, Fenton W. Disorders of transsulfuration. In: Scriver C, Beaudet A, Sly W, Valle D, Childs B, Kinzler K, Vogelstein B, editors. *The metabolic and molecular bases of inherited disease*. 8th ed. New York, NY: Mc Graw-Hill; 2001. p. 2007–56.
32. Visy JM, Le Coz P, Chadefaux B, Fressinaud C, Woimant F, Marquet J, et al. Homocystinuria due to 5,10-methylenetetrahydrofolate reductase deficiency revealed by stroke in adult sibs. *Neurology*. 1991;41(8):1313–5.
33. McCully KS. Vascular pathology of homocysteinemia: implications for the pathogenesis of arteriosclerosis. *Am J Pathol*. 1969;56(1):111–28.
34. Refsum H, Nurk E, Smith AD, Ueland PM, Gjesdal CG, Bjelland I, et al. The Hordaland Homocysteine Study: a community-based study of homocysteine, its determinants, and associations with disease. *J Nutr*. 2006;136(6 Suppl):1731S–40.
35. Nygard O, Nordrehaug JE, Refsum H, Ueland PM, Farstad M, Vollset SE. Plasma homocysteine levels and mortality in patients with coronary artery disease. *N Engl J Med*. 1997;337(4):230–6.
36. Wald DS, Law M, Morris JK. Homocysteine and cardiovascular disease: evidence on causality from a meta-analysis. *BMJ*. 2002;325(7374):1202.
37. Anderson JL, Muhlestein JB, Horne BD, Carlquist JF, Bair TL, Madsen TE, et al. Plasma homocysteine predicts mortality independently of traditional risk factors and C-reactive protein in patients with angiographically defined coronary artery disease. *Circulation*. 2000;102(11):1227–32.

38. Seshadri S, Beiser A, Selhub J, Jacques PF, Rosenberg IH, D'Agostino RB, et al. Plasma homocysteine as a risk factor for dementia and Alzheimer's disease. *N Engl J Med.* 2002;346(7):476–83.
39. Daly S, Cotter A, Molloy AE, Scott J. Homocysteine and folic acid: implications for pregnancy. *Semin Vasc Med.* 2005;5(2):190–200.
40. Gjesdal CG, Vollset SE, Ueland PM, Refsum H, Drevon CA, Gjessing HK, et al. Plasma total homocysteine level and bone mineral density: the Hordaland Homocysteine Study. *Arch Intern Med.* 2006;166(1):88–94.
41. Perla-Kajan J, Twardowski T, Jakubowski H. Mechanisms of homocysteine toxicity in humans. *Amino Acids.* 2007;32(4):561–72.
42. Lusis AJ. Atherosclerosis. *Nature.* 2000;407(6801):233–41.
43. Ross R. Atherosclerosis—an inflammatory disease. *N Engl J Med.* 1999;340(2):115–26.
44. Lentz SR. Mechanisms of homocysteine-induced atherothrombosis. *J Thromb Haemost.* 2005;3(8):1646–54.
45. Hofmann MA, Lalla E, Lu Y, Gleason MR, Wolf BM, Tanji N, et al. Hyperhomocysteinemia enhances vascular inflammation and accelerates atherosclerosis in a murine model. *J Clin Invest.* 2001;107(6):675–83.
46. Mudd SH, Skovby F, Levy HL, Pettigrew KD, Wilcken B, Pyeritz RE, et al. The natural history of homocystinuria due to cystathionine beta-synthase deficiency. *Am J Hum Genet.* 1985;37(1):1–31.
47. Strauss KA, Morton DH, Puffenberger EG, Hendrickson C, Robinson DL, Wagner C, et al. Prevention of brain disease from severe 5,10-methylenetetrahydrofolate reductase deficiency. *Mol Genet Metab.* 2007;91(2):165–75.
48. Lawrence de Koning AB, Werstuck GH, Zhou J, Austin RC. Hyperhomocysteinemia and its role in the development of atherosclerosis. *Clin Biochem.* 2003;36(6):431–41.
49. Durga J, van Boxtel MP, Schouten EG, Kok FJ, Jolles J, Katan MB, et al. Effect of 3-year folic acid supplementation on cognitive function in older adults in the FACIT trial: a randomised, double blind, controlled trial. *Lancet.* 2007;369(9557):208–16.
50. Spence JD, Bang H, Chambless LE, Stampfer MJ. Vitamin intervention for stroke prevention trial: an efficacy analysis. *Stroke.* 2005;36(11):2404–9.
51. Lonn E, Yusuf S, Arnold MJ, Sheridan P, Pogue J, Micks M, et al. Homocysteine lowering with folic acid and B vitamins in vascular disease. *N Engl J Med.* 2006;354(15):1567–77.
52. Bonna KH, Njolstad I, Ueland PM, Schirmer H, Tverdal A, Steigen T, et al. Homocysteine lowering and cardiovascular events after acute myocardial infarction. *N Engl J Med.* 2006;354(15):1578–88.
53. Wang X, Qin X, Demirtas H, Li J, Mao G, Huo Y, et al. Efficacy of folic acid supplementation in stroke prevention: a meta-analysis. *Lancet.* 2007;369(9576):1876–82.
54. Hankey GJ, Eikelboom JW, Yi Q, Lees KR, Chen C, Xavier D, et al. Antiplatelet therapy and the effects of B vitamins in patients with previous stroke or transient ischaemic attack: a post-hoc subanalysis of VITATOPS, a randomised, placebo-controlled trial. *Lancet Neurol.* 2012;11:512–20.
55. Ebbing M, Bonna KH, Arnesen E, Ueland PM, Nordrehaug JE, Rasmussen K, et al. Combined analyses and extended follow-up of two randomized controlled homocysteine-lowering B-vitamin trials. *J Intern Med.* 2010;268(4):367–82.
56. Smith AD, Smith SM, de Jager CA, Whitbread P, Johnston C, Agacinski G, et al. Homocysteine-lowering by B vitamins slows the rate of accelerated brain atrophy in mild cognitive impairment: a randomized controlled trial. *PLoS One.* 2010;5(9):e12244.
57. de Jager CA, Oulhaj A, Jacoby R, Refsum H, Smith AD. Cognitive and clinical outcomes of homocysteine-lowering B-vitamin treatment in mild cognitive impairment: a randomized controlled trial. *Int J Geriatr Psychiatry.* 2012;27(6):592–600.
58. Zhang C, Cai Y, Adachi MT, Oshiro S, Aso T, Kaufman RJ, et al. Homocysteine induces programmed cell death in human vascular endothelial cells through activation of the unfolded protein response. *J Biol Chem.* 2001;276(38):35867–74.

59. Hossain GS, van Thienen JV, Werstuck GH, Zhou J, Sood SK, Dickhout JG, et al. TDAG51 is induced by homocysteine, promotes detachment-mediated programmed cell death, and contributes to the development of atherosclerosis in hyperhomocysteinemia. *J Biol Chem.* 2003;278(32):30317–27.
60. Roybal CN, Yang S, Sun CW, Hurtado D, Vander Jagt DL, Townes TM, et al. Homocysteine increases the expression of vascular endothelial growth factor by a mechanism involving endoplasmic reticulum stress and transcription factor ATF4. *J Biol Chem.* 2004;279(15):14844–52.
61. Kerkeni M, Tnani M, Chuniaud L, Miled A, Maaroufi K, Trivin F. Comparative study on in vitro effects of homocysteine thiolactone and homocysteine on HUVEC cells: evidence for a stronger proapoptotic and proinflammatory homocysteine thiolactone. *Mol Cell Biochem.* 2006;291(1–2):119–26.
62. Mattson MP, Shea TB. Folate and homocysteine metabolism in neural plasticity and neurodegenerative disorders. *Trends Neurosci.* 2003;26(3):137–46.
63. Jakubowski H. Proofreading in vivo: editing of homocysteine by methionyl-tRNA synthetase in the yeast *Saccharomyces cerevisiae*. *EMBO J.* 1991;10(3):593–8.
64. Jakubowski H. The determination of homocysteine-thiolactone in biological samples. *Anal Biochem.* 2002;308(1):112–9.
65. Jakubowski H, Goldman E. Editing of errors in selection of amino acids for protein synthesis. *Microbiol Rev.* 1992;56(3):412–29.
66. Tuite NL, Fraser KR, O'Byrne CP. Homocysteine toxicity in *Escherichia coli* is caused by a perturbation of branched-chain amino acid biosynthesis. *J Bacteriol.* 2005;187(13):4362–71.
67. Sikora M, Jakubowski H. Homocysteine editing and growth inhibition in *Escherichia coli*. *Microbiology.* 2009;155(Pt 6):1858–65.
68. Jakubowski H. Molecular basis of homocysteine toxicity in humans. *Cell Mol Life Sci.* 2004;61(4):470–87.
69. Jakubowski H. Pathophysiological consequences of homocysteine excess. *J Nutr.* 2006;136(6 Suppl):1741S–9.
70. Jacobsen DW. Homocysteine targeting of plasma proteins in hemodialysis patients. *Kidney Int.* 2006;69(5):787–9.
71. Jacobsen DW, Catanescu O, Dibello PM, Barbato JC. Molecular targeting by homocysteine: a mechanism for vascular pathogenesis. *Clin Chem Lab Med.* 2005;43(10):1076–83.
72. Glowacki R, Bald E, Jakubowski H. Identification and origin of Nepsilon-homocysteinyl-lysine isopeptide in humans and mice. *Amino Acids.* 2010;39(5):1563–9.
73. Jakubowski H. Metabolism of homocysteine thiolactone in human cell cultures. Possible mechanism for pathological consequences of elevated homocysteine levels. Possible mechanism for pathological consequences of elevated homocysteine levels. *J Biol Chem.* 1997;272(3):1935–42.
74. Jakubowski H, Zhang L, Bardeguet A, Aviv A. Homocysteine thiolactone and protein homocysteinyl-lysine in human endothelial cells: implications for atherosclerosis. *Circ Res.* 2000;87(1):45–51.
75. Jakubowski H. Translational incorporation of S-nitrosomethionine into protein. *J Biol Chem.* 2000;275(29):21813–6.
76. Jakubowski H. Translational accuracy of aminoacyl-tRNA synthetases: implications for atherosclerosis. *J Nutr.* 2001;131(11):2983S–7.
77. Jakubowski H. Homocysteine-thiolactone and S-nitroso-homocysteine mediate incorporation of homocysteine into protein in humans. *Clin Chem Lab Med.* 2003;41(11):1462–6.
78. Jakubowski H. Protein homocysteinyl-lysine: possible mechanism underlying pathological consequences of elevated homocysteine levels. *FASEB J.* 1999;13(15):2277–83.
79. Jakubowski H. Homocysteine is a protein amino acid in humans. Implications for homocysteine-linked disease. *J Biol Chem.* 2002;277(34):30425–8.

80. Teng YW, Mehedint MG, Garrow TA, Zeisel SH. Deletion of betaine-homocysteine S-methyltransferase in mice perturbs choline and 1-carbon metabolism, resulting in fatty liver and hepatocellular carcinomas. *J Biol Chem.* 2011;286(42):36258–67.
81. Jakubowski H. Calcium-dependent human serum homocysteine thiolactone hydrolase. A protective mechanism against protein N-homocysteinylation. *J Biol Chem.* 2000;275(6):3957–62.
82. Jakubowski H. tRNA synthetase editing of amino acids. In: *Encyclopedia of life sciences.* Chichester, UK: Wiley; 2005. <http://www.els.net/doi/10.1038/npg.els.0003933>
83. Jakubowski H. Accuracy of aminoacyl-tRNA synthetases: proofreading of amino acids. In: Ibba M, Francklyn C, Cusack S, editors. *The aminoacyl-tRNA synthetases.* Georgetown, TX: Landes Bioscience/Eurekah.com; 2005. p. 384–96.
84. Jakubowski H. Mechanism of the condensation of homocysteine thiolactone with aldehydes. *Chemistry.* 2006;12(31):8039–43.
85. Zimny J, Sikora M, Guranowski A, Jakubowski H. Protective mechanisms against homocysteine toxicity: the role of bleomycin hydrolase. *J Biol Chem.* 2006;281(32):22485–92.
86. Zaabczyk M, Glowacki R, Machnik A, Herod P, Kazek G, Jakubowski H, et al. Elevated concentrations of Nvarepsilon-homocysteinyl-lysine isopeptide in acute myocardial infarction: links with ADMA formation. *Clin Chem Lab Med.* 2011;49(4):729–35.
87. Refsum H, Smith AD, Ueland PM, Nexø E, Clarke R, McPartlin J, et al. Facts and recommendations about total homocysteine determinations: an expert opinion. *Clin Chem.* 2004;50(1):3–32.
88. Gerritsen T, Vaughn JG, Waisman HA. The identification of homocystine in the urine. *Biochem Biophys Res Commun.* 1962;9:493–6.
89. Frimpter GW. The disulfide of L-cysteine and L-homocysteine in urine of patients with cystinuria. *J Biol Chem.* 1961;236:PC51–3.
90. Schneider JA, Bradley KH, Seegmiller JE. Identification and measurement of cysteine-homocysteine mixed disulfide in plasma. *J Lab Clin Med.* 1968;71(1):122–5.
91. Kang SS, Wong PW, Becker N. Protein-bound homocyst(e)ine in normal subjects and in patients with homocystinuria. *Pediatr Res.* 1979;13(10):1141–3.
92. Smolin LA, Benevenga NJ. Accumulation of homocyst(e)ine in vitamin B-6 deficiency: a model for the study of cystathionine beta-synthase deficiency. *J Nutr.* 1982;112(7):1264–72.
93. Chwatko G, Boers GH, Strauss KA, Shih DM, Jakubowski H. Mutations in methylenetetrahydrofolate reductase or cystathionine beta-synthase gene, or a high-methionine diet, increase homocysteine thiolactone levels in humans and mice. *FASEB J.* 2007;21(8):1707–13.
94. Chwatko G, Jakubowski H. The determination of homocysteine-thiolactone in human plasma. *Anal Biochem.* 2005;337(2):271–7.
95. Chwatko G, Jakubowski H. Urinary excretion of homocysteine-thiolactone in humans. *Clin Chem.* 2005;51(2):408–15.
96. Glowacki R, Jakubowski H. Cross-talk between Cys34 and lysine residues in human serum albumin revealed by N-homocysteinylation. *J Biol Chem.* 2004;279(12):10864–71.
97. Medici V, Peerson JM, Stabler SP, French SW, Gregory 3rd JF, Virata MC, et al. Impaired homocysteine transsulfuration is an indicator of alcoholic liver disease. *J Hepatol.* 2010;53(3):551–7.
98. Stabler SP, Lindenbaum J, Savage DG, Allen RH. Elevation of serum cystathionine levels in patients with cobalamin and folate deficiency. *Blood.* 1993;81(12):3404–13.
99. Santhosh-Kumar CR, Deutsch JC, Kolhouse JC, Hassell KL, Kolhouse JF. Measurement of excitatory sulfur amino acids, cysteine sulfinic acid, cysteic acid, homocysteine sulfinic acid, and homocysteic acid in serum by stable isotope dilution gas chromatography–mass spectrometry and selected ion monitoring. *Anal Biochem.* 1994;220(2):249–56.
100. Stamler JS, Osborne JA, Jaraki O, Rabbani LE, Mullins M, Singel D, et al. Adverse vascular effects of homocysteine are modulated by endothelium-derived relaxing factor and related oxides of nitrogen. *J Clin Invest.* 1993;91(1):308–18.

101. Lee JS, Kang Decker N, Chatterjee S, Yao J, Friedman S, Shah V. Mechanisms of nitric oxide interplay with Rho GTPase family members in modulation of actin membrane dynamics in pericytes and fibroblasts. *Am J Pathol.* 2005;166(6):1861–70.
102. Mudd SH, Finkelstein JD, Refsum H, Ueland PM, Malinow MR, Lentz SR, et al. Homocysteine and its disulfide derivatives: a suggested consensus terminology. *Arterioscler Thromb Vasc Biol.* 2000;20(7):1704–6.
103. Refsum H, Helland S, Ueland PM. Radioenzymic determination of homocysteine in plasma and urine. *Clin Chem.* 1985;31(4):624–8.
104. Sass JO, Nakanishi T, Sato T, Sperl W, Shimizu A. S-homocysteinylation of transthyretin is detected in plasma and serum of humans with different types of hyperhomocysteinemia. *Biochem Biophys Res Commun.* 2003;310(1):242–6.
105. Lim A, Sengupta S, McComb ME, Theberge R, Wilson WG, Costello CE, et al. In vitro and in vivo interactions of homocysteine with human plasma transthyretin. *J Biol Chem.* 2003;278(50):49707–13.
106. Hortin GL, Seam N, Hoehn GT. Bound homocysteine, cysteine, and cysteinylglycine distribution between albumin and globulins. *Clin Chem.* 2006;52(12):2258–64.
107. Eagle H, Oyama VI, Piez KA. The reversible binding of half-cystine residues to serum protein, and its bearing on the cystine requirement of cultured mammalian cells. *J Biol Chem.* 1960;235:1719–26.
108. King TP. On the sulfhydryl group of human plasma albumin. *J Biol Chem.* 1961;236:PC5.
109. Malloy MH, Rassin DK, Gaull GE. A method for measurement of free and bound plasma cyst(e)ine. *Anal Biochem.* 1981;113(2):407–15.
110. Hanyu N, Shimizu T, Yamauchi K, Okumura N, Hidaka H. Characterization of cysteine and homocysteine bound to human serum transthyretin. *Clin Chim Acta.* 2009;403(1–2):70–5.
111. Mansoor MA, Svardal AM, Ueland PM. Determination of the in vivo redox status of cysteine, cysteinylglycine, homocysteine, and glutathione in human plasma. *Anal Biochem.* 1992;200(2):218–29.
112. Muscat JE, Kleinman W, Colosimo S, Muir A, Lazarus P, Park J, et al. Enhanced protein glutathiolation and oxidative stress in cigarette smokers. *Free Radic Biol Med.* 2004;36(4):464–70.
113. Jakubowski H, Perla-Kajan J, Finnell RH, Cabrera RM, Wang H, Gupta S, et al. Genetic or nutritional disorders in homocysteine or folate metabolism increase protein N-homocysteinylation in mice. *FASEB J.* 2009;23(6):1721–7.
114. Svardal A, Refsum H, Ueland PM. Determination of in vivo protein binding of homocysteine and its relation to free homocysteine in the liver and other tissues of the rat. *J Biol Chem.* 1986;261(7):3156–63.
115. Jakubowski H, Boers GH, Strauss KA. Mutations in cystathionine β -synthase or methylenetetrahydrofolate reductase gene increase N-homocysteinylation levels in humans. *FASEB J.* 2008;22(12):4071–6.
116. Kerins DM, Koury MJ, Capdevila A, Rana S, Wagner C. Plasma S-adenosylhomocysteine is a more sensitive indicator of cardiovascular disease than plasma homocysteine. *Am J Clin Nutr.* 2001;74(6):723–9.
117. Stabler SP, Allen RH. Quantification of serum and urinary S-adenosylmethionine and S-adenosylhomocysteine by stable-isotope-dilution liquid chromatography-mass spectrometry. *Clin Chem.* 2004;50(2):365–72.
118. Maclean KN, Sikora J, Kozich V, Jiang H, Greiner LS, Kraus E, et al. Cystathionine β -synthase null homocystinuric mice fail to exhibit altered hemostasis or lowering of plasma homocysteine in response to betaine treatment. *Mol Genet Metab.* 2010;101(2–3):163–71.
119. Quinn CT, Griener JC, Bottiglieri T, Hyland K, Farrow A, Kamen BA. Elevation of homocysteine and excitatory amino acid neurotransmitters in the CSF of children who receive methotrexate for the treatment of cancer. *J Clin Oncol.* 1997;15(8):2800–6.
120. Omori S, Kodama H, Ikegami T, Mizuhara S, Oura T. Unusual sulfur-containing amino acids in the urine of homocystinuric patients: III. Homocysteic acid, homocysteine sulfinic acid,

- S-(carboxymethylthio) homocysteine, and S-(3-hydroxy-3-carboxy-n-propyl). *Physiol Chem Phys.* 1972;4(3):286–94.
121. Hasegawa T, Ichiba M, Matsumoto SE, Kasanuki K, Hatano T, Fujishiro H, et al. Urinary homocysteic acid levels correlate with mini-mental state examination scores in Alzheimer's disease patients. *J Alzheimers Dis.* 2012;31(1):59–64.
 122. Frauscher G, Karnaukhova E, Muehl A, Hoeger H, Lubec B. Oral administration of homocysteine leads to increased plasma triglycerides and homocysteic acid-additional mechanisms in homocysteine induced endothelial damage? *Life Sci.* 1995;57(8):813–7.
 123. Vijayanathan V, Gulinello M, Ali N, Cole PD. Persistent cognitive deficits, induced by intrathecal methotrexate, are associated with elevated CSF concentrations of excitotoxic glutamate analogs and can be reversed by an NMDA antagonist. *Behav Brain Res.* 2011;225(2):491–7.
 124. Hasegawa T, Mikoda N, Kitazawa M, LaFerla FM. Treatment of Alzheimer's disease with anti-homocysteic acid antibody in 3xTg-AD male mice. *PLoS One.* 2010;5(1):e8593.
 125. Waller SJ, Kilpatrick IC, Chan MW, Evans RH. The influence of assay conditions on measurement of excitatory dibasic sulphinic and sulphonic alpha-amino acids in nervous tissue. *J Neurosci Methods.* 1991;36(2–3):167–76.
 126. Kopoldova J, Liebster J, Gross E. Radiation chemical reactions in aqueous solutions of methionine and its peptides. *Radiat Res.* 1967;30(2):261–74.
 127. Bern M, Saladino J, Sharp JS. Conversion of methionine into homocysteic acid in heavily oxidized proteomics samples. *Rapid commun mass spectrom.* 2010;24(6):768–72.
 128. Parker ET, Cleaves HJ, Dworkin JP, Glavin DP, Callahan M, Aubrey A, et al. Primordial synthesis of amines and amino acids in a 1958 Miller H₂S-rich spark discharge experiment. *Proc Natl Acad Sci USA.* 2011;108(14):5526–31.
 129. Van Trump JE, Miller SL. Prebiotic synthesis of methionine. *Science.* 1972;178(4063):859–60.
 130. Salojin KV, Cabrera RM, Sun W, Chang WC, Lin C, Duncan L, et al. A mouse model of hereditary folate malabsorption: deletion of the PCFT gene leads to systemic folate deficiency. *Blood.* 2011;117(18):4895–904.
 131. Carrillo-Carrasco N, Chandler RJ, Venditti CP. Combined methylmalonic acidemia and homocystinuria, cblC type. I. Clinical presentations, diagnosis and management. *J Inherit Metab Dis.* 2012;35(1):91–102.
 132. Carrillo-Carrasco N, Venditti CP. Combined methylmalonic acidemia and homocystinuria, cblC type. II. Complications, pathophysiology, and outcomes. *J Inherit Metab Dis.* 2012;35(1):103–14.
 133. Undas A, Jakubowski H. Letter by Undas and Jakubowski regarding article, "Relationship between homocysteine and mortality in chronic kidney disease". *Circulation.* 2006;114(16):e547. author reply e548.
 134. Jakubowski H. Anti-N-homocysteinylated protein autoantibodies and cardiovascular disease. *Clin Chem Lab Med.* 2005;43(10):1011–4.
 135. Undas A, Jankowski M, Twardowska M, Padjas A, Jakubowski H, Szczeklik A. Antibodies to N-homocysteinylated albumin as a marker for early-onset coronary artery disease in men. *Thromb Haemost.* 2005;93(2):346–50.
 136. Chambers JC, Obeid OA, Kooner JS. Physiological increments in plasma homocysteine induce vascular endothelial dysfunction in normal human subjects. *Arterioscler Thromb Vasc Biol.* 1999;19(12):2922–7.
 137. Chambers JC, Ueland PM, Wright M, Dore CJ, Refsum H, Kooner JS. Investigation of relationship between reduced, oxidized, and protein-bound homocysteine and vascular endothelial function in healthy human subjects. *Circ Res.* 2001;89(2):187–92.
 138. Jakubowski H, Goldman E. Synthesis of homocysteine thiolactone by methionyl-tRNA synthetase in cultured mammalian cells. *FEBS Lett.* 1993;317(3):237–40.
 139. Jakubowski H. Homocysteine thiolactone: metabolic origin and protein homocysteinylolation in humans. *J Nutr.* 2000;130(2S Suppl):377S–81.

140. Borowczyk K, Shih DM, Jakubowski H. Metabolism and neurotoxicity of homocysteine thiolactone in mice: evidence for a protective role of paraoxonase 1. *J Alzheimers Dis.* 2012;30(2):225–31.
141. Borowczyk K, Tisonczyk J, Jakubowski H. Metabolism and neurotoxicity of homocysteine thiolactone in mice: protective role of bleomycin hydrolase. *Amino Acids.* 2012;43(3):1339–48.
142. Van Aerts LA, Klaasboer HH, Postma NS, Pertijs JC, Peereboom JH, Eskes TK, et al. Stereospecific in vitro embryotoxicity of L-homocysteine in pre- and post-implantation rodent embryos. *Toxicol In Vitro.* 1993;7(6):743–9.
143. Jakubowski H. The molecular basis of homocysteine thiolactone-mediated vascular disease. *Clin Chem Lab Med.* 2007;45(12):1704–16.
144. Zinellu A, Sotgia S, Scanu B, Pintus G, Posadino AM, Cossu A, et al. S-homocysteinylated LDL apolipoprotein B adversely affects human endothelial cells in vitro. *Atherosclerosis.* 2009;206(1):40–6.
145. Jacovina AT, Deora AB, Ling Q, Broekman MJ, Almeida D, Greenberg CB, et al. Homocysteine inhibits neoangiogenesis in mice through blockade of annexin A2-dependent fibrinolysis. *J Clin Invest.* 2009;119(11):3384–94.
146. Barbato JC, Catanescu O, Murray K, DiBello PM, Jacobsen DW. Targeting of metallothionein by L-homocysteine: a novel mechanism for disruption of zinc and redox homeostasis. *Arterioscler Thromb Vasc Biol.* 2007;27(1):49–54.
147. Harker LA, Ross R, Slichter SJ, Scott CR. Homocystine-induced arteriosclerosis. The role of endothelial cell injury and platelet response in its genesis. *J Clin Invest.* 1976;58(3):731–41.
148. Mudd SH, Levy HL, Skovby F. Disorders of transsulfuration. In: Scriver CR, Beaudet AL, Sly WS, Valle D, editors. *The metabolic and molecular bases of inherited disease*, vol. 1. 6th ed. New York, NY: Mc Graw-Hill; 1995. p. 1279–327.
149. Endo N, Nishiyama K, Otsuka A, Kanouchi H, Taga M, Oka T. Antioxidant activity of vitamin B6 delays homocysteine-induced atherosclerosis in rats. *Br J Nutr.* 2006;95(6):1088–93.
150. Donahue S, Struman JA, Gaull G. Arteriosclerosis due to homocyst(e) inemia. Failure to reproduce the model in weanling rabbits. *Am J Pathol.* 1974;77(2):167–74.
151. Makheja AN, Bombard AT, Randazzo RL, Bailey JM. Anti-inflammatory drugs in experimental atherosclerosis. Part 3. Evaluation of the atherogenicity of homocystine in rabbits. *Atherosclerosis.* 1978;29(1):105–12.
152. Jakubowski H, Ambrosius WT, Pratt JH. Genetic determinants of homocysteine thiolactonase activity in humans: implications for atherosclerosis. *FEBS Lett.* 2001;491(1–2):35–9.
153. Jakubowski H. Biosynthesis and reactions of homocysteine thiolactone. In: Jacobson D, Carmel R, editors. *Homocysteine in health and disease*. Cambridge: Cambridge University Press; 2001. p. 21–31.
154. Rosenquist TH, Ratashak SA, Selhub J. Homocysteine induces congenital defects of the heart and neural tube: effect of folic acid. *Proc Natl Acad Sci USA.* 1996;93(26):15227–32.
155. Maestro de las Casas C, Epeldegui M, Tudela C, Varela-Moreiras G, Perez-Miguelsanz J. High exogenous homocysteine modifies eye development in early chick embryos. *Birth Defects Res A Clin Mol Teratol.* 2003;67(1):35–40.
156. Spence AM, Rasey JS, Dwyer-Hansen L, Grunbaum Z, Livesey J, Chin L, et al. Toxicity, biodistribution and radioprotective capacity of L-homocysteine thiolactone in CNS tissues and tumors in rodents: comparison with prior results with phosphorothioates. *Radiother Oncol.* 1995;35(3):216–26.
157. Folbergrova J. Anticonvulsant action of both NMDA and non-NMDA receptor antagonists against seizures induced by homocysteine in immature rats. *Exp Neurol.* 1997;145(2 Pt 1):442–50.
158. Langmeier M, Folbergrova J, Haugvicova R, Pokorny J, Mares P. Neuronal cell death in hippocampus induced by homocysteic acid in immature rats. *Epilepsia.* 2003;44(3):299–304.

159. Sprince H, Parker CM, Josephs Jr JA, Magazino J. Convulsant activity of homocysteine and other short-chain mercaptoacids: protection therefrom. *Ann N Y Acad Sci.* 1969;166(1):323–5.
160. Greene ND, Dunlevy LE, Copp AJ. Homocysteine is embryotoxic but does not cause neural tube defects in mouse embryos. *Anat Embryol (Berl).* 2003;206(3):185–91.
161. Najib S, Sanchez-Margalet V. Homocysteine thiolactone inhibits insulin signaling, and glutathione has a protective effect. *J Mol Endocrinol.* 2001;27(1):85–91.
162. Najib S, Sanchez-Margalet V. Homocysteine thiolactone inhibits insulin-stimulated DNA and protein synthesis: possible role of mitogen-activated protein kinase (MAPK), glycogen synthase kinase-3 (GSK-3) and p70 S6K phosphorylation. *J Mol Endocrinol.* 2005;34(1):119–26.
163. Li Y, Jiang C, Xu G, Wang N, Zhu Y, Tang C, et al. Homocysteine upregulates resistin production from adipocytes in vivo and in vitro. *Diabetes.* 2008;57(4):817–27.
164. Mercie P, Garnier O, Lascoste L, Renard M, Closse C, Durrieu F, et al. Homocysteine-thiolactone induces caspase-independent vascular endothelial cell death with apoptotic features. *Apoptosis.* 2000;5(5):403–11.
165. Huang RF, Huang SM, Lin BS, Wei JS, Liu TZ. Homocysteine thiolactone induces apoptotic DNA damage mediated by increased intracellular hydrogen peroxide and caspase 3 activation in HL-60 cells. *Life Sci.* 2001;68(25):2799–811.
166. Kamudhamas A, Pang L, Smith SD, Sadovsky Y, Nelson DM. Homocysteine thiolactone induces apoptosis in cultured human trophoblasts: a mechanism for homocysteine-mediated placental dysfunction? *Am J Obstet Gynecol.* 2004;191(2):563–71.
167. Rodgers GM, Kane WH. Activation of endogenous factor V by a homocysteine-induced vascular endothelial cell activator. *J Clin Invest.* 1986;77(6):1909–16.
168. Yang X, Gao Y, Zhou J, Zhen Y, Yang Y, Wang J, et al. Plasma homocysteine thiolactone adducts associated with risk of coronary heart disease. *Clin Chim Acta.* 2006;364(1–2):230–4.
169. Capasso R, Sambri I, Cimmino A, Salemme S, Lombardi C, Acanfora F, et al. Homocysteinylated albumin promotes increased monocyte-endothelial cell adhesion and up-regulation of MCP1, Hsp60 and ADAM17. *PLoS One.* 2012;7(2):e31388.
170. Ferretti G, Bacchetti T, Moroni C, Vignini A, Nanetti L, Curatola G. Effect of homocysteinylated low density lipoproteins on lipid peroxidation of human endothelial cells. *J Cell Biochem.* 2004;92(2):351–60.
171. Paoli P, Sbrana F, Tiribilli B, Caselli A, Pantera B, Cirri P, et al. Protein N-homocysteinylated albumin induces the formation of toxic amyloid-like protofibrils. *J Mol Biol.* 2010;400(4):889–907.
172. Undas A, Perla J, Lacinski M, Trzeciak W, Kazmierski R, Jakubowski H. Autoantibodies against N-homocysteinylated proteins in humans: implications for atherosclerosis. *Stroke.* 2004;35(6):1299–304.
173. Undas A, Stepień E, Glowacki R, Tisonczyk J, Tracz W, Jakubowski H. Folic acid administration and antibodies against homocysteinylated proteins in subjects with hyperhomocysteinemia. *Thromb Haemost.* 2006;96(3):342–7.
174. Undas A, Brozek J, Jankowski M, Siudak Z, Szczeklik A, Jakubowski H. Plasma homocysteine affects fibrin clot permeability and resistance to lysis in human subjects. *Arterioscler Thromb Vasc Biol.* 2006;26(6):1397–404.
175. Sauls DL, Lockhart E, Warren ME, Lenkowski A, Wilhelm SE, Hoffman M. Modification of fibrinogen by homocysteine thiolactone increases resistance to fibrinolysis: a potential mechanism of the thrombotic tendency in hyperhomocysteinemia. *Biochemistry.* 2006;45(8):2480–7.
176. Wang H, Yoshizumi M, Lai K, Tsai JC, Perrella MA, Haber E, et al. Inhibition of growth and p21ras methylation in vascular endothelial cells by homocysteine but not cysteine. *J Biol Chem.* 1997;272(40):25380–5.

177. Ingrosso D, Cimmino A, Perna AF, Masella L, De Santo NG, De Bonis ML, et al. Folate treatment and unbalanced methylation and changes of allelic expression induced by hyperhomocysteinaemia in patients with uraemia. *Lancet*. 2003;361(9370):1693–9.
178. Yi P, Melnyk S, Pogribna M, Pogribny IP, Hine RJ, James SJ. Increase in plasma homocysteine associated with parallel increases in plasma S-adenosylhomocysteine and lymphocyte DNA hypomethylation. *J Biol Chem*. 2000;275(38):29318–23.
179. Devlin AM, Bottiglieri T, Domann FE, Lentz SR. Tissue-specific changes in H19 methylation and expression in mice with hyperhomocysteinemia. *J Biol Chem*. 2005;280(27):25506–11.
180. Caudill MA, Wang JC, Melnyk S, Pogribny IP, Jernigan S, Collins MD, et al. Intracellular S-adenosylhomocysteine concentrations predict global DNA hypomethylation in tissues of methyl-deficient cystathionine beta-synthase heterozygous mice. *J Nutr*. 2001;131(11):2811–8.
181. Maclean KN, Greiner LS, Evans JR, Sood SK, Lhotak S, Markham NE, et al. Cystathionine protects against endoplasmic reticulum stress-induced lipid accumulation, tissue injury, and apoptotic cell death. *J Biol Chem*. 2012;287(38):31994–2005.
182. Shi Q, Savage JE, Hufeisen SJ, Rauser L, Grajkowska E, Ernberger P, et al. L-homocysteine sulfinic acid and other acidic homocysteine derivatives are potent and selective metabotropic glutamate receptor agonists. *J Pharmacol Exp Ther*. 2003;305(1):131–42.
183. Parsons RB, Waring RH, Ramsden DB, Williams AC. In vitro effect of the cysteine metabolites homocysteic acid, homocysteine and cysteic acid upon human neuronal cell lines. *Neurotoxicology*. 1998;19(4–5):599–603.
184. Kim JP, Koh JY, Choi DW. L-homocysteate is a potent neurotoxin on cultured cortical neurons. *Brain Res*. 1987;437(1):103–10.
185. Schwarz S, Zhou GZ. N-methyl-D-aspartate receptors and CNS symptoms of homocystinuria. *Lancet*. 1991;337(8751):1226–7.
186. Fritzer-Szekeres M, Blom HJ, Boers GH, Szekeres T, Lubec B. Growth promotion by homocysteine but not by homocysteic acid: a role for excessive growth in homocystinuria or proliferation in hyperhomocysteinemia? *Biochim Biophys Acta*. 1998;1407(1):1–6.
187. Baernstein HD. A modification of the method for determining methionine in proteins. *J Biol Chem*. 1934;106:451–6.
188. Jakubowski H. Facile syntheses of [35S]homocysteine-thiolactone, [35S]homocystine, [35S]homocysteine, and [S-nitroso-35S]homocysteine. *Anal Biochem*. 2007;370(1):124–6.
189. Racker E. Glutathione-homocystine transhydrogenase. *J Biol Chem*. 1955;217(2):867–74.
190. Jakubowski H, Guranowski A. Metabolism of homocysteine-thiolactone in plants. *J Biol Chem*. 2003;278(9):6765–70.
191. Benesch RE, Benesch R. The acid strength of the -SH group in cysteine and related compounds. *J Am Chem Soc*. 1955;77:5877–81.
192. Reuben DM, Bruice TC. Reaction of thiol anions with benzene oxide and malachite green. *J Am Chem Soc*. 1976;98(1):114–21.
193. Jakubowski H. Proofreading in vivo. Editing of homocysteine by aminoacyl-tRNA synthetases in *Escherichia coli*. *J Biol Chem*. 1995;270(30):17672–3.
194. Gao W, Goldman E, Jakubowski H. Role of carboxy-terminal region in proofreading function of methionyl-tRNA synthetase in *Escherichia coli*. *Biochemistry*. 1994;33(38):11528–35.
195. Wolfenden R. The mechanism of hydrolysis of amino acyl RNA. *Biochemistry*. 1963;2:1090–2.
196. Schuber F, Pinck M. On the chemical reactivity of aminoacyl-tRNA ester bond. I. Influence of pH and nature of the acyl group on the rate of hydrolysis. *Biochimie*. 1974;56(3):383–90.
197. Jakubowski H. Proofreading in vivo: editing of homocysteine by methionyl-tRNA synthetase in *Escherichia coli*. *Proc Natl Acad Sci USA*. 1990;87(12):4504–8.
198. Dudman NP, Hicks C, Lynch JF, Wilcken DE, Wang J. Homocysteine thiolactone disposal by human arterial endothelial cells and serum in vitro. *Arterioscler Thromb*. 1991;11(3):663–70.

199. Jakubowski H. Aminoacylation of coenzyme A and pantetheine by aminoacyl-tRNA synthetases: possible link between noncoded and coded peptide synthesis. *Biochemistry*. 1998;37(15):5147–53.
200. Jakubowski H. Facile syntheses of [(35)S]homocysteine-thiolactone, [(35)S]homocystine, [(35)S]homocysteine, and [S-nitroso-(35)S]homocysteine. *Anal Biochem*. 2007;370(1):124–6.
201. Stekol JA. Preparation and determination of sulfur amino acids and related compounds. *Methods Enzymol*. 1957;3:578–600.
202. du Vigneaud V, Patterson WI, Hunt M. Opening of the ring of the thiolactone of homocysteine. *J Biol Chem*. 1938;126:217–31.
203. Benesch R, Benesch RE. Formation of peptide bonds by aminoacylation of homocysteine thiolactones. *J Am Chem Soc*. 1956;78:618–22.
204. Abadi DM, Wilcox PE. Chemical derivatives of alpha-chymotrypsinogen. III. Reaction with N-acetyl-DL-homocysteine thiolactone. *J Biol Chem*. 1960;235:396–404.
205. Benesch R, Benesch RE. Thiolation of proteins. *Proc Natl Acad Sci USA*. 1958;44(9):848–53.
206. Hough DW, Shall S. Inhibition of enzymically active N-acetyl-homocysteiny-ribonuclease by silver ions. *FEBS Lett*. 1970;8(5):243–6.
207. Leanza WJ, Chupak LS, Tolman RL, Marburg S. Acidic derivatives of homocysteine thiolactone: utility as anionic linkers. *Bioconjug Chem*. 1992;3(6):514–8.
208. Lundeberg P, Lynd NA, Zhang Y, Zeng X, Krogstad DV, Paffen T, et al. ph-triggered self-assembly of biocompatible histamine-functionalized triblock copolymers. *Soft Matter*. 2013;9(1):82–9.
209. Kumar A, Advani S, Dawar H, Talwar GP. A simple method for introducing a thiol group at the 5'-end of synthetic oligonucleotides. *Nucleic Acids Res*. 1991;19(16):4561.
210. Jakubowski H, Fersht AR. Alternative pathways for editing non-cognate amino acids by aminoacyl-tRNA synthetases. *Nucleic Acids Res*. 1981;9(13):3105–17.
211. Refsum H, Ueland PM, Nygard O, Vollset SE. Homocysteine and cardiovascular disease. *Annu Rev Med*. 1998;49:31–62.
212. Marczak L, Sikora M, Stobiecki M, Jakubowski H. Analysis of site-specific N-homocysteinylation of human serum albumin in vitro and in vivo using MALDI-ToF and LC-MS/MS mass spectrometry. *J Proteomics*. 2011;74(7):967–74.
213. Sikora M, Marczak L, Twardowski T, Stobiecki M, Jakubowski H. Direct monitoring of albumin lysine-525 N-homocysteinylation in human serum by liquid chromatography/mass spectrometry. *Anal Biochem*. 2010;405(1):132–4.
214. Zang T, Dai S, Chen D, Lee BW, Liu S, Karger BL, et al. Chemical methods for the detection of protein N-homocysteinylation via selective reactions with aldehydes. *Anal Chem*. 2009;81(21):9065–71.
215. Sikora M, Marczak L, Suszynska-Zajczyk J, Jakubowski H. Monitoring site-specific N-homocysteinylation in fibrinogen in vitro and in vivo as a potential marker of thrombosis in CBS-deficient patients. In: 22nd International Fibrinogen Workshop: July 4, 2012; Brighton, UK: International Fibrinogen Research Society (IFRS); 2012: p. 94.
216. Liu G, Nellaiappan K, Kagan HM. Irreversible inhibition of lysyl oxidase by homocysteine thiolactone and its selenium and oxygen analogues. Implications for homocystinuria. *J Biol Chem*. 1997;272(51):32370–7.
217. Deitrich RA, Petersen D, Vasiliou V. Removal of acetaldehyde from the body. *Novartis Found Symp*. 2007;285:23–40. discussion 40–51, 198–199.
218. Andrades ME, Lorenzi R, Berger M, Guimaraes JA, Moreira JC, Dal-Pizzol F. Glycolaldehyde induces fibrinogen post-translational modification, delay in clotting and resistance to enzymatic digestion. *Chem Biol Interact*. 2009;180(3):478–84.
219. Wriston Jr JC, Mackenzie CG. Synthesis and metabolism of 1, 3-thiazane-4-carboxylic acid derived from formaldehyde and homocysteine. *J Biol Chem*. 1957;225(2):607–13.

220. Glowacki R, Bald E, Jakubowski H. An on-column derivatization method for the determination of homocysteine-thiolactone and protein N-linked homocysteine. *Amino Acids*. 2011;41(1):187–94.
221. Senger B, Despons L, Walter P, Jakubowski H, Fasiolo F. Yeast cytoplasmic and mitochondrial methionyl-tRNA synthetases: two structural frameworks for identical functions. *J Mol Biol*. 2001;311(1):205–16.
222. Cohn VH, Lyle J. A fluorometric assay for glutathione. *Anal Biochem*. 1966;14(3):434–40.
223. Mukai Y, Togawa T, Suzuki T, Ohata K, Tanabe S. Determination of homocysteine thiolactone and homocysteine in cell cultures using high-performance liquid chromatography with fluorescence detection. *J Chromatogr B Analyt Technol Biomed Life Sci*. 2002;767(2):263–8.
224. Togawa T, Mukai Y, Ohata K, Suzuki T, Tanabe S. Measurement of homocysteine thiolactone hydrolase activity using high-performance liquid chromatography with fluorescence detection and polymorphisms of paraoxonase in normal human serum. *J Chromatogr B Analyt Technol Biomed Life Sci*. 2005;819(1):67–72.
225. Daneshvar P, Yazdanpanah M, Cuthbert C, Cole DE. Quantitative assay of plasma homocysteine thiolactone by gas chromatography/mass spectrometry. *Rapid Commun Mass Spectrom*. 2003;17(4):358–62.
226. Chen SJ, Chang HT. Nile red-adsorbed gold nanoparticles for selective determination of thiols based on energy transfer and aggregation. *Anal Chem*. 2004;76(13):3727–34.
227. Chen X, Zhou Y, Peng X, Yoon J. Fluorescent and colorimetric probes for detection of thiols. *Chem Soc Rev*. 2010;39(6):2120–35.
228. Lim II, Ip W, Crew E, Njoki PN, Mott D, Zhong CJ, et al. Homocysteine-mediated reactivity and assembly of gold nanoparticles. *Langmuir*. 2007;23(2):826–33.
229. Huang CC, Tseng WL. Role of fluorosurfactant-modified gold nanoparticles in selective detection of homocysteine thiolactone: remover and sensor. *Anal Chem*. 2008;80(16):6345–50.
230. Reynolds NM, Lazazzera BA, Ibba M. Cellular mechanisms that control mistranslation. *Nat Rev Microbiol*. 2010;8(12):849–56.
231. Fersht A. *Structure and mechanism in protein science*. New York, NY: WH Freeman and Company; 2000.
232. Old JM, Jones DS. The aminoacylation of transfer ribonucleic acid. Recognition of methionine by *Escherichia coli* methionyl-transfer ribonucleic acid synthetase. *Biochem J*. 1977;165(2):367–73.
233. Fersht AR, Dingwall C. An editing mechanism for the methionyl-tRNA synthetase in the selection of amino acids in protein synthesis. *Biochemistry*. 1979;18(7):1250–6.
234. Jakubowski H. Aminoacyl thioester chemistry of class II aminoacyl-tRNA synthetases. *Biochemistry*. 1997;36(37):11077–85.
235. Zubay J. *Biochemistry*. 4th ed. Dubuque, IA: Wm. C. Brown; 1998.
236. Lewin B. *Genes VIII*. New York: Oxford University Press; 2004.
237. Jakubowski H. Synthesis of homocysteine thiolactone in normal and malignant cells. In: Rosenberg IH, Graham I, Ueland PM, Refsum H, editors. *Homocysteine metabolism: from basic science to clinical medicine*. Norwell, MA: Kluwer Academic; 1997. p. 157–65.
238. Kim HY, Ghosh G, Schulman LH, Brunie S, Jakubowski H. The relationship between synthetic and editing functions of the active site of an aminoacyl-tRNA synthetase. *Proc Natl Acad Sci USA*. 1993;90(24):11553–7.
239. Serre L, Verdon G, Choinowski T, Hervouet N, Risler JL, Zelwer C. How methionyl-tRNA synthetase creates its amino acid recognition pocket upon L-methionine binding. *J Mol Biol*. 2001;306(4):863–76.
240. Jakubowski H. The synthetic/editing active site of an aminoacyl-tRNA synthetase: evidence for binding of thiols in the editing subsite. *Biochemistry*. 1996;35(25):8252–9.
241. Nadarajan SP, Mathew S, Deepankumar K, Yun H. An in silico approach to evaluate the polyspecificity of methionyl-tRNA synthetases. *J Mol Graph Model*. 2012;39C:79–86.

242. Crepin T, Schmitt E, Mechulam Y, Sampson PB, Vaughan MD, Honek JF, et al. Use of analogues of methionine and methionyl adenylate to sample conformational changes during catalysis in *Escherichia coli* methionyl-tRNA synthetase. *J Mol Biol.* 2003;332(1):59–72.
243. Jakubowski H. Proofreading in trans by an aminoacyl-tRNA synthetase: a model for single site editing by isoleucyl-tRNA synthetase. *Nucleic Acids Res.* 1996;24(13):2505–10.
244. Jakubowski H. Synthesis of cysteine-containing dipeptides by aminoacyl-tRNA synthetases. *Nucleic Acids Res.* 1995;23(22):4608–15.
245. Jakubowski H. Amino acid selectivity in the aminoacylation of coenzyme A and RNA minihelices by aminoacyl-tRNA synthetases. *J Biol Chem.* 2000;275(45):34845–8.
246. Mocibob M, Ivic N, Bilokapic S, Maier T, Luic M, Ban N, et al. Homologs of aminoacyl-tRNA synthetases acylate carrier proteins and provide a link between ribosomal and nonribosomal peptide synthesis. *Proc Natl Acad Sci USA.* 2010;107(33):14585–90.
247. Jarvis D, Bondanszky M, du Vigneaud V. The synthesis of 1-(hemi-homocysteine)-oxytocin and a study of some of its pharmacological properties. *J Am Chem Soc.* 1961;83:4780–4.
248. Daruzzaman A, Clifton IJ, Adlington RM, Baldwin JE, Rutledge PJ. The crystal structure of isopenicillin N synthase with a dipeptide substrate analogue. *Arch Biochem Biophys.* 2013;530(1):48–53.
249. Lima B, Forrester MT, Hess DT, Stamler JS. S-nitrosylation in cardiovascular signaling. *Circ Res.* 2010;106(4):633–46.
250. Perla-Kajan J, Jakubowski H. Paraoxonase 1 protects against protein N-homocysteinylation in humans. *FASEB J.* 2010;24(3):931–6.
251. Suszynska J, Tisonczyk J, Lee HG, Smith MA, Jakubowski H. Reduced homocysteine-thiolactonase activity in Alzheimer's disease. *J Alzheimers Dis.* 2010;19(4):1177–83.
252. Marsillach J, Mackness B, Mackness M, Riu F, Beltran R, Joven J, et al. Immunohistochemical analysis of paraoxonases-1, 2, and 3 expression in normal mouse tissues. *Free Radic Biol Med.* 2008;45(2):146–57.
253. Shih DM, Gu L, Xia YR, Navab M, Li WF, Hama S, et al. Mice lacking serum paraoxonase are susceptible to organophosphate toxicity and atherosclerosis. *Nature.* 1998;394(6690):284–7.
254. Bhattacharyya T, Nicholls SJ, Topol EJ, Zhang RL, Yang X, Schmitt D, et al. Relationship of paraoxonase 1 (PON1) gene polymorphisms and functional activity with systemic oxidative stress and cardiovascular risk. *JAMA.* 2008;299(11):1265–76.
255. Bayrak A, Bayrak T, Tokgozoglu SL, Volkan-Salanci B, Deniz A, Yavuz B, et al. Serum PON-1 activity but not Q192R polymorphism is related to the extent of atherosclerosis. *J Atheroscler Thromb.* 2012;19(4):376–84.
256. Jakubowski H. Paraoxonase 1 (PON1), a Junction between the metabolisms of homocysteine and lipids. In: Mackness B, Mackness M, Aviral M, Paragh G, editors. *Proteins and cell regulation*, vol. 6. Dordrecht: Springer; 2008. p. 87–102.
257. Perla-Kajan J, Jakubowski H. Paraoxonase 1 and homocysteine metabolism. *Amino Acids.* 2012;43(4):1405–17.
258. Dantoine TF, Debord J, Merle L, Lacroix-Ramiandrisoa H, Bourzeix L, Charmes JP. Paraoxonase 1 activity: a new vascular marker of dementia? *Ann N Y Acad Sci.* 2002;977:96–101.
259. Paragh G, Balla P, Katona E, Seres I, Egerhazi A, Degrell I. Serum paraoxonase activity changes in patients with Alzheimer's disease and vascular dementia. *Eur Arch Psychiatry Clin Neurosci.* 2002;252(2):63–7.
260. Erlich PM, Lunetta KL, Cupples LA, Abraham CR, Green RC, Baldwin CT, et al. Serum paraoxonase activity is associated with variants in the PON gene cluster and risk of Alzheimer disease. *Neurobiol Aging.* 2012;33(5):1015.e7–1015.e23.
261. Lacinski M, Skorupski W, Cieslinski A, Sokolowska J, Trzeciak WH, Jakubowski H. Determinants of homocysteine-thiolactonase activity of the paraoxonase-1 (PON1) protein in humans. *Cell Mol Biol (Noisy-le-Grand).* 2004;50(8):885–93.

262. Wehr H, Bednarska-Makaruk M, Graban A, Lipczynska-Lojkowska W, Rodo M, Bochynska A, et al. Paraoxonase activity and dementia. *J Neurol Sci.* 2009;283(1–2):107–8.
263. Harel M, Aharoni A, Gaidukov L, Brumshtein B, Khersonsky O, Meged R, et al. Structure and evolution of the serum paraoxonase family of detoxifying and anti-atherosclerotic enzymes. *Nat Struct Mol Biol.* 2004;11(5):412–9.
264. Ben-David M, Elias M, Filippi JJ, Dunach E, Silman I, Sussman JL, et al. Catalytic versatility and backups in enzyme active sites: the case of serum paraoxonase 1. *J Mol Biol.* 2012;418(3–4):181–96.
265. Jarvik GP, Hatsukami TS, Carlson C, Richter RJ, Jampsa R, Brophy VH, et al. Paraoxonase activity, but not haplotype utilizing the linkage disequilibrium structure, predicts vascular disease. *Arterioscler Thromb Vasc Biol.* 2003;23(8):1465–71.
266. Jarvik GP, Rozek LS, Brophy VH, Hatsukami TS, Richter RJ, Schellenberg GD, et al. Paraoxonase (PON1) phenotype is a better predictor of vascular disease than is PON1(192) or PON1(55) genotype. *Arterioscler Thromb Vasc Biol.* 2000;20(11):2441–7.
267. Bayrak A, Bayrak T, Demirpence E, Kilinc K. Differential hydrolysis of homocysteine thiolactone by purified human serum (192)Q and (192)R PON1 isoenzymes. *J Chromatogr B Analyt Technol Biomed Life Sci.* 2011;879(1):49–55.
268. Mackness B, Davies GK, Turkie W, Lee E, Roberts DH, Hill E, et al. Paraoxonase status in coronary heart disease: are activity and concentration more important than genotype? *Arterioscler Thromb Vasc Biol.* 2001;21(9):1451–7.
269. Domagała TB, Łacinski M, Trzeciak WH, Mackness B, Mackness MI, Jakubowski H. The correlation of homocysteine-thiolactonase activity of the paraoxonase (PON1) protein with coronary heart disease status. *Cell Mol Biol (Noisy-le-Grand).* 2006;52(5):4–10.
270. Robert K, Chasse JF, Santiard-Baron D, Vayssettes C, Chabli A, Aupetit J, et al. Altered gene expression in liver from a murine model of hyperhomocysteinemia. *J Biol Chem.* 2003;278(34):31504–11.
271. Lazo JS, Humphreys CJ. Lack of metabolism as the biochemical basis of bleomycin-induced pulmonary toxicity. *Proc Natl Acad Sci USA.* 1983;80(10):3064–8.
272. Schwartz DR, Homanics GE, Hoyt DG, Klein E, Abernethy J, Lazo JS. The neutral cysteine protease bleomycin hydrolase is essential for epidermal integrity and bleomycin resistance. *Proc Natl Acad Sci USA.* 1999;96(8):4680–5.
273. Takeda A, Higuchi D, Yamamoto T, Nakamura Y, Masuda Y, Hirabayashi T, et al. Purification and characterization of bleomycin hydrolase, which represents a new family of cysteine proteases, from rat skin. *J Biochem (Tokyo).* 1996;119(1):29–36.
274. Kamata Y, Itoh Y, Kajiya A, Karasawa S, Sakatani C, Takekoshi S, et al. Quantification of neutral cysteine protease bleomycin hydrolase and its localization in rat tissues. *J Biochem (Tokyo).* 2007;141(1):69–76.
275. Nishimura C, Tanaka N, Suzuki H, Tanaka N. Purification of bleomycin hydrolase with a monoclonal antibody and its characterization. *Biochemistry.* 1987;26(6):1574–8.
276. Sebt SM, Mignano JE, Jani JP, Srimatkadada S, Lazo JS. Bleomycin hydrolase: molecular cloning, sequencing, and biochemical studies reveal membership in the cysteine proteinase family. *Biochemistry.* 1989;28(16):6544–8.
277. Bromme D, Rossi AB, Smeekens SP, Anderson DC, Payan DG. Human bleomycin hydrolase: molecular cloning, sequencing, functional expression, and enzymatic characterization. *Biochemistry.* 1996;35(21):6706–14.
278. Zheng W, Johnston SA, Joshua-Tor L. The unusual active site of Gal6/bleomycin hydrolase can act as a carboxypeptidase, aminopeptidase, and peptide ligase. *Cell.* 1998;93(1):103–9.
279. Niemer I, Muller G, Strobel G, Bandlow W. Bleomycin hydrolase (Blh1p), a multi-sited thiol protease in search of a distinct physiological role. *Curr Genet.* 1997;32(1):41–51.
280. Okamura Y, Nomoto S, Hayashi M, Hishida M, Nishikawa Y, Yamada S, et al. Identification of the bleomycin hydrolase gene as a methylated tumor suppressor gene in hepatocellular carcinoma using a novel triple-combination array method. *Cancer Lett.* 2011;312(2):150–7.

281. Kajiyama A, Kaji H, Isobe T, Takeda A. Processing of amyloid beta-peptides by neutral cysteine protease bleomycin hydrolase. *Protein Pept Lett.* 2006;13(2):119–23.
282. Papassotiropoulos A, Bagli M, Jessen F, Frahnert C, Rao ML, Maier W, et al. Confirmation of the association between bleomycin hydrolase genotype and Alzheimer's disease. *Mol Psychiatry.* 2000;5(2):213–5.
283. Lefterov IM, Koldamova RP, Lefterova MI, Schwartz DR, Lazo JS. Cysteine 73 in bleomycin hydrolase is critical for amyloid precursor protein processing. *Biochem Biophys Res Commun.* 2001;283(4):994–9.
284. Kajiyama A, Kaji H, Isobe T, Takeda A. Processing of amyloid beta-peptides by neutral cysteine protease bleomycin hydrolase. *Protein Pept Lett.* 2006;13(2):119–23.
285. Ratovitski T, Chighladze E, Waldron E, Hirschhorn RR, Ross CA. Cysteine proteases bleomycin hydrolase and cathepsin Z mediate N-terminal proteolysis and toxicity of mutant huntingtin. *J Biol Chem.* 2011;286(14):12578–89.
286. Kamata Y, Maejima H, Watarai A, Saito N, Katsuoka K, Takeda A, et al. Expression of bleomycin hydrolase in keratinization disorders. *Arch Dermatol Res.* 2012;304(1):31–8.
287. Kamata Y, Taniguchi A, Yamamoto M, Nomura J, Ishihara K, Takahara H, et al. Neutral cysteine protease bleomycin hydrolase is essential for the breakdown of deiminated filaggrin into amino acids. *J Biol Chem.* 2009;284(19):12829–36.
288. O'Farrell PA, Gonzalez F, Zheng W, Johnston SA, Joshua-Tor L. Crystal structure of human bleomycin hydrolase, a self-compartmentalizing cysteine protease. *Structure.* 1999;7(6):619–27.
289. van Guldener C, Stehouwer CD. Homocysteine metabolism in renal disease. *Clin Chem Lab Med.* 2003;41(11):1412–7.
290. Carson NA, Dent CE, Field CM, Gaull GE. Homocystinuria: clinical and pathological review of ten cases. *J Pediatr.* 1965;66:565–83.
291. Freeman JM, Finkelstein JD, Mudd SH. Folate-responsive homocystinuria and "schizophrenia". A defect in methylation due to deficient 5,10-methylenetetrahydrofolate reductase activity. *N Engl J Med.* 1975;292(10):491–6.
292. Rassin DK, Longhi RC, Gaull GE. Free amino acids in liver of patients with homocystinuria due to cystathionine synthase deficiency: effects of vitamin B6. *J Pediatr.* 1977;91(4):574–7.
293. Kanwar YS, Manaligod JR, Wong PW. Morphologic studies in a patient with homocystinuria due to 5, 10-methylenetetrahydrofolate reductase deficiency. *Pediatr Res.* 1976;10(6):598–609.
294. Stein WH, Moore S. The free amino acids of human blood plasma. *J Biol Chem.* 1954;211(2):915–26.
295. Glushchenko AV, Jacobsen DW. Molecular targeting of proteins by L-homocysteine: mechanistic implications for vascular disease. *Antioxid Redox Signal.* 2007;9(11):1883–98.
296. Noel JK, Hunter MJ. Bovine mercaptalbumin and non-mercaptalbumin monomers. Interconversions and structural differences. *J Biol Chem.* 1972;247(22):7391–406.
297. Jakubowski H. New method for the determination of protein N-linked homocysteine. *Anal Biochem.* 2008;380(2):257–61.
298. Perla-Kajan J, Marczak L, Kajan L, Skowronek P, Twardowski T, Jakubowski H. Modification by homocysteine thiolactone affects redox status of cytochrome c. *Biochemistry.* 2007;46(21):6225–31.
299. Akchiche N, Bossenmeyer-Pourie C, Kerek R, Martin N, Pourie G, Koziel V, et al. Homocysteinylation of neuronal proteins contributes to folate deficiency-associated alterations of differentiation, vesicular transport, and plasticity in hippocampal neuronal cells. *FASEB J.* 2012;26(10):3980–92.
300. Uji Y, Motomiya Y, Hanyu N, Ukaji F, Okabe H. Protein-bound homocystamide measured in human plasma by HPLC. *Clin Chem.* 2002;48(6 Pt 1):941–4.
301. Perna AF, Satta E, Acanfora F, Lombardi C, Ingrosso D, De Santo NG. Increased plasma protein homocysteinylation in hemodialysis patients. *Kidney Int.* 2006;69(5):869–76.

302. Beltowski J, Wojcicka G, Jakubowski H. Modulation of paraoxonase 1 and protein N-homocysteinylation by leptin and the synthetic liver X receptor agonist T0901317 in the rat. *J Endocrinol.* 2010;204(2):191–8.
303. Ishimine N, Usami Y, Nogi S, Sumida T, Kurihara Y, Matsuda K, et al. Identification of N-homocysteinylation apolipoprotein AI in normal human serum. *Ann Clin Biochem.* 2010;47(Pt 5):453–9.
304. Bostom A, Brosnan JT, Hall B, Nadeau MR, Selhub J. Net uptake of plasma homocysteine by the rat kidney in vivo. *Atherosclerosis.* 1995;116(1):59–62.
305. Gupta S, Kuhnisch J, Mustafa A, Lhotak S, Schlachterman A, Slifker MJ, et al. Mouse models of cystathionine beta-synthase deficiency reveal significant threshold effects of hyperhomocysteinemia. *FASEB J.* 2009;23(3):883–93.
306. Rusek M, Jakubowski H. Cystathionine beta synthase deficiency increases collagen N-homocysteinylation in mice. *Clin Chem Lab Med.* 2012;50(2):A31.
307. Pexa A, Fischer K, Deussen A, Henle T. Homocysteine in food. *Eur Food Res Technol.* 2008;226:933–5.
308. Borowczyk K, Jakubowski H. N-Homocysteinylation causes hair keratin damage in humans and animals. *Clin Chem Lab Med.* 2012;50(2):A52.
309. Robert K, Maurin N, Ledru A, Delabar J, Janel N. Hyperkeratosis in cystathionine beta synthase-deficient mice: an animal model of hyperhomocysteinemia. *Anat Rec A Discov Mol Cell Evol Biol.* 2004;280(2):1072–6.
310. Perla J, Undas A, Twardowski T, Jakubowski H. Purification of antibodies against N-homocysteinylation proteins by affinity chromatography on Nomega-homocysteinylation-aminohexyl-Agarose. *J Chromatogr B Analyt Technol Biomed Life Sci.* 2004;807(2):257–61.
311. Sibrian-Vazquez M, Escobedo JO, Lim S, Samoei GK, Strongin RM. Homocystamides promote free-radical and oxidative damage to proteins. *Proc Natl Acad Sci USA.* 2010;107(2):551–4.
312. Glowacki R, Bald E. Fully automated method for simultaneous determination of total cysteine, cysteinylglycine, glutathione and homocysteine in plasma by HPLC with UV absorbance detection. *J Chromatogr B Analyt Technol Biomed Life Sci.* 2009;877(28):3400–4.
313. Mazur P, Kozynacka A, Durajski L, Glowacki R, Pfitzner R, Fijorek K, et al. Nvarepsilon-homocysteinylation-lysine isopeptide is associated with progression of peripheral artery disease in patients treated with folic acid. *Eur J Vasc Endovasc Surg.* 2012;43(5):588–93.
314. Kolarz M, Glowacki R, Stompor T, Wyrosiak J, Undas A. Elevated levels of Nepsilon-homocysteinylation-lysine isopeptide in patients on long-term hemodialysis. *Clin Chem Lab Med.* 2012;50(8):1373–8.
315. du Vigneaud V, Ressler C, Swan JM, Roberts CW, Katsoyannis PG. The synthesis of oxytocin. *J Am Chem Soc.* 1954;76:3115–21.
316. Kosfeld M, Heinrichs M, Zak PJ, Fischbacher U, Fehr E. Oxytocin increases trust in humans. *Nature.* 2005;435(7042):673–6.
317. Di Simplicio M, Massey-Chase R, Cowen PJ, Harmer CJ. Oxytocin enhances processing of positive versus negative emotional information in healthy male volunteers. *J Psychopharmacol.* 2009;23(3):241–8.
318. Jarvis D, Ferrier BM, Du Vigneaud V. The effect of increasing the size of the ring present in deamino-oxytocin by one methylene group on its biological properties. The synthesis of 1-gamma-mercaptobutyric acid-oxytocin. *J Biol Chem.* 1965;240(9):3553–7.
319. Hope DB, Du Vigneaud V. Synthesis of desamino-desoxyoxytocin, a biologically active analogue of oxytocin. *J Biol Chem.* 1962;237:3146–50.
320. Ferretti G, Bacchetti T, Marotti E, Curatola G. Effect of homocysteinylation on human high-density lipoproteins: a correlation with paraoxonase activity. *Metabolism.* 2003;52(2):146–51.

321. Gerasimova YV, Knorre DD, Shakirov MM, Godovikova TS. Human serum albumin as a catalyst of RNA cleavage: N-homocysteinylation and N-phosphorylation by oligonucleotide affinity reagent alter the reactivity of the protein. *Bioorg Med Chem Lett*. 2008;18(20):5396–8.
322. Knorre DG, Kudryashova NV, Godovikova TS. Chemical and functional aspects of post-translational modification of proteins. *Acta Naturae*. 2009;1(3):29–51.
323. Peters TJ. All about albumin. San Diego, CA: Academic; 1996.
324. Christodoulou J, Sadler PJ, Tucker A. A new structural transition of serum albumin dependent on the state of Cys34. Detection by ¹H-NMR spectroscopy. *Eur J Biochem*. 1994;225(1):363–8.
325. Gates AT, Lowry M, Fletcher KA, Murugesu A, Rusin O, Robinson JW, et al. Capillary electrophoretic screening for the inhibition of homocysteine thiolactone-induced protein oligomerization. *Anal Chem*. 2007;79(21):8249–56.
326. Sauls DL, Warren M, Hoffman M. Homocysteinylation of fibrinogen forms disulfide-linked complexes with albumin. *Thromb Res*. 2011;127(6):576–81.
327. Koopman J, Haverkate F, Grimbergen J, Engesser L, Novakova I, Kerst AF, et al. Abnormal fibrinogens IJmuiden (B beta Arg14—Cys) and Nijmegen (B beta Arg44—Cys) form disulfide-linked fibrinogen-albumin complexes. *Proc Natl Acad Sci USA*. 1992;89(8):3478–82.
328. Koopman J, Haverkate F, Grimbergen J, Lord ST, Mosesson MW, DiOrio JP, et al. Molecular basis for fibrinogen Dusart (A alpha 554 Arg—>Cys) and its association with abnormal fibrin polymerization and thrombophilia. *J Clin Invest*. 1993;91(4):1637–43.
329. Marchi R, Lundberg U, Grimbergen J, Koopman J, Torres A, de Bosch NB, et al. Fibrinogen Caracas V, an abnormal fibrinogen with an Aalpha 532 Ser—>Cys substitution associated with thrombosis. *Thromb Haemost*. 2000;84(2):263–70.
330. Hanss M, Biot F. A database for human fibrinogen variants. *Ann N Y Acad Sci*. 2001;936:89–90.
331. La Corte AL, Ali M, Glowacki R, Jakubowski H, Ridger V, Pease R, et al. In vivo N-homocysteinylation of fibrinogen and its role in thrombosis. *J Thromb Haemost*. 2011;9(SI, Suppl 2):142.
332. Brown MS, Goldstein JL. Lipoprotein metabolism in the macrophage: implications for cholesterol deposition in atherosclerosis. *Annu Rev Biochem*. 1983;52:223–61.
333. Steinberg D, Parthasarathy S, Carew TE, Khoo JC, Witztum JL. Beyond cholesterol. Modifications of low-density lipoprotein that increase its atherogenicity. *N Engl J Med*. 1989;320(14):915–24.
334. Weisgraber KH, Innerarity TL, Mahley RW. Role of lysine residues of plasma lipoproteins in high affinity binding to cell surface receptors on human fibroblasts. *J Biol Chem*. 1978;253(24):9053–62.
335. Vidal M, Sainte-Marie J, Philippot J, Bienvenue A. Thiolation of low-density lipoproteins and their interaction with L2C leukemic lymphocytes. *Biochimie*. 1986;68(5):723–30.
336. Naruszewicz M, Olszewski AJ, Mirkiewicz E, McCully KS. Thiolation of low density lipoproteins by homocysteine thiolactone causes increased aggregation and altered interaction with cultured macrophages. *Nutr Metab Cardiovasc Dis*. 1994;4:70–7.
337. Vignini A, Nanetti L, Bacchetti T, Ferretti G, Curatola G, Mazzanti L. Modification induced by homocysteine and low-density lipoprotein on human aortic endothelial cells: an in vitro study. *J Clin Endocrinol Metab*. 2004;89(9):4558–61.
338. Jakubowski H, Boers GH, Strauss KA. Mutations in cystathionine beta-synthase or methylenetetrahydrofolate reductase gene increase N-homocysteinylation levels in humans. *FASEB J*. 2008;22(12):4071–6.
339. Strauss KA, Morton DH, Puffenberger EG, Hendrickson C, Robinson DL, Wagner C, et al. Prevention of brain disease from severe 5,10-methylenetetrahydrofolate reductase deficiency. *Mol Genet Metab*. 2007;91(2):165–75.

340. Virupaksha TK, Tarver H. The reaction of insulin with N-acetyl-DL-homocysteine thiolactone: some chemical and biological properties of the products. *Biochemistry*. 1964;3:1507–11.
341. Jalili S, Yousefi R, Papari MM, Moosavi-Movahedi AA. Effect of homocysteine thiolactone on structure and aggregation propensity of bovine pancreatic insulin. *Protein J*. 2011;30(5):299–307.
342. Yousefi R, Jalili S, Alavi P, Moosavi-Movahedi AA. The enhancing effect of homocysteine thiolactone on insulin fibrillation and cytotoxicity of insulin fibril. *Int J Biol Macromol*. 2012;51(3):291–8.
343. O'Harte FP, Boyd AC, McKillop AM, Abdel-Wahab YH, McNulty H, Barnett CR, et al. Structure, antihyperglycemic activity and cellular actions of a novel diglycated human insulin. *Peptides*. 2000;21(10):1519–26.
344. Farah MA, Bose S, Lee JH, Jung HC, Kim Y. Analysis of glycated insulin by MALDI-TOF mass spectrometry. *Biochim Biophys Acta*. 2005;1725(3):269–82.
345. Wemheuer WM, Benestad SL, Wrede A, Schulze-Sturm U, Wemheuer WE, Hahmann U, et al. Similarities between forms of sheep scrapie and Creutzfeldt-Jakob disease are encoded by distinct prion types. *Am J Pathol*. 2009;175(6):2566–73.
346. Li J, Liu D, Sun L, Lu Y, Zhang Z. Advanced glycation end products and neurodegenerative diseases: mechanisms and perspective. *J Neurol Sci*. 2012;317(1–2):1–5.
347. Stroylova YY, Chobert JM, Muronetz VI, Jakubowski H, Haertle T. N-homocysteinylation of ovine prion protein induces amyloid-like transformation. *Arch Biochem Biophys*. 2012;526(1):29–37.
348. Khodadadi S, Riazi GH, Ahmadian S, Hoveizi E, Karima O, Aryapour H. Effect of N-homocysteinylation on physicochemical and cytotoxic properties of amyloid beta-peptide. *FEBS Lett*. 2012;586(2):127–31.
349. Desai A, Mitchison TJ. Microtubule polymerization dynamics. *Annu Rev Cell Dev Biol*. 1997;13:83–117.
350. Goedert M, Spillantini MG, Jakes R, Rutherford D, Crowther RA. Multiple isoforms of human microtubule-associated protein tau: sequences and localization in neurofibrillary tangles of Alzheimer's disease. *Neuron*. 1989;3(4):519–26.
351. Panda D, Samuel JC, Massie M, Feinstein SC, Wilson L. Differential regulation of microtubule dynamics by three- and four-repeat tau: implications for the onset of neurodegenerative disease. *Proc Natl Acad Sci USA*. 2003;100(16):9548–53.
352. Mandelkow EM, Schweers O, Drewes G, Biernat J, Gustke N, Trinczek B, et al. Structure, microtubule interactions, and phosphorylation of tau protein. *Ann N Y Acad Sci*. 1996;777:96–106.
353. Karima O, Riazi G, Khodadadi S, Aryapour H, Nasiri Khalili MA, Yousefi L, et al. Altered tubulin assembly dynamics with N-homocysteinylation of human 4R/1N tau in vitro. *FEBS Lett*. 2012;586(21):3914–9.
354. Stroylova YY, Zimny J, Yousefi R, Chobert JM, Jakubowski H, Muronetz VI, et al. Aggregation and structural changes of alpha(S1)-, beta- and kappa-caseins induced by homocysteinylation. *Biochim Biophys Acta*. 2011;1814(10):1234–45.
355. Khazaei S, Yousefi R, Alavian-Mehr MM. Aggregation and fibrillation of eye lens crystallins by homocysteinylation; implication in the eye pathological disorders. *Protein J*. 2012;31(8):717–27.
356. Ferguson E, Parthasarathy S, Joseph J, Kalyanaraman B. Generation and initial characterization of a novel polyclonal antibody directed against homocysteine thiolactone-modified low density lipoprotein. *J Lipid Res*. 1998;39(4):925–33.
357. Perla-Kajan J, Stanger O, Luczak M, Ziolkowska A, Malendowicz LK, Twardowski T, et al. Immunohistochemical detection of N-homocysteinylation of proteins in humans and mice. *Biomed Pharmacother*. 2008;62(7):473–9.

358. Perna AF, Capasso R, Lombardi C, Acanfora F, Satta E, Ingrosso D. Hyperhomocysteinemia and macromolecule modifications in uremic patients. *Clin Chem Lab Med.* 2005;43(10):1032–8.
359. Wang W, Escobedo JO, Lawrence CM, Strongin RM. Direct detection of homocysteine. *J Am Chem Soc.* 2004;126(11):3400–1.
360. Wang W, Rusin O, Xu X, Kim KK, Escobedo JO, Fakayode SO, et al. Detection of homocysteine and cysteine. *J Am Chem Soc.* 2005;127(45):15949–58.
361. Mosesson MW, Sherry S. The preparation and properties of human fibrinogen of relatively high solubility. *Biochemistry.* 1966;5(9):2829–35.
362. Gu W, Lu J, Yang G, Dou J, Mu Y, Meng J, et al. Plasma homocysteine thiolactone associated with risk of macrovasculopathy in Chinese patients with type 2 diabetes mellitus. *Adv Ther.* 2008;25(9):914–24.
363. Kokame K, Kato H, Miyata T. Homocysteine-responsive genes in vascular endothelial cells identified by differential display analysis. GRP78/BiP and novel genes. *J Biol Chem.* 1996;271(47):29659–65.
364. Outinen PA, Sood SK, Liaw PC, Sarge KD, Maeda N, Hirsh J, et al. Characterization of the stress-inducing effects of homocysteine. *Biochem J.* 1998;332(Pt 1):213–21.
365. Althausen S, Paschen W. Homocysteine-induced changes in mRNA levels of genes coding for cytoplasmic- and endoplasmic reticulum-resident stress proteins in neuronal cell cultures. *Brain Res Mol Brain Res.* 2000;84(1–2):32–40.
366. Kokame K, Agarwala KL, Kato H, Miyata T. Herp, a new ubiquitin-like membrane protein induced by endoplasmic reticulum stress. *J Biol Chem.* 2000;275(42):32846–53.
367. Kaufman RJ. Stress signaling from the lumen of the endoplasmic reticulum: coordination of gene transcriptional and translational controls. *Genes Dev.* 1999;13(10):1211–33.
368. Mori K. Tripartite management of unfolded proteins in the endoplasmic reticulum. *Cell.* 2000;101(5):451–4.
369. Werstuck GH, Lentz SR, Dayal S, Hossain GS, Sood SK, Shi YY, et al. Homocysteine-induced endoplasmic reticulum stress causes dysregulation of the cholesterol and triglyceride biosynthetic pathways. *J Clin Invest.* 2001;107(10):1263–73.
370. Anfinsen CB. Principles that govern the folding of protein chains. *Science.* 1973;181(96):223–30.
371. Stefani M. Protein misfolding and aggregation: new examples in medicine and biology of the dark side of the protein world. *Biochim Biophys Acta.* 2004;1739(1):5–25.
372. Mallamaci F, Zoccali C, Tripepi G, Fermo I, Benedetto FA, Cataliotti A, et al. Hyperhomocysteinemia predicts cardiovascular outcomes in hemodialysis patients. *Kidney Int.* 2002;61(2):609–14.
373. Perla-Kaján J, Stanger O, Ziółkowska A, Melandowicz LK, Twardowski T, Jakubowski H. Immunohistochemical detection of N-homocysteinylated proteins in cardiac surgery patients. *Clin Chem Lab Med.* 2007;45(5):A36.
374. Libby P. Inflammation and cardiovascular disease mechanisms. *Am J Clin Nutr.* 2006;83(2):456S–60.
375. Forrester JS, Libby P. The inflammation hypothesis and its potential relevance to statin therapy. *Am J Cardiol.* 2007;99(5):732–8.
376. Binder CJ, Shaw PX, Chang MK, Boullier A, Hartvigsen K, Horkko S, et al. The role of natural antibodies in atherogenesis. *J Lipid Res.* 2005;46(7):1353–63.
377. Libby P, Ridker PM, Maseri A. Inflammation and atherosclerosis. *Circulation.* 2002;105(9):1135–43.
378. Lopes-Virella MF, Thorpe SR, Derrick MB, Chassereau C, Virella G. The immunogenicity of modified lipoproteins. *Ann N Y Acad Sci.* 2005;1043:367–78.
379. Undas A, Kolarz M, Kopec G, Glowacki R, Placzkiewicz-Jankowska E, Tracz W. Autoantibodies against N-homocysteinylated proteins in patients on long-term haemodialysis. *Nephrol Dial Transplant.* 2007;22(6):1685–9.

380. Bogdanski P, Pupek-Musialik D, Dytfield J, Lacinski M, Jablecka A, Jakubowski H. Plasma homocysteine is a determinant of tissue necrosis factor-alpha in hypertensive patients. *Biomed Pharmacother.* 2008;62(6):360–5.
381. Durga J, van Tits LJ, Schouten EG, Kok FJ, Verhoef P. Effect of lowering of homocysteine levels on inflammatory markers: a randomized controlled trial. *Arch Intern Med.* 2005;165(12):1388–94.
382. Folsom AR, Desvarieux M, Nieto FJ, Boland LL, Ballantyne CM, Chambless LE. B vitamin status and inflammatory markers. *Atherosclerosis.* 2003;169(1):169–74.
383. Ravaglia G, Forti P, Maioli F, Servadei L, Martelli M, Arnone G, et al. Plasma homocysteine and inflammation in elderly patients with cardiovascular disease and dementia. *Exp Gerontol.* 2004;39(3):443–50.
384. Peeters AC, van Aken BE, Blom HJ, Reitsma PH, den Heijer M. The effect of homocysteine reduction by B-vitamin supplementation on inflammatory markers. *Clin Chem Lab Med.* 2007;45(1):54–8.
385. Friso S, Jacques PF, Wilson PW, Rosenberg IH, Selhub J. Low circulating vitamin B(6) is associated with elevation of the inflammation marker C-reactive protein independently of plasma homocysteine levels. *Circulation.* 2001;103(23):2788–91.
386. Rohde LE, Hennekens CH, Ridker PM. Survey of C-reactive protein and cardiovascular risk factors in apparently healthy men. *Am J Cardiol.* 1999;84(9):1018–22.
387. Holven KB, Aukrust P, Retterstol K, Hagve TA, Morkrid L, Ose L, et al. Increased levels of C-reactive protein and interleukin-6 in hyperhomocysteinemic subjects. *Scand J Clin Lab Invest.* 2006;66(1):45–54.
388. Aso Y, Yoshida N, Okumura K, Wakabayashi S, Matsutomo R, Takebayashi K, et al. Coagulation and inflammation in overt diabetic nephropathy: association with hyperhomocysteinemia. *Clin Chim Acta.* 2004;348(1–2):139–45.
389. Shai I, Stampfer MJ, Ma J, Manson JE, Hankinson SE, Cannuscio C, et al. Homocysteine as a risk factor for coronary heart diseases and its association with inflammatory biomarkers, lipids and dietary factors. *Atherosclerosis.* 2004;177(2):375–81.
390. Widner B, Leblhuber F, Frick B, Laich A, Artner-Dworzak E, Fuchs D. Moderate hyperhomocysteinemia and immune activation in Parkinson's disease. *J Neural Transm.* 2002;109(12):1445–52.
391. Powers RW, Majors AK, Cerula SL, Huber HA, Schmidt BP, Roberts JM. Changes in markers of vascular injury in response to transient hyperhomocysteinemia. *Metabolism.* 2003;52(4):501–7.
392. Holven KB, Scholz H, Halvorsen B, Aukrust P, Ose L, Nenseter MS. Hyperhomocysteinemic subjects have enhanced expression of lectin-like oxidized LDL receptor-1 in mononuclear cells. *J Nutr.* 2003;133(11):3588–91.
393. Wang G, Woo CW, Sung FL, Siow YL, O K. Increased monocyte adhesion to aortic endothelium in rats with hyperhomocysteinemia: role of chemokine and adhesion molecules. *Arterioscler Thromb Vasc Biol.* 2002; 22(11):1777–83.
394. Zhang R, Ma J, Xia M, Zhu H, Ling W. Mild hyperhomocysteinemia induced by feeding rats diets rich in methionine or deficient in folate promotes early atherosclerotic inflammatory processes. *J Nutr.* 2004;134(4):825–30.
395. Lee H, Kim JM, Kim HJ, Lee I, Chang N. Folic acid supplementation can reduce the endothelial damage in rat brain microvasculature due to hyperhomocysteinemia. *J Nutr.* 2005;135(3):544–8.
396. Keating AK, Freehauf C, Jiang H, Brodsky GL, Stabler SP, Allen RH, et al. Constitutive induction of pro-inflammatory and chemotactic cytokines in cystathionine beta-synthase deficient homocystinuria. *Mol Genet Metab.* 2011;103(4):330–7.
397. Robert K, Nehme J, Bourdon E, Pivert G, Friguet B, Delcayre C, et al. Cystathionine beta synthase deficiency promotes oxidative stress, fibrosis, and steatosis in mice liver. *Gastroenterology.* 2005;128(5):1405–15.

398. Vanzin CS, Biancini GB, Sitta A, Wayhs CA, Pereira IN, Rockenbach F, et al. Experimental evidence of oxidative stress in plasma of homocystinuric patients: a possible role for homocysteine. *Mol Genet Metab.* 2011;104(1-2):112-7.
399. Dalal S, Parkin SM, Homer-Vanniasinkam S, Nicolaou A. Effect of homocysteine on cytokine production by human endothelial cells and monocytes. *Ann Clin Biochem.* 2003;40(Pt 5):534-41.
400. Zhang L, Jin M, Hu XS, Zhu JH. Homocysteine stimulates nuclear factor kappaB activity and interleukin-6 expression in rat vascular smooth muscle cells. *Cell Biol Int.* 2006;30(7):592-7.
401. Den Heijer M, Lewington S, Clarke R. Homocysteine, MTHFR and risk of venous thrombosis: a meta-analysis of published epidemiological studies. *J Thromb Haemost.* 2005;3(2):292-9.
402. Eyre DR, Weis MA, Wu JJ. Advances in collagen cross-link analysis. *Methods.* 2008;45(1):65-74.
403. Kang AH, Trelstad RL. A collagen defect in homocystinuria. *J Clin Invest.* 1973;52(10):2571-8.
404. Lubec B, Fang-Kircher S, Lubec T, Blom HJ, Boers GH. Evidence for McKusick's hypothesis of deficient collagen cross-linking in patients with homocystinuria. *Biochim Biophys Acta.* 1996;1315(3):159-62.
405. Robert K, Maurin N, Vayssettes C, Siauve N, Janel N. Cystathionine beta synthase deficiency affects mouse endochondral ossification. *Anat Rec A Discov Mol Cell Evol Biol.* 2005;282(1):1-7.
406. Jones DP, Go YM. Mapping the cysteine proteome: analysis of redox-sensing thiols. *Curr Opin Chem Biol.* 2011;15(1):103-12.
407. Markus G, Kraush F. The disulfide bonds of human serum albumin and bovine r-globulin. *J Am Chem Soc.* 1957;79:134-9.
408. Zinellu A, Lepedda Jr A, Sotgia S, Zinellu E, Marongiu G, Usai MF, et al. Albumin-bound low molecular weight thiols analysis in plasma and carotid plaques by CE. *J Sep Sci.* 2010;33(1):126-31.
409. Fan SW, George RA, Haworth NL, Feng LL, Liu JY, Wouters MA. Conformational changes in redox pairs of protein structures. *Protein Sci.* 2009;18(8):1745-65.
410. Christodoulou J, Sadler PJ, Tucker A. ¹H NMR of albumin in human blood plasma: drug binding and redox reactions at Cys34. *FEBS Lett.* 1995;376(1-2):1-5.
411. Sengupta S, Chen H, Togawa T, DiBello PM, Majors AK, Budy B, et al. Albumin thiolate anion is an intermediate in the formation of albumin-S-S-homocysteine. *J Biol Chem.* 2001;276(32):30111-7.
412. Sengupta S, Wehbe C, Majors AK, Ketterer ME, DiBello PM, Jacobsen DW. Relative roles of albumin and ceruloplasmin in the formation of homocystine, homocysteine-cysteine-mixed disulfide, and cystine in circulation. *J Biol Chem.* 2001;276(50):46896-904.
413. Rostom AA, Sunde M, Richardson SJ, Schreiber G, Jarvis S, Bateman R, et al. Dissection of multi-protein complexes using mass spectrometry: subunit interactions in transthyretin and retinol-binding protein complexes. *Proteins.* 1998;Suppl 2:3-11.
414. Falk RH, Comenzo RL, Skinner M. The systemic amyloidoses. *N Engl J Med.* 1997;337(13):898-909.
415. Suzuki T, Azuma T, Tsujino S, Mizuno R, Kishimoto S, Wada Y, et al. Diagnosis of familial amyloidotic polyneuropathy: isolation of variant prealbumin. *Neurology.* 1987;37(4):708-11.
416. Theberge R, Connors L, Skinner M, Skare J, Costello CE. Characterization of transthyretin mutants from serum using immunoprecipitation, HPLC/electrospray ionization and matrix-assisted laser desorption/ionization mass spectrometry. *Anal Chem.* 1999;71(2):452-9.
417. Suhr OB, Svendsen IH, Ohlsson PI, Lendoire J, Trigo P, Tashima K, et al. Impact of age and amyloidosis on thiol conjugation of transthyretin in hereditary transthyretin amyloidosis. *Amyloid.* 1999;6(3):187-91.

418. Zhang Q, Kelly JW. Cys10 mixed disulfides make transthyretin more amyloidogenic under mildly acidic conditions. *Biochemistry*. 2003;42(29):8756–61.
419. Yang C, Gu ZW, Yang M, Gotto Jr AM. Primary structure of apoB-100. *Chem Phys Lipids*. 1994;67–68:99–104.
420. Zinellu A, Zinellu E, Sotgia S, Formato M, Cherchi GM, Deiana L, et al. Factors affecting S-homocysteinylolation of LDL apoprotein B. *Clin Chem*. 2006;52(11):2054–9.
421. Zinellu A, Loriga G, Scanu B, Pisanu E, Sanna M, Deiana L, et al. Increased low-density lipoprotein S-homocysteinylolation in chronic kidney disease. *Am J Nephrol*. 2010;32(3):242–8.
422. Zinellu A, Sotgia S, Pisanu E, Loriga G, Deiana L, Satta AE, et al. LDL S-homocysteinylolation decrease in chronic kidney disease patients undergone lipid lowering therapy. *Eur J Pharm Sci*. 2012;47(1):117–23.
423. Zinellu A, Sotgia S, Scanu B, Deiana L, Talanas G, Terrosu P, et al. Low density lipoprotein S-homocysteinylolation is increased in acute myocardial infarction patients. *Clin Biochem*. 2012;45(4–5):359–62.
424. Armstrong VW, Walli AK, Seidel D. Isolation, characterization, and uptake in human fibroblasts of an apo(a)-free lipoprotein obtained on reduction of lipoprotein(a). *J Lipid Res*. 1985;26(11):1314–23.
425. Seed M, Hoppichler F, Reaveley D, McCarthy S, Thompson GR, Boerwinkle E, et al. Relation of serum lipoprotein(a) concentration and apolipoprotein(a) phenotype to coronary heart disease in patients with familial hypercholesterolemia. *N Engl J Med*. 1990;322(21):1494–9.
426. Wild SH, Fortmann SP, Marcovina SM. A prospective case–control study of lipoprotein(a) levels and apo(a) size and risk of coronary heart disease in Stanford Five-City Project participants. *Arterioscler Thromb Vasc Biol*. 1997;17(2):239–45.
427. Foody JM, Milberg JA, Robinson K, Pearce GL, Jacobsen DW, Sprecher DL. Homocysteine and lipoprotein(a) interact to increase CAD risk in young men and women. *Arterioscler Thromb Vasc Biol*. 2000;20(2):493–9.
428. Herrmann W, Quast S, Ellgass A, Wolter K, Kiessig ST, Molinari E, et al. An increased serum level of free Apo(a) in renal patients is more striking than that of Lp(a) and is influenced by homocysteine. *Nephron*. 2000;85(1):41–9.
429. Smith EB, Cochran S. Factors influencing the accumulation in fibrous plaques of lipid derived from low density lipoprotein. II. Preferential immobilization of lipoprotein (a) (Lp(a)). *Atherosclerosis*. 1990;84(2–3):173–81.
430. Harpel PC, Chang VT, Borth W. Homocysteine and other sulfhydryl compounds enhance the binding of lipoprotein(a) to fibrin: a potential biochemical link between thrombosis, atherogenesis, and sulfhydryl compound metabolism. *Proc Natl Acad Sci USA*. 1992;89(21):10193–7.
431. Whiteman P, Hutchinson S, Handford PA. Fibrillin-1 misfolding and disease. *Antioxid Redox Signal*. 2006;8(3–4):338–46.
432. Hutchinson S, Aplin RT, Webb H, Kettle S, Timmermans J, Boers GH, et al. Molecular effects of homocysteine on cbEGF domain structure: insights into the pathogenesis of homocystinuria. *J Mol Biol*. 2005;346(3):833–44.
433. Hubmacher D, Tiedemann K, Bartels R, Brinckmann J, Vollbrandt T, Batge B, et al. Modification of the structure and function of fibrillin-1 by homocysteine suggests a potential pathogenetic mechanism in homocystinuria. *J Biol Chem*. 2005;280(41):34946–55.
434. Hubmacher D, Cirulis JT, Miao M, Keeley FW, Reinhardt DP. Functional consequences of homocysteinylolation of the elastic fiber proteins fibrillin-1 and tropoelastin. *J Biol Chem*. 2010;285(2):1188–98.
435. Singh P, Carraher C, Schwarzbauer JE. Assembly of fibronectin extracellular matrix. *Annu Rev Cell Dev Biol*. 2010;26:397–419.

436. Majors AK, Sengupta S, Willard B, Kinter MT, Pyeritz RE, Jacobsen DW. Homocysteine binds to human plasma fibronectin and inhibits its interaction with fibrin. *Arterioscler Thromb Vasc Biol.* 2002;22(8):1354–9.
437. Hubmacher D, Sabatier L, Annis DS, Mosher DF, Reinhardt DP. Homocysteine modifies structural and functional properties of fibronectin and interferes with the fibronectin-fibrillin-1 interaction. *Biochemistry.* 2011;50(23):5322–32.
438. Cirulis JT, Bellingham CM, Davis EC, Hubmacher D, Reinhardt DP, Mecham RP, et al. Fibrillins, fibulins, and matrix-associated glycoprotein modulate the kinetics and morphology of in vitro self-assembly of a recombinant elastin-like polypeptide. *Biochemistry.* 2008;47(47):12601–13.
439. Brown PL, Mecham L, Tisdale C, Mecham RP. The cysteine residues in the carboxy terminal domain of tropoelastin form an intrachain disulfide bond that stabilizes a loop structure and positively charged pocket. *Biochem Biophys Res Commun.* 1992;186(1):549–55.
440. Jenny RJ, Pittman DD, Toole JJ, Kriz RW, Aldape RA, Hewick RM, et al. Complete cDNA and derived amino acid sequence of human factor V. *Proc Natl Acad Sci USA.* 1987;84(14):4846–50.
441. Kalafatis M, Rand MD, Mann KG. The mechanism of inactivation of human factor V and human factor Va by activated protein C. *J Biol Chem.* 1994;269(50):31869–80.
442. Undas A, Williams EB, Butenas S, Orfeo T, Mann KG. Homocysteine inhibits inactivation of factor Va by activated protein C. *J Biol Chem.* 2001;276(6):4389–97.
443. Lentz SR, Piegors DJ, Fernandez JA, Erger RA, Arning E, Malinow MR, et al. Effect of hyperhomocysteinemia on protein C activation and activity. *Blood.* 2002;100(6):2108–12.
444. Flood EC, Hajjar KA. The annexin A2 system and vascular homeostasis. *Vascul Pharmacol.* 2011;54(3–6):59–67.
445. Hajjar KA. Homocysteine-induced modulation of tissue plasminogen activator binding to its endothelial cell membrane receptor. *J Clin Invest.* 1993;91(6):2873–9.
446. Hajjar KA, Mauri L, Jacovina AT, Zhong F, Mirza UA, Padovan JC, et al. Tissue plasminogen activator binding to the annexin II tail domain. Direct modulation by homocysteine. *J Biol Chem.* 1998;273(16):9987–93.
447. Ling Q, Jacovina AT, Deora A, Febbraio M, Simantov R, Silverstein RL, et al. Annexin II regulates fibrin homeostasis and neoangiogenesis in vivo. *J Clin Invest.* 2004;113(1):38–48.
448. Dayal S, Chauhan AK, Jensen M, Leo L, Lynch CM, Faraci FM, et al. Paradoxical absence of a prothrombotic phenotype in a mouse model of severe hyperhomocysteinemia. *Blood.* 2012;119(13):3176–83.
449. Antony AC, Utley C, Van Horne KC, Kolhouse JF. Isolation and characterization of a folate receptor from human placenta. *J Biol Chem.* 1981;256(18):9684–92.
450. Antony AC. Folate receptors. *Annu Rev Nutr.* 1996;16:501–21.
451. Xiao X, Tang YS, Mackins JY, Sun XL, Jayaram HN, Hansen DK, et al. Isolation and characterization of a folate receptor mRNA-binding trans-factor from human placenta. Evidence favoring identity with heterogeneous nuclear ribonucleoprotein E1. *J Biol Chem.* 2001;276(44):41510–7.
452. Sun XL, Antony AC. Evidence that a specific interaction between an 18-base cis-element in the 5'-untranslated region of human folate receptor-alpha mRNA and a 46-kDa cytosolic trans-factor is critical for translation. *J Biol Chem.* 1996;271(41):25539–47.
453. Tang YS, Khan RA, Zhang Y, Xiao S, Wang M, Hansen DK, et al. Incrimination of heterogeneous nuclear ribonucleoprotein E1 (hnRNP-E1) as a candidate sensor of physiological folate deficiency. *J Biol Chem.* 2011;286(45):39100–15.
454. Xiao S, Tang YS, Khan RA, Zhang Y, Kusumanchi P, Stabler SP, et al. Influence of physiological folate deficiency on human papillomavirus type 16 (HPV16)-harboring human keratinocytes in vitro and in vivo. *J Biol Chem.* 2012;287(15):12559–77.
455. Maret W. Oxidative metal release from metallothionein via zinc-thiol/disulfide interchange. *Proc Natl Acad Sci USA.* 1994;91(1):237–41.

456. Khachigian LM. Early growth response-1 in cardiovascular pathobiology. *Circ Res.* 2006;98(2):186–91.
457. Stuhlinger MC, Oka RK, Graf EE, Schmolzer I, Upson BM, Kapoor O, et al. Endothelial dysfunction induced by hyperhomocyst(e)inemia: role of asymmetric dimethylarginine. *Circulation.* 2003;108(8):933–8.
458. Stuhlinger MC, Stanger O. Asymmetric dimethyl-L-arginine (ADMA): a possible link between homocyst(e)ine and endothelial dysfunction. *Curr Drug Metab.* 2005;6(1):3–14.
459. Ogawa T, Kimoto M, Sasaoka K. Occurrence of a new enzyme catalyzing the direct conversion of NG, NG-dimethyl-L-arginine to L-citrulline in rats. *Biochem Biophys Res Commun.* 1987;148(2):671–7.
460. Stuhlinger MC, Tsao PS, Her JH, Kimoto M, Balint RF, Cooke JP. Homocysteine impairs the nitric oxide synthase pathway: role of asymmetric dimethylarginine. *Circulation.* 2001;104(21):2569–75.
461. Rocha MS, Teerlink T, Janssen MC, Kluijtmans LA, Smulders Y, Jakobs C, et al. Asymmetric dimethylarginine in adults with cystathionine beta-synthase deficiency. *Atherosclerosis.* 2012;222(2):509–11.
462. Frey D, Braun O, Briand C, Vasak M, Grutter MG. Structure of the mammalian NOS regulator dimethylarginine dimethylaminohydrolase: a basis for the design of specific inhibitors. *Structure.* 2006;14(5):901–11.
463. Reuben DM, Bruice TC. Reaction of thiol anions with benzene oxide and malachite green. *J Am Chem Soc.* 1976;98(1):114–21.

Index

A

- α 1-acid glycoprotein, 9–10, 123
- α -crystallin, 26, 65, 93
- Acetaldehyde, 24, 27–28
- AdoHcy, 4, 7–9, 11–12, 17, 72
- AdoMet, 7, 9, 17, 72
- Albumin, 55–56, 59–61, 65–67, 69–70, 78–82, 121, 123–124
- Annexin A2, 131, 132
- Aminoacyl-tRNA synthetases (AARS), 33, 34, 36, 41, 42
- Aminopterin, 37, 55
- ApoE^{-/-} mice
 - atherosclerotic lesions, 99, 111
 - N-Hcy-protein, 99, 111
- Apolipoprotein A1 (ApoA1), 9, 66, 85–86, 99–100
- Apolipoprotein B (ApoB-100), 126–127
- Asymmetrical dimethylarginine (ADMA), 8, 72, 75, 134–135
- Atherosclerosis
 - anti-N-Hcy-protein autoantibody, 113–115
 - chronic inflammatory disease, 111–112
 - hyperhomocysteinemia, 3–4
 - innate immune response, 115
 - N-Hcy-albumin, 82

B

- Betaine–Hcy methyltransferase (BHMT), 7
- Bleomycin hydrolase (Blmh), 8, 15
 - D-, D,L-, and L-Hcy-thiolactone, 48–49
 - Hcy-thiolactone-induced neurotoxicity, 47, 49–50
- hyperhomocysteinemia, 49

substrate specificity, 48

- Blmh^{-/-} mice, 47, 49–50
- Brain, 3–4, 12, 17, 45–49, 63, 76, 133, 135

C

- Calcium-binding epidermal growth factor-like (cbEGF), 127
- Cardiac surgery patients
 - aorta, 11
 - myocardium, 11
 - N-Hcy-protein, 11
- cbIC/D, 125
- Cbs^{-/-} mice, 67–69, 116, 119, 132
- CBS and MTHFR gene, 62, 110
- Chronic kidney disease (CKD), 126, 127
- Circular dichroism (CD) spectral analyses
 - N-Hcy-albumin, 88
 - N-Hcy-insulin, 90
 - N-Hcy-amyloid- β -peptide, 91
 - N-Hcy-caseins, 92
- Collagen, 67–68, 118–119, 129
- Cse^{-/-} mice, 68–68
- Coronary artery disease (CAD), 16, 111, 113–114
- C-reactive protein (CRP), 53, 112, 114–116
- Cysteine, 1, 4, 7, 9–10, 14, 29, 32–33, 41, 43, 44, 48, 76, 78–81, 83, 121–135
- Cystathionine γ -lyase (Cse), 7
- Cystathionine, 9, 11–12, 18
- Cystathionine β -synthase (CBS), 3–4, 10–12, 14, 16–17, 36, 51–52, 55, 62–63, 66–69, 75, 84, 89, 93, 95, 104–105, 107, 101–110, 113, 116–119, 125, 129–130, 132, 135
- Cytochrome c, 26, 60, 65, 82–83, 86–87

D

- Diabetes patients
 - macrovasculopathy, 52
 - hemodialysis, 98
 - uremia, 98, 110
- Dihydrofolate reductase (Dhfr), 42–43
- Dimethylarginine dimethylaminohydrolase (DDAH), 134–135
- δ -L- α -aminoadipoyl-L-homocysteiny-D-valine (AhCV), 43
- Dynamic light scattering (DLS) analysis, 87
- Dynein, 61, 69–70, 93–94, 108

E

- Edman degradation analysis, 61
- Electrospray ionization-mass spectroscopy (ESI-MS), 103, 125
- Endoplasmic reticulum (ER), 15, 107, 108
- Endothelial cells, 8, 13–17, 30, 36–37, 42–45, 55, 81, 85, 95, 108, 110, 113–114, 116, 126, 131, 134–135

F

- folic acid, 4, 36, 44, 56, 75, 108, 110, 114, 117
- Fibrillins, 127–130
- Fibrin clot, 83–84
 - properties, 83
 - structure, 84, 117–118
- Fibrinogen, 10, 26, 52, 59–62, 65–66, 70, 78, 80, 83–84, 86, 96, 102, 104–105, 117–118
- Fibronectin, 129
- Fluorosurfactant (FSN), 32–33
- Folate metabolism
 - human MTHFR, 3, 7–8, 36, 39, 52
 - mouse Dhfr, 42–43
 - mouse Mthfr, 62–63, 69
 - mouse Pcft, 62–63
- Formaldehyde, 24, 27–28

G

- Gas chromatography/mass spectrometry (GC-MS), 32
- Glutathione (GSH), 10, 14, 30, 121–126, 134
- γ -Globulin, 9–10, 13, 59, 65–66, 87, 121, 123–124
- γ -Thiobutyrolactone, 25, 46, 48, 64
- Gold nanoparticle (AuNP) sensor, 32–33

H

- Heart, 10, 63, 99, 107, 115, 131
- Hemoglobin, 8, 10, 26, 61, 65–67, 73–74, 77, 80, 86–87, 96, 98, 101–102, 112
- Heterogenous nuclear ribonucleoprotein E1 (hnRNP-E1), 132–133
- High-density lipoprotein (HDL), 9–10, 44–46, 52, 56, 65–66, 78, 85–86, 96, 99, 114, 123
- High-performance liquid chromatography (HPLC) assay
 - fluorescence detection
 - 7-fluorobenzo-2-oxa-1,3-diazole-4-sulfonate, 98
 - 4-fluoro-7-sulfamoyl-benzofurazan, 98
 - OPA derivatization, 96–98
- Hcy-thiolactone
 - glutathione-OPA reaction, 30
 - urinary Hcy-thiolactone, 31–32
 - UV absorbance, 30
 - UV detection, 95–96
- Homocysteic acid (HCA), 11–12, 18
 - agonist of glutamate receptors, 18
 - prebiotic synthesis, 12
- Homocysteine
 - atherosclerosis, 3–4
 - B-vitamin supplementation trials, 4
 - folic acid supplementation, 4, 117
 - Hcy-lowering therapy, 4, 66, 110, 115–117
 - Hcy-thiolactone and *N*-Hcy-protein, 5
 - Hcy-thiolactone and *S*-nitroso-Hcy, 4–5
 - homocystinuria, 3
 - hyperhomocysteinemia, 2–3
 - methionine source, 2
 - reactivity, 4
 - toxic metabolite, 4
- Homocysteine metabolism
 - CBS, 7
 - concentration value, 8, 9
 - cystathionine, 11
 - Hcy-thiolactone, 8, 10
 - HSA and HCA, 11–12
 - methionine, 7
 - methionine synthase (MS), 7
 - methionyl-tRNA synthetase, 7–8
 - Ne*-Hcy-Lys, 8, 10–11
 - N*-Hcy-protein, 10–11
 - S*-adenosylhomocysteine, 11
 - schematic representation, 1–2
 - S*-homocysteiny-protein, 9–10
 - S*-nitroso-Hcy, 8
 - total Hcy, 9
 - toxicity

- cystathionine, 18
 - free reduced Hcy, 13
 - HCA, 18
 - Hcy-thiolactone (*see* Homocysteine-thiolactone)
 - N*-Hcy-Lys, 16
 - N*-Hcy-protein, 16
 - S*-adenosylhomocysteine, 17
 - S*-Hcy-protein, 13–14
 - Homocysteine sulfinic acid (HSA), 11–12
 - Homocysteine-thiolactone
 - acute treatment, 14–15
 - cell lines transformation, 16
 - chemical synthesis
 - acid-dependent homocysteine cyclization, 21–22
 - methionine demethylation, 19–21
 - chronic treatment, 14
 - clinical significance, 51–53
 - detrimental effects, 14
 - direct UV monitoring, 29
 - enzymatic turnover
 - bleomycin hydrolase, 48–50
 - paraoxonase 1, 45–47
 - gas chromatography/mass spectrometry, 32
 - gold nanoparticle homocysteine-thiolactone sensor, 32–33
 - high-performance liquid chromatography
 - with fluorescence detection, 30–32
 - with UV detection, 30
 - human endothelial cells, 15–16, 38
 - HUVECs, 15–16, 38–39, 43–44
 - intraperitoneal injection model, 15
 - methionyl-tRNA synthetase
 - involvement of, 33–37
 - S*-NO-Hcy, 42–44
 - synthetic/editing active site, 37, 39–41
 - thiol-binding subsite, 41–42
 - physicochemical properties
 - vs.* Hcy, 22
 - pK_a value, 23
 - reactivity, 25–28
 - stability, 23–24
 - UV spectrum, 22
 - radiolabeling, 29
 - urinary excretion, 50–51
 - Human papillomavirus (HPV), 133
 - Human papilloma virus 16 (HPV16), 133
 - Human umbilical vein endothelial cells (HUVECs), 15, 16, 38, 43, 44, 95
 - Hydriodic acid, 19, 21
 - Hydrochloric acid, 19, 21, 23
 - HCl, 42, 94–96
 - Hydrogen atom transfer (HAT), 77
 - Hydrogen peroxide, 12, 81, 145
 - Hyperhomocysteinemia
 - causes, 36
 - Hcy-thiolactone hypothesis, 109–110
 - MTHFR/CBS* gene mutation, 52
 - pathology, 108–109
 - plasma Hcy-thiolactone levels, 39
 - protein *N*-linked Hcy, 110–111
 - treatment, 37
- I**
- Inflammation, 16, 53, 75, 109, 112, 115
 - Innate immune response, 111–112, 115–116
 - Intracellular adhesion molecule (ICAM-1), 81, 116
 - Iron
 - cytochrome c, 82–83
 - ferritin, 65
 - Isoleucyl-tRNA synthetase, 35
- K**
- Keyhole limpet hemocyanin, 53, 99, 112
 - Kidney, 7, 10, 17, 28, 31, 49, 63, 115, 126, 131
 - Kinesin, 70, 94
- L**
- Lactoglobulin, 25, 92
 - Leptin, 64
 - Leucyl-tRNA, 23
 - Leucyl-tRNA synthase, 35
 - Liver, 7–8, 10, 17, 45, 63, 68, 73–74, 78, 107–108, 116
 - Lipoprotein [a] (Lp[a]), 127
 - Liquid chromatography/mass spectrometry analysis
 - N*-Hcy-albumin, 102–104
 - N*-Hcy-fibrinogen, 104–105
 - N*-Hcy-dynein, 70, 94
 - Low-density lipoproteins (LDL), 10, 60, 65, 75, 84–85, 96, 108, 112, 116, 126, 127
 - Lung, 10, 63, 129, 131
 - Lysine
 - free, 24, 26–27, 59, 61
 - protein, 57, 59, 72–73, 77–78, 109

M

Metallothionein, 13–14, 134

Methionine demethylation

hydriodic acid digestion, 19, 20

hydrochloric acid, 19, 21

sulfuric acid, 19

Methionine

degradation to HCA, 12

essential amino acid, 2

high-Met diet, 3, 7–8, 51, 110–111,
128, 131

life span, 3

loading test, 3

metabolism, 7

prebiotic formation, 12

toxicity, 2–3

tRNA aminoacylation, 33, 35, 40, 43

Methionyl-tRNA synthetase (MetRS)

aminoacyl-tRNA synthetases, 33, 34

Chinese hamster ovary cells, 36

E. coli, 36, 37

Hcy editing reaction, 34–35

homocysteinyl adenylate (Hcy-AMP), 2, 34

human endothelial cells, 36, 38

hyperhomocysteinemia, 36–37, 39

microorganisms, 34–35

S-NO-Hcy

AhCV, 43

posttranslational Hcy incorporation, 43, 44

relative binding, editing, and tRNA
aminoacylation, 42, 43

substrate, 42

translational Hcy incorporation, 43–44

synthetic/editing active site

Asp52 interaction, 40, 41

organisms, 40–41

specificity subsite, 37, 39

Tyr15 and Trp253 role, 39, 40

thiol-binding subsite, 41–42

Methylenetetrahydrofolate reductase

(MTHFR), 3, 7, 10, 12, 16–17, 36,

39, 52–53, 55, 62–63, 66, 68–69, 75,

89, 107, 110, 113

Microtubule

binding domain of dynein, 70

proteins, 92, 94

Monocyte chemoattractant protein (MCP), 81, 116

Mthfr^{-/-} mice, 10, 17, 68–69

N

N-Acetyl-Hcy-thiolactone, 25, 90

Ne-homocysteinyl-lysine, 8, 10–11

biological formation, 73–74

chemical synthesis, 71–73

clinical significance, 75

physicochemical properties, 73

quantification, 74

toxicity, 16

Neuromodulator brain, 76

N-homocysteinyl-lysine (N-Hcy) protein

adaptive autoimmune response

animal models, 112

anti-N-Hcy-protein, 113–115

atherosclerosis, 111–112

autoimmunogenic, 112–113

collagen and connective tissues, 118–119

innate immune responses, 115–117

N-Hcy-fibrinogen and thrombosis,
117–118

aminopterin treatment, 55–56

CHOP/GADD153 gene, 107

ER function, 107, 108

folic acid, 108

hyperhomocysteinemia

Hcy-thiolactone hypothesis, 109–110

pathology, 108–109

protein N-linked Hcy, 110–111

kinetics, 56

misfolded/aggregated protein, 108

schematic structure, 57

N-homocysteinyl-lysine

Ne-homocysteinyl-lysine

biological formation, 73–74

chemical synthesis, 71–73

clinical significance, 75

physicochemical properties, 73

quantification, 74

quantification

aldehyde reaction, 100–102

extracellular and cellular protein, 94

HPLC assay (*see* High-performance

liquid chromatography

(HPLC) assay)

immunoassay, 99

LC-MS method (*see* Liquid

chromatography/mass spectrometry
analysis)

radiolabeling method, 38, 95

Western blot immunoassay, 99–100

structure/functional study

classical peptide chemistry

method, 76

cysteine residue, 76

fibrinogen and fibrin clot property,
83–84

- HAT process, 77
 HDL function, 85–86
 LDL function, 84–85
 oxytocin, 76
 protein aggregation/amyloid structure
 (see Protein aggregation)
 protein modification reaction, 78
 redox function (see Redox function)
 thiol, 77
- in vitro synthesis
 adduct's structure, 59
 Edman degradation analysis, 61
 fibrinogen and LDL, 60
 Hcy-thiolactone reaction, 24, 61
 lysine and serum albumin, 24, 59
 mass spectrometric analyses, 61
 polyacrylamide gel electrophoretic
 analyses, 59–60
 protein lysine residue, 60, 61
 protein purification, 26, 60
 pseudo-first-order rate
 constant, 24, 61
- in vivo
 blood protein, 65–67
 CBS and MTHFR gene, 62
 cellular protein, 65
 collagen, 67–68
 genetic and dietary factor, 62
 genetic/nutritional disorder, 62–63
 hair keratin, 68–69
 milk protein, 68
 PON1 gene, 62, 64
 site-specific N-Hcy, 69–71 (see also
 Liquid chromatography/mass
 spectrometry analysis)
 wild-type C57BL/6 J mice, 63–64
- N-methyl-D-aspartate receptor (NMDA), 18
 NMR, 59, 72
- O**
- o*-phthalaldehyde (OPA), 27, 28, 30–32, 96–98
- Oxidative
 damage, 77–78, 81, 85
 stress, 127, 134
- Oxytocin
- Analogs
 Hcy-oxytocin, 76
 1 β -mercaptopyrrolic acid-oxytocin, 76
 1 γ -butyric acid-oxytocin, 76
 biological activity, 43, 76
 cysteine residue, 76
 loss of activity, 76
 neuromodulator, 76
 sexual reproduction, 76
 social attachment and affiliation, 76
 structure and function, 76
- P**
- Paraoxonase 1 (PON1)
 Alzheimer's disease, 45
 cardiovascular disease, 47
 Hcy-thiolactonase activity, 45–47
 Hcy-thiolactone-induced neurotoxicity,
 46–47
 high-density lipoprotein, 45–46
 N-Hcy-protein, 64
 paraoxonase activity, 46
 penicillamine, 46
 PON1 gene, 62, 64
 PON1-R192 allele, 47
 substrate specificity, 46
- Phenyl acetate, 46, 64
- Phenylthiohydantoin derivative of Hcy,
 44, 61
- pK_a value, 23, 50, 61, 122
- Pyridoxal phosphate, 27
- Polyacrylamide gel electrophoretic analyses,
 59–60
- Polysulfoethylaspartamide (PSEA) cation
 exchange column, 30–31, 95–97
- Pon1^{-/-} mice, 46–47
- Protein aggregation
 N-Hcy-albumin
 atomic force microscopy image, 89
 CBS deficiency, 89
 CD spectral analysis, 88
 DLS analysis, 87
 α -helical structure, 86
 physiological condition, 88
 seeding experiment, 87–88
 N-Hcy-amyloid β -peptide, 91
 N-Hcy-caseins, 92–93
 N-Hcy-crystallin, 93
 N-Hcy-dynein, 93–94
 N-Hcy-insulin, 90
 N-Hcy-prion, 91
 N-Hcy-tau, 92
- Protein carbonyls, 77, 116
- Proton-coupled folate transporter (Pcft),
 11–12, 62–63, 113
- Pseudo-first-order rate constant, 24, 27, 49,
 61, 71

R

- Reactivity, Hcy-thiolactone
- amino groups
 - lysine derivatives, 26–27
 - N*-acetyl-Hcy-thiolactone, 25
 - proteins, 25–26
 - thiol functionality, 25
 - carbonyl compounds
 - acetaldehyde, 27–28
 - formaldehyde, 27, 28
 - o*-phthalaldehyde, 28
- Redox function
- N*-Hcy-albumin
 - atherosclerotic lesion, 82
 - cell adhesion, 81
 - HPLC analysis, 79–80
 - mechanism of, 79–80
 - molecular/physiological form, 78–79
 - structural transition, 81
 - structure and function, 78
 - thiol-disulfide exchange reaction, 79–81
 - N*-Hcy-cytochrome *c*, 82–83

S

- S*-homocysteinylated proteins
- blood homeostasis
 - annexin A2, 131–132
 - factor Va, 130–131
 - extracellular matrix
 - fibrillins, 127–128
 - fibronectin, 129
 - tropoelastin, 129–130
 - intracellular proteins
 - DDAH, 134–135
 - hnRNP-E1, 132–133
 - metallothionein, 134
 - ionizations, 122
 - physiological pH, 121
 - plasma
 - apolipoprotein B, 126–127
 - lipoprotein [a], 127
 - serum albumin, 123–124
 - transthyretin, 124–126
 - types, 121
- S*-homocysteinylation
- kinetics, 56
 - 2-mercaptoethanol treatment, 55
 - schematic structure, 57
- S*-nitroso-Hcy (*S*-NO-Hcy), 4, 8, 22, 40, 42–43
- Stability, 23–24
- Staurosporine, 16

- Streptomycin, 27–28
- Sulfur
- amino acids, 1, 28
 - prebiotic formation, 8
 - DDAH-Hcy complex, 135
 - MetRS-Met complex, 39
 - thioether activation, 7

T

- Thioether
- methionine 7
 - N*-Hcy-Lys CMQT derivative 73
- Thioester
- Hcy-thiolactone, 2, 7, 22–23, 25, 29, 34, 40, 41, 59, 108
 - Met-S-CoA, 23, 41
 - Met-S-pantetheine, 41
 - Met-thioesters, 40–41
- Thrombosis, 3, 14, 84, 115, 117–118, 131–132
- Thyl radical, 77, 83, 116
- Tissue plasminogen activator (TPA), 13, 131
- TNF-alpha, 81, 115–116
- Total Hcy, 9
- Transferrin, 26, 80–81, 87, 123
- Trichloroacetic acid, 56
- Tris(2-carboxyl)phosphine (TCEP), 74, 98
- tRNA, 33–35, 40, 42–43
- Hcy-tRNA, 42
 - Met-tRNA, 2, 37, 40
 - S*-NO-Hcy-tRNA, 40, 43
- Transthyretin, 9, 10, 67, 124–126
- Tropoelastin, 129–130

U

- Unfolded protein response (UPR), 15, 107–108
- Urinary excretion, 15, 50–52
- UV spectrum, 22, 73

V

- VCAM-1, 81, 11–116

W

- Western blot immunoassay, 66, 99–100

Z

- Zinc, 13, 122, 134